



THE UNIVERSITY *of* EDINBURGH

This thesis has been submitted in fulfilment of the requirements for a postgraduate degree (e.g. PhD, MPhil, DClinPsychol) at the University of Edinburgh. Please note the following terms and conditions of use:

This work is protected by copyright and other intellectual property rights, which are retained by the thesis author, unless otherwise stated.

A copy can be downloaded for personal non-commercial research or study, without prior permission or charge.

This thesis cannot be reproduced or quoted extensively from without first obtaining permission in writing from the author.

The content must not be changed in any way or sold commercially in any format or medium without the formal permission of the author.

When referring to this work, full bibliographic details including the author, title, awarding institution and date of the thesis must be given.



THE UNIVERSITY *of* EDINBURGH

Fetal programming of adult disease:
Causes and consequences of metabolic
dysregulation in an ovine model of PCOS

Katarzyna Siemienowicz

The University of Edinburgh

Thesis submitted for the fulfilment of the degree of
Doctor of Philosophy

August 2017

Contents

Acknowledgements	ii
Abstract	iii
Lay abstract	v
Presentations relating to this thesis	vii
Abbreviations	viii
Chapter 1 Literature Review	1
1.1 Female reproductive function.....	2
1.1.1 Mammalian reproductive development.....	2
1.1.2 The hypothalamic-pituitary-ovarian axis	3
1.1.3 Folliculogenesis.....	4
1.1.4 Female puberty.....	6
1.1.5 Human ovarian cycle.....	7
1.1.5.1 The follicular phase.....	7
1.1.5.2 The luteal phase	7
1.1.6 Ovarian steroidogenesis	8
1.1.7 Adrenal steroidogenesis	9
1.1.8 Ovarian and adrenal androgens in adult females	10
1.1.9 Ovarian and adrenal androgens in adolescent girls.....	12
1.1.10 Reproduction in sheep	12
1.1.11 Regulation of pubertal transition in sheep	13
1.2 Role of adipose tissue in metabolism	14
1.2.1 Adipocyte development and growth	15
1.2.2 Lipolysis and triglyceride formation.....	16
1.2.3 WAT as an endocrine organ.....	16
1.2.3.1 Leptin.....	17
1.2.3.2 Adiponectin.....	18
1.2.4 Adipose tissue depot differences between SAT and VAT	19
1.2.5 Central obesity	20
1.2.6 Obesity and WAT	20
1.2.7 Role of brown adipose tissue in energy homeostasis	22
1.2.8 Adipose tissue and sexual dimorphism	23
1.3 Clinical features and diagnostic criteria of PCOS	24
1.3.1 Clinical features and diagnostic criteria of PCOS in adolescent girls.....	26
1.3.2 Prevalence of PCOS.....	26

1.3.3	Metabolic characteristics of adult women with PCOS	27
1.3.3.1	Insulin resistance	27
1.3.3.2	Type 2 diabetes mellitus.....	27
1.3.3.3	Obesity	28
1.3.3.4	Adipose tissue dysfunction.....	29
1.3.3.5	Metabolic syndrome	30
1.3.3.6	Non-alcoholic fatty liver disease	31
1.3.3.7	Dyslipidaemia.....	31
1.3.3.8	Cardiovascular disease	32
1.3.4	Metabolic characteristics of adolescent girls with PCOS	32
1.3.4.1	Insulin resistance	32
1.3.4.2	Obesity	33
1.3.4.3	Metabolic syndrome	34
1.3.5	Pathophysiology of PCOS	35
1.3.6	Management of PCOS	38
1.3.6.1	Insulin sensitisers	38
1.3.6.2	Oral contraceptives.....	39
1.4	Aetiology of PCOS	40
1.4.1	Heritability of PCOS	40
1.4.2	Genetics of PCOS.....	40
1.4.3	Prenatal programming of PCOS	42
1.5	Animal models of PCOS.....	45
1.5.1	Non-human primate model.....	45
1.5.2	Ovine model	45
1.6	The objectives of this thesis	47
Chapter 2	Materials and Methods	49
2.1	Introduction.....	50
2.2	Animal husbandry	50
2.2.1	Mating and pregnant ewe husbandry.....	50
2.2.2	Pregnant ewe treatment	51
2.2.2.1	Maternal Injections.....	51
2.2.2.2	Fetal Injections	51
2.2.3	Non-pregnant treatment.....	52
2.2.4	Husbandry of offspring.....	52
2.2.5	Animal sacrifice and specimen collection	53

2.2.5.1	Animal sacrifice	53
2.2.5.2	Tissue and plasma collection	53
2.3	Histology	55
2.3.1	Tissue Processing	55
2.3.2	De-waxing and rehydration.....	55
2.3.3	Haematoxylin and Eosin Staining	55
2.3.4	Immunohistochemistry.....	56
2.3.5	Antigen Retrieval	56
2.3.6	Blocking	56
2.3.7	Incubation with Primary and Secondary Antibody	57
2.3.8	Detection and Counterstaining.....	57
2.3.9	Imaging	58
2.4	Western Blotting.....	58
2.4.1	Protein Extraction.....	58
2.4.2	Protein Quantification	58
2.4.3	Western Blotting Protocol.....	59
2.5	ELISA.....	60
2.6	Multiplex immunoassay	60
2.7	Gene expression.....	61
2.7.1	RNA extraction	61
2.7.1.1	RNA extraction from liver tissue	61
2.7.1.2	RNA extraction from adipose tissue	61
2.7.1.3	RNA extraction from skeletal muscle.....	62
2.7.2	Measurement of RNA concentration.....	62
2.7.3	Complementary DNA synthesis.....	62
2.7.4	Quantitative Real-Time Polymerase Chain Reaction.....	64
2.7.5	SYBR Green DNA-binding dye.....	64
2.7.6	SYBR Green protocol and analysis.....	65
2.7.7	The selection of the optimal reference genes using geNorm	66
2.7.8	Primer Design.....	66
2.8	Statistical analysis.....	67
Chapter 3	The effect of prenatal androgenisation on the function of WAT	69
3.1	Introduction	70
3.2	Materials and Methods	72
3.2.1	Experimental animals.....	72

3.2.2	Gene expression analysis using qRT-PCR	73
3.2.3	Western Blotting.....	74
3.2.4	Intravenous Glucose Tolerance Test	74
3.2.5	Glucose and insulin measurements.....	75
3.2.6	Measurement of other plasma analytes.....	75
3.2.7	Plasma leptin concentration.....	75
3.2.8	Plasma adiponectin concentration	76
3.2.9	Adipocyte morphometric analysis	76
3.2.10	Statistical analysis	76
3.3	Results.....	77
3.3.1	Adipocyte differentiation in adolescent VAT and SAT	77
3.3.2	Link between altered adipogenesis and dyslipidaemia.....	80
3.3.3	Leptin and adiponectin levels during adolescence	81
3.3.4	Adiponectin and insulin signalling in adipose tissue during adolescence	83
3.3.5	Inflammation markers in adipose tissue	85
3.3.6	Adipocyte differentiation in SAT in fetal and early life.....	86
3.3.7	Temporal androgenisation of sheep did not result in altered adipogenesis	87
3.3.8	The effect of different steroid classes on adipogenesis	88
3.3.9	Metabolic parameters of adult prenatally androgenised sheep	89
3.3.10	Markers of adipogenesis in adult SAT and VAT	91
3.3.11	Histological analysis of VAT and SAT.....	93
3.3.12	Consequences of adipocyte hypertrophy in adult SAT	95
3.4	Discussion.....	97
Chapter 4	The effect of prenatal androgenisation on energy expenditure.....	107
4.1	Introduction.....	108
4.2	Methods.....	112
4.2.1	Experimental animals	112
4.2.2	Measuring postprandial thermogenesis	112
4.2.3	Gene expression analysis using qRT-PCR.	113
4.2.4	Immunohistochemistry	114
4.2.5	Noradrenaline ELISA	114
4.2.6	Statistical analysis	115
4.3	Results.....	116
4.3.1	PPT is decreased in adult PCOS-like sheep	116
4.3.2	Gene expression of uncoupling proteins in adipose tissue depots.....	118

4.3.3	Immunohistochemical examination of the UCP1 and UCP3 expression in adipose tissue depots.	119
4.3.4	Insulin resistance in adult PCOS-like sheep correlates with decreased PPT .	121
4.3.5	Noradrenaline levels and β -adrenergic receptors expression	123
4.3.6	Expression of beige adipocyte markers is depot specific.....	125
4.3.7	Thermogenic potential of skeletal muscles	126
4.3.8	Expression of thermogenic genes across different developmental stages.....	127
4.4	Discussion.....	130
Chapter 5	The effect of prenatal androgens on hepatic phenotype	143
5.1	Introduction	144
5.2	Methods	149
5.2.1	Experimental animals.....	149
5.2.2	Gene expression analysis using qRT-PCR.....	149
5.2.3	Oil Red O Lipid Staining and Analysis.....	151
5.2.4	Measurement of plasma analytes	151
5.2.5	Statistical analysis	151
5.3	Results	152
5.3.1	Hepatic FA uptake in adolescent animals	152
5.3.2	Hepatic de novo lipogenesis in livers of 11 months old animals.	153
5.3.3	Hepatic fatty acid utilisation and storage in adolescent animals.....	153
5.3.4	Gluconeogenesis in adolescent PCOS-like animals.....	154
5.3.5	Hepatic expression of insulin and growth hormone receptors	155
5.3.6	Correlation of insulin with selected hepatic gene expression	156
5.3.7	Liver lipid content in adult animals.....	157
5.3.8	Hepatic FA uptake in adult old animals.	158
5.3.9	Hepatic de novo lipogenesis in adult animals.	159
5.3.10	Hepatic fatty acid utilisation and storage in adult animals.	159
5.3.11	Gluconeogenesis regulation in adult animals.....	160
5.3.12	Hepatic expression of insulin and growth hormone receptors	161
5.3.13	Correlation of insulin with selected hepatic gene expression	162
5.4	Discussion.....	163
Chapter 6	Role of FGF21 and irisin in the metabolic phenotype of PCOS-like sheep.171
6.1	Introduction	172
6.2	Methods	176

6.2.1	Experimental animals	176
6.2.2	Measuring gene expression using qRT-PCR.....	176
6.2.3	FGF21 ELISA	177
6.2.4	Irisin ELISA	178
6.2.5	Statistical analysis	178
6.3	Results.....	179
6.3.1	FGF21 expression in adolescents and adult PCOS-like sheep	179
6.3.2	Potential regulatory mechanisms underlying altered levels of FGF21	181
6.3.3	Autocrine regulation of FGF21 expression	182
6.3.4	FGF21 and endoplasmic reticulum stress.....	184
6.3.5	Association between FGF21 and metabolic parameters.....	185
6.3.6	FGF21 signalling in adipose tissue.....	187
6.3.7	Downstream FGF signalling in adipose tissue	188
6.3.8	FGF21 signalling in muscle tissue.....	190
6.3.9	Insulin and adiponectin signalling in muscle tissue	192
6.3.10	Expression of ER stress markers in muscle tissue	193
6.3.11	Prenatal androgenisation does not affect levels of irisin	194
6.3.12	Correlation of irisin with metabolic parameters.....	195
6.4	Discussion.....	196
Chapter 7 General Discussion		213
7.1	Future work.....	225

List of Figures

Figure 1.1. The two cell, two gonadotrophin, model.....	6
Figure 1.2. The hormonal profile over the human ovarian cycle.....	8
Figure 1.3 Ovarian and adrenal steroidogenesis.....	10
Figure 1.4 Major white adipose tissue depots in humans.....	14
Figure 1.5 Pathological obesity-induced changes in white adipose tissue.....	21
Figure 1.6 Differentiation of white and brown adipocytes.....	22
Figure 3.1 Adipogenesis markers expression in VAT in adolescent animals.....	77
Figure 3.2 Adipogenesis markers expression in SAT in adolescent animals.....	78
Figure 3.3 PPAR γ protein level in VAT and SAT samples from adolescent animals.....	79
Figure 3.4 Plasma fasting TG and FFA in adolescent animals.....	80
Figure 3.5 Plasma fasting leptin and adiponectin in adolescent animals.....	81
Figure 3.6 Correlation of plasma leptin and adiponectin in adolescent animals.....	82
Figure 3.7 Expression of adiponectin receptors in VAT and SAT in adolescent animals.....	83
Figure 3.8 Insulin signalling in VAT and SAT of adolescent animals.....	84
Figure 3.9 Expression of inflammation markers in VAT and SAT of adolescent animals.....	85
Figure 3.10 Expression of adipogenesis markers in SAT in fetal and juvenile animals.....	86
Figure 3.11 Expression of adipogenesis markers in SAT in animals temporally treated with testosterone.....	87
Figure 3.12 Effect of direct fetal steroid injections on the expression of adipogenesis markers in SAT in adolescent animals.....	88
Figure 3.13 Birthweight and postnatal weight in androgenised animals. Weight of omental fat in adult animals.....	89
Figure 3.14 Effect of prenatal androgenisation on glucose and insulin dynamics in adult animals.....	90
Figure 3.15 Adipogenesis markers expression in VAT in adult animals.....	91
Figure 3.16 Adipogenesis markers expression in SAT in adult animals.....	92
Figure 3.17 Representative adipose tissue sections from VAT and SAT of adult animals.....	93
Figure 3.18 Adipocyte count in VAT and SAT in adult animals.....	94
Figure 3.19 Fasting plasma FFA in adult animals.....	95
Figure 3.20 Expression of inflammation markers in VAT and SAT in adult animals.....	96
Figure 4.1 Characteristics of animals selected for thermogenesis study.....	116
Figure 4.2 Postprandial thermogenesis in adult animals.....	117

Figure 4.3 Expression of <i>UCP1</i> , <i>UCP2</i> and <i>UCP3</i> in different adipose tissue depots of adult animals.	118
Figure 4.4 Correlation of expression of UCPs mRNA in different fat depots with change in postprandial temperature in adult animals.....	119
Figure 4.5 Immunohistochemical examination of the UCP1 and UCP3 expression in adipose tissue depots.	120
Figure 4.6 The association between fasting insulin levels and changes in postprandial thermogenesis dynamics. Relationship between mRNA expression of <i>UCP1</i> in different fat depots and fasting insulin levels.....	122
Figure 4.7 Expression of <i>ADRB1</i> , <i>ADRB2</i> and <i>ADRB3</i> in four different adipose tissue depots in adult animals.	123
Figure 4.8 Noradrenaline concentrations in different adipose tissue depots	124
Figure 4.9 Correlation of fasting FFA with postprandial temperature change and with average noradrenaline level in four different anatomical adipose tissue location	125
Figure 4.10 Expression of selected beige adipocyte markers in four different adipose tissue locations.	126
Figure 4.11 Expression of UCPs mRNA and genes involved in calcium cycling in muscles of adult animals	127
Figure 4.12 Expression of UCP genes in SAT in fetal and juvenile animals	128
Figure 4.13 Expression of UCP genes and selected beige adipocyte markers in SAT in adolescent animals.....	129
Figure 5.1 Hepatic expression of genes associated with FA uptake in adolescent animals .	152
Figure 5.2 Hepatic expression of genes involved in <i>de novo</i> lipogenesis in adolescent animals	153
Figure 5.3 Hepatic expression of genes associated with FA utilisation and storage in adolescent animals	153
Figure 5.4 Hepatic expression of genes associated with gluconeogenesis in adolescent animals.	154
Figure 5.5 Hepatic expression of insulin and growth hormone receptors, <i>STAT5A</i> and <i>STAT5B</i> in adolescent animals.....	155
Figure 5.6 Correlation of insulin level at 15min of IVGTT with hepatic expression of <i>INSR</i> , <i>SREBF1</i> , <i>PEPCK</i> and <i>G6PC</i> in adolescent animals	156
Figure 5.7 Liver lipid content, plasma liver analytes and cholesterol level in adult animals	157
Figure 5.8 Hepatic expression of genes associated with FA uptake in adult animals	158

Figure 5.9 Hepatic expression of genes associated with <i>de novo</i> lipogenesis in adult animals	159
Figure 5.10 Hepatic expression of genes associated with fatty acid utilisation and storage in adult animals	159
Figure 5.11 Hepatic expression of genes associated with gluconeogenesis in adult animals	160
Figure 5.12 Hepatic expression of insulin and growth hormone receptors, <i>STAT5A</i> and <i>STAT5B</i> in adult animals.....	161
Figure 5.13 Correlation of insulin level at 15min of IVGTT with hepatic expression of <i>INSR</i> , <i>SREBF1</i> , <i>PEPCK</i> and <i>G6PC</i> in adult animals	162
Figure 6.1 FGF21 levels in adolescent and adult animals	180
Figure 6.2 Correlation of hepatic <i>FGF21</i> expression with hepatic <i>PPARA</i> and <i>PPARGCIA</i> expression in adolescent and adult animals	181
Figure 6.3 Hepatic expression of <i>KLB</i> and FGF receptors in adolescent and adult animals.	183
Figure 6.4 Hepatic expression of endoplasmic reticulum stress markers in adolescent and adult animals.....	184
Figure 6.5 Correlation of FGF21 with metabolic parameters in adolescent animals	185
Figure 6.6 Correlation of FGF21 with metabolic parameters in adult animals	186
Figure 6.7 FGF21 signalling in SAT and VAT in adolescent and adult animals	187
Figure 6.8 Correlation of <i>KLB</i> expression with <i>PPARG</i> and <i>ADIPOQ</i> in SAT and VAT in adolescent and adult animals.	189
Figure 6.9 Expression of <i>SLC2A1</i> in SAT and VAT of adolescent and adult animals.....	190
Figure 6.10 Expression of <i>KLB</i> , <i>FGFR1</i> and <i>PPARG</i> in skeletal muscle of adolescent and adult animals.....	191
Figure 6.11 Expression of <i>INSR</i> , <i>IRS1</i> , <i>IRS2</i> , <i>ADIPOR1</i> and <i>ADIPOR2</i> in skeletal muscle of adolescent and adult animals	192
Figure 6.12 Expression of selected ER stress markers in skeletal muscle of adolescent and adult animals	193
Figure 6.13 Expression of <i>FNDC5</i> in skeletal muscles and level of circulating irisin in adolescent and adult animals	194
Figure 6.14 Association of circulating irisin with selected metabolic parameters in adolescent and adult animals	195
Figure 7.1 An adolescent PCOS-like model of prenatally androgenised sheep.....	219
Figure 7.2 An adult PCOS-like model of prenatally androgenised sheep.....	222

List of Tables

Table 1.1 Criteria for diagnosis of PCOS according to different guidelines.....	25
Table 1.2 Summary of main clinical manifestations of PCOS across the life course	34
Table 2.1 Table of treatments and animal numbers used in studies documented in this thesis.	52
Table 2.2 Ovine tissue collected at the time of sacrifice from different cohorts of animals..	54
Table 2.3 Components and concentration of the TaqMan Reverse Transcription kit used for cDNA synthesis.....	63
Table 2.4 Reference genes used in qRT-PCR studies.	66
Table 3.1 Treatment regime, age and corresponding sample numbers of experimental animals discussed in chapter.3.....	72
Table 3.2 Forward and reverse primer sequences and product size for genes analysed in the fetal and postnatal adipose tissue using SYBR Green qRT-PCR.....	73
Table 3.3 List of primary and secondary antibodies used for western blotting.....	74
Table 4.1 Treatment regime, age, and corresponding sample numbers of experimental animals discussed in chapter.4.....	112
Table 4.2 Forward and reverse primer sequences and product size for genes analysed in the fetal and postnatal adipose tissue using SYBR Green qRT-PCR.....	113
Table 4.3 Details of antibodies used for immunohistochemistry in the adult adipose tissue samples.	114
Table 5.1 Treatment regime, age and corresponding sample numbers of experimental animals discussed in chapter.5.....	149
Table 5.2 Forward and reverse primer sequences and product size for genes analysed in the postnatal liver tissue using SYBR Green qRT-PCR.	150
Table 6.1 Treatment regime, age, and corresponding sample numbers of experimental animals discussed in chapter 6.....	176
Table 6.2 Forward and reverse primer sequences and product size for genes analysed in the liver tissue using SYBR Green qRT-PCR.....	177

Declaration

I hereby declare that the work in this thesis was carried out by the author, and if others contributed they are acknowledged. This thesis is submitted for the fulfilment of the degree of Doctor of Philosophy, and not for any other degree or qualification.

Katarzyna Siemienowicz

August 2017

Acknowledgements

There are number of people that I would like to thank for helping me to complete my PhD. First and foremost, I would like to thank my PhD supervisors, Prof. Colin Duncan and Prof. Mick Rae for giving me this great opportunity, for believing in me and giving me the confidence to become a scientist. I couldn't have asked for better supervisors. They have made my PhD an excellent experience. I would like to thank them for their guidance, encouragement, support, motivation, enthusiasm, passion for science, immense knowledge, a very approachable attitude and incredible patience and understanding. I have learned so much from you. Furthermore, I would like to thank Colin for teaching me the importance of telling a good and coherent story, but also his huge generosity, wonderful lab lunches, amazing conferences and all the Tequila bottles at Christmas.

I would like to thank Lyndsey Boswell for teaching me techniques and Linda Nicol for her assistance, advice and help during my last months of PhD. I would like to express my sincere gratitude to Dr Forbes Howie, for his help with measuring protein and glucose concentrations, for teaching me RIA, and his ELISA's advice as well as an incredible sense of humour. Forbes has always been supporting, welcoming, friendly and very approachable. In addition, I would like to thank Flavien Coukan for performing morphometric analysis of adipose tissue and Grace Cathal for assisting me with a geNorm analysis.

A big thank you to the staff at the Marshall building in Roslin, Joan Docherty, Marjorie Thomson and John Hogg for their wonderful support, patience, experience and for providing fantastic animal husbandry.

My sincere thanks also go to everyone in the CRH for providing me with a great learning environment, expert knowledge and excellent facilities, and to my office buddies for their support and all the fun I have had in the past four years.

Last but not the least, I would like to thank my family: my wonderful husband Jarek and beautiful and perfect daughter Zosia for their love, support, encouragement and unbelievable patience. I would like to thank my amazing and loving parents, my brilliant and talented sister Jola and my fantastic granny for their reassurance, inspiration, and for believing in me. Without you I would never achieve this. Thank you very much for everything.

Abstract

Polycystic ovary syndrome (PCOS) is a common and complex endocrine condition with reproductive and metabolic complications, affecting up to 10% of reproductive-age women. Hyperandrogenemia, ovulatory dysfunction, and luteinising hormone hypersecretion are characteristic traits of PCOS however, it seems that the most concerning long-term key issues are metabolic problems associated with the syndrome, such as hyperinsulinemia, insulin resistance, obesity, dyslipidaemia and non-alcoholic liver disease.

Despite the numerous studies on PCOS, its origin and pathophysiology are still not fully understood. However, there is increasing evidence that the adult PCOS phenotype is programmed in fetal life by androgen excess. Exposure to increased levels of testosterone *in utero* in rodents, sheep and monkeys result in adult reproductive and metabolic pathologies that parallel those seen in PCOS women. Since hyperandrogenemia is a hallmark of PCOS and daughters of PCOS mothers have elevated levels of androgens at birth, it is likely that prenatal androgenisation during early life predispose to the future development of PCOS.

Animal models of PCOS provide an opportunity to examine the developmental aetiology and molecular mechanisms underlying the pathogenesis of this condition. Over last 10 years our lab has successfully utilised a well-established ovine model of PCOS, where pregnant ewes were treated with testosterone propionate (TP) through mid-gestation. From this model, we had a large sample bank of fixed and frozen tissues from the fetal, lamb and adolescent prenatally androgenised animals that allowed to carry a broad range of experiments. In addition, a new cohort of prenatally androgenised adult sheep enabled additional *in vivo* analysis. Past research documented that prenatal androgenisation result in hyperinsulinemia with altered pancreas structure and function, and early fatty liver without difference in body weight in adolescent sheep. This thesis examines the effects and consequences of increased *in utero* androgen exposure on metabolic dysregulation in adolescent and adult female sheep.

During puberty, but not fetal or early life, there was decreased adipogenesis in subcutaneous adipose tissue (SAT), but not visceral adipose tissue (VAT), accompanied by decreased circulating concentrations of fibroblast growth factor 21 (FGF21), leptin and adiponectin, and increased concentrations of fasting free fatty acids (FFA) in prenatally androgenised sheep. This was countered by upregulated expression of FFA transporters in liver. As adults, TP-exposed animals had increased body weight, elevated fasting insulin and FFA concentrations but normal FGF21, leptin and adiponectin levels. Histological analysis revealed that adult TP-exposed animals had SAT hypertrophy, which was associated with increased expression of

inflammatory markers and correlated with increased fasting FFA. Therefore, it is likely that impaired preadipocyte differentiation in SAT during adolescence resulted in hypertrophy and inflammation of adult SAT. This consequently lowered capacity of SAT to safely store fat and potentially explains metabolic perturbations observed in PCOS-like female sheep.

To further investigate potential causes of obesity in adult PCOS-like sheep postprandial thermogenesis (PPT), an important constituent of energy expenditure, was measured through implantation of datalogger thermometers into interscapular adipose tissue. Adult prenatally androgenised sheep had decreased amplitude of PPT, without difference in basal body temperature, despite receiving the same caloric intake, and independent of obesity. These findings indicate that adult PCOS-like sheep have reduced capacity for energy expenditure, which is mirrored in women with PCOS. This reduced capacity for postprandial thermogenesis was correlated with hyperinsulinemia decreased noradrenaline levels and reduced thermogenic potential of brown and/or beige adipose tissue. This suggests that women with PCOS might be prenatally programmed to become obese.

In summary, findings documented in this thesis provide better understanding into the pathophysiology of PCOS from puberty to adulthood and give opportunities for early clinical intervention to ameliorate the metabolic phenotype of PCOS.

Lay abstract

Polycystic ovary syndrome (PCOS) is a common hormonal disorder with reproductive and metabolic complications, affecting up to 10% of reproductive-age women. The characteristic traits of the syndrome are increased level of male hormones, known as androgens, irregular menstruation, ovaries containing many small follicles, and difficulty getting pregnant as a result of irregular ovulation. However, it seems that the most concerning long-term key issues are metabolic problems associated with the syndrome, such as insensitivity to the action of insulin, resulting in compensatory increased production of insulin by pancreas, potentially resulting in type 2 diabetes, obesity, abnormal amount of lipids in the blood, and accumulation of fat in the liver and around internal organs, which might lead to further health complications.

Despite the numerous studies on PCOS the exact cause of this syndrome is unknown. PCOS often runs in families and there is increasing evidence that this condition might result from exposure of the female fetus to increased levels of androgens during pregnancy. Studies demonstrated that exposure of experimental animals to increased levels of androgens in fetal life result in the same reproductive and metabolic problems in adult life, as in women with PCOS.

Therefore, animal models of PCOS provide an opportunity to examine the cause and mechanisms underlying the development of this syndrome. Over past years our lab has successfully utilised a sheep model of PCOS, where pregnant sheep were treated with androgen through mid-pregnancy. Previous research by the members of our lab documented that females that were prenatally exposed to increased levels of androgens in fetal life had increased levels of insulin, and presence of fat deposits in the liver in adolescence. This thesis examines the effects and consequences of increased prenatal androgen exposure on metabolic dysregulation in adolescent and adult female sheep.

Results demonstrated that in adolescence, sheep that were exposed to increased levels of androgens in fetal life, had decreased development of fat cells in subcutaneous adipose tissue (SAT), a fat tissue located beneath the skin. This led to decreased levels of beneficial proteins normally secreted from this fat tissue, leptin and adiponectin. Leptin and adiponectin regulate appetite and insulin sensitivity, thus decreased levels of those proteins could result in future insulin insensitivity and weigh gain. In addition, decreased development of fat cells in SAT indicated decreased capacity of that tissue to safely store any excess fat, which was reflected in increased levels of lipids in a blood. Further, this was countered by upregulated expression

of proteins in the liver that transport fat into that organ, potentially explaining presence of fat deposits in that tissue, as previously detailed.

As adults, androgen-exposed animals had increased body weight, elevated insulin and lipid concentration in blood however, normal leptin and adiponectin levels. Analysis of cells from SAT revealed that PCOS-like animals had significantly enlarged fat cells within this fat depot, which was associated with increased level of inflammatory markers. Therefore, it is likely that reduced adipocyte development during adolescence resulted in fat cell enlargement and inflammation of adult SAT.

To further investigate potential causes of obesity in adult PCOS-like sheep postprandial thermogenesis, a heat production due to metabolism after a meal, was measured through implantation of datalogger thermometers into adipose tissue. Adult sheep prenatally exposed to increased levels of androgens had decreased maximal body temperature after a meal, without difference in basal body temperature, despite receiving the same caloric intake, and independent of obesity. These findings indicate that adult PCOS-like sheep have reduced ability to burn energy, which was also documented in women with PCOS. In addition, this reduced ability to burn energy was associated with increased insulin levels and reduced thermogenic potential of brown and/or beige adipose tissue, the tissue that is specialized in heat production and excess energy expenditure. This suggests that women with PCOS might be prenatally programmed to become obese.

In summary, findings documented in this thesis provide better understanding into the mechanisms underlying PCOS from puberty to adulthood and give opportunities for early clinical intervention to ameliorate the metabolic problems associated with PCOS.

Presentations relating to this thesis

Chapter 3

Poster presentation

“Altered adipocytes in an ovine model of polycystic ovary syndrome”

Siemienowicz K., Coukan F., Lerner A., Franks S., Rae M., Duncan C.

Society for Endocrinology, Edinburgh 2015

Oral presentation

“Impaired adipose function in PCOS – evidence that the primary abnormalities are in subcutaneous rather than visceral fat”

Siemienowicz K., Coukan F., Lerner A., Franks S., Rae M., Duncan C.

European Congress of Endocrinology, Munich 2016

Chapter 4

Oral presentation

“Obesity in PCOS: a consequence of prenatally programmed reduced energy expenditure”

Siemienowicz K., Rae M., Lerner A., Franks S., Duncan C.

Society of Reproduction and Fertility, Oxford 2015

Chapter 5

Oral presentation

“Exaggerated metabolic changes during puberty precede adult obesity and hyperlipidemia in an ovine model of Polycystic Ovary Syndrome (PCOS)”

Siemienowicz K., Coukan F., Lerner A., Franks S., Rae M., Duncan C.

Society of Reproduction and Fertility, Winchester 2016

Chapter 6

Oral presentation

“Potential role of FGF21 in the metabolic pathophysiology of an ovine model of polycystic ovary syndrome”

Siemienowicz K., Rae M., Duncan C.

Society of Reproduction and Fertility, Edinburgh 2014

Abbreviations

A4	Androstenedione
ABC	Avidin biotin complex
ACACA (ACC1)	Acetyl coenzyme A carboxylase alpha
ACTB	Actin
ACTH	Adrenocorticotrophic hormone
ADIPOQ	Adiponectin
ADIPOR	Adiponectin receptor
ADR	Adrenergic receptor
AES	Androgen Excess Society
ALT	Alanine transaminase
AMH	anti-Müllerian hormone
AMPK	Adenosine monophosphate activated protein kinase
ANOVA	Analysis of variance
AR	Androgen receptor
ASRM	American Society for Reproductive Medicine
AST	Aspartate transaminase
ATF	Activating transcription factor
ATGL	Adipose triglyceride lipase
ATP	Adenosine triphosphate
ATP2A	ATPase sarcoplasmic/endoplasmic reticulum Ca ²⁺ transporting
AUC	Area under the curve
BAT	Brown adipose tissue
BLAST	Basic local alignment search tool
BMI	Body mass index
BMR	Basal metabolic rate
BP	Base pairs
BSA	Bovine serum albumin
C	Control
C/EBP	CCAAT/enhancer binding protein
CAH	Congenital adrenal hyperplasia
CAV	Caveolin
CCL2	C-C motif chemokine ligand 2
cDNA	Complementary deoxyribonucleic acid
ChREBP	Carbohydrate responsive element binding protein
CO	Control obese
COCP	Combined oral contraceptive
CRP	C reactive protein
Ct	Cycle threshold
CT	Computed tomography
CV	Coefficients of variation

CVD	Cardiovascular disease
CYP	Cytochrome
D	Day
DAB	3,3'-diaminobenzidine
DES	Diethylstilbestrol
DEX	Dexamethasone
dH ₂ O	Distilled water
DHEA	Dehydroepiandrosterone
DHEAS	Dehydroepiandrosterone sulfate
DHEA-ST	Dehydroepiandrosterone sulfotransferase
DHT	5 α -dihydrotestosterone
DIO	Diet induced obesity
DIT	Diet induced thermogenesis
DNA	Deoxyribonucleic acid
EDTA	Ethylenediaminetetraacetic acid
EIF2AK3	Eukaryotic translation initiation factor 2 alpha kinase 3
ELISA	Enzyme-linked immunosorbent assay
ER	Endoplasmic reticulum
ERN1	Endoplasmic reticulum to nucleus signalling 1
ESHRE	European Society for Human Reproduction and Embryology
FABP	Fatty acid binding protein
FAI	Free androgen index
FAS (FASN)	Fatty acid synthase
FATP	Fatty acid transporter proteins
FFA	Free fatty acids
F-FDG-PET	Fludeoxyglucose-Positron emission tomography
FGF21	Fibroblast growth factor 21
FGFR	Fibroblast growth factor receptor
FI	Fetal injection
FNDC5	Fibronectin type III domain containing 5
FOXL2	Forkhead box L2
FOXO1	Forkhead box O1
FRS2	Fibroblast growth factor receptor substrate
FSH	Follicle stimulating hormone
FST	Follistatin
G	G force
G:I	Glucose to insulin ratio
G6PC	Glucose-6-phosphatase
GDM	Gestational diabetes mellitus
GH	Growth hormone
GHR	Growth hormone receptor
GIT	Glucose induced thermogenesis
GLUT	Insulin-regulated glucose transporter
GnRH	Gonadotrophin-releasing hormone

GnRHR	Gonadotrophin-releasing hormone receptor
GWAS	Genome-wide association study
H	Hour
H&E	Haematoxylin and eosin
H ₂ O ₂	Hydrogen peroxide
HA	Hyperandrogenism
HCL	Hydrogen chloride
HDL	High density lipoprotein
HEPES	4-(2-hydroxyethyl)-1-piperazineethanesulfonic acid
HIF-1 α	Hypoxia inducible factor 1-alpha
HMW	High molecular weight
HOMA-IR	Homeostatic model assessment of insulin resistance
HPG	Hypothalamic pituitary gonadal
HPO	Hypothalamic pituitary ovarian
HRP	Horse radish peroxidase
HSD	Hydroxysteroid dehydrogenases
HSL	Hormone sensitive lipase
IGT	Impaired glucose tolerance
IHC	Immunohistochemistry
IL-6	Interleukin-6
IM	Intramuscularly
INSR	Insulin receptor
IR	Insulin resistance
IRDye	Infrared dye
IRS	Insulin receptor substrate
IV	Intravenous
IVGTT	Intravenous glucose tolerance test
JAK-STAT3	Janus kinase signal transducer and activator of transcription 3
KLB	Klotho beta
KNDy	Kisspeptin/neurokinin B/dynorphin
KO	Knockout
LDL	Low density lipoprotein
LEP	Leptin
LEPR	Leptin receptor
LFT	Liver function tests
LH	Luteinising hormone
LMW	Low molecular weight
LPL	Lipoprotein lipase
M	Month
MAPK	Mitogen-activated protein kinase
MCP-1	Monocyte chemoattractant protein1
MDH1	Malate dehydrogenase 1
ME	Mercaptoethanol
MetS	Metabolic syndrome

MGL	Monoglyceride lipase
MI	Maternal injection
Min	Minute
MLXIPL	MLX interacting protein like
MMW	Middle molecular weight
MRI	Magnetic resonance imaging
mRNA	Messenger ribonucleic acid
Myf5	Myogenic factor 5
NAFLD	Non-alcoholic fatty liver disease
NASH	Non-alcoholic steatohepatitis
NCBI	National Center for Biotechnology Information
NF	Nuclease free
NIH	National Institutes of Health
OA	Oligoanovulation
OGTT	Oral glucose tolerance test
ORO	Oil Red O
OS	Oxidative stress
P450 _{scc}	Cytochrome P450 side chain cleavage enzyme
PBS	Phosphate buffered saline
PBST	Phosphate buffered saline with Tween
PCO	Polycystic ovaries
PCOS	Polycystic ovary syndrome
PCR	Polymerase chain reaction
PEPCK	Phosphoenolpyruvate carboxykinase
PGC	Primordial germ cell
PI3K	Phosphatidylinositol 3-kinase
PKB	Protein kinase B
PPAR	Peroxisome proliferator activated receptor
PPARGC1A	Peroxisome proliferator activated receptor gamma coactivator 1 alpha
PPT	Postprandial thermogenesis
PRDM16	PR domain-containing protein 16
PVDF	Polyvinylidene difluoride
qRT-PCR	Quantitative real-time polymerase chain reaction
RBP4	Retinol binding protein 4
RER	Rough endoplasmic reticulum
RIPA	Radioimmunoprecipitation assay
RNA	Ribonucleic acid
ROS	Reactive oxygen species
RPS26	Ribosomal protein S26
RT	Reverse transcriptase
RYR1	Ryanodine receptor 1
S.E.M	Standard error of the mean
SAT	Subcutaneous adipose tissue
SCD1	Sterol CoA desaturase 1

SDS	Sodium dodecyl sulfate
Sec	Second
SHBG	Sex-hormone binding globulin
SIRT1	Sirtuin 1
SLC27A	Solute Carrier Family 27 Member
SLC2A1	Solute Carrier Family 2 Member
SNP	Single nucleotide polymorphism
SNS	Sympathetic nervous system
SREBF1	Sterol regulatory element binding transcription factor 1
SREBP1c	Sterol regulatory element binding protein 1C
SRY	Sex-determining region of Y
StAR	Steroidogenic acute regulatory protein
STAT	Signal transducer and activator of transcription
T	Testosterone
T1DM	Type 1 diabetes mellitus
T2DM	Type 2 diabetes mellitus
TEF	Thermic effect of food
TG	Triglycerides
TLE3	Transducin like enhancer of split 3
TMEM26	Transmembrane protein 26
TNF	Tumour necrosis factor
TP	Testosterone propionate
TZD	Thiazolidinedione
UCP	Uncoupling protein
VAT	Visceral adipose tissue
VLDL	Very low density lipoproteins
W	Week
WAT	White adipose tissue
WHR	Waist-to-hip ratio
WNT4	Wingless-type MMTV integration site family member 4
WT	Wild-type
XBP1	X-box-binding protein 1

Chapter 1 Literature Review

1.1 Female reproductive function

1.1.1 Mammalian reproductive development

In mammals, sexual dimorphism has a genetic origin. The presence or absence of the Y chromosome, or precisely the sex-determining region of Y (SRY) gene, determines the genotypic sex (1,2). However, the development of the phenotype depends largely on endocrine induced differentiation. This hormonally induced phenotype is then a major determinant for further development of the individual and its capacity for reproduction, but also for sex-related differences in health and disease (3-5). Therefore, presence or absence of specific sex hormones early in fetal life, affects sexual differentiation in a permanent manner (5).

The early development of the gonads is common in both sexes, and begins as paired thickenings of the coelomic epithelium that arise within the intermediate mesoderm, on either side of the central dorsal aorta (6). These genital ridge primordia develop at approximately the fifth week of gestation in humans, giving rise to bipotential gonads (6). This is followed by primordial germ cell (PGC) migration from the yolk sac into genital ridge primordia, which is completed by sixth week of gestation (6). Subsequently, PGCs start to cumulate and proliferate, maintaining their bipotentiality until differentiation (7,8). Correspondingly, a second group of cells, derived from the columnar coelomic epithelium, migrate in as columns forming primitive sex cords (9). The further development of these sex cords depends on presence, or absence, of SRY gene.

In male fetuses, expression of the SRY gene in the somatic cells, which are precursors of Sertoli cells, initiates testicular cord formation, and enclosure of PGCs within the cords (9). In female fetuses, due to absence of SRY gene, and in the presence of genes such as wingless-type mouse mammary tumour virus integration site family, member 4 (WNT4), follistatin (FST) and forkhead box L2 (FOXL2), sex cords condense cortically around PGCs (oogonia), initiating the formation of primordial ovarian follicles (10,11). Thus, in primordial ovarian follicles, the granulosa cells originate from condensing cord cells, while oogonia give rise to oocytes (11). From this point onwards, the gonads themselves direct sexual differentiation. In contrast to male gonads, which actively secrete androgens and anti-Müllerian hormone (AMH), endocrine activity of the ovaries is not essential for sexual differentiation (12). In female fetuses, in the absence of androgens and AMH, the Wolffian ducts regress spontaneously, whereas the Müllerian ducts persist, giving rise to oviducts, uterus, cervix and upper vagina (13). Furthermore, the lack of androgens in female fetuses permits formation of female external genitalia from, common for both sexes, bipotential primordia of the external

genitalia. In males however, androgens maintain the Wolffian ducts, which consequently develop into epididymis, vas deferens and seminal vesicles, whereas AMH provokes regression of Müllerian ducts (14). In addition, the presence of androgens in male fetuses results in the formation of male external genitalia. Therefore, the differentiation process is highly androgen-dependent. The exposure of female fetuses to high levels of androgen *in utero* causes masculinisation of external genitalia. In congenital adrenal hyperplasia (CAH), due to congenital defect in corticosteroid synthesising enzymes, the fetal adrenal glands secrete large quantities of androgens, which in turn, stimulate development of male external genitalia in females (15,16). Moreover, some female patients with CAH demonstrate behavioural traits typically associated with male behaviour (15,16).

1.1.2 The hypothalamic-pituitary-ovarian axis

The reproductive cycle is regulated by the hypothalamic-pituitary-ovarian (HPO) axis. Signalling is initiated in the hypothalamus, a small region at the base of the brain. Hypothalamus comprises of numerous nuclei that control neuroendocrine, behavioural and autonomic functions. The pituitary gland is located just below hypothalamus, and consists of two main lobes, the anterior lobe, connected to hypothalamus through portal capillary system, and posterior lobe, connected with the hypothalamus through magnocellular neurons (17). The anterior lobe of the pituitary consists of various cell types, including the gonadotrophs, basophilic cells that synthesise, store and secrete the gonadotrophins, luteinising hormone (LH) and follicle stimulating hormone (FSH), controlled upon pulsatile stimulation of hypothalamic gonadotrophin-releasing hormone (GnRH) that binds to GnRH receptors (GnRHR) located on the gonadotroph (17). Therefore, the changes in FSH and LH secretion could be attributed to alterations in amplitude and frequency of the GnRH pulses or by modulating the actual response of gonadotrophs to GnRH pulses. Conversely, kisspeptin/neurokinin B/dynorphin pathway (KNDy neurons) play a key role in regulating GnRH secretion (18,19). Kisspeptin, through binding to kisspeptin receptors, expressed on GnRH neurons, directly controls GnRH pulsatility. Kisspeptin neurones, which are located in close proximity to GnRH neurons, also co-express neurokinin B and dynorphin, which, in turn, via neurokinin B receptor and kappa opioid peptide receptor, regulate pulsatile kisspeptin secretion, with neurokinin B being stimulatory and dynorphin inhibitory (19). There is also a dynamic relationship between ovary and pituitary. Estrogen and progesterone secreted from the ovary through the negative feedback mechanism control GnRH, FSH and LH secretion through action on both hypothalamus and anterior pituitary. It has been shown that kisspeptin neurons express both estrogen and progesterone receptors and that kisspeptin, neurokinin B

and dynorphin activity, and subsequently GnRH and LH secretion, is modulated by sex steroids (19). In addition, significant elevation in the plasma concentrations of estrogen during the late follicular phase of the ovarian cycle, through positive feedback mechanism, can induce LH and FSH secretion. There is evidence suggesting that kisspeptin might be also involved in mediating the positive estrogenic feedback (20).

1.1.3 Folliculogenesis

Throughout fetal life, ovaries grow slowly and assume a pelvic location, while ovarian germ cells undergo major changes. Formation of follicles starts shortly after sexual differentiation (21). At approximately day 45 in the ovine fetus and 7 to 9 weeks of gestation in the human, mitotically active oogonia interact with adjacent mesonephric cells to form the ovigerous cords, the oogonia-pregranulosa cell complexes surrounded by a basal lamina (21). During mid-gestation, the maximum number of germ cells is achieved, with approximately 6 million present in the fetal human ovary (22). After day 75 of gestation in sheep and 20 weeks of gestation in humans first follicles start to form through breakdown of germ cell clusters and subsequent interaction with pre-granulosa cells, which form a single layer around each oocyte (23). Oogonial germ cells enter first meiotic division, and arrest their progress at first meiotic prophase, thereby becoming primary oocytes (23). The majority of germ cells undergo atresia before birth (11), with an average of 1 million follicles present at birth in the human ovary however, at the time of puberty this number may be reduced further (22,24). Throughout reproductive life there is a further depletion of number of follicles and, as the result of ovarian follicle exhaustion, menopause occurs on average at about 51 years of age (24). An existing dogma states, that mammalian females are born with a total pool of non-renewing primordial follicles that they will have throughout reproductive life span. However, an existence of mitotically active germ cells in human and mice ovaries has been reported (25,26).

After a primordial follicle is activated it grows through stages of development, primary (preantral), secondary (antral), and tertiary (preovulatory). Throughout the neonatal and pre-pubertal life follicles can grow as far as the early antral phase however, only after puberty follicles can be activated to progress to the large antral, dominant and ovulatory stage. It has been estimated that the entire growth phase of a follicle from primordial to antral stage is much greater than 220 days or eight ovarian cycles (24,27).

In the preantral phase of follicular growth, the follicle increases in size, due to growth of oocyte and proliferation of granulosa cells, which become several layers thick. In addition, zona pellucida is formed, a layer of glycoproteins, which separates the oocyte from granulosa cells, and condensation of ovarian cells on the outer membrana propria will eventually become theca cells (24,27).

In the antral phase, granulosa and theca cells further proliferate and increase in size and a follicular antrum is formed. This is a collection of fluid within the follicle mainly secreted from growing granulosa cells. Theca cells divide into two layers, the outer theca externa and the inner theca interna. As follicular antrum expands, the oocyte become suspended in follicular fluid and is left surrounded only by the cumulus oophorus, a dense mass of granulosa cells encompassing the oocyte (28).

Whereas follicular development from primordial to early antral stage is independent of gonadotrophic regulation, further progression requires the action of FSH and LH from the anterior pituitary (24). In the absence of external signals from the pituitary, atresia of antral follicles occurs (29). FSH binds to FSH receptors, distributed in granulosa cells, while LH binds to LH receptors located on theca interna cells (30). Under the stimulation of LH, the theca interna cells synthesise androgens, mainly androstenedione, although testosterone is also produced to lesser extent, which are then aromatised into estrogen in granulosa cells, under the control of FSH (30). Fig. 1.1 summarises the two cell, two gonadotrophin, model of follicular steroidogenesis. In addition, androgens from theca cells, stimulate aromatase activity, and together with FSH stimulate the proliferation of granulosa cells, therefore increasing the thecal output of androgens, resulting in a matched increase in estrogens, which further stimulates the proliferation of granulosa cells (31). Finally, estrogen, together with FSH, stimulates the expression of LH receptors on granulosa cells of the dominant follicle.

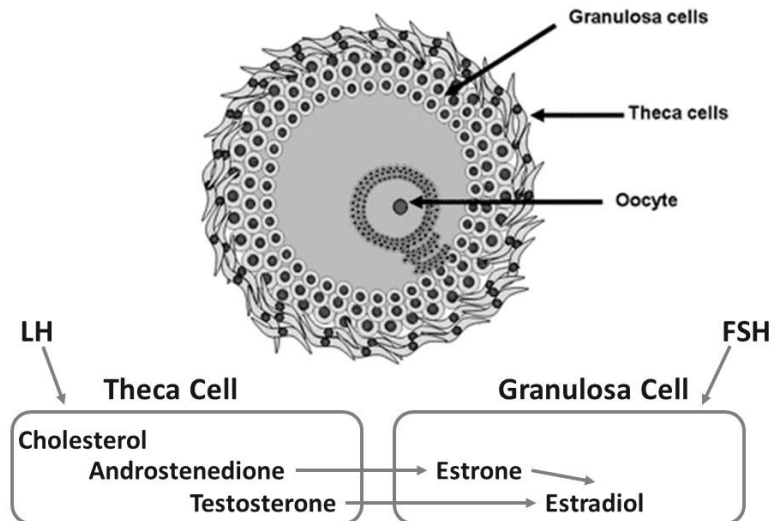


Figure 1.1. The two cell, two gonadotrophin, model. The image illustrates mechanism of estradiol production in the preovulatory follicle.

Adapted from Catalano *et al.* (32)

1.1.4 Female puberty

Puberty, a process of transition, involves physiological, morphological and behavioural changes that lead to gain of reproductive capability. In pre-pubertal girls, the HPO axis is suppressed, the ovary is quiescent, and consequently circulating gonadotrophin and sex hormones are at low levels (33). Approximately 2-4 years before puberty, adrenarche and gonadarche take place, an increase in sex steroids from the adrenal glands and the gonads respectively (33). Puberty is triggered by the activation of hypothalamic GnRH secretion, which is associated with increased pulse frequency of kisspeptin and sensitization of GnRH neurons to kisspeptin. This subsequently results in increase in the magnitude and frequency of nocturnal LH pulses and is associated with a growth spurt, and development of secondary sexual characteristics, such as maturation of the genitalia, development of breast tissue and the growth of pubic and axillary hair (18,33). Menarche follows 1-2 years later and is correlated with body fat mass. Observational studies reported that a threshold weight of 46 kg, or more precisely 22% total body fat content, is required to initiate menarche (34,35). An adipokine, leptin, has been indicated as a permissive signal in the progression into puberty and the maintenance of normal hypothalamic-pituitary-gonadal function thereafter (36). That is why, the increasing prevalence of obesity in children was highlighted as a potential cause of growing incidence of precocious puberty in children.

1.1.5 Human ovarian cycle

The human ovarian cycle lasts on average 28 days, although it can be highly variable, ranging from 25 to 30 days, and begins with the first day of menstruation (17). Menstruation, the external measure of cyclicity in women, ensues at the end of the luteal and the beginning of the follicular phase, and on average, lasts for 3–6 days (37). The ovarian cycle is composed of two distinct phases, which are separated by ovulation on day 14 of the cycle, the follicular phase and the luteal phase, each usually lasting 14 days (Fig 1.2). Irregularity in cycle length is mostly attributed to variability in the duration of the follicular phase of the cycle (38). The ovarian cycle is tightly controlled by endocrine, autocrine and paracrine factors regulating follicular development, ovulation, luteinisation and luteolysis.

1.1.5.1 The follicular phase

In regularly cycling women during the luteal–follicular transition, on average four days before menstruation, levels of estrogen and progesterone begin to decline resulting in an increase in FSH and LH (39), due to decreased negative feedback. This rise in FSH resumes growth of multiple antral follicles, accompanied by an increase in ovarian estrogen and androgen secretion. This, in turn, gradually re-establishes a negative feedback, resulting in temporary decrease of FSH level and steady levels of LH. The selection of the dominant follicle, by upregulating LH-receptor and downregulating FSH-receptor expression on its granulosa cells, results in a further estrogen surge (40). This turn, through a positive feedback effect, triggers a rapid increase in LH and FSH, which consequently initiates ovulation (38). The resulting follicular collapse and formation of corpus luteum, means levels of estrogen decrease again, together with FSH and LH, whereas levels of progesterone increase (24,38).

1.1.5.2 The luteal phase

The luteal phase of the cycle is characterised by rising concentrations of plasma progesterone and estrogen, which peak 6-8 days after ovulation, which through negative feedback, and other luteal peptide hormones such as inhibin A, suppresses circulating gonadotrophins (17). The low level of FSH suppresses the growth of antral follicles. The increasing estrogen from the corpus luteum does not induce an LH surge because of the increased levels of progesterone at the same time (38). At the end of luteal phase, if conception has not occurred, levels of progesterone and estrogen decline, during luteolysis, decreasing in negative feedback, and FSH and LH start to rise again, thereby resuming antral growth and initiating another cycle.

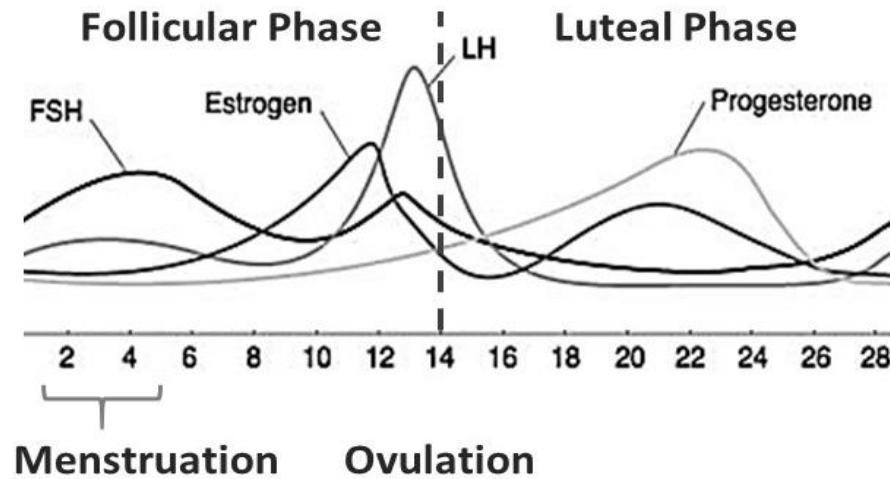


Figure 1.2. The hormonal profile over the human ovarian cycle. The ovarian cycle is composed of two distinct phases, which are separated by ovulation on day 14 of the cycle, the follicular phase and the luteal phase, each usually lasting 14 days.

Adapted from Johnson 2007 (17)

1.1.6 Ovarian steroidogenesis

In adult females, the ovary is a major source of steroid hormones. During the follicular phase of the ovulatory cycle, ovary predominantly secretes estrogens and androgens, whereas during the luteal phase mainly progestogens, with additional estrogens and androgens. The steroidogenic pathway begins with transport of free cytoplasmic cholesterol across the mitochondrial membrane by steroidogenic acute regulatory protein (StAR), encoded by *STAR* gene (17). Then, two main classes of enzymes, the cytochrome (CYP) P450 enzymes and the hydroxysteroid dehydrogenases (HSD), modulate the consecutive conversion of cholesterol (41). The conversion of cholesterol to pregnenolone marks the first step in the formation of the major steroid hormones is rate-limiting and is controlled by cytochrome P450 side chain cleavage enzyme (P450_{scc}), encoded by *CYP11A1* gene (42). Pregnenolone is then transported to smooth endoplasmic reticulum. Pregnenolone can be converted to progesterone through action of 3 β -HSD type 2 (3 β -HSD2), encoded by *HSD3B2* gene. Biosynthesis of androgens is controlled by an additional critical cytochrome enzyme: 17 α -hydroxylase, encoded by *CYP17A1* that regulates two consecutive catalytic reactions, leading to the formation of androgenic precursors, dehydroepiandrosterone (DHEA) and androstenedione (A4) (42). DHEA is then converted to A4 by the action of 3 β -HSD2, whereas 17 β -HSD type 3 (17 β -HSD3), encoded by *HSD17B3* gene, converts A4 to testosterone (T) (43). Biosynthesis

of estrogens requires action of aromatase, encoded by *CYP19A1* gene, which converts androgenic substrates, A4 into estrone, and T into estradiol (42). In addition, estrone can be converted to estradiol by the action of 17 β -HSD type 1 (17 β -HSD1), encoded by *HSD17B1* gene. 17 α -hydroxylase is found in theca cells, while aromatase is located in granulosa cells, however, both theca and preovulatory granulosa cells express StAR, P450_{scc}, and 3 β -HSD2 (42). This indicates that both, theca and preovulatory granulosa cells, are therefore capable of making pregnenolone and progesterone from cholesterol. However, in follicular phase, there is no direct blood supply to granulosa cells therefore, these cells have limited access to cholesterol, which result in low synthesis level of progestagens. In contrast, in the luteal phase, due to formation of the corpus luteum, these cells have an abundant blood supply and access to cholesterol, and synthesise large amounts of progesterone (41). Figure 1.3 summarises ovarian and adrenal steroidogenesis.

1.1.7 Adrenal steroidogenesis

The adrenal glands are another source of steroid hormones, and are composed of the inner medullary region, which controls the secretion of catecholamines, adrenaline and noradrenaline, and the outer cortical region, cortex, secreting corticosteroids, mineralocorticoids and sex steroids. The cortex consists of three zones, responsible for the secretion of hormones. Androgens, DHEA, DHEA sulfate (DHEAS), A4 and T are synthesised in the zona reticularis; glucocorticoids, cortisol and corticosterone, in the zona fasciculata; the mineralocorticoid, aldosterone, is synthesised in the zona glomerulosa (42). Androgens are synthesised, like in ovary from conversion of cholesterol by the action of P450_{scc}, 17 α -hydroxylase, 3 β -HSD2, and 17 β -HSD3. The conversion of the androgen DHEA into DHEAS is catalysed by DHEA sulfotransferase 2A1 (DHEA-ST), encoded by *SULT2A1* gene (17).

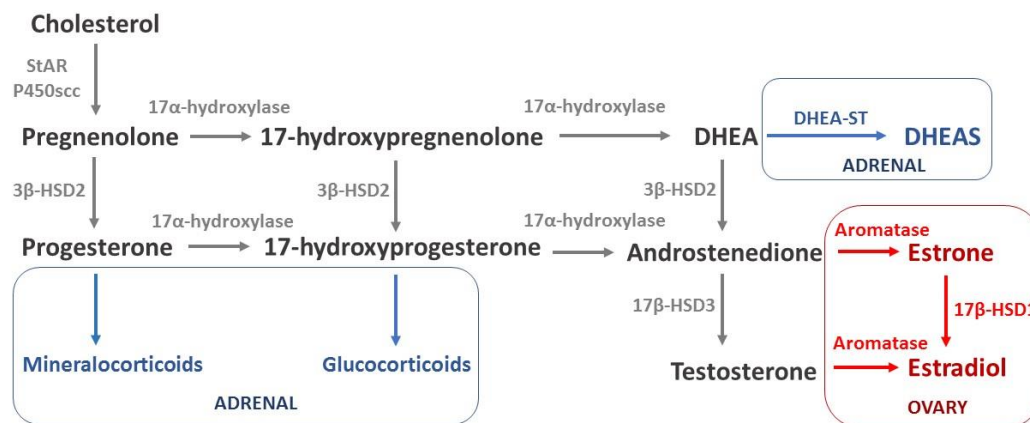


Figure 1.3 Ovarian and adrenal steroidogenesis. In black/grey common pathway; in blue adrenal specific; in red ovarian specific.

1.1.8 Ovarian and adrenal androgens in adult females

Androgens are 19 carbon steroids that are synthesised from cholesterol as the substrate or via conversion from other androgens or precursor steroids. Quantitatively, women secrete more androgens than estrogens (43). The main circulating androgens in adult females, in descending order of concentration in a serum, are DHEAS (1–4 µg/mL), DHEA (1-10 ng/ml), A4 (0.5-2ng/ml), T (0.2-0.7ng/ml), and 5 α -dihydrotestosterone (DHT) with a concentration of 0.02ng/ml (43). However, only T and DHT bind to the androgen receptor, whereas DHEAS, DHEA and A4 can be viewed as pro-androgens, as they need to be converted to T, to induce a biological action (43). In normal adult women, A4 is derived in approximately equal amounts from the ovarian theca cells and the adrenal zona fasciculata however, it shows circadian level variation and peak concentrations during the middle of ovarian cycle. Testosterone is derived 25% from the ovaries, 25% from the adrenals, and 50% from peripheral conversion of A4. The concentration of T varies throughout the ovarian cycle, with T concentrations being the lowest at early follicular phase, followed by a pre-ovulatory increase, and relatively higher concentration in luteal phase as compared to the beginning of the cycle. Testosterone shows circadian variation, with the highest concentration in the morning. In the circulation, approximately 65-75% of T is carried bound to sex-hormone binding globulin (SHBG), and 25-35% bound to albumin, with estimated of only 1–2% of T being free or biologically available (43). A free androgen index (FAI), ratio of total T to SHBG multiplied by 100, is a

method of calculating bioavailable testosterone. It has been demonstrated that T concentrations do not change significantly during menopausal transition, but rather decrease with age (44), however, there is significant decrease in SHBG during menopause, therefore an increased concentrations of free T is observed across during this transition (45). DHT is a potent, non-aromatisable androgen, almost exclusively derived from peripheral conversion of T by the action of 5α -reductase, although small quantity is secreted from the adrenals (43). DHEA and DHEAS are mainly secreted from adrenal zona reticularis, with approximately 80% of DHEA and 90% of DHEAS produced in the adrenals (46). Serum concentrations of DHEAS and DHEA increase from adrenarche, peak in third decade of life, followed by a steady decline with age (47). There is no significant fluctuation of both DHEAS and DHEA during ovarian cycle. The regulation of androgen secretion involves stimulation by adrenocorticotrophic hormone (ACTH) in adrenal and LH in ovary together with intraglandular paracrine and autocrine mechanisms (46). Liver, adipose tissue, and skin express 3β -HSD, 17β -HSD, aromatase and steroid sulfatase, and thus can catalyse conversion of androgenic precursors into androgen and estrogen (48). Therefore, substantial androgen production originates from conversion of circulating DHEAS in target tissues.

There is increasing evidence for widespread anatomical distribution of androgen receptors in women, in areas as diverse as breast, bone and brain (44). Therefore, it is likely that androgens and their metabolites may have an important role not only in sexual differentiation, growth and metabolism, but also in other biological processes (49). Our current knowledge of androgen action is still primarily based on measuring serum levels of these hormones and their metabolites however, the specific intracellular actions of these hormones is less well understood but is likely to be of critical importance to their biological significance. Studies on rhesus monkeys demonstrated widespread tissue distribution of the steroidogenic enzymes, 3β -HSD, 17β -HSD, steroid sulfatase, 5α -reductase and aromatase, suggesting that all that tissue, 114 out of 132 sites studied, could possibly form biologically active sex steroids (50). Therefore, this could indicate that the active androgens and estrogens synthesised in peripheral tissues could exert their activity in the cells of origin, without diffusing into the circulation (48).

1.1.9 Ovarian and adrenal androgens in adolescent girls

Before adrenarche, circulating levels of androgens are similar in male and female children. During puberty, plasma levels of DHEA and DHEAS reach adult levels first, followed by A4 and T (43,51). The pattern of increase in DHEA and DHEAS is comparable in boys and girls, and coincides with the development of the zona reticularis in the adrenal glands however, this is not mirrored by an increase in ACTH (51).

1.1.10 Reproduction in sheep

Sheep are seasonal breeders as their HPO axis, and thus reproductive function, is controlled by the hours of light to which the ewe is exposed. As pregnancy in sheep lasts on average 147 days, fertility has evolved to ensure that lambs are born in the spring, when warmer weather and ample access to food safeguard lamb survival and growth (52). Prolonged melatonin secretion from pineal gland during the hours of darkness, directly signals to the hypothalamus and activates the HPO axis. Thus, in temperate zones, in autumn, when daylight to darkness ratio decreases, the hypothalamic GnRH pulses are activated and estrus cycle commence, while in springtime, as nights becoming shorter, secretion of melatonin decreases, estrus cycling ends, and the ewes enter anestrus.

Reproductive cyclicity in sheep and other non-primate mammals, is termed the estrus cycle. The estrus cycle of the ewe is fundamentally analogous to the ovarian cycles of women, with the comparable neuroendocrine mechanisms controlling both cycles, however, there are some differences (52). In the estrus cycle menstruation does not occur, and cycle consists of four different stages, estrus, metaestrus, di-estrus and pro-estrus (53). In ewes, the estrus cycle lasts usually 17 days, with short follicular phase, taking 2-3 days, and pro-longed luteal phase lasting approximately 15 days, although environmental stressors, such as poor nutrition and severe weather, may disrupt cycle regularity (54,55). Estrus, is a period of 24-36 hours, in which the ewe is receptive to the ram. Preovulatory LH surge occurs at the start of estrus, so that ovulation occurs, on average, 24–30 hours after the onset of estrus behaviour (53). Luteal phase consists of metaestrus, with the formation of the corpus luteum and increase in progesterone levels, di-estrus in which progesterone reaches peak levels and pro-estrus, when the corpus luteum regresses and progesterone levels decline (53). In the estrus cycle, tonic LH secretion in pulsatile manner occurs throughout the cycle, regulated by the negative feedback actions of ovarian hormones, and the LH surge is triggered by high circulating concentrations of estradiol, which induces ovulation and formation of the corpus luteum. FSH concentrations decrease at the beginning of the follicular phase, and increase together with LH surge. After

ovulation, FSH level, analogous to LH concentration, decline again however, unlike LH, FSH increases again, 20–28 hours after the LH surge, followed by a sharp drop (53). A gradual rise in FSH concentration is frequently observed between fourth and sixth day of the luteal phase, which correlates with waves of antral follicle development, as unlike in women, the corpus luteum does not produce estradiol and inhibin A, and therefore FSH is not suppressed and follicular development can occur in the luteal phase (53).

1.1.11 Regulation of pubertal transition in sheep

At birth, the lambs are well developed and have similar birth weight to newborn humans, on average 3.5-4.5 kg, depending on the breed (56), however, lambs grow much more rapidly. By 30 weeks of age lambs can increase their birthweight up to ten times, while human infants only double their birthweight (56,57). Like in other organisms, sufficient growth is necessary to gain reproductive function therefore, sheep, due to their fast growth, enter puberty on average between 6 and 12 months. In the developing sheep there is strong correlation between weight with GnRH and LH pulsatility, which could indicate a potential role of adipose tissue and leptin in regulating timing of puberty (57). It was demonstrated that leptin can stimulate LH secretion in prepubertal males, but not females, indicating potential sex differences in factors controlling timing of the pubertal increase in GnRH secretion (58,59). However, it seems that one of the most important factors contributing to pubertal transition in female sheep is sensitivity to photoperiod and action of melatonin, as lambs can enter puberty only during breeding season, regardless of the month of birth, with the exception of females born in the autumn.

1.2 Role of adipose tissue in metabolism

White adipose tissue (WAT) is a specialised loose connective tissue, consisting of several distinct anatomical depots (60). WAT has mainly been considered as an energy storage depot, thermal insulator, and mechanical cushion however, it is now recognised as an endocrine organ (61). The mass of adipose tissue in humans is highly variable, ranging from 5% to 60% of total body weight (62) and is influenced by many factors, including sex and hormones, age, diet, physical activity level, and drugs (61). Subcutaneous adipose tissues (SAT), an adipose tissue layer found between the dermis and the aponeuroses and fasciae of the muscles, includes abdominal, gluteal and femoral compartments, and stores approximately 80% of total body fat in the body (63). Conversely, visceral adipose tissue (VAT), which is associated with internal organs, and include omental, mesenteric and retroperitoneal fat, represent 10–20% of total body fat in men, and 5–10% in women (63). There are also smaller depots of adipose tissue surrounding heart (epi/pericardial) and kidneys (perirenal), as well as intermuscular fat (60). In other large mammals, such as sheep, the location and relative size of these principal depots are comparable.

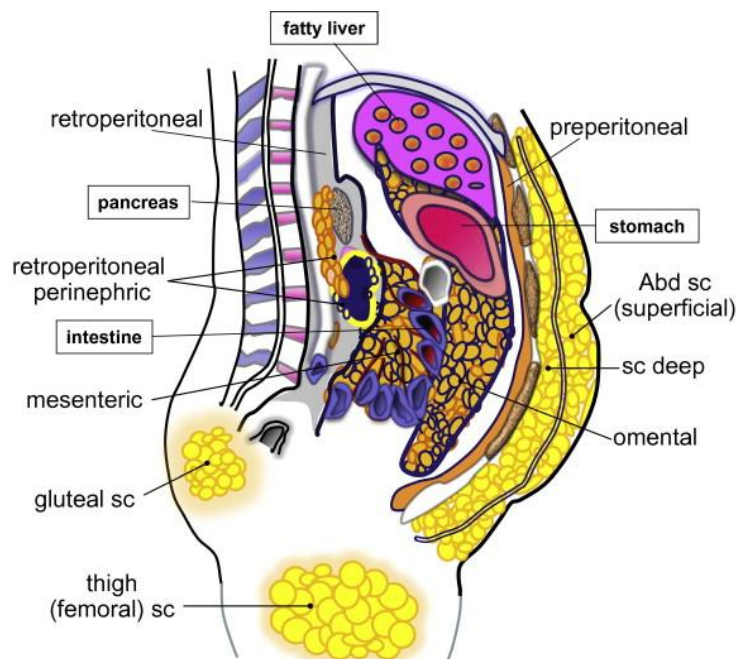


Figure 1.4 Major white adipose tissue depots in humans. Subcutaneous adipose tissue (sc) include abdominal, gluteal and femoral depots. Visceral adipose tissue is associated with internal organs, including stomach (omental), intestine (mesenteric), perinephric (kidneys) and retroperitoneal fat in retroperitoneal compartment.

Taken from Lee *et al.* (62)

WAT is a heterogeneous organ, consisting of adipocytes, macrophages, fibroblasts, stromal cells, monocytes and preadipocytes, with an estimated 1–2 million adipocytes and 4–6 million other cells, per gram of WAT (62). Adipocytes constitute approximately 90% of the WAT volume, due to their relatively large cell size, ranging from 20 to 200 μm , in which 95% of the cell volume is occupied by a unilocular lipid droplet (62). There are some sex dependent differences in adipocyte size. Women tend to have smaller adipocytes in VAT than in SAT, while in men and extremely obese individuals, adipocyte size is comparable in both adipose depots. In addition, there is higher number of preadipocytes in SAT, as compared with VAT (64).

1.2.1 Adipocyte development and growth

In humans, preadipocyte differentiation into adipocytes occurs between the 14th and the 16th weeks of gestation (65), likewise in sheep it ensues in third month of gestation (66). In rodents, however, majority of adipose tissue is formed after birth (67). In humans, adipocyte proliferation tends to decrease in late gestation, and adiposity is increased primarily by filling of predetermined adipocytes until puberty, after which another intensified proliferation of adipocytes occurs (68). Therefore, the adolescent period sets the total number of adipocytes that the individual will have as an adult, although, the differentiation potential of preadipocytes into mature adipocytes is present throughout life, and depends on the body energy status and the storage needs. However, in adult life, the capacity of preadipocytes to become fully functional mature adipocytes declines (69,70). There is a constant turnover of adipocytes, with an estimated 8% of adipocytes per year in humans, and 0.6% per day in mice, being replaced (68). This stage of accelerated adipocyte proliferation in adolescence is paralleled by higher expression of peroxisome proliferator activated receptor gamma (PPARG), the master regulator of adipogenesis (71). It has been demonstrated, that diminished expression of PPARG results in reduced mitochondrial function and accumulation of lipids in nonadipose tissues, due to the decreased storage capacity of WAT, which consequently leads to lipotoxicity and metabolic perturbations (72,73). Therefore, inability of an individual to increase adipose cell number results in the development of hypertrophic adipocytes, which might increase risk of metabolic diseases (74).

1.2.2 Lipolysis and triglyceride formation

The main role of WAT is to store free fatty acids (FFA) in form of triglycerides (TG) during times of energy abundance and to release them back during periods of energy shortage, by the integration of several biochemical pathways. In adipocytes, TG are synthesised from esterification of FFA, which are mainly delivered through breakdown of circulating TG through lipoprotein lipase (LPL), although the direct uptake of circulating FFA also contributes (62). Lipolysis is defined as hydrolysis of TG into FFA and glycerol. Adipose triglyceride lipase (ATGL), hydrolyses TG into diacylglycerol and fatty acids, which are further broken down to FFA and glycerol by hormone sensitive lipase (HSL) and monoglyceride lipase (MGL) (73). Lipolysis occurs during fasting, under the control of glucagon and catecholamines, which stimulate various lipases in adipocytes, resulting in secretion of FFA from the adipocyte to the circulation. FFA are then bound to albumin and are transported to muscle, liver, heart and other tissues for their oxidation or re-esterification (75). In the fed state, increased insulin concentrations inhibit lipolytic enzymes, thus decreasing lipid mobilisation from adipose tissue.

1.2.3 WAT as an endocrine organ

WAT has previously been considered as a metabolically inert tissue however, there is now significant evidence that WAT is also a dynamic endocrine organ, regulating metabolism and energy homeostasis, in an endocrine, paracrine and autocrine manner, through the secretion of adipokines (73). Furthermore, as adipose tissue is also involved in additional processes such as steroid metabolism, angiogenesis and the immune response, it is therefore vital that WAT maintains its functionality, which is lost in obesity (73).

The number of identified adipokines is constantly increasing. Leptin, adiponectin, resistin, serpin, retinol binding protein 4 (RBP4), vaspin, visfatin, omentin, apelin, and chemerin are only some of them. In addition, there are number of cytokines and chemokines, that exert inflammatory response and cell migration, including tumour necrosis factor alpha (TNF α) and interleukin 6 (IL6) as well as monocyte-chemoattractant protein 1 (MCP1) however, for the purpose of this thesis only leptin and adiponectin will be reviewed in the section below.

1.2.3.1 Leptin

In 1994 the first adipocyte-secreted protein was identified by Friedman and colleagues and was named leptin, from the Greek word leptos, meaning thin (76). Leptin, is a protein coded by *LEP (OB)* gene and is considered a metabolic signal of energy sufficiency (76,77). Leptin is secreted mainly by white adipose tissue, and its expression and concentration directly reflects the volume of body fat, and thus the amount of energy stored (78), however, it can also indicate acute changes in caloric intake (79). Leptin acts on the central nervous system to adjust food intake, through activation of anorexigenic (appetite-diminishing) and orexigenic (appetite-stimulating) neuropeptides, according to the needs of the body (77). In addition, there is some evidence showing that in mice, leptin can regulate energy expenditure, through elevating sympathetic nerve activity (80) and activation of thermogenesis in brown adipose tissue (81). Leptin also plays a critical function as neuroendocrine integrator linking the magnitude of body energy stores with the reproductive system. Leptin is an vital factor in the metabolic control of puberty and fertility, having a stimulatory/permissive effect on the hypothalamic-pituitary-gonadal (HPG) axis (82,83). Moreover, the presence of leptin receptors on ovarian theca and granulosa cells has been documented, however, in contrary to the role of leptin on the HPG axis, there is evidence showing that leptin can have an inhibitory effect on ovarian steroidogenesis (84,85) and act as inhibitor of ovarian follicle development (86).

Leptin induces its effects by binding to specific leptin receptors (LEPR) expressed in the brain and in peripheral tissues, including liver, skeletal muscle, pancreas, kidney, heart, adrenal glands, ovaries and testes (87). Alternative splicing generates several isoforms of LEPR. The long LEPR isoform mediates complete signal transduction initiated by leptin, and it is associated with energy homeostasis and neuroendocrine function, while the short LEPR isoform is thought to play an important role in transporting leptin across the blood–brain-barrier (77). Downstream of the LEPR, leptin activates numerous signal transduction pathways, including Janus kinase signal transducer and activator of transcription 3 (JAK-STAT3), which is important for regulation of energy homeostasis (88), and phosphatidylinositol 3-kinase (PI3K), which is important in regulation appetite and glucose homeostasis (89). Leptin deficiency or resistance, resulting from *LEP* or *LEPR* gene mutation, results in severe obesity in humans and transgenic animals (90,91). Leptin replacement therapy, in patients with leptin deficiency, causes reduced food intake and enhanced response to satiety signals (92), which consequently results in decreased body weight (93). Likewise, lipodystrophy is associated with hypoleptinemia, thus leptin treatment in patients with lipodystrophy has been shown to decrease insulin resistance and hyperlipidemia, and to

reverse hepatic steatosis (94,95). Interestingly, in women with lipoatrophy and features of the PCOS, leptin treatment restored menstrual cycles, decreased T, and increased SHBG levels (96). However, majority of obese humans have high levels of circulating leptin, which reflect increased levels of adiposity, but are leptin resistant (78). The proposed mechanism underlying leptin resistance include defects in downstream signalling of LEPR in hypothalamus or changes in the leptin transport across the blood–brain barrier (97).

1.3.2.2 Adiponectin

Adiponectin was first identified by Scherer and colleagues in 1995, as an adipocyte secretory protein (98) however, since it was discovered independently by several laboratories at around the same time, it has few different names such as, adipocyte related complement protein (Acrp30), adipose most abundant gene transcript 1 (apM1), adipose-specific gene (ADIPOQ), and gelatin-binding protein of 28 kDa (GBP28) (99).

Adiponectin is the protein product of the *ADIPOQ* gene transcript, and is secreted exclusively from adipose tissue, in the form of a trimer as the low-molecular-weight (LMW) form, a combination of two trimers as a middle-molecular-weight (MMW) form, or as six trimers as a high-molecular-weight (HMW) form. Adiponectin is one of the most abundantly secreted adipokines, constituting 0.05% of the total serum proteins, and circulates either as a trimer or an oligomer. Adiponectin mediates its effects through two receptors ADIPOR1 and ADIPOR2 (100). Downstream of its receptors, adiponectin stimulates the phosphorylation and subsequent activation of adenosine monophosphate activated protein kinase (AMPK) and peroxisome proliferators activated receptors (PPARs), thereby regulating both glucose and lipid metabolism, in skeletal muscle and the liver (100). ADIPOR1 is highly expressed in skeletal muscle, while ADIPOR2 is particularly abundant in liver. Expression of adipocyte receptors in insulin target organs, is upregulated during fasting and suppressed during postprandial states.

Adiponectin is an insulin sensitising adipokine. Levels of mRNA and circulating adiponectin are significantly decreased in obese and lipodystrophic humans, as well as in animal models of obesity and type 2 diabetes mellitus (T2DM) (101,102). Administration of recombinant adiponectin restores insulin sensitivity, decreases levels of glucose, FFA, TG, and reduces body weight (103-105). Studies demonstrated that adiponectin decreases insulin resistance by reducing TG content in muscle and liver, through increasing FFA oxidation and energy dissipation. In addition, adiponectin has been shown to suppress gluconeogenesis in liver (106) and increase glucose uptake in muscle and adipose tissue (107,108). Therefore, it has been

postulated that decreased adiponectin level contribute to the development of insulin resistance, metabolic syndrome, T2DM and atherosclerosis (99,109).

A role for adiponectin in reproduction has also been investigated. Both adiponectin receptors were detected in human pituitary and hypothalamus neurons (110,111), suggesting potential impact of this adipokine on the central reproductive endocrine axis. Adiponectin has been shown to acutely reduce basal and GnRH-stimulated LH secretion through increased phosphorylation of AMPK, with no impact on FSH levels (112), therefore, low levels of adiponectin can lead to increased LH concentrations. Adiponectin receptors have been also detected in ovarian granulosa and theca cells (113,114), and it was found that adiponectin reduced steroidogenesis in theca cells. Conversely, testosterone has been shown to selectively reduce adiponectin levels by inhibiting its secretion from adipocytes (115) and a negative correlation between circulating adiponectin and testosterone has been reported (116), which might indicate a potential role of adiponectin in the pathophysiology of PCOS.

1.2.4 Adipose tissue depot differences between SAT and VAT

There is strong evidence showing differences between SAT and VAT biology, including adipokine secretion and rates of lipolysis and TG synthesis (117). Two mechanisms have been proposed to explain this phenomenon, which are not mutually exclusive. Firstly, differences resulting from distinctive innervation and links with the circulatory system, such as, the direct venous drainage of VAT into the portal circulation, resulting in hepatic exposure to by-products of fat metabolism and adipokines. Secondly, the cell-autonomous depot-specific differences in adipocyte physiology, such as distinct gene expression in VAT and SAT preadipocytes, even after isolation and prolonged passage under identical conditions (68,118). Further, experimental studies demonstrated that transplantation of VAT into a subcutaneous position has minor effects while, transplanting SAT to the visceral compartment results in overall reduced adiposity and improvement in glucose homeostasis (119). It has been demonstrated that adipocytes in the VAT depot exhibit increased lipolysis when stimulated with adrenergic agonists, mainly due to decreased expression of antilipolytic $\alpha 2$ -adrenergic receptors (ADR) and increased expression of lipolytic $\beta 3$ -ADR. In addition, there is evidence showing that adipocytes in VAT are less sensitive to the antilipolytic effects of insulin therefore, in the states of increased circulating insulin, the contribution of VAT-derived FFA may become more significant, up to 40%. In addition, it has been demonstrated that, FFA release from VAT to the hepatic portal vein is paralleled by increasing VAT, thus, individuals with central (visceral) obesity are more likely to have altered hepatic function (120). On the contrary, VAT is not significant contributor of FFA in the systemic peripheral circulation as

studies show that only 6% to 13% of total FFA in circulation originate from VAT. In addition, some studies demonstrated that in VAT macrophages are more prevalent and the production of proinflammatory cytokines is higher, therefore, this could also contribute to hepatic pathology in obesity, although these results are not consistent (121,122). These results indicate that there are intrinsic differences between depots and also imply that subcutaneous fat may have beneficial effects on metabolism.

1.2.5 Central obesity

Central obesity, so called apple or android fat distribution, refers mainly to increased visceral adiposity, however, it also includes fat accumulation in abdominal SAT, is considered a significant risk for metabolic complications (123,124). In contrast preferential fat accumulation in the gluteofemoral region and leg, namely pear-shaped or gynoid fat distribution, is believed to be associated with lower risk, or as some authors suggested, it may be protective. Therefore, it has been proposed that calculating waist-to-hip ratio (WHR) is a better determinant than body weight in estimating a risk for developing metabolic complications in obese individuals.

1.2.6 Obesity and WAT

Obesity is characterised by increased storage of FFA and subsequent expansion of adipose tissue, mainly through hypertrophy. It has been demonstrated that, in times of energy excess, adipose cells expand first by hypertrophy until they reach a critical threshold of 0.7–0.8 $\mu\text{g}/\text{cell}$, after which signals are secreted that induce the proliferation and/or differentiation of preadipocytes (125). Overfeeding for several months caused increase in cell size but not cell number (126), however, a study by Tchoukalova *et al.* reported that overnutrition induces hypertrophy in upper-body SAT but hyperplasia in depots below the waist (127). Nevertheless, once adipocytes are gained, they are hard to lose, as even significant weight loss is associated with a reduction in adipocyte volume, but not number (128). Increase in fat mass is accompanied by changes in blood flow and hypoxia of the adipose tissue, with activation of the hypoxia-inducible factor 1 alpha (HIF1 α), which in turn, may lead to metabolic dysfunction (129). When the expansion capacity is saturated, either due to decreased expandability of adipose cells, decreased recruitment of fat cell progenitors or augmented differentiation to new adipocytes, adipose cells start to release their lipid content. This starts an inflammatory process, with increased macrophage infiltration and pro-inflammatory cytokine production, such TNF α and IL6 as well as MCP1 (130). Conversely, elevated MCP1, can promote the recruitment of circulating monocytes, while upregulated expression of TNF α

and IL6 can impair insulin signalling and FFA oxidation in hepatocytes, skeletal muscles and adipose tissue (131). Histologically, macrophages can be observed as crown-like structures surrounding adipocytes, with tendency to cluster around dead or dying adipocytes, which underlie their irregular distribution in the WAT (68). Furthermore, this pathological process deregulates secretion of adipokines, such as leptin and adiponectin, which leads to further increased caloric consumption and reduced energy expenditure as well as decreased insulin sensitivity in peripheral tissue and ectopic lipid accumulation. Figure 1.5 summarizes pathological changes in WAT resulting from expansion of adipose tissue in obesity.

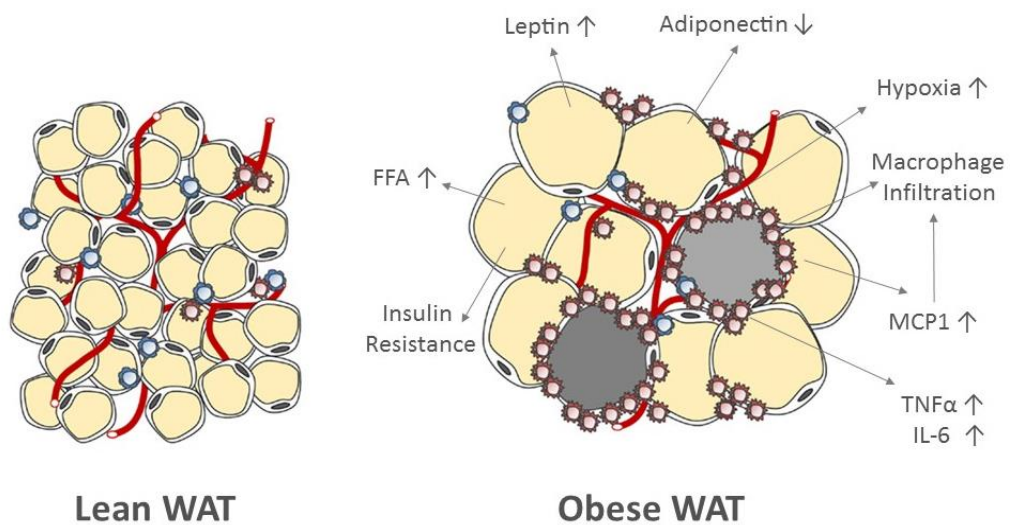


Figure 1.5 Pathological obesity-induced changes in white adipose tissue resulting in enhanced production of pro-inflammatory cytokines and macrophage infiltration, increased release of free fatty acids, altered secretion of adipokines and insulin resistance. On the systemic level, dysregulated adipokine secretion may lead to increased food intake, decreased energy expenditure and reduced insulin sensitivity as well as ectopic lipid deposition and inflammation.

Adapted from Choe *et al.* (132)

1.2.7 Role of brown adipose tissue in energy homeostasis

Brown adipose tissue (BAT), discovered recently in adult humans, is a highly vascularised oxidative tissue containing multilocular fat cells with abundant mitochondria. Myogenic factor 5 (Myf5) positive cells are common progenitors for brown adipocytes and myocytes in skeletal muscle (133). In humans BAT is mostly localised to the supraclavicular and neck regions (134). It is specialised in heat production and energy expenditure through the capacity of brown adipocytes to dissipate energy from glucose and lipids via uncoupling protein 1 (UCP1) (135). Therefore, BAT might play a role in protecting against obesity and obesity-associated metabolic alterations, since reduced BAT activity in obesity was reported (136). Recently an endocrine role of BAT was also put forward, showing that BAT releases factors that can act in autocrine and paracrine manner (135).

There is also growing evidence for presence of cells exhibiting a brown adipocyte thermogenic phenotype (including UCP1 expression), named 'beige' or 'brite' (brown-in-white), in WAT, after thermogenic activation (137). These cells are predominantly present in SAT depots (133). Stimulation of adipocyte receptors such as β 3-ADR and PPARG can induce activation of beige adipocytes within WAT. There are two possible sources of beige adipocytes in WAT, conversion of mature white adipocytes or *de novo* generation from distinct progenitor cells (133). As shown in rodent models, beige adipocyte activation can have protective effects against obesity and improve glucose homeostasis in T2DM (138).

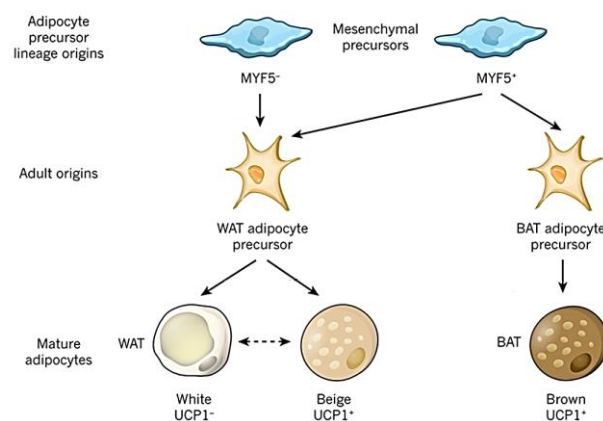


Figure 1.6 Differentiation of white and brown adipocytes. WAT adipocyte precursors derive from both MYF5⁻ and MYF5⁺ mesenchymal precursor cells while BAT adipocyte precursors derive exclusively from MYF5⁺ mesenchymal precursor cells. Beige adipocytes can derive from WAT adipocyte precursors and potentially directly from mature white adipocytes.

Taken from Peirce *et al.* (139)

1.2.8 Adipose tissue and sexual dimorphism

Body fat distribution patterns are sexually dimorphic. In general, women are characterised by a higher body fat percentage than men, with a greater proportion of adipose tissue in gluteal and femoral regions, while men tend to have more adipose tissue accumulated in the abdominal region (140). However, in both sexes, a large accumulation of visceral fat (omental, mesenteric and retroperitoneal) is associated with metabolic syndrome (141). Sex hormones play an important role in the regulation of body fat distribution. However, to fully understand relationship between sex steroids and adipose tissue the role of steroid-converting enzymes needs to be recognized (140). This may be particularly important with regards to androgens, which modulate adipocyte function and affect the size and distribution of adipose tissue (142). An inhibitory effect of testosterone on lipoprotein lipase in adipose tissue was reported, which supports an inhibitory effect of androgens on lipid accumulation. Furthermore, it was described that androgens can inhibit preadipocyte differentiation (142).

In men, low plasma testosterone is linked to abdominal obesity (143). Conversely, androgen treatment in female-to-male transsexuals results in increased visceral fat accumulation and insulin resistance (144). In women increased levels of androgens are thought to be associated with abdominal obesity. This idea is largely based on the observation that hyperandrogenism seen in PCOS patients is often accompanied by abdominal obesity and hyperinsulinemia (145).

Besides the well-known impact of sex hormones on WAT distribution, there is some evidence that there is also sexual dimorphism in distribution and function of BAT. Women have been found to have greater volume of BAT, than men (146,147). Further, studies on rodents demonstrated that, there is sex-specific composition of lipids in BAT (148), mitochondrial function and sensitivity of BAT to adrenergic stimulation (149). Female mice are more responsive to browning of WAT during β -adrenergic stimulation than males (150), and have higher UCP1 expression in BAT (151).

1.3 Clinical features and diagnostic criteria of PCOS

PCOS was first described in 1935 by Irving Stein and Michael Leventhal, in report entitled “Amenorrhea associated with polycystic ovaries”, where the authors described seven patients with enlarged ovaries, detected using radiologic techniques, amenorrhea, sterility, pain, and hirsutism (152). Since then more than 30,000 scientific reports on this topic have been published, and this clinical triad of polycystic ovaries, hyperandrogenism, and oligo/amenorrhea, has been the foundation for diagnostic criteria of PCOS in different guidelines (153).

However, PCOS is a heterogenous syndrome and the clinical presentation of PCOS varies broadly. Polycystic ovaries (PCO) are common findings in patients with PCOS, hence the name of the syndrome. PCO are defined as an ovarian volume of greater than 10 millilitres and/or presence of 12 or more follicles measuring 2–9 mm in diameter in each ovary (154). It is estimated that PCO are present more than 75% of patients with PCOS (155) however, 20% of women in general population also have PCO (156). Menstrual disturbances associated with PCOS include oligomenorrhea, amenorrhea, and prolonged erratic menstrual bleeding, yet nearly one third of patients have a normal menstrual cycle (157). Increased androgen plasma concentrations (hyperandrogenaemia), and its clinical manifestation (hyperandrogenism) of hirsutism and/or acne is another common presentation in PCOS. In the large study of patients presenting with clinically evident androgen excess, it was found that 82% had PCOS (158). Excess hair growth is reported in 50-70% of PCOS women (158-160), while acne and alopecia are less prevalent, with 15-30%, and 22%, respectively of adult women affected (158,161,162). Further, 40-60% women with PCOS have elevated LH levels (163,164). Infertility is also a common complication in patients with PCOS. PCOS is considered most frequent cause of anovulatory infertility and it accounts for 90% of patients attending infertility clinics with anovulation, yet 60% of women with PCOS are fertile (165).

The diagnosis of PCOS requires the exclusion of other ovarian, pituitary and adrenal causes of androgen excess in reproductive-age women. Until now three different diagnostic criteria have been proposed, as summarised in Table 1. In 1990, the National Institutes of Health (NIH) established definition of the disorder and diagnostic criteria, which advised that clinical or biochemical presence of hyperandrogenism (HA) and chronic oligo-anovulation (OA) were needed to diagnose PCOS (166). In 2003, during a consensus workshop in Rotterdam, new diagnostic criteria were proposed by the European Society for Human Reproduction and Embryology/American Society for Reproductive Medicine (ESHRE/ASRM), which included,

in addition to previous guidelines, presence of polycystic ovaries on ultrasound, as a diagnostic criterion for the syndrome (154). Expansion of PCOS classification, to include women who either had PCO in combination with HA and/or OA, resulted in a significant increase in the number of patients diagnosed with PCOS, and extended the heterogeneity of PCOS phenotypes as compared with the NIH guidelines (167). Recently, a novel phenotypic approach to classifying PCOS has been introduced by a panel of specialists during the NIH Evidence-based Methodology Workshop, recommending use of the following phenotype classification: phenotype A: HA+OA+PCO; phenotype B: HA+OA; phenotype C: HA+PCO; and phenotype D: OA+PCO, with phenotypes A and B being the highest risk for metabolic dysfunction (168-170). Finally, in 2006, The Androgen Excess Society (AES) issued new recommendations, which stated that PCOS should be primarily considered a disorder of androgen excess and that diagnosis of PCOS should be based on the presence of clinical or biochemical HA in combination with OA and/or PCO, therefore excluding a non-hyperandrogenic phenotype, which was proposed in the 2003 Rotterdam criteria (155). The rationale for proposing these new criteria was based on the that evidence that HA seemed to be the most robust determinant of the PCOS pathophysiology and a central factor contributing to the associated metabolic dysfunction (167,171). Interestingly, some studies demonstrated that with age, women with PCOS, may regain menstrual cyclicality (172) and present with decrease in ovarian volume and number of follicles (173,174) however, their androgen levels remain elevated when compared with age matched controls (175).

NIH 1990	ESHRE/ASRM 2003	AES 2006	NIH 2012
Exclusion of other ovarian, pituitary and adrenal causes of androgen excess in reproductive-age women			
All criteria required	Two of three criteria required	All criteria required	Identification of different PCOS phenotypes
HA OA	HA OA PCO	HA OA and/or PCO	A: HA+OA+PCO B: HA+OA C: HA+PCO D: OA+PCO

Table 1.1 Criteria for diagnosis of PCOS according to different guidelines. HA: hyperandrogenism, OA: oligo-anovulation, PCO: polycystic ovaries. Adapted from Lizneva *et al.* 2016 (167).

1.3.1 Clinical features and diagnostic criteria of PCOS in adolescent girls

In general, the diagnostic criteria for PCOS in adolescent girls follows the guidelines outlined for adult women however, hormonal and reproductive differences associated with pubertal transition need to be taken into consideration. Irregular menstrual cycles are frequent in adolescent girls, with up to 85% anovulatory cycles during the first year after menarche (176). PCO is also very common, with up to 40% of the adolescent girls demonstrating PCO morphology two years after menarche as documented in ultrasonographic studies (177). Premature pubarche, the appearance of sexual hair before the age of 8 years in girls, is considered a potential predictor of PCOS in future life, as it has been demonstrated that girls with premature pubarche have a risk of developing PCOS (178). In turn, premature pubarche is a sign of premature adrenarche and increased adrenal androgens, which might be the first manifestation of steroidogenic dysregulation in girls with PCOS (179-181). HA has been found to be the strongest predictor of PCOS in adolescent girls (176). That is why, all three diagnostic criteria (HA+OA+PCO) should be present in adolescent girls to identify PCOS, with OA present for at least 2 years after menarche, according the ESHRE/ASRM consensus from 2010 (160).

1.3.2 Prevalence of PCOS

PCOS is the most common endocrine disorder among women of reproductive age (182). The global prevalence of PCOS and its different phenotypes varies greatly based on geographical location, ethnicity and diagnostic criteria used with worldwide occurrence ranging from 4% to 21% (182). Depending on diagnostic criteria applied, the prevalence oscillates between 5% to 10% with NIH 1990 guidelines; from 10% to 15% according to the AES 2006 recommendations, and from 6% to 21% with ESHRE/ASRM 2003 criteria (167). Higher prevalence of PCOS with the ESHRE/ASRM 2003 and AES 2006 criteria can be mainly attributed to their broader definition with inclusion of additional phenotypes. The prevalence of specific phenotype among women with PCOS was recently evaluated, with phenotype A (HA+OA+PCO) accounting for 66%, phenotype B (HA+OA) for 13%, phenotype C (HA+PCO) for 11% and phenotype D (OA+PCO) for 9% (167). The estimated prevalence of PCOS in adolescent girls varies between 0.81-5% however, it is likely to be underdiagnosed in this population (183-186).

1.3.3 Metabolic characteristics of adult women with PCOS

1.3.3.1 Insulin resistance

PCOS is clearly a reproductive disorder however, it seems that metabolic comorbidities associated with the syndrome have more pronounced implications across the lifespan and pose a significant health and economic burden. It was estimated that 40% of total PCOS health care costs were attributed to diabetes associated with the syndrome (187). Although not diagnostic criteria, insulin resistance (IR) and associated hyperinsulinemia are the most common metabolic complications in PCOS. Insulin resistance is defined as pathological state, in which there is diminished cellular response to the insulin, and as a consequence, an increased amount of insulin is required to stimulate the biological response (188). Increased insulin secretion by pancreatic β -cells is the physiological compensatory mechanism and as long as hyperinsulinemia overcomes insulin resistance, glucose levels remain normal. However, when ability of β -cells to secrete insulin deteriorates, relative or absolute insulin insufficiency develops, with impaired glucose tolerance (IGT) and T2DM (188). Women with PCOS have increased frequency of IR than age- and body mass index (BMI)-matched controls, and obesity has disproportionately greater impact on IR in PCOS than in general population (189). In a recent meta-analysis of 28 published euglycemic–hyperinsulinemic clamp studies, it was found, that women with PCOS have 27% worse insulin sensitivity than controls, independent of BMI, age or diagnostic criteria (189). It is estimated that 50-70% of PCOS patients are IR (190) however, a recent cross-sectional study reported that 75% of lean and 95% of overweight women with PCOS had decreased insulin sensitivity (191). IR is more pronounced in the classic PCOS phenotypes, phenotype A and B, compared with PCOS patients who have either normal androgen levels or regular menstrual cycles (189). It has been suggested that PCOS patients manifest intrinsic insulin hypersecretion, elevated β -cell function together with decreased insulin clearance and insulin signalling abnormalities, which in consequence lead to IR, which is further exacerbated by increased body weight and adiposity (192-195). IR and hyperinsulinemia are the key pathophysiological features of PCOS contributing to reproductive, endocrine and metabolic disturbances.

1.3.3.2 Type 2 diabetes mellitus

T2DM is a metabolic disorder characterised by hyperglycaemia and a distorted lipid profile caused by pancreatic β cells being unable to secrete adequate insulin to overcome insulin resistance. In turn, chronic hyperglycaemia and hyperlipidaemia, through glucotoxic and lipotoxic mechanisms, including rough endoplasmic reticulum (RER) stress, accelerate β -cell failure, which might result in the need for insulin therapy (196). T2DM is a significant risk

factor for heart disease and stroke, end-stage renal failure, non-traumatic lower-limb amputations, and is the leading cause of blindness among adults aged 20–74 years (196).

Women with PCOS are at increased risk of developing T2DM and have higher conversion rate from IGT to T2DM than general female population (197,198). PCOS has been identified as a significant non-modifiable risk factor for T2DM by the International Diabetes Federation (199). Legro *et al.* estimated that PCOS patients contribute to 20% of IGT and 40% of T2DM cases in reproductive-aged women in US (200). Moreover, women with PCOS are at increased risk of developing gestational diabetes mellitus (GDM) (201,202). A large prospective cohort study documented a remarkably high incidence (22%) of GDM in PCOS women (203), compared to 7% in general female population (204). GDM, in turn, is a significant lifetime risk for developing T2DM, with 35% - 60% of women with GDM progressing to T2DM within 10 years postpartum (205,206)

1.3.3.3 Obesity

Epidemiological studies provide a clear evidence for the close link between PCOS and obesity, showing that 38%–88% women with PCOS are overweight or obese (207), and conversely, that the prevalence of PCOS is high in unselected obese female population, with up to 28% of all cases (208,209). Therefore, considering the high prevalence of obesity in PCOS, some authors postulated that women with PCOS might have a unique predisposition to obesity, and that these women might face additional barriers to effective weight management (210). Indeed, decreased basal metabolic rate (BMR) (211) and reduced postprandial thermogenesis (212) have been reported in women with PCOS. However, as not every obese woman develops PCOS, it should be noted that, obesity does not cause PCOS but rather exacerbates its symptoms. It has been demonstrated that obesity can further increase prevalence of irregular menstrual cycles, amplify androgen concentrations and elevate risk for pregnancy complications (213). Obesity is also linked to a reduced response to infertility treatment (213). Conversely, even modest weight loss in obese PCOS women can significantly improve reproductive and metabolic characteristics of the syndrome (207).

1.3.3.4 Adipose tissue dysfunction

Numerous studies demonstrated that there is a strong relationship between fat mass and the severity of PCOS phenotype however, the mechanisms underlying this association are not completely understood. Increased abdominal (visceral) adiposity is thought to be correlated with adverse metabolic profile, mainly due to its proximity to hepatic portal vein, and thus direct effects of FFA and cytokines released from this depot on liver, while subcutaneous adipose tissue is believed to be inert, or even protective (214,215). Previous studies indicated that overweight/obese women with PCOS have increased abdominal adiposity when compared with BMI-matched controls (216,217). This hypothesis has gained wide acceptance, as it explained increased frequency of metabolic disturbances in women with PCOS, as compared with women in general population (218). However, more recent studies, using magnetic resonance imaging (MRI) techniques, has challenged this assumption, showing that there is no difference in adipose tissue distribution between PCOS and BMI-matched controls (219). Moreover, Barber and colleagues demonstrated that women with PCOS remained more insulin resistant than control women, thus indicating that increased insulin resistance in PCOS women is unlikely to emerge from increased visceral adiposity (219). Interestingly, in a study by Dolfing *et al.*, again employing MRI imaging, it was found that lean PCOS women had less visceral fat than the control women (220), while Horejsi *et al.* reported that young, lean PCOS patients had significantly decreased SAT volume, especially on the legs, when compared with age- and BMI- matched controls (145). Moreover, there is evidence showing link between partial lipodystrophy and PCOS (221-226). Lipodystrophy is a clinical disorder characterised by adipocyte malfunction, resulting in maldistribution of body fat, with a partial lack of adipose tissue (lipoatrophy) in certain body areas, with excess of adipose tissue (lipohypertrophy) elsewhere, with resulting hyperinsulinemia, insulin resistance, and abnormalities of glucose homeostasis (222). Therefore, aforementioned evidence might indicate potential role of the intrinsic adipocyte dysfunction in the development of PCOS.

Indeed, there are increasing numbers of reports showing that women with PCOS have adipose tissue dysfunction, independent of obesity. Insulin and androgens, both main culprits in PCOS, affect adipose tissue function, however, insulin and androgens have opposing regulatory effects on the differentiation of preadipocytes to adipocytes. There is evidence that insulin stimulate adipogenesis (227), while androgens inhibit preadipocyte differentiation (228), thus hormonal and metabolic derangements are likely to play an important role in adipose tissue function in PCOS. Wang *et al.* documented that in subcutaneous adipocytes from PCOS patients, expression of testosterone synthesising enzymes was higher, while expression of aromatase was decreased, suggesting increased local androgen action (229). It has been

reported, that adipocytes in SAT of women with PCOS are hypertrophic (230). Conversely, adipocyte hypertrophy is strongly associated with insulin resistance and increased inflammation. Furthermore, a decrease in hormone-sensitive lipase expression and activity and catecholamine-induced lipolysis in SAT, and an increase in the VAT, in PCOS women, was also reported (231,232), which might partially elucidate adipocyte hypertrophy in the SAT depot. Moreover, an increase in the expression of CD36, a FFA transporter, in adipocytes from women with PCOS, was also described (233). In addition, PCOS women were found to have decreased adiponectin levels, independent of BMI, which can further contribute to metabolic perturbations in those females, considering the insulin sensitising properties of adiponectin (230,234-236). There is evidence showing that adiponectin can suppress theca cell androgen synthesis, and therefore decreased levels of adiponectin in PCOS may contribute to enhanced ovarian androgen production (237). In PCOS, there is also evidence of a low-grade chronic inflammation of adipose tissue, with increased secretion of pro-inflammatory mediators, such as TNF α and IL6, which might be a consequence of adipocyte hypertrophy (238). These inflammatory cytokines can in turn exacerbate the metabolic and ovarian dysfunctions of the syndrome, such as insulin resistance, T2DM, cardiovascular disease (CVD), hyperandrogenism and disordered ovarian cyclicity (238).

1.3.3.5 Metabolic syndrome

Metabolic syndrome (MetS), also known as syndrome X, the insulin resistance syndrome, and the deadly quartet, is a cluster of metabolic abnormalities, which occur together more often than by chance alone. They include insulin resistance, (central) obesity, dyslipidaemia, and hypertension, and are well documented risk factors for both T2DM and CVD (239). In fact, MetS poses a 5-fold increased risk for developing T2DM and a 2-fold risk for CVD (240). There are different definitions of MetS, however, these definitions agree on the main components of the syndrome, glucose intolerance, obesity, hypertension, and dyslipidaemia (239). Insulin resistance is accepted as the central factor in the pathophysiology of MetS (239). It leads to decreased suppression of lipolysis in WAT and therefore, elevated FFA in circulation. Conversely, a major contributor to the development of IR is an excess of circulating FFA, which alter the downstream signalling of insulin in peripheral tissue, with decreased glucose uptake in skeletal muscle and WAT (239), and impair a pancreatic β -cell function (241). In addition, with increased FFA flux to the liver, there is amplified production of triglycerides, and apoB-containing triglyceride-rich very low density lipoproteins (VLDL), resulting in dyslipidaemia and non-alcoholic fatty liver disease (NAFLD) (239).

MetS is common in reproductive-age women with PCOS, with an estimated prevalence of 35-45% (242-246) compared to 6% in females age 20–29, and 15% in females age 30–39, in the general population (247). Therefore, it has been suggested that PCOS is an ovarian manifestation of MetS, and that the name ‘PCOS’ should be changed to ‘female metabolic syndrome’ or ‘syndrome XX’, to mirror its strong link with cardio-metabolic abnormalities (248). Interestingly, hyperandrogenic sisters of women with PCOS, and women with increased androgens, but no PCOS, also have an increased prevalence of MetS (249,250). The prevalence of MetS was twofold higher in the PCOS population with hyperandrogenism compared with PCOS with normal androgen levels and control groups, supporting hypothesis that androgens may play a role in the adverse metabolic profile seen in PCOS (251). Indeed, free testosterone and fasting insulin levels were found to be strong predictors of MetS in women with PCOS (245,246) supporting the common aetiological role of insulin resistance in both PCOS and the metabolic syndrome.

1.3.3.6 Non-alcoholic fatty liver disease

NAFLD is the most common chronic liver disorder in Western countries, with estimated prevalence of 20-30% in general population (252). NAFLD is often considered the hepatic manifestation of MetS, with incidence as high as 75-95% in the morbidly obese population (253-255). NAFLD refers to the accumulation of fat in the liver of subjects who drink little or no alcohol, and comprises of spectrum of hepatic manifestations, ranging from simple hepatic steatosis to non-alcoholic steatohepatitis (NASH), associated with hepatic inflammation and fibrosis (252). An increased incidence of NAFLD and NASH in women with PCOS was reported, with an estimated 39-69% of women affected, independent of BMI, depending on ethnicity and diagnostic criteria used (256,257). PCOS and NAFLD have common risk factors, including insulin resistance and obesity however, the increased prevalence of NAFLD in PCOS patients, especially lean ones, is not fully understood.

1.3.3.7 Dyslipidaemia

Dyslipidaemia is a spectrum of qualitative lipid abnormalities reflecting perturbations in the structure, metabolism, and biological activities of both atherogenic lipoproteins, including increased levels of apolipoprotein B, TGs, VLDL and low density lipoprotein (LDL) cholesterol, and decreased level of anti-atherogenic high density lipoprotein (HDL) cholesterol (258). Dyslipidaemia is another common finding in PCOS, independent of BMI and insulin resistance and obesity can further exacerbate lipid disorders (259-261). It is estimated that 70% of PCOS patients exhibit abnormal serum lipid levels (262). Women with PCOS often display increased TGs and LDL cholesterol levels combined with decreased HDL cholesterol

(259-262). Moreover, in women younger than 40 years, PCOS might be the main cause of dyslipidaemia (259). In addition, PCOS patients were reported to have elevated levels of FFA (263,264). Both, IR and increased androgen levels, have been indicated as possible causes of dyslipidaemia in PCOS (265). Conversely, FFA have been demonstrated to increase adrenal androgen precursors *in vivo* (266) and exacerbate both insulin resistance and hyperinsulinemia, mainly due to interfering with insulin signalling, inhibiting insulin-stimulated glucose uptake, glucose oxidation and glycogen synthesis in skeletal muscle and liver (267,268). Increased FFA have also been demonstrated to directly stimulate pancreatic insulin secretion (269).

1.3.3.8 Cardiovascular disease

Life-long metabolic dysfunctions in women with PCOS, such as IR, T2DM, obesity and dyslipidaemia, exaggerate the risk for CVD (270). This is significant, since CVD is the leading cause of mortality in women (271). Patients with PCOS have increased early clinical and subclinical markers of vascular dysfunction and atherosclerosis and elevated blood pressure, when compared with general female population, however, cardiovascular risk profiles may vary with PCOS phenotype, age, ethnicity and BMI (251,270,272). Furthermore, PCOS patients were found to have elevated markers of low-grade chronic inflammation, which have also been implicated in the pathogenesis of CVD, including C reactive protein (CRP), fibrinogen and white blood cell count (273). In addition, PCOS patients were documented to have elevated risk of ischaemic stroke, ischaemic heart disease and overall mortality (274,275). Increased androgen levels might contribute to overall risk of CVD in women with PCOS. It has been demonstrated that in females high testosterone levels contribute to atherosclerosis and CVD development independently of age, adiposity, ovarian function, and smoking (276,277). Particularly, androgens have been demonstrated to stimulate inflammation and oxidative stress (OS) in vascular endothelium, as well as induce renal reabsorption of sodium and water, contributing to development of atherosclerosis and hypertension, respectively (278).

1.3.4 Metabolic characteristics of adolescent girls with PCOS

1.3.4.1 Insulin resistance

Impaired glucose metabolism, insulin resistance and hyperinsulinemia are common metabolic dysregulations in adolescent PCOS girls, across the spectrum of BMI, and may be a central factor underlying the pathogenesis of PCOS (279). It was reported that the prevalence of IR among adolescent girls with PCOS was 69.4%, independent of age and BMI (181,279-282). Increased body weight and adiposity, like in adult women with PCOS, further exacerbate insulin resistance. Obese girls with PCOS, when compared with BMI-matched controls, were

reported to have a 50% reduction in peripheral tissue insulin sensitivity, evidence of hepatic insulin resistance, and compensatory hyperinsulinemia (283). Interestingly, a study by Kent *et al.* demonstrated that daughters in the latter stages of puberty, but not sons, of PCOS women had significantly increased levels of insulin during a two hour oral glucose tolerance test (OGTT), when compared with BMI-matched control girls (284). However, authors did not find evidence of increased androgen levels in those girls, although testosterone levels were elevated in the sons of PCOS mothers (285). Comparable results were reported by Sir-Petermann *et al.*, showing that pre-pubertal and pubertal daughters of PCOS mothers had increased insulin levels after a two hour OGTT, when compared with controls (286). In addition, it was demonstrated that although androgen levels were normal in pre-pubertal girls, they were elevated during puberty. These findings suggest that hyperinsulinemia might precede reproductive perturbations in girls at increased risk of developing PCOS (286).

1.3.4.2 Obesity

Obesity frequently co-exist with PCOS and there is a correlation between incidence of PCOS in adolescent girls and elevated BMI, however, population studies are scarce. One study found that the overall prevalence of PCOS in 137,502 adolescent girls aged 15-19 years was 1.14%, however, compared with normal and underweight girls, the odds ratios for confirmed PCOS diagnosis were 3.85 for overweight, 10.25 for moderately obese, and 23.10 for extremely obese adolescents (185). However, authors also noted that the association between PCOS and obesity was lost when a subset of girls with suspected PCOS, based on medical records, were included into analysis, suggesting that obese girls are more likely to seek medical help and receive a diagnosis of PCOS, leading to a potential bias and overestimation of the association of PCOS with obesity (185). Moreover, longitudinal, population-based studies found that pubertal obesity and weight gain after adolescence was associated with an increased risk of having symptoms of PCOS in later life (287,288). In addition, a prospective study on 244 randomly selected postmenarchal girls reported PCO morphology in 61.1% of the obese girls, 36.2% in overweight girls, and 32.1% in the normal weight girls, indicating that obesity might be a contributing factor (183). Obesity often exaggerate hyperandrogenemia and hyperinsulinemia in normal pre-pubertal and pubertal girls, which might further accelerate development of PCOS in predisposed girls (289,290). Conversely, hyperandrogenemia can increase adiposity and alter adipose tissue distribution towards visceral fat, which in turn further contributes to the metabolic and endocrine disturbances in PCOS.

1.3.4.3 Metabolic syndrome

Childhood and adolescent MetS might predict adult morbidity and premature mortality (291-293). The increased prevalence of MetS, and its individual components, in girls with PCOS has been reported in numerous studies (294-299). In a retrospective study of 205 teenage girls, it was found that 10.8% of adolescent girls with PCOS had MetS, defined as presence of three or more risk factors, compared with 1.7% in those without PCOS (297). However, since girls in control group in this study had a medical history of irregular menses or hyperandrogenemia, but not PCOS, it can be speculated that the difference in the prevalence of MetS in adolescent PCOS, when compared with pubertal girls in the general population, might be even higher. Adolescents with PCOS were reported to have increased BMI, blood pressure, TG, and decreased HDL (297), therefore, it could be argued that obesity is the major factor contributing to the elevated risk of MetS in girls with PCOS. However, it was found that adolescent girls with PCOS had a 4.5 times higher prevalence of MetS, than age- and BMI-matched girls from the general adolescent population (294). Interestingly, in this study, hyperandrogenemia was reported to be the strongest predictor of MetS in adolescent PCOS girls, independent of obesity and insulin resistance (294). Adolescent girls with PCOS were also reported to have persistent elevations of FFA, hyperinsulinemia, and elevated cardiovascular disease risk markers, such as arterial stiffening and atherogenic lipoprotein lipid profiles (294,298,300).

Clinical Concerns	Childhood	Adolescence	Reproductive Years	Peri- and Post-Menopause
Hirsutism/Acne		→	→	→
Oligo/Anovulation		→	→	→
Infertility			→	→
Obesity	→	→	→	→
Diabetes		→	→	→
CVD			→	→

Table 1.2 Summary of main clinical manifestations of PCOS across the life course. Adapted from National Institutes of Health Evidence-Based Methodology Workshop on PCOS, 2012 (301).

1.3.5 Pathophysiology of PCOS

The pathophysiology of PCOS is complex and despite over 80 years of research, remains elusive. However, it is widely accepted that androgens and insulin play central role in the pathogenesis of PCOS.

In a normal ovary, androgens are synthesised from cholesterol in the theca cell layer of the ovarian follicle, under the stimulation of LH secreted from the anterior pituitary gland, which bind to LH receptors located on theca interna cells (302). Subsequently, androgens are converted into estrogen in the granulosa cells, under the regulation of FSH, by the action of the aromatase enzyme (302). In addition, in normal ovary, inhibin promotes androgen synthesis, whereas androgens, in turn, stimulate inhibin production. Activin opposes the effects of inhibin (302). Women with PCOS have elevated LH serum concentration (163) and increased LH pulse amplitude and frequency (303,304), but normal FSH levels, which in turn, lead to LH:FSH imbalance and elevated androgen synthesis (303,304). However, some women with PCOS have normal levels of LH, but remain hyperandrogenic, which point to additional mechanisms underlying hormonal dysregulation. Indeed, it was demonstrated that theca cells of PCOS women have intrinsic steroidogenic defect, and are hyper-responsive to gonadotrophins, thus secrete excess androgens even under normal LH levels, which might be further potentiated by increased LH and insulin concentrations (305,306). As indicated in *in vitro* studies, the enhanced steroidogenic potential of PCOS theca cells resides in the increased enzyme activities of P450_{scc}, 17 α -hydroxylase, and 3 β -HSD and increased expression of the transcription factor GATA-6, which regulates the promoter activity of *CYP11A* and *CYP17A1* (305,306,307).

Conversely, increased androgen levels may decrease the sensitivity of the hypothalamic GnRH pulse generator to steroid inhibition resulting in enhanced LH secretion (308). Further, women with PCOS have increased serum concentrations of inhibin B, which in turn, might lead to decreased levels of FSH, and thus decreased stimulation of aromatase by FSH, consequently resulting in the reduced conversion of androgen to estrogen, further aggravating the ovarian androgen excess (309,310). This also could perpetuate the vicious cycle of increased androgens in PCOS women (309,310). It has been demonstrated that androgens stimulate the development of smaller antral follicles, but inhibit the growth of larger antral follicles (302,311,312). In consequence, increased androgen levels in PCOS patients cause the development of a polycystic ovary, an ovary with many small antral follicles.

Although the ovaries are the primary source of androgen excess in PCOS, there is some evidence that women with PCOS frequently also display increased adrenal androgen production (313). This adrenal androgen excess, defined by high circulating levels of the metabolite DHEAS, is present in 20-30% of women with PCOS, and it is likely to be intrinsic (313). As there is no evidence of increased ACTH levels in patients with PCOS, this might be due to aberrant adrenocortical biosynthesis or increased sensitivity to ACTH (314,315).

Elevated insulin, as a potential consequence of insulin resistance, acts synergistically with LH to increase the generation and release of androgens from ovarian theca cells, through activation of 17α -hydroxylase, a key enzyme in ovarian androgen biosynthesis (316). Moreover, insulin suppresses hepatic production of SHBG, further enhancing the concentrations of free, biologically available, testosterone. In addition, insulin promotes the arrest of preantral follicle development, thus leading to both hyperandrogenemia and menstrual disturbance. Experimental studies demonstrated that insulin can increase LH pulse amplitude in pituitary tissue and adrenal androgen production, by enhancing adrenal sensitivity to ACTH, further exacerbating hyperandrogenemia (316,317). Considering insulin resistance, the action of insulin might seem paradoxical however, it has been demonstrated that insulin, downstream of its cellular receptor, acts via two key pathways, phosphatidylinositol 3-kinase (PI3K), which include insulin receptor substrates (IRS), IRS1 and IRS2, and mitogen-activated protein kinase (MAPK) pathways (318). In general, metabolic action of insulin is mediated through the PI3K pathway, whereas mitogenic and steroidogenic effects via MAPK pathway (318). In insulin resistant patients, including T2DM and PCOS, PI3K pathway deteriorates however, the MAPK pathway remains relatively intact, therefore the selective insulin resistance in women with PCOS results in defects in insulin-mediated glucose metabolism, but continued high insulin levels lead to upregulated steroidogenesis (319). Conversely, a decrease in insulin levels, resulting from improvement in insulin sensitivity in PCOS, achieved through either weight loss or drug therapy, leads to improved ovulatory function, menstrual cyclicity and fertility.

Insulin resistance in women with PCOS has been attributed to impaired insulin stimulated glucose uptake and post-receptor defects of the insulin-signalling system in adipose tissue and skeletal muscles. Impaired insulin stimulated tyrosine phosphorylation of IRS1 has been postulated as one of the mechanism leading to insulin resistance in PCOS women. Furthermore, decreased expression of the insulin-regulated glucose transporter 4 (GLUT4), encoded by *SLC2A4* gene, was shown in adipocytes of PCOS women (320). Interestingly, *in vitro* experimentation showed that testosterone can directly induce insulin resistance in SAT,

via androgen receptor (AR), selective for metabolic signalling pathways, independent of PI3K pathway (319). In skeletal muscle, reduced insulin receptor (INSR) tyrosine kinase activity due to increased serine phosphorylation was indicated as a potential cause for insulin resistance in PCOS.

It has been demonstrated that women with PCOS have decreased levels of circulating adiponectin, an insulin-sensitising adipokine, regardless of their level of adiposity, which positively correlated with IR and negatively with testosterone and FAI (321-322). Adiponectin in turn, has been shown to reduce the synthesis of androgens from ovarian theca cells (321-322), therefore, enhanced ovarian androgen production in women with PCOS could be also attributed to reduced adiponectin.

Obesity with associated increased adiposity further exacerbate the hormonal imbalance in PCOS patients. Obesity aggravates insulin resistance and hyperinsulinemia, but also hyperandrogenemia. Numerous studies report a positive relationship between BMI and androgens in both the paediatric and adult female population, opposite to what is observed in males (142,143). Although typically, women with PCOS were thought to have primarily increased visceral adiposity when compared with BMI-matched controls, employment of more sensitive imaging techniques revealed that there is no difference in volume of visceral, abdominal and gluteal subcutaneous adipose tissue depots between obese PCOS and weighed matched controls (219). Interestingly, one study reported decreased visceral adiposity in young, lean PCOS women when compared with BMI- matched controls (220). Therefore, it seems that women with PCOS appear to manifest global adiposity, with similar distribution to BMI-matched control women.

Nevertheless, excessive adiposity, and particularly android versus gynoid body fat distribution, has been suggested as an important factor in hyperandrogenemia. Android distribution, with increased VAT, was associated with decreased SHBG and increased free and total T concentrations, when compared with the gynoid distribution. The different distribution of steroidogenic enzymes, with increased 17β -HSD, converting A4 to T, in VAT versus increased aromatase, catalysing conversion of androgens to estrogens in SAT, has been proposed as a potential mechanism underlying different body fat distribution and elevated androgens levels in females with central adiposity. Conversely, increased expression of AR in VAT depots, as compared with the SAT was documented. In addition, obesity leads to dysfunction of adipose tissue, resulting in altered levels of circulating adipokines and

increased pro-inflammatory cytokines, which can further impair insulin resistance and stimulate steroidogenic enzymes in the ovary, accelerating androgen synthesis (130).

1.3.6 Management of PCOS

The complex pathophysiology and the broad clinical spectrum of PCOS entails a multidimensional therapeutic approach, however, lifestyle modification leading to sustained reduction of body weight remain central in improving the clinical, metabolic and hormonal characteristics of PCOS. Weight loss, through combination of balanced diet and regular exercise, should be undoubtedly encouraged in obese and overweight women, however, evidence has shown that even lean PCOS women can benefit from employing healthier life choices (323,324). It has been shown that even modest weight loss, by 10% of initial body weight, can increase frequency of ovulation, and improve the hormonal and metabolic profile, even if the women remain obese (325-328).

1.3.6.1 Insulin sensitisers

Insulin sensitisers, metformin and thiazolidinediones (TZDs) are commonly prescribed to women with PCOS, as evidence has shown that these pharmaceuticals can be beneficial in the management of this syndrome. Metformin is a biguanide generally used as an antihyperglycaemic agent, however, it has been also extensively evaluated as a potential treatment of infertility in PCOS. Metformin primarily improves insulin sensitivity, inhibits hepatic glucose production, and decreases intestinal glucose uptake, but also facilitates weight loss, reduces visceral adiposity and hyperandrogenemia, partially through direct action on ovarian theca cells, overall resulting in more favourable metabolic and hormonal profile (329-333). In addition, studies have shown that metformin improved ovulation rate, likely due to reducing insulin levels and altering the effect of insulin on ovarian androgen biosynthesis (329).

TZDs, namely rosiglitazone and pioglitazone, have also been found to be useful in decreasing IR and hyperandrogenemia, as well as restoring ovulation in PCOS. A study on the effects of six months of rosiglitazone treatment on obese and insulin-resistant PCOS women, demonstrated a decline in T and DHEAS levels, an increase in insulin sensitivity and SHBG, and the number of ovulatory cycles, without changes in body weight (334). Studies comparing TZDs and metformin did not find differences in their insulin-sensitising effects however, TZDs have more side effects and treatment with metformin is preferable (332). Interestingly, TZDs have a variety of beneficial effects in adipose tissue, including insulin sensitisation, induction of browning, and anti-inflammation. Unfortunately, the clinical utility of TZDs has

been limited by their unfavourable side effect profile, including fluid retention, osteoporosis, and (possibly) increased risk of cardiovascular events.

1.3.6.2 Oral contraceptives

If pregnancy is not desired, the combined oral contraceptive pill (COCP), might be prescribed to regulate menstrual cyclicality and to attenuate the clinical signs of hyperandrogenism in PCOS. Treatment with COCP lowers both, LH and FSH and additionally, increases the hepatic production of SHBG, decreases adrenal androgen secretion, and reduces the risk of endometrial hyperplasia, which is associated with chronic anovulation (333). However, since PCOS is associated with metabolic comorbidities, treatment with COCP might not be sufficient. Some studies raise concerns that treatment with COCP might actually result in the deterioration of insulin sensitivity, glucose tolerance and lipid profile, especially in obese PCOS patients.

1.4 Aetiology of PCOS

1.4.1 Heritability of PCOS

Despite the numerous studies on PCOS, its origin is still not fully understood. It has been suggested that this syndrome has a heterogeneous aetiology, developing from a mixture of genetic and environmental factors, additionally modified by sexual maturation and ageing. The PCOS phenotype shows familial clustering and appears to be transmitted between generations with hyperandrogenemia and insulin resistance being the most common characteristics (335-340). It is estimated that 20-40% of first-degree female relatives of women with PCOS are also affected by this syndrome (335-340). Sisters of PCOS women have increased frequency of hyperandrogenemia and PCO morphology, higher LH and plasma insulin concentrations, decreased insulin sensitivity, and greater incidence of obesity than women in the general population (341). In addition, male siblings or sons of PCOS women were found to have increased metabolic and hormonal perturbations, including IR and hyperinsulinemia, greater TG and cholesterol levels, elevated LH and FSH responses to GnRH agonist stimulation and higher DHEAS concentrations (342-346). Moreover, it has been documented that monozygotic twins shared twice as many features of PCOS than dizygotic twins, thus potentially supporting the hypothesis of a genetically inherited origin of PCOS (347). Although, since monozygotic twins are more likely to be exposed to an identical intrauterine environment than dizygotic twins, it could be argued that this could equally support the hypothesis of developmental programming of PCOS. Nevertheless, numerous studies have tried to ascertain the genetic basis of the syndrome, however, a robust genotype has not been identified.

1.4.2 Genetics of PCOS

Over than 100 PCOS-related candidate genes have been examined through candidate gene association studies. In this method, relationship of a genetic variation of candidate genes, usually a frequency of single-nucleotide polymorphism (SNP), with trait or disease, is investigated in case-control studies (348). More recently, the genome-wide association study (GWAS) technique was employed, in which an extensive number of SNPs are tested for association with a disease in a large number of selected individuals (349)

The main categories of candidate-genes studied in PCOS included, genes involved in the biosynthesis and the action of androgens, genes related to metabolism, and genes correlated with inflammatory cytokines.

Several studies investigated link of specific alleles of *CYP11A1* and *CYP17A1* genes, key regulators in androgen biosynthesis, with PCOS however, results are contradictory. While some reported a positive association of *CYP11A1* and *CYP17A1* with hyperandrogenemia in PCOS (350-352), others did not confirm these findings (353-357). Polymorphisms in androgen receptors and their potential links with PCOS were also studied. In a study by Ibanez *et al.*, shorter CAG trinucleotide repeat length in the *AR* gene was found to be an indicative of increased androgen sensitivity and elevated risks for precocious pubarche, and subsequent ovarian hyperandrogenism in postpubertal girls (358), and women with PCOS (359). Furthermore, it has been demonstrated that polymorphisms of short CAG repeats in *AR* can impact the positive association between insulin resistance and free testosterone in women with PCOS (359). However, the results are inconsistent (360-363).

Since PCOS is also strongly correlated with insulin resistance and metabolic syndrome, genes closely related with insulin signalling and obesity were also assessed. *INSR* is considered as an important candidate gene for PCOS, as number of different nucleotide polymorphism of the *INSR* gene has been found to be associated with this syndrome (364-367). However, a recent meta-analysis of studies on polymorphism of *INSR* and PCOS found no significant evidence for association with PCOS (368). Insulin receptor substrates are critical downstream factors involved in insulin signalling, therefore, these were also considered plausible candidates for PCOS susceptibility. Several studies on polymorphisms of IRSs have been conducted but the results are inconclusive. A weak correlation between polymorphisms in *IRS1*, but not *IRS2*, and PCOS was found (369,370). However, there was no correlation between *IRS1* polymorphisms and the characteristic features of PCOS (369,370).

An obesity-associated gene, *FTO*, has been identified as a strong candidate gene for PCOS. It was found that a *FTO* polymorphism is associated with PCOS (371), which correlated with hyperandrogenism (370,371), and insulin resistance (372). While the majority of the studies found that the *FTO* polymorphism was a strong predictor of obesity and adiposity in PCOS (371-374), one study reported that this association was independent of BMI (375).

PCOS is associated with low grade inflammation, therefore it was speculated that genes associated with chronic inflammation, such as *TNF* and *IL6*, might contribute to the incidence of PCOS, although this may be secondary to hyperandrogenism, insulin resistance and obesity. Although some studies reported link between PCOS and polymorphisms in *TNF* (376) and *IL6* genes (377), a more recent meta-analysis did not confirm those findings (378).

To date, five GWAS studies were conducted on women with PCOS with different ethnicity, including Han Chinese (378,379), Korean (378,379) and European ancestry populations (380). From these studies, 15 risk loci have been identified, with genes associated with gonadotrophin action, folliculogenesis, ovulation, T2DM, T1DM and cell proliferation, and although these studies provided new clues for understanding the genetic components and cellular pathways in PCOS, we are still far from understanding its pathogenetic mechanisms. This is likely due to PCOS being a polygenic condition with a cluster of different molecular pathologies and clinical complications.

1.4.3 Prenatal programming of PCOS

As postulated by Barker *et al.* the maternal–fetal environment plays an important role in the developmental programming of adult disease by epigenetic modifications of genetic susceptibility (382-384). There is growing evidence that perturbed intrauterine environment during critical periods of development can permanently alter the trajectory of the growing fetus and predispose to adult chronic disease. Well known examples of insults resulting in developmental programming include maternal under- and overnutrition (385-387), smoking (388), stress (389), and hormonal imbalance. One of the most recognised studies on developmental programming is the Dutch famine study, documenting long-term metabolic effects in people born during or after the Dutch hunger winter of 1944-45 (390-391). Prenatal undernutrition resulted in a low-birth weight in offspring, and in adult life this cohort of people had significantly increased frequency of diabetes, cardiovascular and pulmonary disease, obesity and cancers (390,391).

Although the molecular mechanism of developmental programming of adult disease are still largely unknown, epigenetic changes induced by an altered intrauterine environment are likely. Epigenetics refers to molecular mechanisms regulating gene expression not caused by DNA sequence variation, including DNA methylation, histone modification and other changes in chromatin structures together with transcriptional and post-transcriptional regulations by noncoding RNAs (392).

There is increasing evidence that the adult PCOS phenotype is programmed in fetal life by androgen excess. It is widely known, that women exposed to increased androgen levels in utero, due to congenital adrenal hyperplasia or virilising tumours, have increased risk of developing a PCOS-like syndrome in adult life, even after eliminating the hyperandrogenemia with postnatal therapies (393,394). Furthermore, testosterone levels in pregnant women with PCOS are higher than in normal pregnant controls throughout pregnancy and a particular

increase in testosterone concentrations in PCOS women was observed from the second trimester of pregnancy (395-397). In daughters of PCOS mothers testosterone levels in the amniotic fluid are elevated (395-397), which is further mirrored in increased testosterone concentrations in the umbilical vein at birth, as compared with control girls (398,399). In addition, it was demonstrated that maternal circulating total testosterone level, within normal physiological range in unselected population, was significantly correlated with early follicular-phase circulating AMH, a marker of enhanced follicular development, in female adolescent offspring (398,399). Likewise, it was reported that three-month old and prepubertal daughters of PCOS mothers had elevated AMH concentrations, suggesting an altered follicular development during infancy and childhood (400,401). Interestingly, Crisosto *et al.* demonstrated that treatment of pregnant PCOS women with metformin, which reduced insulin and androgen levels in those women, reduced AMH levels in their newborns, as compared with the daughters of untreated PCOS women and comparable to levels seen in offspring from normal mothers (400,401). In a retrospective study by Bridges *et al.* it was reported that most women diagnosed with PCOS in adulthood already had polycystic ovaries during childhood and puberty (402).

Yet, despite this evidence, the hypothesis of prenatal androgenisation as an aetiological factor in PCOS was questioned for many years, as the human fetus is protected from the effects of excessive maternal androgens by a combination of high level of placental aromatase activity, which metabolises androgens to estrogens, and increased concentrations of plasma binding proteins, which decrease free testosterone in the circulation (403). However, there is data demonstrating that placenta from PCOS women show macroscopic and microscopic alterations, as compared to healthy controls (404), and increased activity of placental 3 β -HSD1 and decreased placental aromatase, which could induce an accumulation of androgenic substrates (404). Further, although mechanisms underlying changes in placental activity of steroidogenic enzymes are not understood, potentially some of them could be attributed to increased insulin levels, as frequently reported in pregnant PCOS females (395,405), as it was demonstrated that in human placental cytotrophoblasts insulin inhibits aromatase activity (406), and promotes 3 β -HSD1 activity (407). Conversely, disorders associated with impaired insulin sensitivity and hyperinsulinemia, such as gestational diabetes and preeclampsia, have been linked with decreased placental aromatase activity and increased AR levels (408). Interestingly, it was also found that in women with gestational diabetes there was a significantly higher concentrations of T and DHT in the amniotic fluid, in both male and female fetuses, when compared with those of their respective gender controls (409). Therefore, it cannot be excluded that fetal hyperandrogenism comes directly from increased fetal

production of androgens, ovarian and/or adrenal, as result of maternal and fetal hyperinsulinemia, which can stimulate androgen hypersecretion.

Therefore, it is likely that combination of increased maternal androgens, decreased placental aromatase activity, and possibly elevated insulin levels, change the fetal environment, which predisposes female fetuses to the future development of PCOS. Animal models of PCOS provide further evidence supporting this hypothesis, which will be discussed in the next section.

1.5 Animal models of PCOS

Animal models of PCOS provide an opportunity to examine the developmental aetiology and molecular mechanisms underlying the pathogenesis of this condition. However, the applicability of rodent models in understanding PCOS is restricted, due to the different patterns of *in utero* development, ovarian development and structure, the presence of several ovulations in any normal estrous cycle and therefore, naturally occurring multi-follicular ovaries (410). In non-rodent animal models however, prenatal androgen exposure of female primate and sheep fetuses clearly leads to a disrupted reproductive phenotype, with altered metabolism and ovarian morphology, neuroendocrine defects, hyperandrogenism and LH excess in adult life, resembling that of women with PCOS (411-416).

1.5.1 Non-human primate model

Female rhesus monkeys have been used as a non-human primate model of PCOS. Rhesus monkeys' genome has a 93% similarity to that of humans, and their reproductive biology and metabolic physiology is analogous to humans. Thus, studies using this model of PCOS deliver the greatest translational relevance for human (417). Numerous studies demonstrated that prenatal exposure to testosterone yields a comprehensive adult PCOS-like phenotype in female rhesus monkeys (418-421). It was reported that prenatally androgenised females exhibited ovarian hyperandrogenism and higher levels of circulating testosterone (414), adrenal hyperandrogenism (420) and LH excess (422). What is more, those females had 50% less menstrual cycles than control females and 40% exhibited polyfollicular ovaries (414). Interestingly, prenatally androgenised female rhesus monkeys also displayed metabolic traits of PCOS, namely: impaired insulin sensitivity and glucose intolerance, T2DM, increased abdominal adiposity and dyslipidaemia (414,418,419). These data provide strong evidence for the role of increased prenatal androgens in the programming of adult PCOS. Unfortunately, as monkeys are very expensive, with poor availability and a long lead-time to adulthood they are not the ideal pre-clinical model.

1.5.2 Ovine model

Sheep have many developmental and reproductive characteristics comparable with humans (423). In sheep, as in humans, ovarian differentiation is completed *in utero* and lambs are well developed at birth. Furthermore, sheep are mono- or bi-ovulatory therefore, compared to poly-ovulatory rodents, are better animal model for studying the reproductive aspects of PCOS. In addition, their adult size is similar to adult humans, thus providing greater opportunity for

detailed and repetitive hormonal and metabolic profiling, and in consequence investigating aspects of metabolism, but also energy expenditure. Sheep are domesticated species therefore, can be kept in their natural environment for most of the time, free from stress associated with caging. Moreover, in comparison with rhesus monkeys, sheep are more cost-effective as an experimental research model. In addition, in comparison to rodents they are outbred with natural variability in phenotypes, like women.

The ovine model of PCOS, like the rhesus monkey model, strongly supports the hypothesis of prenatal programming of PCOS. Numerous studies provided evidence that prenatal androgen exposure of female sheep, both with T and DHT, disrupts reproductive cyclicity and various aspects of metabolism (423). However, the severity of perturbations depends on the treatment window, with prenatal androgenisation from fetal day 30, of 147 day of gestation, causing masculinisation of female external genitalia and increased aggressive behaviour, while treatment from fetal day 60 to 90 results in less severe phenotype with normal external genitalia (423).

Regardless of window treatment however, prenatally androgenised sheep have been shown to have altered cyclicity (424,425), with progressive deterioration of the reproductive phenotype with aging, and postnatal overfeeding (426,427). Moreover, prenatally androgenised ewes were reported to have elevated GnRH-induced LH response, leading to LH hypersecretion and acyclicity in adulthood (428), PCO morphology (429), increased androgenic capacity and altered gene expression of theca cells (412) and reduced fertility (430). In addition, these sheep were found to have decreased insulin sensitivity (411,426), altered pancreas morphology, with increased β -cell number (431), increased circulating FFA (423) and fatty liver (411).

1.6 The objectives of this thesis

As discussed in the introduction of this thesis, PCOS is a complex condition with reproductive, endocrine and metabolic complications, however it seems that metabolic problems associated with the syndrome, such as obesity, insulin resistance and NAFLD, are the most concerning long-term issues. The ovine model of PCOS will be used. Previous research utilising this clinically realistic model of PCOS reported hyperinsulinemia and early fatty liver changes, with no difference in body weight and adiposity, in adolescence. This thesis will principally focus on the effects of prenatal androgen exposure on metabolic health, mainly in adolescent and adult female sheep, although data from fetal and juvenile animals will also be included in selected chapters.

Chapter 3 will investigate the role of prenatally increased androgens on the development and function of adipose tissue depots, VAT and SAT, in fetal, juvenile, adolescent and adult PCOS-like sheep. Particularly, this chapter will examine expression of genes associated with adipocyte differentiation, insulin sensitivity and inflammation in SAT and VAT. In addition, this chapter will provide results of morphometric analysis of adipocytes from SAT and VAT in adult animals. In addition, the effects of direct treatment with steroids *in utero* on the development of SAT in adolescent females will be assessed.

Chapter 4 will determine the role of postprandial thermogenesis, an important constituent of energy expenditure, in the development of obesity in adult PCOS-like sheep. In addition, this chapter will evaluate the expression of thermogenic genes in different depots of adipose tissue, in both adolescent and adult animals. Finally, noradrenaline levels in the adipose tissue depots in adult animals will be evaluated.

Chapter 5 will investigate the causes and consequences of presence of fatty liver in adolescent PCOS-like sheep. Further, this chapter will evaluate fat liver content in adult animals and hepatic expression of genes associated with fatty acid uptake and processing.

Finally, chapter 6, will determine potential role of novel metabolic regulators, fibroblast growth factor 21 (FGF21) and irisin in metabolic phenotype of adolescent and adult PCOS-like sheep.

The results presented in this thesis provide better understanding into the metabolic pathophysiology of PCOS from puberty to adulthood and give opportunities for early clinical intervention to ameliorate the metabolic phenotype of PCOS.

Chapter 2 Materials and Methods

2.1 Introduction

This chapter will list the general materials and methods that were utilised in this thesis, while more detailed methods will be described in the individual results chapters. Any work that was not carried out directly by author of this thesis will be acknowledged in the appropriate sections. All reagents and chemicals were obtained from Merc, former Sigma-Aldrich (Gillingham, Dorset, UK), unless otherwise stated.

2.2 Animal husbandry

Scottish Greyface ewes were used for these studies and housed and cared for at the Marshall Building, Roslin, East Lothian. All experiments were conducted under a UK Home Office project licence (PPL60/4401) after local ethical committee approval.

2.2.1 Mating and pregnant ewe husbandry

Prior to mating, ewes were assessed by body condition score and only those with a good score of 2-3 were chosen. To obtain a similar time of pregnancy across the cohort, estrous cycles of previously selected ewes were synchronised with Chronogest CR sponges infused with 20mg flugestone acetate, a synthetic progesterone (Intervet UK Ltd., Buckinghamshire, UK), which was implanted vaginally for 10-12 days. After the withdrawal of the sponges, to terminate luteal phase, 0.5ml of prostaglandin estrumate (Schering Plough Animal Health, Welwyn Garden City, UK) was administered intramuscularly (IM). Approximately 48h later, ewes came into heat, and the Scottish Greyface ewes were mated with Texel rams, marked with raddle crayons, under natural seasonal breeding conditions from November to January. Ewes that were not mated, as indicated by the lack of a reference paint on their hind, were returned for mating a second time. Pregnancies and number of fetuses per pregnancy were confirmed by ultrasound scan, and pregnant ewes with single, twin (or rarely) triplet pregnancies were evenly divided amongst treatment groups. Pregnant ewes were housed in groups in spacious enclosures, unless dominant ewes prevented smaller ewes from feeding, in which case smaller ewes were housed separately. Animals were fed hay *ad libitum*, supplemented with Excel Ewe Nuts (0.5-1.0kg/day; Carrs Billington, Lancashire, UK) and Crystalyx Extra High Energy Lick (Caltech Solway Mills, Cumbria, UK). To prevent Clostridial diseases and Pasteurellosis, 4-6 weeks before lambing ewes received Heptavac P Plus (Intervet UK Ltd.).

2.2.2 Pregnant ewe treatment

Treatment methods used for this thesis include maternal treatment and fetal treatment. When a twin pregnancy resulted in two female offspring or fetuses only one from each pregnancy was included in the analysis to avoid any possibility of genetic bias.

2.2.2.1 Maternal Injections

In the maternal injection (MI) cohort, pregnant sheep were treated intra-muscularly with 100mg testosterone propionate (TP) (AMS Biotechnology (Europe) Ltd., Abingdon, UK), dissolved in 5% ethanol and added to vegetable oil (Sainsburys's SO organic range) under aseptic conditions to achieve a final volume of 1ml, and stored in an incubator at 37°C until use, to prevent steroid precipitate formation. Control (C) ewes were treated with the 1ml of vehicle only, containing same proportion of 5% ethanol and vegetable oil, and stored in an incubator at 37°C. To avoid masculinisation of external genitalia, seen in animals treated from day 30 of gestation, treatment was started at day 62 of gestation. Animals were treated twice weekly from day 62 until day 102 of gestation, with pregnancy lasting on average 147 days. The dose and method of testosterone treatment were selected based on published data, with regards to postnatal reproductive disruptions.

2.2.2.2 Fetal Injections

In the fetal injection (FI) cohort, on day 62 and day 82 of gestation, mothers were anaesthetised by initial sedation with Xylazine, 10mg; IM, (Rompun; Bayer PLC Animal Health Division, Berkshire, UK), followed by Ketamine, 2mg/kg; intravenously (IV), (Ketaset; Fort Dodge Animal Health, Southampton, UK). All subsequent procedures were conducted under surgical aseptic conditions. Fetuses were injected via ultrasound guidance using a vaginal probe into the fetal flank with 20G Quincke spinal needle (BD Biosciences, Oxford, UK) with following according to treatment group: C, 0.2ml vehicle (5% ethanol in vegetable oil); TP, 20mg TP in 0.2ml vehicle; 50µg diethylstilbestrol (DES) in 0.2ml vehicle, or 100µg dexamethasone (DEX) in 0.2ml vehicle (Table 2.1). Immediately after surgical procedure all treated ewes received prophylactic antibiotics (1ml/25kg of Streptacare, Animalcare Ltd, UK) and were then monitored during recovery; no significant adverse effects of these procedures were observed. The fetal injection commenced on the same day of pregnancy as maternal injections and were carried 20 days apart to best replicate the length of fetal exposure in maternal injection cohort. When twin pregnancy was involved, both fetuses were injected with the same compound. Ultrasound was performed by Prof. Colin Duncan, while Prof. Alan McNeilly, Prof. Mick Rae, Dr Kirsten Hogg and Dr Fiona Connolly carried out the fetal injection, in accordance with personal licences issued by the UK Home Office.

2.2.3 Non-pregnant treatment

In addition, non-pregnant ewes were treated intra-muscularly with 100mg TP (AMS Biotechnology (Europe) Ltd., Abingdon, UK), in 1 ml vegetable oil, twice weekly for two weeks. Controls (C) were treated with the same volume of vehicle only.

Maternal Treatment			
Treatment Period	Collection Stage	Treatment	Sample Size
D62- sacrifice	D70 fetus	C	3
		TP	6
D62- sacrifice	D90 fetus	C	6
		TP	8
D62-102	D112 fetus	C	9
		TP	4
D62-102	11 weeks lambs	C	8
		TP	8
D62-102	11 months ewes	C	5
		TP	9
D62-102	30 months ewes	C	11
		TP	4
Fetal treatment			
D62 and 82	11 months ewes	C	12
		TP	7
		DES	8
		DEX	11
Contemporary androgen treatment			
2 weeks	30 months ewes	C	5
		TP	5

Table 2.1 Table of treatments and animal numbers used in studies documented in this thesis.

2.2.4 Husbandry of offspring

Lambs were suckled or fed with powdered lamb milk substitute (Shepherdess, SCA Mill, North Yorkshire, UK), then gradually weaned at 3 months, and fed hay or grass *ad libitum*, until sacrifice. Lambs were vaccinated with Heptavac P Plus (Intervet UK Ltd.) at 3 and 7 weeks of age.

2.2.5 Animal sacrifice and specimen collection

2.2.5.1 Animal sacrifice

In pregnancies where fetal tissue was collected, ewes were sacrificed on either D70, D90 or D112 of gestation with sodium pentobarbital, 150mg/kg; IV, (Euthatal; Merial Animal Health Ltd., Essex, UK). The gravid uterus was immediately removed, fetal sex and weight recorded, and tissue collected. In pregnancies carried to term, females were sacrificed and tissue collected at 11 weeks, 11 months, and 30 months of age. For 11 months old sheep, since animals were collected during breeding season, prior to euthanasia, sheep estrous cycles were synchronized with two injections of prostaglandin estrumate, 125mg (0.5ml); IM, (Schering Plough Animal Health) 11 days apart to ensure that all cycles were aligned. Adult, 30 months old ewes were sacrificed in non-breeding season. Euthanasia was performed with single lethal injection of sodium pentobarbital, 150mg/kg; IV (Euthetal; Medial Animal Health Ltd., Essex, UK), in accordance with the regulatory guideline of Schedule 1: Appropriate Methods of Humane Killing of Animals (Scientific Procedures) Act 1986.

2.2.5.2 Tissue and plasma collection

Prior to euthanasia, animals were fasted overnight and Intravenous Glucose Tolerance Test (IVGTT) was performed. Peripheral basal blood was sampled, followed by intravenous administration of bolus glucose (500mg/ml in 20ml) followed by another blood sample collection at 15 min. Blood was collected into heparinised tubes, centrifuged at 1200g at 4°C for 15 min and the plasma stored at -20°C. Animals were immediately sacrificed and tissue collected. Tissues (listed in Table 2.2) were fixed in Bouins solution for 24h, to prevent tissue degradation, and then transferred to 70% ethanol, before processing and embedding in paraffin wax, and/or snap frozen, to prevent RNA degradation, and stored at -80°C. In addition, liver samples were collected from adolescent and adult animals and embedded in cassettes containing OCT compound, (VWR International, Leicestershire, UK), snap frozen and stored at -80°C. Omental fat from each adolescent and adult animal was removed and weighed.

Tissue	Collection Stage			
	Fetal	11 weeks	11 months	30 months
Adrenal	✓	✓	✓	✓
Cerebellum				✓
Fat marrow				✓
Fat scapular	✓			✓
Fat supraclavicular				✓
Fat subcutaneous	✓*	✓*	✓*	✓
Fat visceral	✓*	✓*	✓*	✓
Frontal cortex				✓
Heart	✓			✓
Hypothalamus	✓	✓	✓	✓
Kidney	✓			✓
Liver	✓	✓	✓	✓
Lung	✓			✓
Mammary gland	✓	✓	✓	✓
Muscle	✓	✓	✓	✓
Ovary	✓	✓	✓	✓
Pancreas	✓	✓**	✓**	✓**
Pituitary	✓	✓	✓	✓
Spleen	✓			✓
Thyroid	✓	✓	✓	✓
Uterus	✓	✓	✓	✓

Table 2.2 Ovine tissue collected at the time of sacrifice from different cohorts of animals. →* Tissue frozen only; →**Tissue fixed only. Only selected tissue from the list above was studied in this thesis.

2.3 Histology

2.3.1 Tissue Processing

To preserve tissue morphology and antigenicity, at the time of collection, tissue samples were fixed in Bouins solution for 24h, and then transferred to 70% ethanol. Samples were processed and embedded in heated liquid paraffin wax and cooled into blocks for long term storage by Prof. Mick Rae. Tissue blocks were sectioned on microtome (Leica, UK) at the thickness of 5µm, and wax ribbons were transferred to a pre-heated to 45°C water bath, mounted on poly-L-lysine-coated microscope slides (Leica Biosystems, Peterborough, UK) and incubated at 50°C for 24h to dry.

2.3.2 De-waxing and rehydration

Prior to any tissue staining protocol, slides were dewaxed in xylene for two separate 5 min incubations, to remove the hydrophobic paraffin wax from the tissue, and next rehydrated in gradient alcohol, 1 min each, in the following concentrations of alcohol 2x 100%, 90%, 80% and 75% and completed with incubation in distilled water (dH₂O).

2.3.3 Haematoxylin and Eosin Staining

For the evaluation of gross tissue morphology haematoxylin and eosin (H&E) staining was utilised. Haematoxylin solution, a mixture of hematein and aluminium ions, has an overall positive charge and binds to negatively charged chromatic material in the cell nucleus, staining cell nuclei with blue/purple colour. Eosin, a negatively charged dye, binds to a positively charged proteins in the cytoplasm, resulting in a pink stain. After the de-waxing and rehydration process in gradient alcohol tissue slides were immersed in haematoxylin for 5 min and washed in dH₂O. Next, tissue was very briefly rinsed in acid alcohol (1% HCL in 70% ethanol), to remove excess background stain, and again rinsed in dH₂O. Slides were placed in Scott's tap water for 30 sec, an alkaline bluing agent, to enhance contrast of the H&E stain. Slides were then washed in dH₂O and immersed in eosin for 30 sec and rinsed again in dH₂O. The tissue slides were subsequently thoroughly dried before undergoing dehydration in increasing grades of alcohol; 75%, 80%, 90% and 2 x 100% and cleared in xylene for 10 min. Slides were then mount with a cover slips using Pertex mounting media (Cell Path, UK) and allowed to dry in a fume hood for 24h.

2.3.4 Immunohistochemistry

Immunohistochemistry (IHC), is a method that allows visualisation of the distribution and localisation of specific antigens, proteins or cellular components in a tissue sections, through utilising a principle of antibody-antigen interaction in a tissue. In a direct method of IHC, a primary antibody, with attached reporter molecule, binds directly to antigen however, this method, due to low abundance of binding, can yield a low signal. To further increase binding and intensify signal, an indirect protocol is often applied, where a secondary antibody conjugated to biotin, specific to primary antibody, i.e. raised against the host species of the primary antibody, is added. The avidin-biotin-peroxidase tertiary complex (ABC), is then utilised to bind the biotinylated portion of the secondary antibody through the high binding affinity of avidin for biotin. The final step of visualisation of the complex is achieved through addition of compound that reacts with the tertiary complex resulting in a stain, usually 3,3'-diaminobenzidine (DAB) which yields brown coloured deposits.

2.3.5 Antigen Retrieval

Antigen retrieval step is often included in IHC protocol to expose the antigen epitopes which could be otherwise masked by fixation process due to protein cross linking, thus potentially obstructing the binding of the primary antibody to its target. Different antigen retrieval strategies exist with heat, digestive enzymes or detergents being widely used. In the experiments detailed in this thesis removing of cross-links was achieved through heating tissue slides in a citrate buffer. Following de-waxing and rehydration (Section 2.4.2), slides were submerged in a container of citrate buffer (0.05M, pH 6), which was then placed in a pressure cooker. Slides were pressured cooked for 5 min and then cooled for 20 min. After removing from pressure cooker slides were rinsed in dH₂O and washed in phosphate buffered saline (PBS) twice for 5 min.

2.3.6 Blocking

In IHC protocols that utilise peroxidases and biotin for the amplification or enzymatic detection of target antigens, it is essential to reduce or mask endogenous forms of these proteins to prevent false positives and high background staining.

To reduce endogenous peroxidase activity, and consequently a non-specific brown staining of DAB, after antigen retrieval (section 2.4.5) slides were immersed in 3% hydrogen peroxide (H₂O₂) diluted with dH₂O for 10 min. Slides were then washed twice in PBS for 5 min each time. To block endogenous biotin activity and therefore, a non-specific staining, an

avidin/biotin kit was used (Vector Laboratories, Peterborough, UK). First, slides were treated with avidin for 15 min at room temperature to block endogenous biotin, washed with PBS for 2 min, treated with biotin for 15 min to saturate any remaining biotin binding sites on avidin, and washed again for 2 min with PBS. Slides were quickly wiped with tissue to remove excess liquid, a water repellent barrier was drawn around tissues with a wax pen, to ensure any added solution would remain on tissue, thus preventing dehydration. Next, to prevent any non-specific binding, tissue was incubated for 1h at room temperature in humidity chamber with serum matching the host species of the secondary antibody diluted in 5% bovine serum albumin (BSA).

2.3.7 Incubation with Primary and Secondary Antibody

After incubation, excess serum was removed from slides and primary antibody, diluted in blocking serum, was applied. An optimal concentration of primary antibody was tested prior to experiment. Tissue covered in blocking serum without primary antibody and non-specific matched immunoglobulins of equivalent concentrations served as negative controls. Details of primary and secondary antibodies used in this thesis can be found in the appropriate experimental chapters. Slides were placed in a humidity chamber and stored at 4°C overnight. Following incubation with the primary antibody, slides were washed in PBS supplemented with 1% Tween 20 (PBST), twice for 5 min. Subsequently, slides were incubated for 1 hour at room temperature with secondary biotinylated antibody, diluted 1 in 500 in blocking serum.

2.3.8 Detection and Counterstaining

After incubation with the secondary antibody, slides were washed twice for 5 minutes in PBST and incubated with the ABC Elite Complex (Vector Laboratories, Peterborough, UL), as per the manufacturer's protocol, for 1 hour at room temperature. Subsequently, slides were washed twice in PBS before colourimetric detection with DAB substrate (Vector Laboratories), as per the manufacturer's instructions, with the same exposure time for each sample, usually lasting for 30 sec to 1 min. The enzymatic reaction was stopped with slides immersion in dH₂O. Slides were washed twice in dH₂O and excess water was removed before adding to haematoxylin for 1 minute for counterstaining. Slides were washed briefly in dH₂O, excess water was removed. Next, slides were added to Scott's Tap water and acid alcohol, and were dehydrated and mounted as described in Section 2.4.3.

2.3.9 Imaging

Images of protein immunolocalisation were captured using the Olympus Provis BX2 microscope (Olympus America Inc., Center Valley, PA, USA) with attached a Canon EOS 30D Microcam camera (Canon Inc. Headquarters, Tokyo, Japan) using Axiovert v4.8 software (Carl Zeiss Ltd., Welwyn Garden City, UK).

2.4 Western Blotting

Western blotting is a method used in research to separate and identify proteins of interest, through antibody probing, in tissues or cells. In this technique, proteins are extracted from samples and separated, based on molecular weight, through gel electrophoresis. These proteins are subsequently transferred to a membrane, using an electric current, generating a band for each protein. Following protein transfer, membranes are blocked in an appropriate blocking buffer preventing nonspecific binding of detecting antibodies, therefore minimising background noise. The membrane is then incubated with primary antibodies specific to the proteins of interest. Several washing steps ensure that the unbound antibodies are washed off, leaving only the bound antibody to the protein of interest. The bound antibodies are then detected, using various methods. In this thesis, secondary fluorescent antibodies were utilised to visualise proteins of interest.

2.4.1 Protein Extraction

Protein extraction was carried using radioimmunoprecipitation assay (RIPA) buffer (ab156034, Abcam, Cambridge, UK). Briefly, a small piece of tissue (approximately 30mg) was cut over dry ice and samples were immediately transferred to 2ml eppendorf tubes containing 500 μ l of RIPA buffer, supplemented with 5 μ l of HaltTM Protease Inhibitor Cocktail and 5 μ l of HaltTM Phosphatase Inhibitor Cocktail (Thermo Scientific Pierce, Rockford, USA). Samples were kept on ice for the subsequent steps. Samples were sonicated with Soniprep 150 ultrasonic disintegrator (MSE, London, UK) for 15 sec with alternating cooling on ice, until homogenous mixture was obtained. Samples were then centrifuged at 17500g at 4°C for 10 min to pellet unwanted cellular material. Supernatants were transferred to fresh eppendorf tubes and stored at -20°C.

2.4.2 Protein Quantification

Protein concentration was quantified using the Bradford assay, a colourimetric assay based on the binding of Coomassie dye to proteins (430). The assay principle is based on the colour

change from brown to blue upon binding of proteins to Coomassie dye under acidic conditions, represented by increased absorbance at 595nm proportional to the amount of protein present in the sample. The Bradford assay was performed by Dr Forbes Howie using the Cobas Fara centrifugal analyser (Roche Diagnostics, Welwyn Garden City, UK). The protein concentration was measured in 25µl of samples diluted with 50µl dH₂O. A standard curve, created from serial dilutions of BSA in dH₂O ranging from 0-100mg/l, was utilised to estimate sample concentration, ensuring all samples read on the linear portion of the obtained standard curve.

2.4.3 Western Blotting Protocol

Protein samples were diluted to given concentration in RIPA buffer and combined with equal volume of 1X Laemmli buffer (0.1M Tris-HCl pH 6.8, 20% glycerol, 2% (w/v) SDS, 0.16% (w/v) bromophenol blue and 3% β-mercaptoethanol (β-ME). Proteins were denatured at 99°C for 6 min and the samples loaded onto 4-20% Tris-HEPES-SDS Precast Polyacrylamide Mini Gels (Thermo Scientific Pierce, Rockford, USA). A full-range PageRuler™ Plus Prestained Protein Ladder (Thermo Scientific Pierce, Rockford, USA) was additionally loaded to one well per gel. Gels were submerged in a 1X Tris-HEPES-SDS Running Buffer (Thermo Scientific Pierce, Rockford, USA) and electrophoresed in Bio-Rad tanks (BioRad Laboratories Ltd.) at 100V at room temperature for 1h. Before proteins were transferred to a PVDF membrane (IPFL00010; Immobilon-FL PVDF; Merck Millipore, Darmstadt, Germany) using fast semi-dry blotter (Thermo Scientific Pierce, Rockford, USA) at 25V for 9 min, the membrane was submerged in methanol for 30 sec and subsequently the gel, membrane and filter papers were soaked in Western Blot Transfer Buffer (Thermo Scientific Pierce, Rockford, USA). Membranes were blocked in Odyssey Blocking Buffer (Li-Cor Biosciences, Ltd., UK) overnight at 4°C. The membranes were then incubated with a primary antibody for a housekeeping protein (loading control) diluted in Odyssey Blocking Buffer/PBS with 0.1% (w/v) Tween 20 (PBST20) for 2h at room temperature. Immunoblots were washed 4 times for 5 min with PBST20 and incubated with the primary antibody of interest diluted in Odyssey Blocking Buffer/PBST20 for 4h at room temperature. Subsequently membranes were washed in PBST20 4 times for 5 min and incubated with two different fluorescently-labelled secondary antibodies diluted in Odyssey Blocking Buffer/PBST20/0.01% (w/v) SDS for 1h at room temperature. Finally immunoblots were washed in PBST20 4 times for 5 min and rinsed with PBS to remove residual Tween 20. Membranes were visualised on the Odyssey Imager (Li-Cor Biosciences, Ltd., UK). The size of the visualised protein band was confirmed with reference to the molecular weight markers. Protein densitometry was analysed with Image

Studio Lite Software (Li-Cor Biosciences, Ltd., UK) with housekeeping protein levels used as an internal reference.

2.5 ELISA

Enzyme-linked immunosorbent assay (ELISA) is a plate-based assay technique, typically performed in 96-well polystyrene plates, designed for detecting and quantifying substances such as proteins, in a solution. The detection principle is based on a highly specific antibody-antigen interaction. In an ELISA, the surface of the plate wells is coated with a capture antibody. In a competitive ELISA, competition for antibody binding sites between labelled antigen and sample antigen takes place, therefore the signal yielded is inversely proportional to the amount of the antigen in a tested sample. Conversely, in a sandwich ELISA, the sample antigen added to the plate binds directly to the capture antibody, and a second detection antibody is added, which binds the antigen. If the primary antibody is not conjugated, an addition of a secondary antibody conjugated to an enzyme is necessary. An addition of a colourimetric substrate results in a reaction, yielding a measurable product (signal). In a sandwich ELISA signal intensity is directly proportional to the amount of antigen present in sample. The reaction is stopped with the addition of stop solution and detection is accomplished spectrophotometrically, usually at 450 nm (ThermoMax Microplate Reader; Molecular Devices, CA, USA). Sample concentration was calculated based on standard curve of analytes with known concentration after subtracting background values of set of blanks.

2.6 Multiplex immunoassay

Multiplex immunoassays utilise the same principle of highly specific antigen-antibody interaction as the sandwich ELISA, however, they allow for detection of multiple analytes of interest in biological samples in a single experiment. These immunoassays utilise an xMAP bead-based technology, with a distinctly coloured bead sets created by the use of two fluorescent dyes at distinct ratios and conjugated with a specific capture antibody attached to beads. These colour-coded beads are used to identify the bound capture antibodies, and a sandwich assay with labelled detector antibodies is then used to measure protein levels. Subsequently, beads are read using a specialised flow cytometer and samples are decoded using a specialised software.

2.7 Gene expression

2.7.1 RNA extraction

RNA extraction from frozen tissue was performed using the RNeasy Kit (Qiagen Ltd., West Sussex, UK) however, depending on the tissue type different kits were used.

2.7.1.1 RNA extraction from liver tissue

RNA from liver tissue was isolated using the Qiagen RNeasy Mini Kit. A representative 3mm cube of tissue was cut over dry ice, to prevent tissue thawing and thus RNA degradation, and transferred immediately to 2ml safe-lock eppendorf tube with an autoclaved metal bead (Qiagen Ltd.), containing 600 μ l RLT lysis buffer with 1% v/v β -ME, to denature proteins and inactivate RNases, that could otherwise degrade RNA. Tissue samples were disrupted and homogenised using a TissueLyser (Qiagen Ltd.) at 25Hz for total of 4 min, with position change of TissueLyser racks after 2 min, to ensure even homogenisation of all samples. Samples were then centrifuged at 11500g for 3 minutes to remove precipitated proteins and cellular debris. The resulting supernatant was transferred to a fresh 1.5ml eppendorf tube and mixed with 600 μ l of 70% ethanol, diluted with nuclease-free (NF) H₂O. Next, samples were transferred to an RNeasy spin column, centrifuged at 11500g, and the flow-through was discarded. Subsequently, columns were washed RW1 buffer, and an additional on column DNA digestion with DNase-1 (Qiagen Ltd.) was then performed to remove residual genomic DNA. Following a 15 min incubation with DNase at room temperature, spin columns were washed with RW1 and RPE buffers, as per the manufacturer's instructions. Total RNA was eluted with 30 μ l NF H₂O through centrifugation of collection tubes at 1150 g for 1 min and stored at -80°C.

2.7.1.2 RNA extraction from adipose tissue

To extract RNA from adipose tissue, a combination of TRI reagent, a monophasic solution of phenol and guanidinium isothiocyanate that simultaneously solubilises biological material and denatures protein, with Qiagen RNeasy Mini Kit was used. A 50mg sample of adipose tissue was cut on dry ice and transferred to 2ml Eppendorf tubess with metal beads, containing 1.5ml TRI reagent. Samples were homogenised using the Qiagen TissueLyser for 6 min at 25Hz and rested for 5 min at room temperature, to promote dissociation of nucleoprotein complexes. Lysates were transferred into new eppendorf tubes, and phase separated with addition of 0.3ml chloroform, to partition RNA into aqueous supernatant for separation, and vigorous mixing for 15 sec. Samples were incubated for additional 5 min at room temperature and centrifuged at 15000g at 4°C for 30 min. The upper aqueous phase containing RNA was collected and

mixed with the same volume of 70% ethanol. Following this step RNA was extracted as per the manufacturer's instruction, eluted in 30µl NF H₂O and stored at -80°C.

2.7.1.3 RNA extraction from skeletal muscle

RNA extraction from skeletal muscles was performed using Qiagen RNeasy Fibrous Tissue Mini Kit as per manufacturer's instruction. A representative 3mm cube of tissue was cut over dry ice and transferred immediately to a 2ml safe-lock eppendorf tube with autoclaved metal bead (Qiagen Ltd.), containing 300µl RLT lysis buffer with 1% v/v β-ME, to denature proteins and inactivate RNases that could otherwise degrade RNA. Tissue samples were disrupted and homogenised using a TissueLyser (Qiagen Ltd.) at 25Hz for total of 4 min, with position change of TissueLyser racks after 2 min, to ensure even homogenisation of all samples. Subsequently, Samples were transferred to new eppendorf tubes and 590µl of NF H₂O and 10µl of proteinase K solution (Qiagen Ltd.) was added, and mixed thoroughly by pipetting. Samples were incubated at 55°C for 10 min and centrifuged at room temperature at 10,000g to pellet down any tissue debris. Supernatants were transferred into new 1.5ml eppendorf tubes and 100% molecular grade ethanol was added (half volume of that of supernatant). Samples were then transferred onto spin columns. Following this step RNA was extracted as described previously, eluted in 30µl NF H₂O and stored at -80°C.

2.7.2 Measurement of RNA concentration

RNA concentration and purity was assessed using a NanoDrop 1000 spectrophotometer (Thermo Fisher Scientific, UK). Samples were kept on ice, 1µl of sample was pipetted onto the lower measurement pedestal, sampling arm was closed and the absorbance was measured at 260nm to calculate RNA concentration. In addition, a ratio at 260nm/280nm was calculated, to estimate RNA purity. Sampling pedestal and arm were wiped with laboratory tissue in between measurement of consecutive samples, to prevent carryover and inaccurate readings.

2.7.3 Complementary DNA synthesis

Complementary DNA (cDNA) was synthesised from RNA template, via reverse transcription. Reverse transcriptase (RT) use an RNA template and a short primer complementary to the 3' end of the RNA to direct the synthesis of the first strand cDNA, which can be used in subsequent downstream quantitative real-time polymerase chain reactions (qRT-PCR), allowing the detection of low abundance RNAs in a sample. Complementary DNA was synthesised using TaqMan RT reagents kit (Applied Biosystems, UK) as per the manufacturer's instruction. In each new set of cDNA samples prepared, a control omitting reverse transcriptase (RT) and reaction replacing cDNA with NF H₂O, were included. Samples

were prepared in 0.2ml PCR tubes (Axygen Inc, Glasgow, UK). Reagents, volumes and end concentrations are displayed in Table 2.3. The cDNA was prepared on G-storm gradient PCR thermocycler (G-Storm GS1, GRI Ltd., Essex, UK) with 1h incubation of samples at 42°C followed by an enzyme inactivation step of 95°C for 10 minutes. Samples are then stored at -20°C for further use.

Reagent	Volume (μ l)	Final Concentration
RT Buffer	5	1X
dNTP's mix	10	2mM
mM MgCl ₂	3.5	1.75mM
Random Hexamers	5	2.5 μ M
RNase Inhibitor	5	1.0U/ μ l
MultiScribe RT	5	2.5U/ μ l
RNA (100ng/ μ l)	5	10ng/ μ l
NF H ₂ O	11.5	
Total volume	50 μ L	

Table 2.3 Components and concentration of the TaqMan Reverse Transcription kit used for cDNA synthesis

2.7.4 Quantitative Real-Time Polymerase Chain Reaction

The Polymerase Chain Reaction (PCR) allows for specific sequences within a DNA or cDNA template to be amplified, using sequence specific primers, heat stable DNA polymerase, and thermal cycling. PCR reaction consists of three steps: denaturation, primer hybridisation and extension. First, a high temperature, approximately 94°C-95°C, is applied to denature double stranded DNA into single stranded DNA, or loosen secondary structures in single-stranded DNA. Next, temperature is lowered to approximately 60°C permitting binding of primers to the gene of interest on the single stranded DNA. Subsequently, the temperature is raised to 72°C, which is an optimal for DNA polymerase activity, and primer extension occurs. Following the extension step, cycle is repeated, resulting in denaturation of the newly created double strand and creation of new complementary strand resulting in exponential amplification of the target DNA. Quantitative Real-Time PCR (qRT-PCR), unlike 'traditional' end-point PCR, in which detection and quantification of amplified sequences are performed at the end of last PCR cycle through gel electrophoresis and image analysis, permits the monitoring of each PCR cycle and allows for determining of the initial quantity of the amplified sequences. This is achieved through increase in fluorescence signal, emitted by fluorescence probes or DNA-binding dyes, measured by PCR instrument, which corresponds to gene amplification.

2.7.5 SYBR Green DNA-binding dye

SYBR Green dye is a fluorescent DNA-binding dye, which binds to the minor groove of any double-stranded DNA. The unbound SYBR Green dye produces little fluorescent signal, while a strong fluorescent signal is emitted during PCR amplification, due to binding to increasing copies of double-stranded DNA. Therefore, the fluorescent signal increases with the number of amplifications and is directly proportional to the number of amplified copies of double stranded DNA. The cycle threshold (Ct) value, representing the cycle number at which the fluorescent signal of the reaction crosses the threshold above background signal during the exponential phase of the reaction, is used to calculate the initial DNA copy number. However, as SYBR Green can be bound to any amplified product, target and non-target, therefore, testing the specificity of an assay is essential. It is normally performed by the analysis of the dissociation curve, a readout of gradual melting of the PCR products after the PCR cycling is completed. This is based on principle that one defined genetic sequence has specific melting temperature, therefore, only one sharp peak, representing denaturation of double-stranded DNA and thus dissociation of SYBR dye, should be present in the melting curve. Occurrence of any additional peaks indicates a non-specific amplification.

2.7.6 SYBR Green protocol and analysis

Real-time quantitative amplification was performed on 384-well plate format (Applied Biosystems), with all samples run in duplicate and housekeeping control genes included in each run, using the ABI 7900HT Fast Real Time PCR system instrument (Applied Biosystems). A 10 μ l volume of final reaction mix was prepared with 5 μ l PowerSYBR Green PCR Master Mix (Applied Biosystems), 0.5 μ l primer pairs, 1 μ l cDNA, and 3.5 μ l NF H₂O. The qRT-PCR cycling program consisted of an initial denaturation (95°C for 10 min), combined annealing and extension step (95°C for 15 sec, 60°C for 1 min), repeated 40 times, and a final dissociation step (95°C, 60°C, and 95°C, 15 sec each). Negative controls were included for each gene and consisted of RT negative (cDNA master mix without RT enzyme), H₂O negative (cDNA master mix with RNA substituted for NF H₂O) and PCR negative (PCR master mix with cDNA substituted for NF H₂O) samples. Ct values were collated using the ABI 7900HT v2.3 software and exported to an Excel file. Ct values of sample duplicates were checked to verify accuracy and the melting curve was assessed to confirm the specificity of PCR product. The expression of the target gene relative to the housekeeping genes, as an internal control determined by geNorm assay of housekeeping genes (Primerdesign Ltd, Southampton, UK) was quantified using the $\Delta\Delta$ Ct method (432), as follows:

$$\Delta \text{ Ct} = \text{mean Ct of gene of interest} - \text{mean Ct of housekeeping genes}$$

$$\Delta \text{ Ct calculated for both control and treatment samples}$$

$$\Delta\Delta \text{ Ct} = \Delta \text{ Ct treatment sample} - \text{mean of all } \Delta \text{ Ct control samples}$$

$$\text{Gene expression} = 2^{- (\Delta\Delta \text{ Ct})}$$

2.7.7 The selection of the optimal reference genes using geNorm

In the qRT-PCR studies a normalisation step is essential. The use of reference (housekeeping) genes is the most effective method however, selection of genes with the most stable expression level unaffected by experimental treatments is critical to ensure the accuracy of qRT-PCR results. Therefore, to select the most stable house-keeping genes in ovine liver and adipose tissue, the geNorm Reference Gene Selection Kit with 12 candidate genes (Primerdesign Ltd, Southampton, UK) was carried as per the manufacturer's instructions. Four samples per each treatment group were included in the assay. The analysis of the data using the provided geNorm software was performed by Grace Cathal. Table 2.4 summarises the most stable, with high reference target stability (geNorm $M \leq 0.5$) housekeeping genes in selected ovine tissues.

Tissue	Gene	Forward Sequence	Reverse Sequence	Product Size (bp)
Liver	<i>ACTB</i>	ATCGAGGACAGGATGCAGAA	CCAATCCACACGGAGTACTTG	101
	<i>MDHI</i>	TTATCTCCGATGGCAACTCC	GGGAGACCTTCAACAACCTTCC	100
Visceral adipose tissue	<i>RPS26</i>	CAAGGTAGTCAGGAATCGCTCT	TTACATGGGCTTTGGTGGAG	106
	<i>18S</i>	CAACTTTCGATGGTAGTCG	CCTTCCTTGGATGTGGTA	110
Subcutaneous adipose tissue	<i>ACTB</i>	ATCGAGGACAGGATGCAGAA	CCAATCCACACGGAGTACTTG	101
	<i>MDHI</i>	TTATCTCCGATGGCAACTCC	GGGAGACCTTCAACAACCTTCC	100

Table 2.4 Reference genes used in qRT-PCR studies.

2.7.8 Primer Design

Forward and reverse primers were designed for amplification of the gene of interest by qRT-PCR using Primer3Plus online software (<http://www.bioinformatics.nl/cgi-bin/primer3plus/primer3plus.cgi>), from DNA sequence obtained at Ensembl Genome Browser (<http://www.ensembl.org/index.html>). Primer regions were selected so that the forward and reverse sequence was intron spanning, primer length was 18-22 bp, primer melting temperature 52-65°C, and primer GC content 50-60%. Primer sequences were further assessed for likelihood of obtaining other similarly sized products using the Basic Local Alignment Search Tool (BLAST) provided by the National Center for Biotechnology Information (NCBI).

Primers were synthesised by Eurofins MWG Operon, Germany. Standard PCR was performed for validation of authenticity of the gene product. Standard PCR was performed on G-storm gradient PCR thermal cycler (Labcare Ltd, UK) using GoTaq Flexi DNA polymerase (Promega Ltd, UK). The PCR thermocycle consisted of an initial denaturation at 95°C for 5 min, combined annealing and extension step (95°C for 30 sec, 60°C for 45 sec and 72°C for 45 sec), repeated 35 times, and a final extension step at 72°C for 10 min. PCR products were visualised on a 2% agarose gel with 0.5% gel red prepared in 1X TAE buffer (0.04M tris acetate buffer, 0.001M EDTA), run alongside a 1000 bp ladder. Gel electrophoresis was carried out at 100V for 45 min and bands subsequently visualised in an ultraviolet light box. Primer efficiency was assessed by generating standard curves in qRT-PCR, constructed using double dilution (1:2) of an representative cDNA template, and by using LinRegPCR software (433) whereas primer binding specificity by including a dissociation (melting) curve post qRT-PCR-cycling, during each run. A linear standard curve generating a straight line with an R² value near to 1.0 and a slope of -3.33, and a single high peak in a dissociation curve implicated suitable primers.

2.8 Statistical analysis

Most of the analysis presented in this thesis involved a comparison between C and TP treated groups. The data was subject to Shapiro-Wilk normality test to assess if the values come from a Gaussian distribution. For comparing means of two treatment groups with equal variances, an unpaired, two-tailed Student's t test was used, unless otherwise stated. If data was not normally distributed, a Mann Whitney test was utilised. To compare multiple sets of data a one-way analysis of variance (1 way-ANOVA) was used. Log transformation was used to approximate the normal distribution for parametric analysis when necessary. Each section provides details of statistical analysis utilised. GraphPad Prism 6.0 (GraphPad Prism Software, San Diego, CA, USA) was used to analyse data. A P value of <0.05 was considered as statistically significant. Results are presented as mean + S.E.M, where * signifies a P<0.05, ** P<0.01 and *** P<0.001.

Chapter 3 The effect of prenatal androgenisation on the function of WAT

3.1 Introduction

PCOS is a complex condition with reproductive, endocrine and metabolic characteristics, however, it seems that the most concerning long term key issues are metabolic problems associated with the syndrome, such as hyperinsulinemia, insulin resistance, obesity and dyslipidaemia (434-436). Obesity and increased visceral obesity are considered key factors contributing to metabolic dysfunction in PCOS (437-440). Accumulation of VAT is correlated with pathologic inflammation and insulin resistance whereas SAT is thought to be protective or at least inert (441-447). Recently our group reported that midgestational androgenisation of female sheep resulted in hyperinsulinemia and early signs of NAFLD, independent of body weight or central obesity in adolescent, 11 months old PCOS-like sheep (411). These pubertal prenatally androgenised animals had no differences in ovulation rate, when compared to controls, during their first breeding season. They did not have a significant increase in basal circulating testosterone, but there was enhanced capacity for androgen synthesis in theca cells and adrenal glands (412) and circulating androgens were increased during adrenal stimulation testing. Interestingly similar results were described in adolescent daughters of PCOS mothers, showing that those girls are hyperinsulinemic without difference in body weight or adiposity and have increased testosterone levels in late puberty (448).

WAT is the body's primary long-term energy store, but it is also an important endocrine organ producing many adipokines and cytokines regulating energy homeostasis, insulin sensitivity and inflammation, therefore, functional WAT is essential in maintaining body homeostasis (73,449-451). WAT has a maximal expansion capacity, which is determined on an individual basis by environmental and genetic factors (452). When the capacity to safely store fat is saturated, lipid overflow occurs. Excess FFA are then deposited in non-adipose tissue such as liver and muscle, causing inflammation and insulin resistance by a lipotoxic mechanisms (453). We therefore hypothesised that altered adipose tissue morphology and function may be a central factor contributing to early metabolic disturbances in PCOS including IR and the early detection of NAFLD.

Adipocytes derive from multipotent mesenchymal stem cells. There are two main phases of adipogenesis, determination and terminal differentiation. During the determination phase commitment of a pluripotent stem cell to the adipocyte lineage occurs, resulting in pre-adipocyte formation. Morphologically preadipocytes cannot be distinguished from the stem cells however, those cells, in contrast to stem cells, do not possess ability to differentiate into different cell types. During terminal differentiation, preadipocytes gain characteristic traits of

mature adipocytes, including ability for lipid transport and synthesis, insulin responsiveness and production, and secretion, of adipokines. Numerous transcription factors are involved in establishing the mature white adipocyte phenotype, however, PPARG and family of CCAAT/enhancer binding protein transcription factors (C/EBP) play a main role in controlling the entire terminal differentiation process (454-456). PPARG is a member of a nuclear-receptor superfamily, and it has been demonstrated to be essential and sufficient for adipocyte differentiation. Studies have demonstrated that this gene is sufficient to induce adipocyte differentiation in fibroblasts and that adipogenesis cannot occur without presence of PPARG. In addition, it has been demonstrated that other pro-adipogenic factors, such as C/EBPs, induce *PPARG* promoters. Moreover, it has been shown that PPARG is also necessary to maintain the fully differentiated state of mature white adipocytes. *In vivo* experiments demonstrated that the knockout of *PPARG* in differentiated adipocytes leads to adipocyte death followed by the generation of new adipocytes. We hence aimed to:

1. examine the expression of molecular markers of adipogenesis and mature adipocytes in adipose tissue of PCOS-like sheep during different stages of development;
2. establish effect of different steroid classes on adipocyte differentiation;
3. characterise the adult metabolic phenotype of PCOS-like sheep;
4. perform morphological analysis of adult WAT.

3.2 Materials and Methods

3.2.1 Experimental animals

The ovine model, the animals used, their husbandry and treatments have been described previously (Section 2.2). The female animals assessed in this chapter are detailed in Table 3.1.

Treatment	Developmental stage	Sample number (n)
Fetal		
Maternal Injection D62-102	Fetal day 112	C=9, TP=4
Juvenile		
Maternal Injections D62-102	Lambs 11 weeks old	C=8, TP=8
Adolescent		
Maternal Injection D62-102	Ewes 11 months old	C=5, TP=9
Fetal Injection D62 and D82		C=12, TP=7, DES=8, DEX=11
Adult		
Maternal Injections D62-102	Ewes 30 months old	C=11, TP=4
Contemporary Injections 2 weeks	Ewes 30 months old	C=5, TP=5

Table 3.1 Treatment regime, age and corresponding sample numbers of experimental animals discussed in this chapter.

3.2.2 Gene expression analysis using qRT-PCR

Extraction of RNA from fetal and postnatal adipose tissue was performed using the combination of TRI reagent and Qiagen RNeasy Mini Kit (Qiagen Ltd., West Sussex, UK), as described in section 2.8.1. Protocols for cDNA synthesis and qRT-PCR are described in section 2.8.3. and 2.8.4, respectively. Forward and reverse primers were designed and validated as stated in section 2.8.6 and primer sequences analysed in this chapter are listed in Table 3.2.

Gene	Forward Sequence	Reverse Sequence	Product Size (bp)
<i>PPARG</i>	TGCAGTGGGGATGTCTCATA	CAGCGGGAAGGACTTTATGT	172
<i>CEBPA</i>	GTGGACAAGAACAGCAACGA	CGCAGTGTGTCCAGTTCG	185
<i>CEBPB</i>	GACAAGCACAGCGACGAGTA	AGCTGCTCCACCTTCTTCTG	158
<i>CEBPD</i>	CGAGTACCGGCAGCGAC	GTCGCGCAGTCCGGC	172
<i>LEP</i>	ATCTCACACACGCAGTCCGT	CCAGCAGGTGGAGAAGGTC	202
<i>ADIPOQ</i>	AGAGATGGCACCCCTGGT	GACCTTCGATCCCAGTGATT	100
<i>ADIPOR1</i>	TCTCCTGGCTCTTCCACACT	AGTCCCCATGATCAGCA	99
<i>ADIPOR2</i>	AGGTCGGGAGCCTCTTGTAG	TGAACCCCTCATCTTCCTGA	107
<i>INSR</i>	CACCATCACTCAGGGGAAAC	CAGGAGGTCTCGGAAGTCAG	247
<i>SLC2A4</i>	CCAGCATCTTTGAGTCAGCA	CAGAAGCAGAGCCACAGTCA	188
<i>IRS1</i>	ATCATCAACCCCATCAGACG	GAGTTTGCCACTACCGCTCT	240
<i>IRS2</i>	TCCAGAACGGCCTCAACTAC	TCAGGTGATGCGTCAAGAAG	246
<i>TNF</i>	GGTGCCTCAGCCTCTTCT	GAACCAGAGGCCTGTTGAAG	132
<i>IL6</i>	AAATGACACCACCCCAAGCA	CTCCAGAAGACCAGCAGTGG	253
<i>CCL2</i>	GCTCCCACGCTGAAGCTTGAAT	GATTGCTTTAGACTCTGGGTTGTGGAG	369

Table 3.2 Forward and reverse primer sequences and product size for genes analysed in the fetal and postnatal adipose tissue using SYBR Green qRT-PCR.

3.2.3 Western Blotting

Western blotting was performed to assess the protein level of PPARG in SAT of 11 months old prenatally androgenised ewes from the maternal injection cohort. Due to unequal sample number between control (n=5) and TP group (n=9), 5 samples from TP group were randomly selected for this analysis. The western blotting protocol is described in Section 2.5 with 20 µg of total protein per sample loaded onto gel columns. The size of the visualised protein band was confirmed with reference to the molecular weight markers. Protein densitometry was analysed with Image Studio Lite Software (Li-Cor, Lincoln, USA) with STAT1 protein levels used as the loading control. Specific details of antibodies used are outlined in Table 3.3.

Primary Antibody	Concentration	Details
PPARG	1:500	Polyclonal Goat (SC-1984; N-20) Santa Cruz Biotechnology
STAT1	1:1000	Polyclonal Rabbit (SC-346; E-23) Santa Cruz Biotechnology
Secondary Antibody	Concentration	Details
IRDye 680RD	1:10000	Donkey anti-Goat (926-68074; Li-Cor)
IRDye 800CW	1:10000	Donkey anti-Rabbit (926-32213; Li-Cor)

Table 3.3 List of primary and secondary antibodies used for western blotting. The antibody suppliers and working concentrations are detailed.

3.2.4 Intravenous Glucose Tolerance Test

Intravenous glucose tolerance tests were performed regularly during animals' development to assess impact of prenatal treatments on glucose-insulin homeostasis. IVGTTs were performed by Prof. Colin Duncan with assistance of the staff at the Marshall Building. Animals were fasted overnight, basal blood samples were collected and an IVGTT performed by administering a bolus glucose injection (10g glucose in 20ml saline). Post-glucose administration, blood was sampled at 15 min intervals for 45 min. Blood samples were decanted into heparinised test-tubes for hormonal/metabolite measurements or S-Monovettes containing sodium fluoride with anti-coagulant (Sarstedt Ltd, numbrecht, Germany) for glucose measurement. Tubes were then centrifuged at 1200g for 15 min at 4°C, and the plasma collected for storage at -20°C.

3.2.5 Glucose and insulin measurements

Serum glucose concentrations were performed by Dr Forbes Howie with enzymatic-colourimetric glucose assay kit (Alpha Laboratories Ltd., Eastleigh, UK) using a Cobas Fara centrifugal analyser (Roche Diagnostics Ltd, UK). Assay sensitivity was 0.2mmol/l. The intra and inter-assay coefficients of variation (CV) were <2% and <3% respectively.

Plasma insulin was measured using the ALPCO Ovine Insulin Elisa kit (80-INSOV-E01; American Laboratory Products Company, Salem) as per the manufacturer's instructions. Immunoassay absorbance was measured at 450nm with a reference wavelength of 630nm using a ThermoMax Microplate Reader (Molecular Devices, CA, USA) and the concentrations were calculated from a cubic spline standard curve. All samples were assayed in duplicate. The assay sensitivity was 0.14ng/ml intra and inter-assay CVs were <5% and <6%, respectively.

3.2.6 Measurement of other plasma analytes

Concentrations of plasma triglycerides and FFA were obtained by Dr Forbes Howie using commercial assay kits (Alpha Laboratories Ltd., Eastleigh, UK) as per manufacturer's instruction, using a Cobas Fara centrifugal analyser (Roche Diagnostics Ltd, UK) with assay sensitivity of 0.05mmol/l and 0.02mmol/l, respectively and CVs <3%.

3.2.7 Plasma leptin concentration

Plasma leptin concentration was obtained using Bio-Plex Human Diabetes Assay (171A7001M; Bio-Rad, Watford, UK), as per the manufacturer's instruction. This assay allows for measurement 10 analytes at the same time although, only leptin results will be discussed in this chapter. The principles of multi-plex immunoassays were discussed in section 2.7. All samples were assayed in duplicate and the results were acquired and calculated using Bio-Plex 200 array reader system with Bio-Plex Manager software (Bio-Rad, Watford, UK). The assay working range for leptin was 0.011-129ng/ml, assay sensitivity 3.1pg/ml, and intra and inter-assay CVs were 3% and 4%, respectively.

3.2.8 Plasma adiponectin concentration

Plasma adiponectin was measured using human Adiponectin ELISA kit (KHP041; Invitrogen, Life Technologies, Paisley, UK), as per the manufacturer's instructions. Immunoassay absorbance was measured at 450nm using a ThermoMax Microplate Reader (Molecular Devices, CA, USA) and the concentrations were calculated from standard curve by plotting the known concentration of standard against the absorbance values. All samples were assayed in duplicate. The assay sensitivity was 0.1ng/ml intra and inter-assay CVs were <5% and <6%, respectively.

3.2.9 Adipocyte morphometric analysis

Morphometric analysis of adipocytes was performed by Flavien Coukan, an undergraduate student, under supervision. For adipocyte morphometric analysis, two 5µm sections were cut for each adipose tissue sample, a minimum of 50µm apart, and mounted on positively charged slides (Superfrost Plus Gold, ThermoScientific, Epsom, UK). Sections were then stained with haematoxylin and eosin following standard protocol, as described in section 2.4.3. Two randomly selected fields per section were captured at x4 magnification using cellSens Dimension (Olympus, Essex, UK). Images were analysed using Adiposoft, ImageJ Software (ImageJ, University of Navarra, Spain) (457). Results were then manually corrected as per Adiposoft instructions and confirmed on a graticuled microscope.

3.2.10 Statistical analysis

Statistical analysis was performed with GraphPad Prism version 6.0 (GraphPad Software, Inc., San Diego, CA). For comparing means of two treatment groups with equal variances an unpaired, two-tailed Student's t test was used. To compare multiple sets of data a one-way ANOVA was used. Log transformation was used to approximate the normal distribution for parametric analysis when necessary. A P value of <0.05 was considered as statistically significant. Results are presented as mean + S.E.M, where * signifies a P<0.05, ** P<0.01 and *** P<0.001. Area under the curve (AUC) was calculated using the trapezoidal method. Correlation was assessed by calculation of the Pearson r co-efficient. A line of best fit was incorporated only in the figures where correlation was statistically significant.

3.3 Results

3.3.1 Adipocyte differentiation in adolescent VAT and SAT

To determine whether metabolic perturbations reported previously in adolescent PCOS-like sheep were associated with altered adipogenesis in VAT, mRNA expression of the master adipogenic regulators was evaluated. There was no difference in the expression of *PPARG*, *CEBPA*, *CEBPB* (Fig. 3.1 A-C) while *CEBPD* level was increased ($P < 0.05$; Fig. 3.1 D) in the VAT of adolescent prenatally androgenised female sheep. To fully confirm adipocyte maturation status, mRNA expression of selected markers of fully mature adipocytes was also assessed. There was no difference in the mRNA levels of *LEP* and *ADIPOQ*, in VAT of adolescent TP treated sheep when compared with controls (Fig. 3.1 E-F).

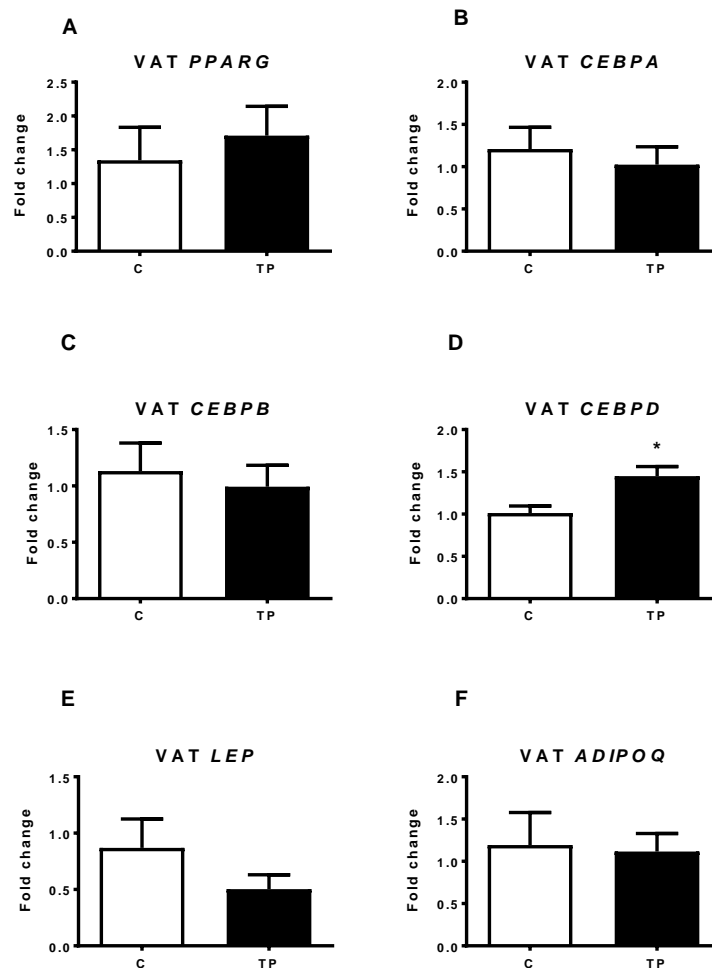


Figure 3.1 Adipogenesis markers expression in VAT in adolescent female controls (C) and prenatally androgenised (TP) ewes, as quantified by qRT-PCR. P value of < 0.05 was considered as statistically significant. Results are presented as mean + S.E.M, where * signifies a $P < 0.05$.

We then looked at the expression of markers of adipogenesis in SAT in the same cohort of animals. Expression of *PPARG*, *CEBPA*, *CEBPB* was significantly downregulated ($P < 0.05$; Fig. 3.2 A-C) with no difference in the expression of *CEBPD* (Fig. 3.2 D). In addition, levels of *LEP* and *ADIPOQ* in SAT were decreased in adolescent prenatally androgenised females ($P < 0.05-0.01$; Fig. 3.2 E-F).

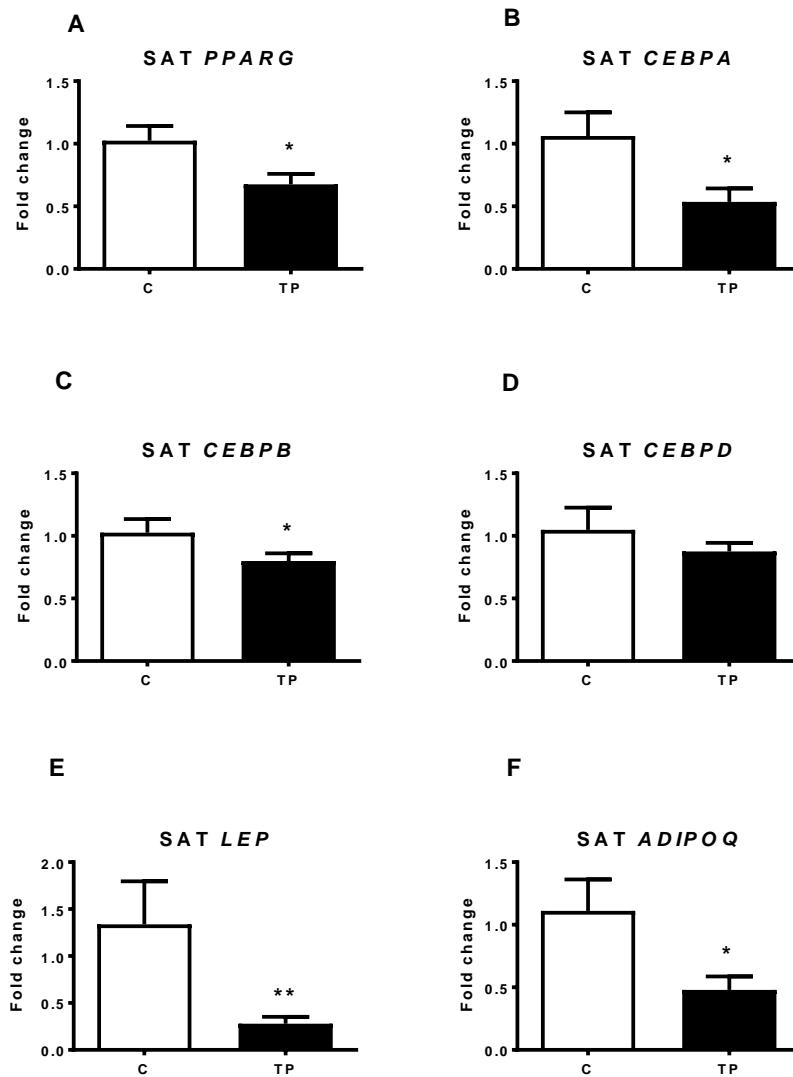


Figure 3.2 Adipogenesis markers expression in SAT in adolescent female controls (C) and prenatally androgenised (TP) ewes, as quantified by qRT-PCR. P value of < 0.05 was considered as statistically significant. Results are presented as mean + S.E.M, where * signifies a $P < 0.05$, ** $P < 0.01$.

We therefore assessed protein levels of PPAR γ in both SAT and VAT (Fig. 3.3 A-B, representative blot). There was no alteration in level of PPAR γ protein in VAT (Fig. 3.3 C; quantified blot) but it was confirmed to be decreased in the SAT ($P < 0.01$; Fig. 3.3 D; quantified blot) of adolescent females exposed to increased concentration of TP *in utero*.

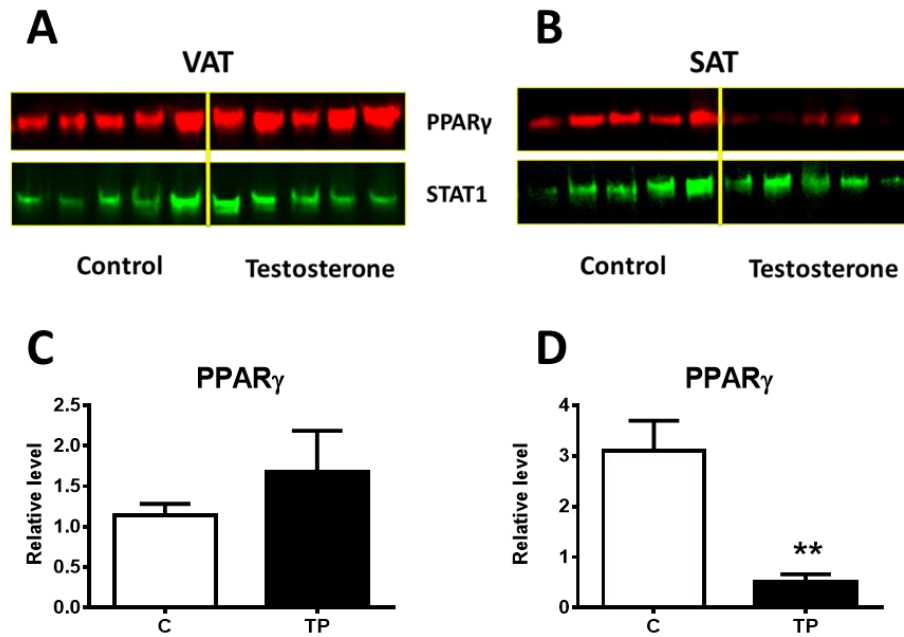


Figure 3.3 PPAR γ protein level in VAT and SAT samples of adolescent control (C) and prenatally androgenised (TP) female sheep, as quantified by Western blot. P value of < 0.05 was considered as statistically significant. Results are presented as mean + S.E.M, where ** signifies a $P < 0.01$.

3.3.2 Link between altered adipogenesis and dyslipidaemia

Downregulated expression of *PPARG* and *C/EBP* family of transcription factors suggested decreased differentiation of preadipocytes into mature adipocytes in SAT of TP exposed adolescent sheep. This consequently could lower capacity of SAT to safely store fat. SAT depot is the main source of FFA, and plasma FFA is the main substrate for hepatic TG production. Therefore, to further evaluate link between metabolic perturbations, especially the early signs of fatty liver reported previously, and alterations in SAT, we evaluated levels of plasma fasting FFA and TG. There was no difference in the levels of plasma TG (Fig. 3.4 A), however fasting FFA levels were increased ($P < 0.05$; Fig. 3.4 B) in adolescent prenatally TP exposed sheep. Increased FFA negatively correlated with mRNA expression of *PPARG*, the master regulator of adipogenesis, in SAT ($P < 0.05$; $r = -0.55$; Fig 3.4 D), but not VAT (Fig. 3.4 C).

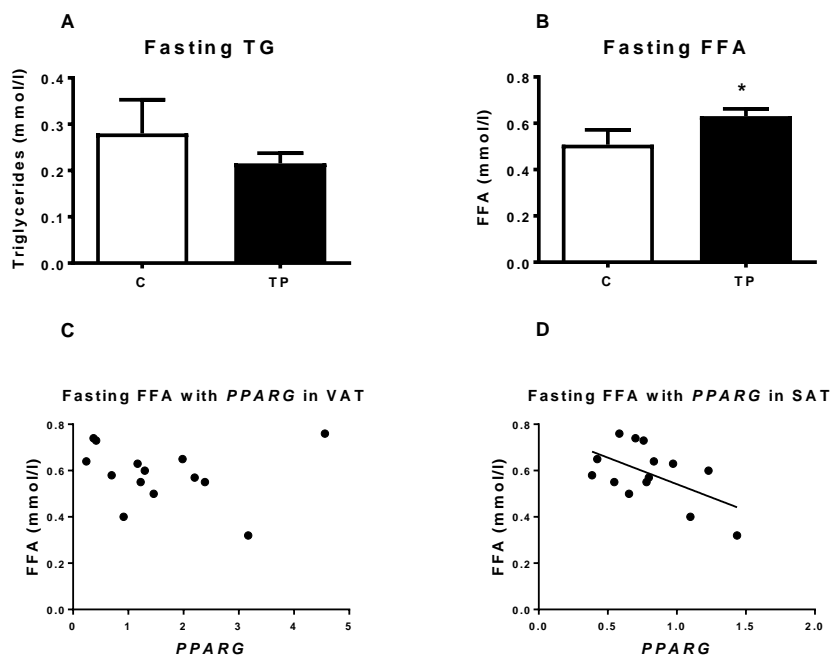


Figure 3.4 Plasma fasting TG and FFA in adolescent control (C) and prenatally androgenised (TP) animals (A-B). Correlation of plasma FFA with *PPARG* mRNA expression in VAT and SAT (C-D). P value of < 0.05 was considered as statistically significant. Results are presented as mean + S.E.M, where * signifies a $P < 0.05$.

3.3.3 Leptin and adiponectin levels during adolescence

To determine whether decreased mRNA expression of *LEP* and *ADIPOQ* in SAT has systemic consequences, levels of circulating leptin and adiponectin were measured. Prenatal androgenisation of adolescent female sheep resulted in decreased concentration of circulating leptin and adiponectin ($P < 0.05$; Fig. 3.5 A-B). In addition, it was observed that circulating leptin levels positively correlated with *LEP* mRNA levels in VAT ($P < 0.01$; $r = 0.65$; Fig. 3.6 A), not with mRNA in SAT (Fig. 3.6 B). In contrast circulating adiponectin levels positively correlated with *ADIPOQ* mRNA levels in SAT ($P < 0.01$; $r = 0.72$; 3.6 D), but not in VAT (Fig. 3.6 C).

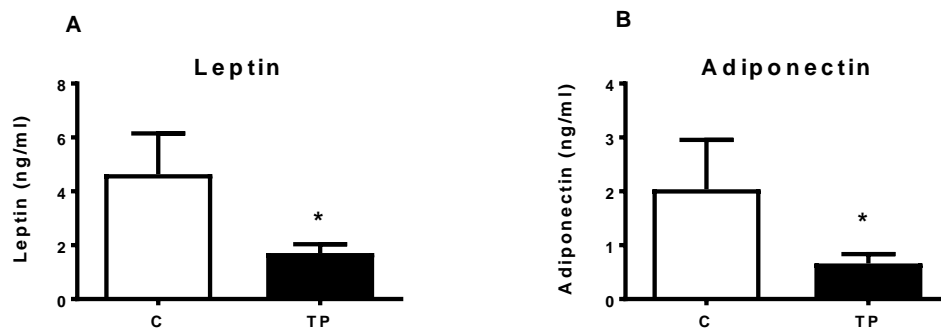


Figure 3.5 Plasma fasting leptin and adiponectin in adolescent control (C) and prenatally androgenised (TP) animals, as measured by ELISA. P value of < 0.05 was considered as statistically significant. Results are presented as mean + S.E.M, where * signifies a $P < 0.05$.

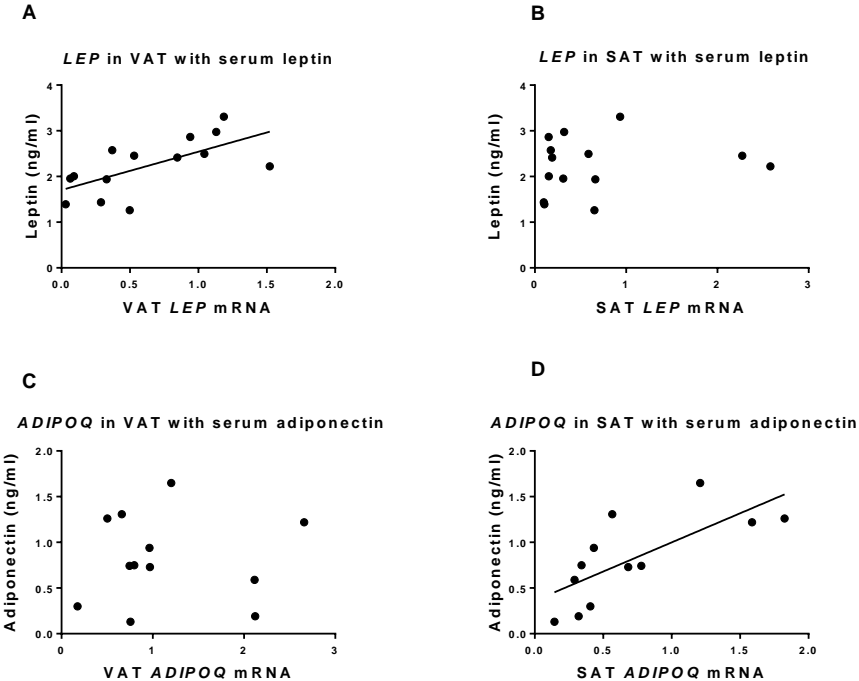


Figure 3.6 Correlation of plasma leptin and adiponectin with *LEP* and *ADIPOQ* gene expression in VAT and SAT in adolescent control (C) and prenatally androgenised (TP) animals.

3.3.4 Adiponectin and insulin signalling in adipose tissue during adolescence

Adiponectin regulates insulin sensitivity and lipid metabolism, mediating its action through adiponectin receptor 1 (ADIPOR1) and 2 (ADIPOR2). Adiponectin can act at endocrine, paracrine and autocrine levels. We therefore assessed mRNA levels of those receptors in VAT and SAT. There was no difference in mRNA expression of *ADIPOR1* and *ADIPOR2* in VAT (Fig. 3.7 A-B), however *ADIPOR2* was significantly downregulated in SAT ($P < 0.05$; Fig. 3.7 D) with no difference in *ADIPOR1* expression (Fig. 3.7 C).

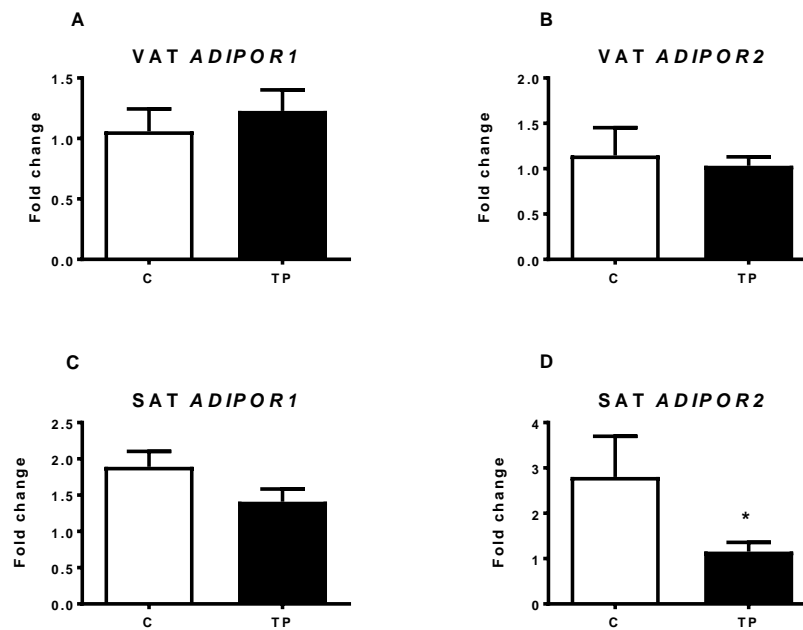


Figure 3.7 Expression of adiponectin receptors *ADIPOR1* and *ADIPOR2* in VAT and SAT of adolescent control (C) and prenatally androgenised (TP) animals, as quantified by qRT-PCR. P value of < 0.05 was considered as statistically significant. Results are presented as mean + S.E.M, where * signifies a $P < 0.05$.

To further evaluate downstream insulin signalling in adipocytes we assessed mRNA levels of *INSR*, *IRS1*, *IRS2* and *SLC2A4*, encoding GLUT4, in VAT and SAT. Exposure to increased androgens levels *in utero* resulted in decreased mRNA levels of *INSR*, *IRS2* and *SLC2A4* ($P < 0.05$; Fig. 3.8 E, F, H, respectively), but no significant change in *IRS1* (Fig. 3.8 G) in SAT, whereas there was no difference in the expression of those genes in VAT between control and TP exposed animals (Fig. 3.8 A-D).

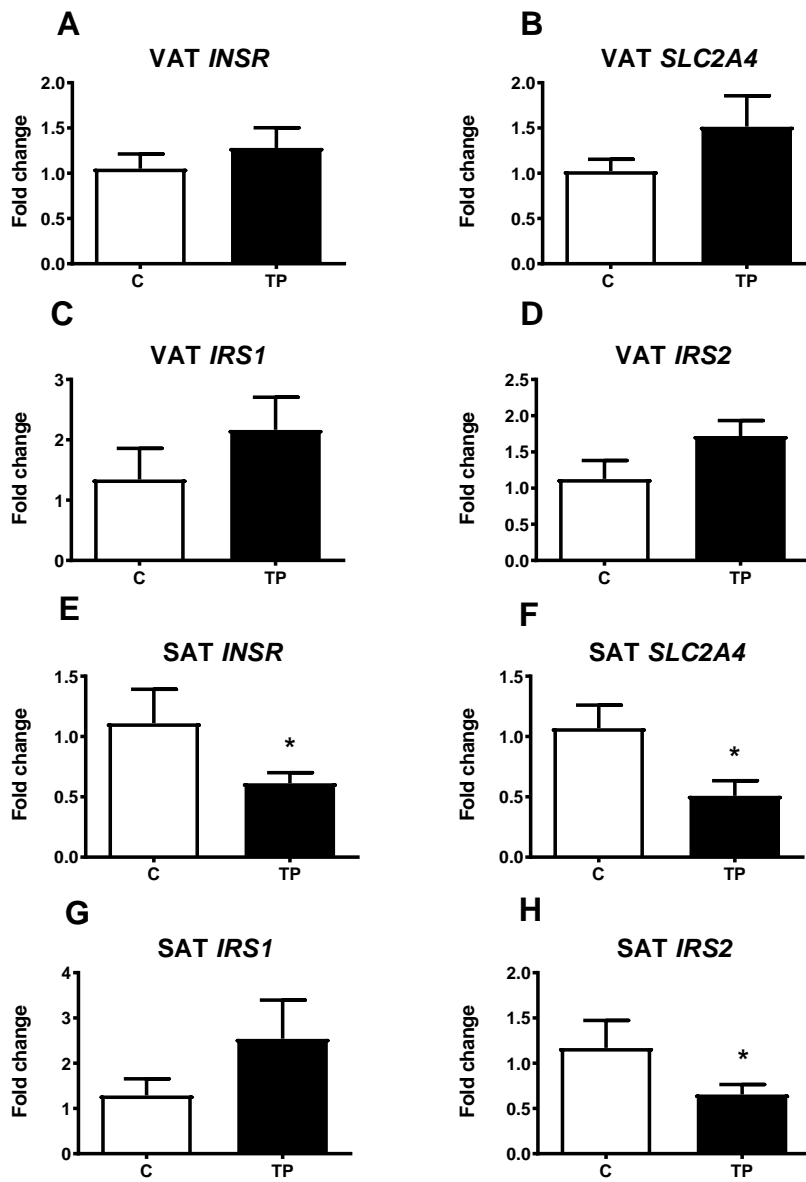


Figure 3.8 Insulin signalling in VAT and SAT of adolescent control (C) and prenatally androgenised (TP) animals, as quantified by qRT-PCR. P value of <0.05 was considered as statistically significant. Results are presented as mean + S.E.M, where * signifies a $P < 0.05$.

3.3.5 Inflammation markers in adipose tissue

It has been shown that increased levels of pro-inflammatory mediators $TNF\alpha$ and $IL6$ downregulate adiponectin expression, therefore we evaluated mRNA expression of TNF and $IL6$ in VAT and SAT of adolescent sheep. Expression of TNF was significantly upregulated in SAT of prenatally androgenised sheep ($P < 0.05$; Fig. 3.9 C) with no difference in the expression of $IL6$ (Fig. 3.9 D). There was no difference in the expression of TNF and $IL6$ in VAT (Fig. 3.9 A-B).

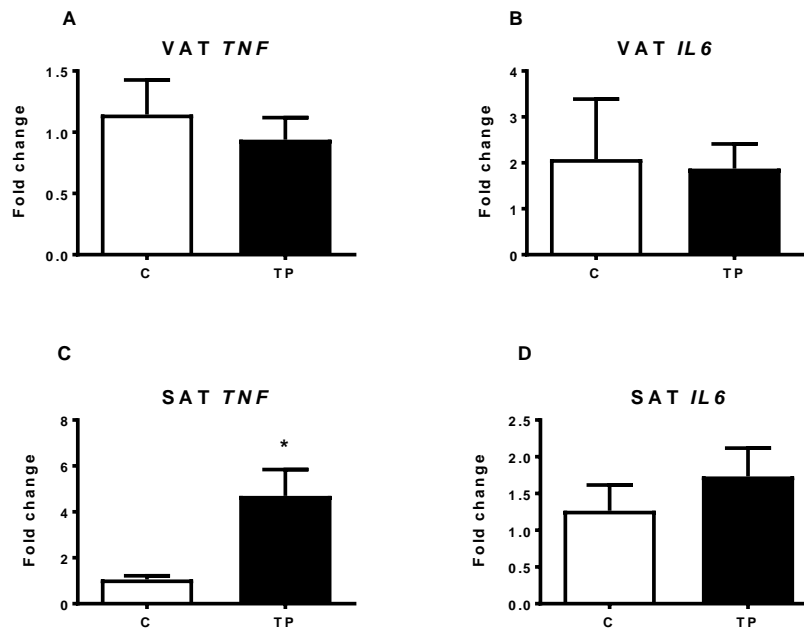


Figure 3.9 Expression of inflammation markers TNF and $IL6$ in VAT and SAT of adolescent control (C) and prenatally androgenised (TP) animals, as quantified by qRT-PCR. P value of < 0.05 was considered as statistically significant. Results are presented as mean + S.E.M, where * signifies a $P < 0.05$.

3.3.6 Adipocyte differentiation in SAT in fetal and early life.

To determine, at what stage of development we can detect changes in adipogenesis, we have investigated expression of adipogenesis markers in SAT of prenatally androgenised female fetuses and juvenile prenatally androgenised sheep. There was no difference in the expression of *PPARG*, *CEBPA*, *CEBPB* and *CEBPD* in SAT of D112 female fetuses (Fig. 3.10 A-D) and 11 weeks old juvenile sheep (Fig. 3.10 E-H).

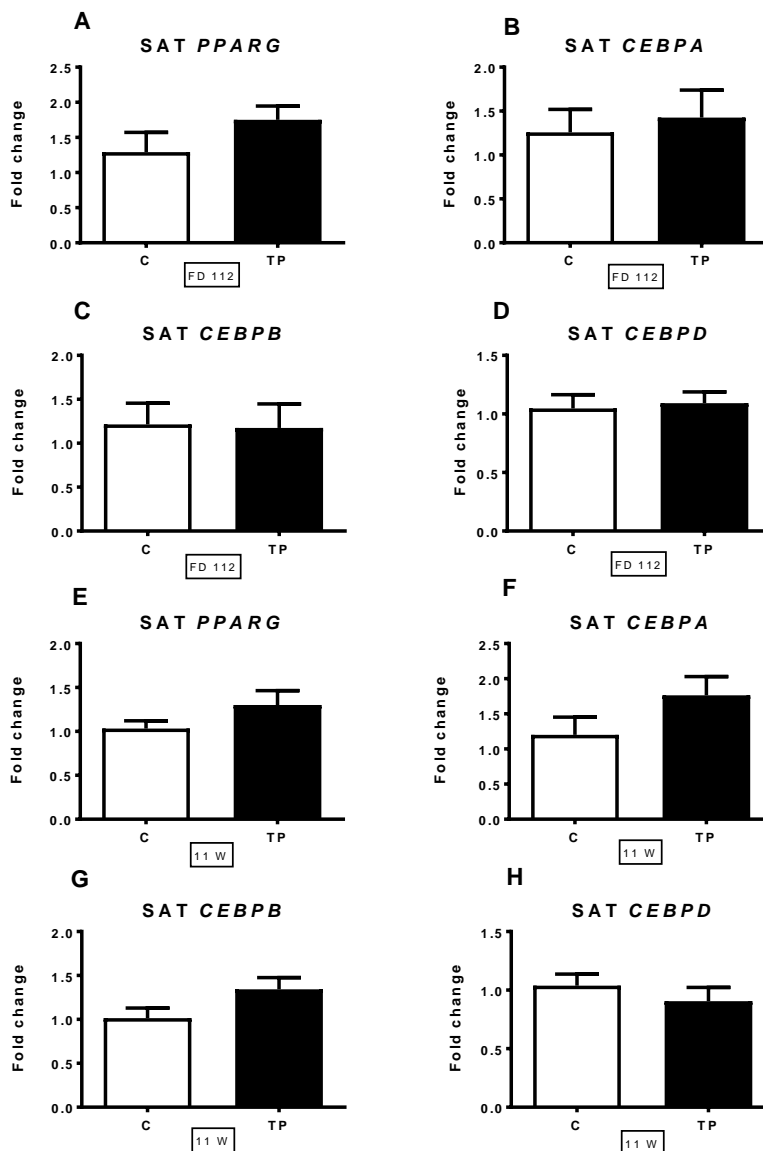


Figure 3.10 Expression of adipogenesis markers in SAT in control (C) and prenatally androgenised (TP) animals at fetal day 112 (A-D) and at 11 weeks of age (E-H), as quantified by qRT-PCR. Results are presented as mean + S.E.M.

3.3.7 Temporal androgenisation of sheep did not result in altered adipogenesis

To assess if temporal androgenisation of sheep might affect adipogenesis, we investigated expression of markers of adipogenesis in SAT of sheep treated with testosterone for two weeks. There was no difference in the expression of *PPARG*, *CEBPA*, *CEBPB* and *CEBPD* in SAT of those adolescent temporally androgenised animals (Fig. 3.11 A-D).

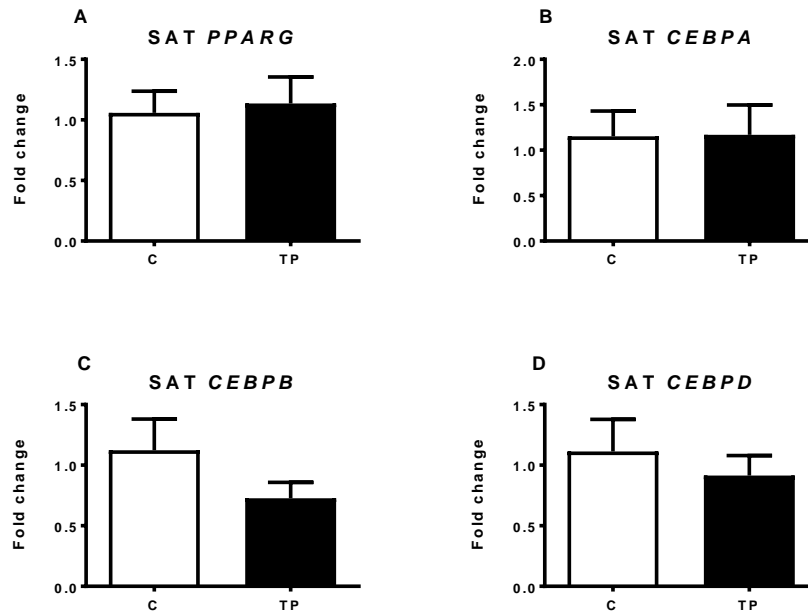


Figure 3.11 Expression of adipogenesis markers in SAT in control (C) and temporally treated with testosterone (TP) normal animals, as quantified by qRT-PCR. Results are presented as mean + S.E.M.

3.3.8 The effect of different steroid classes on adipogenesis

To establish if perturbations in adipocyte development in SAT is due to direct treatment with testosterone or indirect effect of estrogen or glucocorticoids, the effect of different steroid classes on adipocyte differentiation was assessed. To ascertain this question, we had a separate cohort of adolescent, 11 months old animals that were directly injected *in utero* with TP, DES and DEX. Direct fetal injection with DES and DEX showed no effect on the expression of *PPARG*, *CEBPA*, *CEBPB* and *CEBPD* in adolescent sheep (Fig. 3.12 A-D). In contrary, direct injection with TP resulted in decreased levels of *PPARG*, *CEBPA* and *CEBPB* ($P < 0.05$; Fig. 3.12 A-C), with no difference in the expression of *CEBPD* (Fig. 3.12 D).

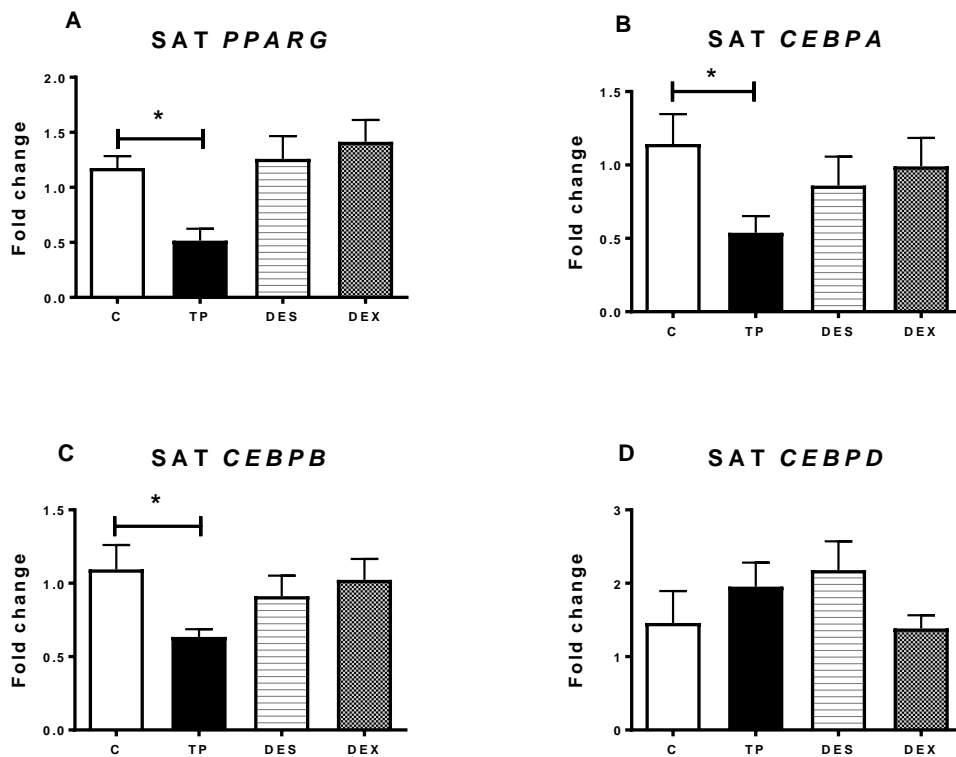


Figure 3.12 Effect of direct fetal steroid injections on the expression of adipogenesis markers in SAT in adolescent control (C), testosterone (TP), diethylstilbestrol (DES), and dexamethasone (DEX) treated animals, as quantified by qRT-PCR. P value of < 0.05 was considered as statistically significant. Results are presented as mean + S.E.M, where * signifies a $P < 0.05$.

3.3.9 Metabolic parameters of adult prenatally androgenised sheep

In adulthood, at 24 and 30 months of age, PCOS-like sheep had increased body weight when compared with control animals (C: $79.73 \pm 1.57\text{kg}$; TP: $85.75 \pm 0.75\text{kg}$) ($P < 0.05$; Fig. 3.13 A), and trend towards increased total abdominal adiposity however, this did not reach statistical significance (C: $1.37 \pm 0.15\text{kg}$; TP: $1.62 \pm 0.23\text{kg}$) (Fig. 3.13 B).

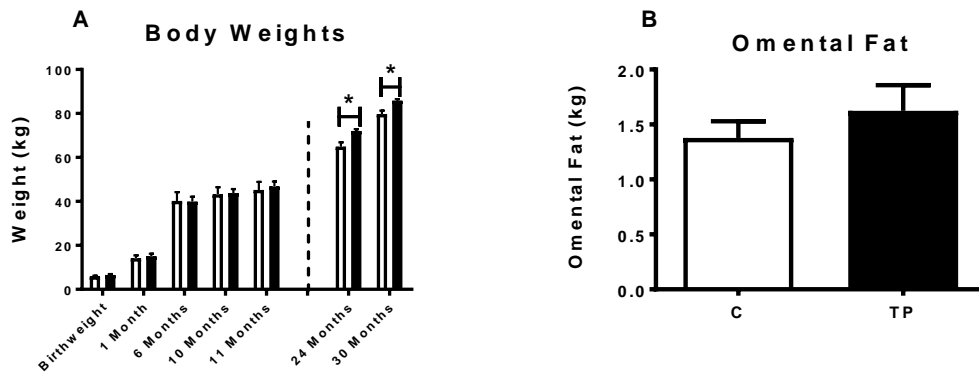


Figure 3.13 A) Birthweight and postnatal weight in control (white bars) and prenatally androgenised animals (black bars). B) Weight of omental fat in adult controls (C) and prenatally androgenised animals (TP), as excised and weighed during the animals' dissection. Results are presented as mean + S.E.M, where * signifies a $P < 0.05$.

Adult, prenatally androgenised animals had increased basal (fasting) insulin concentrations and decreased basal G:I ratio ($P < 0.05$; Fig 3.14 A and B, respectively), suggesting decreased insulin sensitivity. Over the duration of the 45 minutes IVGTT there was no difference in AUCglucose (Fig. 3.14 C), however AUCinsulin was significantly elevated in TP exposed adult ewes as compared to vehicle controls ($P < 0.05$; Fig. 3.14 D).

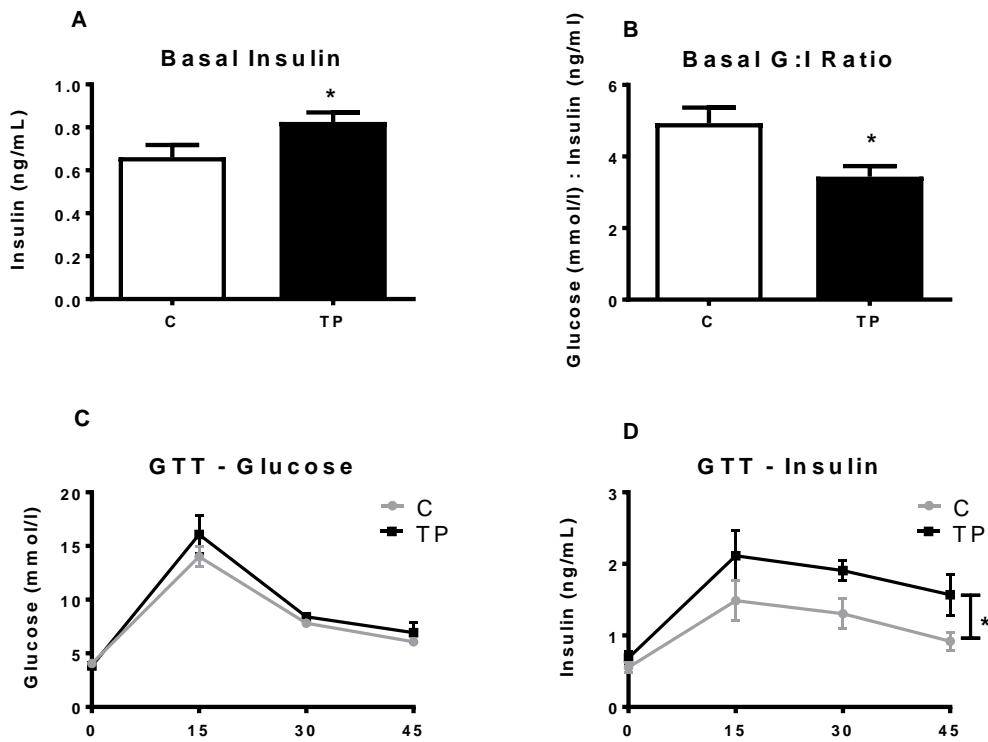


Figure 3.14 Effect of prenatal androgenisation on A) Fasting glucose B) Fasting insulin C) Glucose dynamics during 45 min IVGTT and D) Insulin dynamics during 45 min IVGTT. P value of <math><0.05</math> was considered as statistically significant. Results are presented as mean + S.E.M, where * signifies

3.3.10 Markers of adipogenesis in adult SAT and VAT

We next investigated expression of adipogenesis markers in adult VAT and SAT. There were no differences in the expression of *PPARG*, *CEBPA*, *CEBPB* and *CEBPD* in adult both VAT (Fig. 3.15 A-D) and SAT (Fig. 3.16 A-D). There were also no differences in the mRNA expression of selected markers of fully differentiated adipocytes (*ADIPOQ* and *LEP*) in VAT and SAT (Fig. 3.15 E-F and 3.16 E-F, respectively).

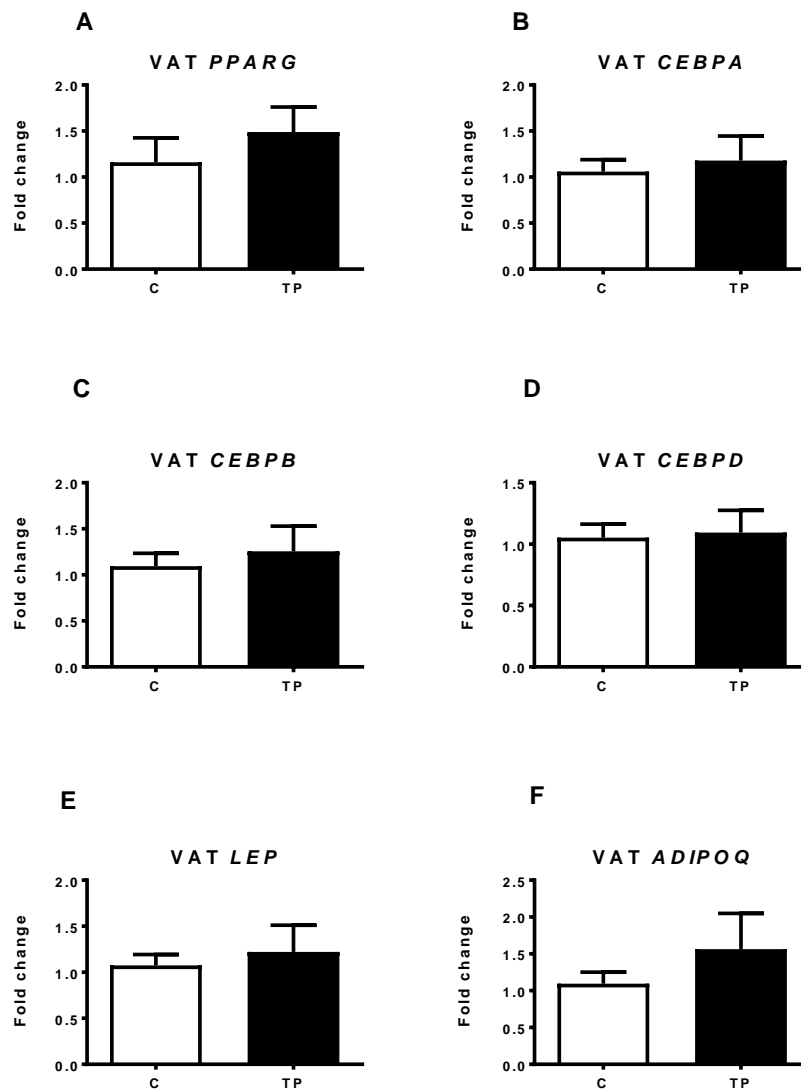


Figure 3.15 Adipogenesis markers expression in VAT in adult female controls (C) and prenatally androgenised (TP) ewes, as quantified by qRT-PCR. Results are presented as mean + S.E.M.

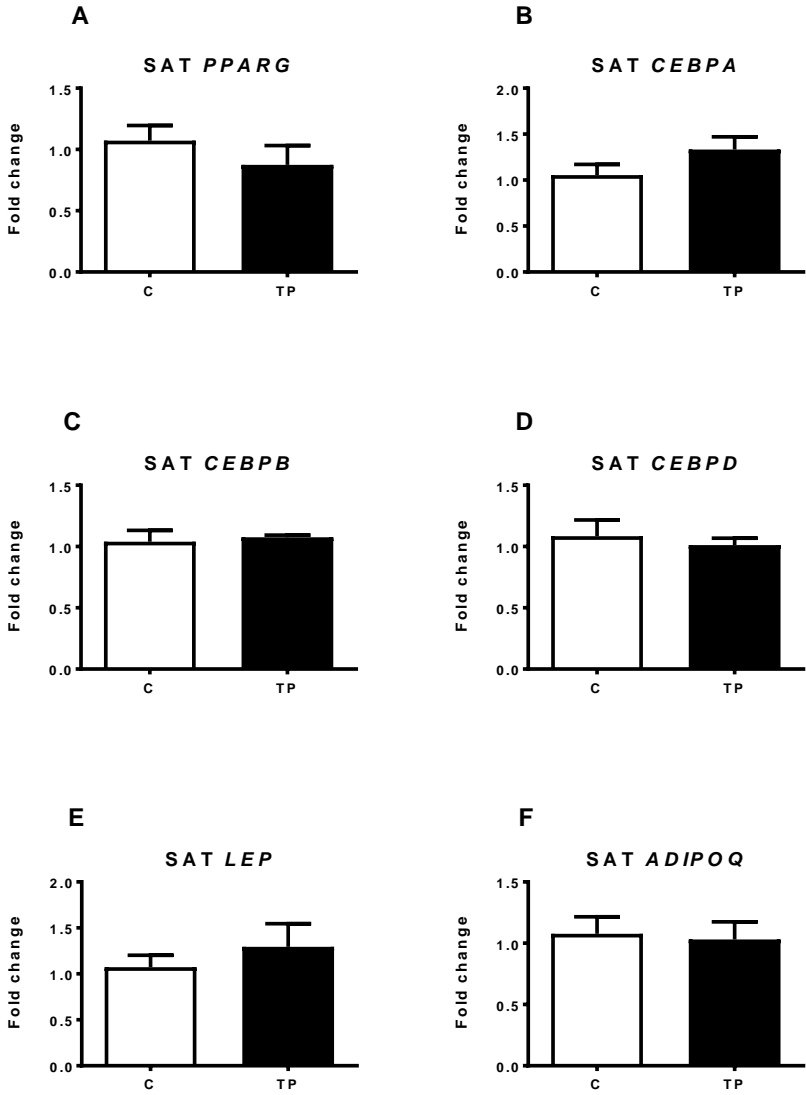


Figure 3.16 Adipogenesis markers expression in SAT in adult female controls (C) and prenatally androgenised (TP) ewes, as quantified by qRT-PCR. Results are presented as mean + S.E.M.

3.3.11 Histological analysis of VAT and SAT

We next performed histological analysis of adult VAT and SAT. Images of representative visceral and subcutaneous sections from control and PCOS-like animals are shown in Fig. 3.17. The mean numbers of adipocytes analysed in visceral and subcutaneous adipose tissue were 1923 ± 111 and 4028 ± 197 cells/animal, respectively. Adipocytes numbers were stratified according to 3 size categories: small ($<1000\mu\text{m}^2$), medium ($1000\text{-}5000\mu\text{m}^2$) and large ($>5000\mu\text{m}^2$). Results from morphometric analysis of adipocytes revealed that although there was no statistically significant difference in the mean size of SAT adipocytes between C and TP animals ($P=0.06$; Fig. 3.18 D), there was increased number of large adipocytes in SAT of TP-exposed animals when compared to vehicle treated controls ($P<0.05$; Fig.3.18 E) and consequently decreased number of total adipocytes per mm^2 of section analysed ($P<0.05$; 3.18 B). There was no alteration in adipocyte size or total number in VAT of adult PCOS-sheep (Fig. 3.18 C, E and A, respectively).

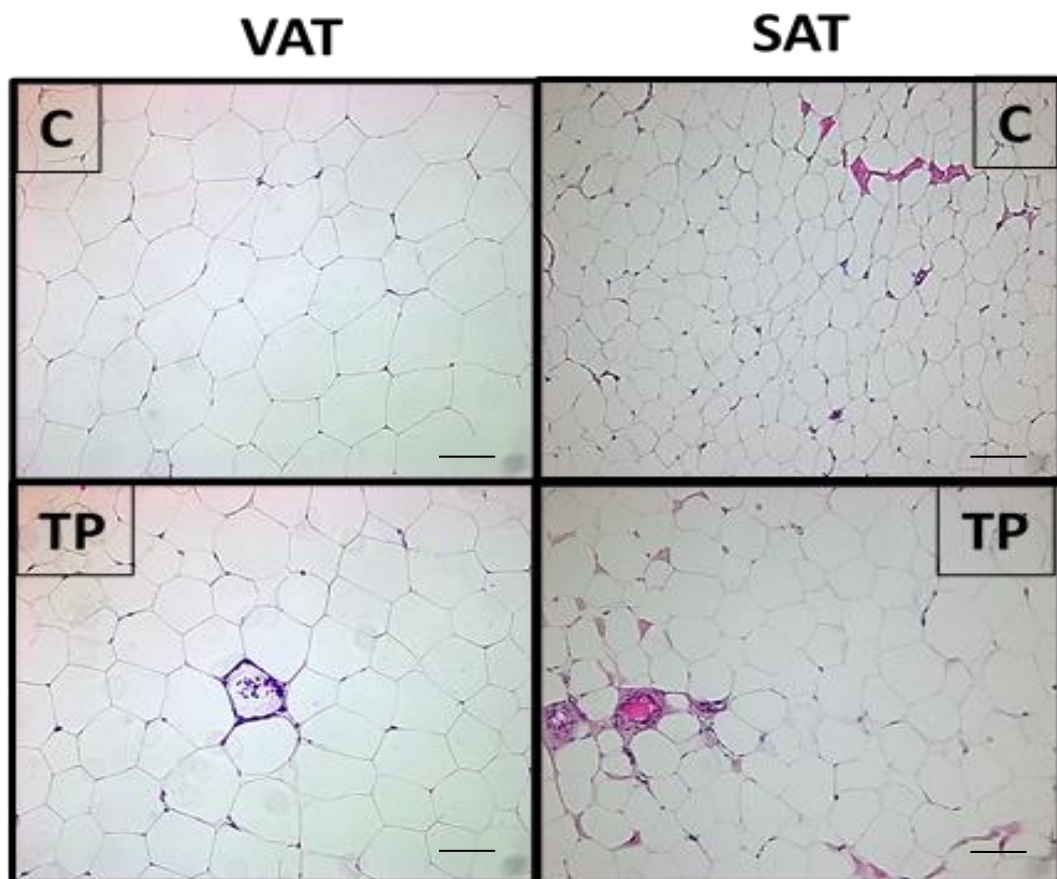


Figure 3.17 Representative adipose tissue sections from VAT and SAT of adult control (C) and prenatally androgenised animals (TP); scale bars = $100\mu\text{m}$.

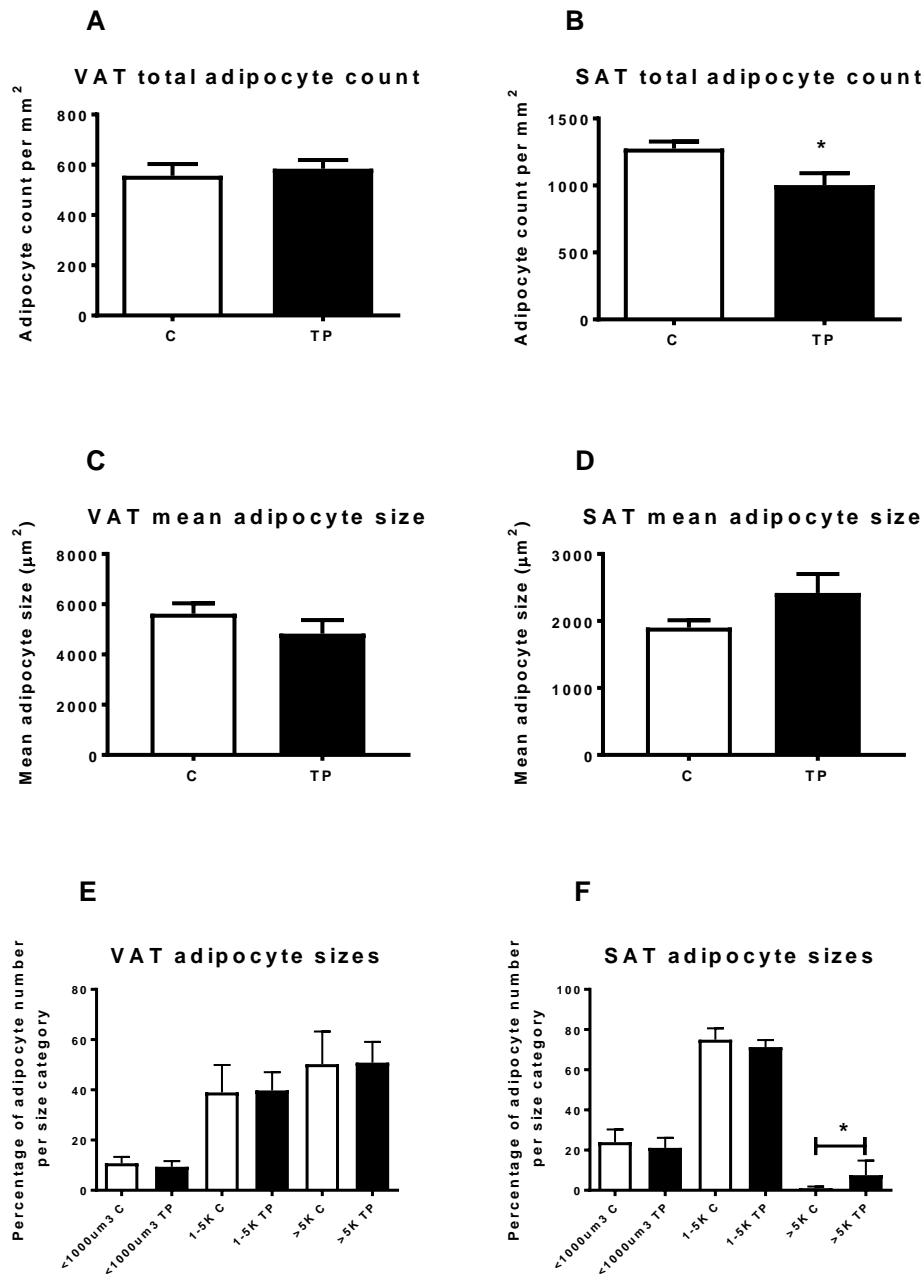


Figure 3.18 Total adipocyte count per mm² in A) VAT and B) SAT. Mean size of adipocytes in C) VAT and D) SAT. Percentage of adipocyte per size category in A) VAT and B) SAT. Two sections per sample were analysed in adult control (C) and prenatally androgenised animals (TP). P value of <0.05 was considered as statistically significant. Results are presented as mean + S.E.M, where * signifies a P<0.05.

3.3.12 Consequences of adipocyte hypertrophy in adult SAT

Adult, TP-exposed animals had increased levels of fasting FFA when compared to controls ($p < 0.05$; Fig. 3.19 A) and there was negative correlation between total number of subcutaneous adipocytes and levels of circulating FFA ($p < 0.05$; $r = -0.61$; Fig. 3.19 B). In addition, expression of inflammation markers *TNF* and *IL6* as well as *CCL2*, encoding MCP-1 protein, was significantly upregulated in SAT ($p < 0.05-0.01$; Fig. 3.20 D-F) but not VAT (Fig. 3.20 A-C) of adult, prenatally androgenised sheep.

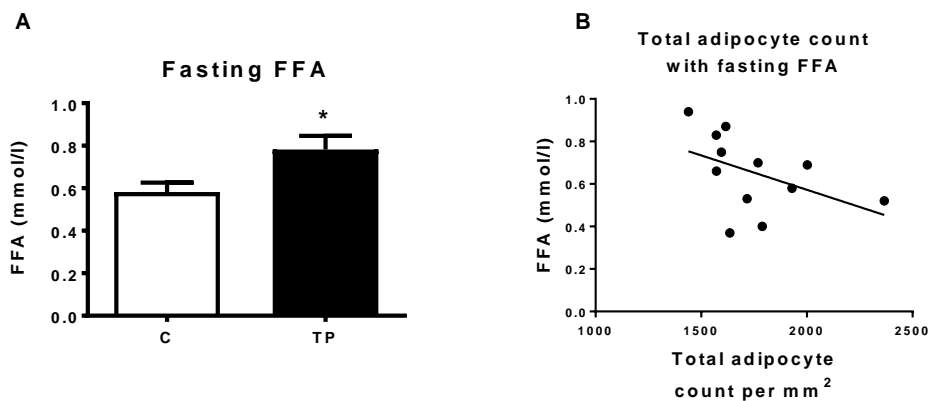


Figure 3.19 A) Fasting plasma FFA in adult control (C) and prenatally androgenised animals (TP); B) correlation of FFA with total adipocyte count per mm² in SAT of adult C and TP animals. P value of < 0.05 was considered as statistically significant. Results are presented as mean + S.E.M, where * signifies a $P < 0.05$.

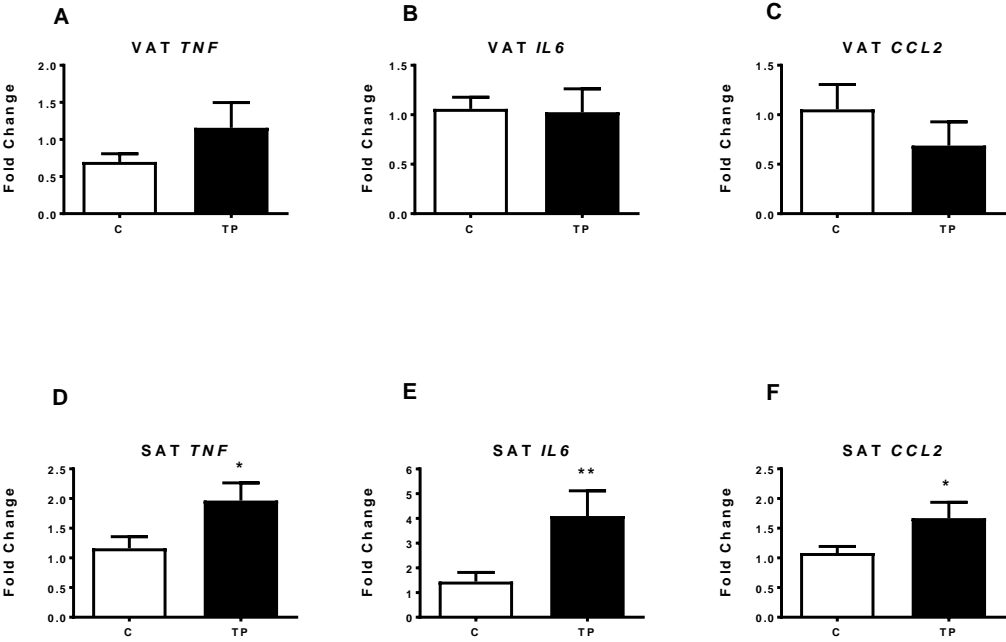


Figure 3.20 Expression of inflammation markers in VAT and SAT in adult control (C) and prenatally androgenised animals (TP), as quantified by qRT-PCR. P value of <0.05 was considered as statistically significant. Results are presented as mean + S.E.M, where * signifies a P<0.05, ** P<0.01.

3.4 Discussion

PCOS is characterised by a broad spectrum of symptoms, with insulin resistance, obesity and increased visceral adiposity playing significant role in its pathophysiology. Furthermore, metabolic problems of women with PCOS worsen with age. It is widely accepted that the degree of insulin resistance increases in parallel with excessive fat mass. However, lipodystrophic patients with insulin resistance or obese people with an otherwise overall healthy profile seem to contradict that. Therefore, it has been postulated that individual capacity for adipose tissue expansion to safely store caloric excess is more essential in determining metabolic health than total fat mass (458). This hypothesis is further supported by studies in animal models, where genetically modified mouse with limitless capacity for adipose tissue expansion remains insulin-sensitive and has no signs of fatty liver, despite having 50% body weight increase (459).

Our lab reported previously that adolescent, 11 months old prenatally androgenised female sheep, were hyperinsulinemic and had early fatty liver changes with no difference in body weight or central obesity (411). We have now found that mRNA and protein expression of *PPARG*, the master regulator of adipogenesis, as well as *CEBPA* and *CEBPB* are downregulated in SAT, but not VAT, in adolescent prenatally TP-exposed animals. This finding suggests decreased differentiation of preadipocytes into mature adipocytes. Interestingly, only the expression of *CEBPD* in SAT was unaltered. Adipocyte differentiation is regulated by sequential expression of adipogenic factors. Early stage of preadipocyte differentiation is marked by increased expression of *CEBPB* and *CEBPD*, which in turn promote expression of *CEBPA* and *PPARG* in the late stage (460). When expressed, *CEBPA* and *PPARG* act in the feedback loop to sustain their expression and direct adipocytes toward terminal differentiation (461). This is accompanied by expression of adipocyte-specific genes such as *SLC2A4*, *LEP* and *ADIPOQ*. No reduced expression of *CEBPD* might suggest that late stage of adipocyte differentiation, rather than early, is affected in SAT of adolescent PCOS-like sheep. Decreased adipogenesis indicates lower capacity of SAT to safely store fat. We also found increased levels of FFA in these animals, which supports evidence for decreased lipid storage volume in SAT. This could potentially explain presence of fatty liver and hyperinsulinemia in the adolescent TP-treated animals, due to increased release of FFA into circulation, subsequent lipotoxicity and decreased insulin sensitivity in peripheral tissue. Unfortunately, we were unable to perform morphological analysis of SAT from 11 month old animals. However, our findings are with agreement with these reported by Keller *et. al* and Veiga-Lopez *et. al.* where perturbed differentiation of subcutaneous adipocytes in prenatally

androgenised female monkeys and sheep were reported, respectively. (462,463). This finding is further supported by studies using the thiazolidinedione class of antidiabetic drugs which are also potent stimulators of adipose tissue differentiation. It has been shown that these drugs ameliorate NAFLD and reduce FFA by promoting adipose tissue expansion (464).

We further investigated at what stage of development we could detect changes in adipocyte differentiation. We did not find any difference in the expression of adipogenesis markers in prenatally androgenised female fetuses during late gestation or in juvenile sheep, suggesting that altered adipogenesis correlates with onset of puberty. There was also no difference in the expression of adipogenesis markers in adult life. This is in agreement with recent findings, showing that number of adipocytes is set during childhood and adolescence, and stays constant in adulthood, with 10% annual turnover, independent of BMI (465). Several studies have now shown that increase or decrease in body weight with corresponding fluctuations in body fat mass leads to changes in adipocyte volume but not the number (128,465-468). SAT represents about 80% of total body adipose tissue and given constant adipocyte number in adulthood, decreased SAT adipogenesis in adolescents would result in decreased storage capacity in adulthood and increased lipid storage in already developed adipocytes, resulting in hypertrophy. This is in agreement with our findings, showing that adult PCOS-like sheep have decreased total number of adipocytes in SAT with a corresponding increase in large, hypertrophic adipocytes. Enlarged adipocytes are less insulin sensitive and individuals with hypertrophic adipocytes in SAT are more insulin resistant than people with comparable adiposity but smaller adipocytes (469-471). In addition, hypertrophic expansion of SAT is associated with altered adipokine secretion, inflammation and fibrosis (461). Interestingly, adult PCOS women were reported to have enlarged subcutaneous adipocytes, lower serum adiponectin levels and lower adipose tissue LPL activity compared to age and BMI matched controls (231,472). In addition, Manneras-Holm *et al.* noted that women with PCOS had increased waist-to-hip ratio compared to BMI matched controls, without differences in abdominal adipose tissue volume, as measured by MRI, potentially suggesting that these women might have lower volume of gluteofemoral adipose tissue (472). Therefore, it can be hypothesised, that due to decreased capacity of SAT in PCOS women and sheep, even normal caloric intake could be relatively excessive, eventually resulting in SAT hypertrophy, leading to subsequent increase in visceral adiposity and insulin resistance. Results from this study support this hypothesis. Despite being on a normal, healthy diet, our experimental, prenatally androgenised animals become obese in their early adulthood, have a trend for increased visceral adiposity, have increased fasting FFA and are hyperinsulinemic. Furthermore, we can

speculate that if these animals were fed a high fat diet, we would observe a faster and exaggerated metabolic perturbations.

Adipogenesis in PCOS patients has not been investigated however, there is growing evidence of decreased adipogenesis in SAT from insulin resistant individuals and subjects with abdominal obesity (473-475). A recent study investigating genome-wide gene expression and DNA methylation in SAT from PCOS women, reported decreased mRNA expression and increased DNA methylation of the *PPARG* gene (476). Authors also reported that *PPARG* gene expression was positively correlated with insulin sensitivity and negatively correlated with adipocyte size and testosterone levels although association was diminished after adjustment for BMI (476). *PPARG*, the master regulator of adipogenesis, also controls gene expression related to a broad spectrum of physiological processes including insulin signalling, adipokine production, lipid transport and metabolism, macrophage function and immunity (477). It has been shown that there is 2-fold higher expression of *PPARG* in SAT than in VAT, *PPARG* adipogenic potential *in vitro* in VAT is reduced, and that *PPARG* agonists cause expansion of SAT, but not VAT (478-480). This evidence suggests that *PPARG* might play a more central role in regulating adipogenesis in SAT rather than VAT, possibly explaining why adipocyte differentiation is only affected in SAT in adolescent PCOS-like sheep.

Decreased expression of *LEP* and *ADIPOQ* in SAT of adolescent prenatally androgenised animals suggest higher number of undifferentiated adipocytes, since these genes are expressed in mature adipose cells. In addition, we found that levels of circulating leptin and adiponectin were correspondingly decreased in adolescent PCOS-like sheep. There was positive correlation of *ADIPOQ* mRNA in SAT, but not VAT, with circulating adiponectin, whereas circulating leptin correlated with *LEP* mRNA in VAT but not SAT. Degawa-Yamauchi *et al.* also reported similar associations, with *ADIPOQ* mRNA in human female SAT, but not VAT, being positively correlated with circulating adiponectin and negatively correlated with BMI, and *LEP* mRNA in VAT correlating with adiposity (481). Therefore, these findings indicate that circulating leptin levels are strongly associated with visceral adiposity, however, we observed decreased leptin levels without significant difference in visceral adiposity in adolescent TP-exposed animals, and therefore it is possible that decreased expression of *LEP* mRNA in SAT impact circulating leptin levels. Leptin is an important adipokine, suppressing food intake, promoting energy balance and regulating body weight. Therefore, low levels of leptin during puberty in TP-exposed sheep might contribute to increased body weight and adiposity in adult PCOS-like animals. Given that there is positive correlation between *ADIPOQ* mRNA in SAT and circulating adiponectin, decreased adiponectin levels might be a

consequence of decreased adipogenesis in SAT of adolescent PCOS-like sheep. This finding is further supported by evidence that both adiponectin and leptin levels are decreased in lipodystrophic patients (482). Adiponectin, primarily secreted from SAT, is an insulin sensitising adipokine, promoting lipid oxidation, inhibiting hepatic gluconeogenesis and reducing plasma concentrations of FFA (483-485). Adiponectin also stimulates glucose uptake in adipocytes by increasing mRNA and translocation of *SLC2A4* (GLUT4), therefore low levels might contribute to insulin resistance (486). Adiponectin was also reported as an autocrine factor regulating adipocyte differentiation and promoting cell differentiation (486,487). Adiponectin levels negatively correlate with BMI, however, decreased circulating adiponectin levels, independent of adiposity, are recurrently reported in adolescent and adult PCOS patients (321,322,448,488-490), suggesting its potential use as a biomarker of PCOS (491-493). As recently reviewed by Li *et al.* there is inconsistent data with regards to relationship of adiponectin and androgen levels in PCOS (236). However, there is evidence that androgens decrease plasma adiponectin *in vitro* and *in vivo* (115,494) and that testosterone administration decreases adiponectin level in men and in female to male transsexuals (495-497). Gender differences in adiponectin levels in adolescence were also described, with significantly lower adiponectin levels in adolescent boys compared with girls, and adiponectin being inversely correlated with testosterone levels (498,499), therefore it is possible that androgens may play a role in dysregulation of adiponectin levels. Simultaneously, the relationship between adiponectin and testosterone concentrations in PCOS women could reflect the direct effect of adiponectin on ovarian steroidogenesis. Adiponectin decreases the production of androgens in theca cells *in vitro* and expression of adiponectin receptors is decreased in theca cells from polycystic ovaries, consequently low levels of adiponectin may contribute to hyperandrogenism in PCOS women (237,500,501). Our group have previously reported enhanced androgen synthesis capacity in theca cells from adolescent PCOS-sheep therefore, it is likely that decreased adiponectin levels in that sheep might contribute to hyperandrogenism during later life (412). Insulin is also implicated as a potential regulator of adiponectin expression, however the exact relationship between insulin and adiponectin is not fully elucidated. Motoshima *et al.* found that insulin stimulates adiponectin secretion from human omental cells but not subcutaneous cell *in vitro* (502). In contrast, study by Fasshauer *et al.* reported that insulin reduced adiponectin mRNA in 3T3-L1 adipocytes in dose- and time dependent manner (503). In addition, it has been shown that hyperinsulinemia reduces circulating levels of adiponectin under euglycemic conditions (504) and that fasting plasma levels of insulin are an independent determinant of plasma adiponectin in multivariate regression analysis (505). Liu and colleagues demonstrated in an *in vitro* study using porcine

adipocytes that insulin inhibits the expression of adiponectin receptors *ADIPOR2* and that rosiglitazone, the PPAR γ agonist, increases the expression of *ADIPOR2* (506). This is in agreement with our findings. We found decreased expression of *PPARG* and *ADIPOR2* in SAT of adolescent PCOS-like sheep, whereas in the previous studies it was demonstrated that these adolescent PCOS-like sheep are hyperinsulinemic, and that altered pancreatic phenotype with increased β -cell numbers may be the primary reason for that increased insulin levels (431). Therefore, it is likely that hyperinsulinemia contributes to the decreased level of adiponectin and that decreased concentrations of adiponectin might exaggerate hyperinsulinemia and lead to insulin resistance in future. Interestingly, we did not observe any difference in the mRNA and circulating level of adiponectin in adult PCOS-like animals. Since low levels of adiponectin are being reported in adolescent and adult PCOS patients, we hypothesise that normal adiponectin levels in adult PCOS-like animals might result from a temporary increase, as a consequence of transition from adolescent to adulthood with an early increase in visceral adiposity, which might contribute to circulating levels of adiponectin. We have also found upregulated expression of *TNF* but not *IL6* in SAT of adolescent prenatally androgenised sheep. Increased levels of TNF α and IL-6 in adipose tissue are typically associated with obesity, hypertrophic adipocytes, inflammation and decreased insulin sensitivity, however, our adolescent PCOS-sheep have normal body weight. Increased TNF α levels have been shown to downregulate adiponectin, and conversely, adiponectin has been shown to decrease levels of inflammatory cytokines, including TNF α , thus it is possible that increased *TNF* expression in adolescent SAT might be the result of a cross-talk with adiponectin, rather than marker of inflammation (485). In adult PCOS-like sheep however, in SAT, but not VAT, there was increased expression of *TNF*, *IL6* and *CCL2* that paralleled adipocyte hypertrophy. It has been proposed that enlarged adipocytes overexpress MCP-1 (*CCL2*) and this induces increased recruitment of proinflammatory M1 macrophages from the blood stream. This in turn increases the production of pro-inflammatory cytokines TNF α and IL-6, promoting altered gene expression and insulin resistance in adipocytes (121).

While there is substantial evidence that hormones are involved in the adipose tissue distribution, hormonal influence on adipogenesis is not fully understood. There is a sex-specific difference in body fat distribution, with women having higher percentage of body fat than men, and preferentially accumulating fat in gluteofemoral region while men tend to have a larger intra-abdominal fat mass. Estrogen promotes accumulation of subcutaneous fat and inversely correlate with visceral adiposity (507). In post-menopausal women there is a redistribution of fat depots with increasing amounts of visceral fat, suggesting that decreasing levels of estrogen may play a role (507). However, since estrogen regulates SHBG (508),

decreased levels of estrogen might result in reduced levels of SHBG and consequently increased levels of free testosterone. Indeed, there are some reports showing that androgen levels are elevated during the menopausal transition (509). Androgens, like estrogens, impact on body fat distribution in humans. In men, low testosterone levels are associated with visceral obesity and metabolic syndrome, and testosterone treatment in hypogonadal men results in decreased adiposity and improved metabolic characteristics. However, supra-physiological androgen treatment in case of female-to-male transsexuals has opposite effects, resulting in increased weight and visceral adiposity (144,510). Interestingly, Elbers *et al.* reported that 1-year treatment with estrogens and antiandrogens in male-to-female transsexuals, SAT volume and adipocyte size were increased together with decreased lipolytic activity (510). The opposite was seen in female-to-male transsexuals, after administration of testosterone for 1 year, SAT and adipocyte size at the gluteal and abdominal depots were decreased, whereas lipolysis was increased significantly at the abdominal level but not at the gluteal level (511). Interestingly, we did not observe any difference in the expression of adipogenesis markers, total adiposity or body weight (data not published) in our adult female sheep temporally treated with testosterone for 2 weeks. This might suggest that only prolonged treatment with testosterone can impact on adipocyte differentiation or, as discussed earlier, it might be related to the accelerated adipogenesis during puberty. Glucocorticoids also play a role in body fat distribution. Elevated levels of circulating cortisol are linked with increasing central, especially visceral adiposity (512). In addition to the adrenal production, local production of cortisol in adipose tissue increases correspondingly with increasing body weight (512). Therefore, to evaluate which class of steroids could affect adipocyte development, we assessed adipogenesis in adolescent, 11 months old female sheep that were directly injected *in utero* with TP, DES and DEX. We found that TP treatment decreased the expression of markers of adipocyte development. This is in agreement with previously published studies since inhibitory effect of androgens on adipogenesis is well documented. Numerous studies have shown that T, DHT and DHEA prevented *in vitro* differentiation and proliferation of various murine preadipocyte cell lines (513-515) and human preadipocytes from both sexes, and from different fat depots (228,516-518). This anti-adipogenic effect was mediated through AR-dependent pathways, since adding AR antagonists blocked this action (513,515). We also found that direct fetal injection with DES showed no alteration in the expression of *PPARG*, *CEBPA*, *CEBPB*, and *CEBPD* in adolescent sheep. There are some conflicting data regarding effect of estrogens on adipogenesis. It has been shown that treatment of 3T3-L1 adipocytes, and ovariectomised mice, with 17 β -estradiol resulted in downregulated expression of adipogenesis-related genes (519). Likewise, 17 β -estradiol decreased the expression of the

adipocyte marker genes and inhibited adipogenesis in ovariectomised rat models and mouse embryonic fibroblasts (520). Interestingly, 17 β -estradiol was also reported to increase proliferation of human (521) and female rat preadipocytes (522).

We did not observe any effect on adipogenesis with DEX treatment. It is well documented that glucocorticoids (GCs) stimulate adipogenesis, however, mechanisms through which GCs regulate adipocyte development are not fully understood. GCs were described to stimulate preadipocyte commitment rather terminal differentiation (523,524) and to prime preadipocytes to adipogenic stimuli through sensitising to insulin signalling. Additionally, it was reported that DEX does not induce adipogenesis alone but rather increase recruitment of adipose progenitors (525). There are also some implications that adipogenic action of GCs might be also depot-specific. It has been shown that GCs treatment of rats increases VAT but not SAT, through upregulating of adipocyte differentiation rather than hypertrophy (526). Unfortunately, we only studied expression of markers of terminal differentiation and did not investigate expression of markers of adipocyte commitment. We also did not investigate markers of adipogenesis in VAT from animals directly treated with steroids therefore we are unable to fully assess effect of glucocorticoids in our model. Nevertheless, adipogenesis was decreased during puberty in PCOS-like sheep therefore it is more likely that hormonal levels during this period will play a significant role in regulating adipocyte differentiation. We know from our previous studies that adolescent PCOS-like sheep have normal levels of systemic cortisol (data not published), estrogen and non-significant increase in systemic testosterone with significantly enhanced capacity for androgen synthesis in theca cells (412) and adrenal glands (data not published). What is more, it has been shown that local testosterone synthesis is increased, while local synthesis of estrone, estradiol and DHT is decreased in SAT of PCOS women (229). Therefore, this data suggests that increased levels of local and systemic testosterone or imbalance in androgen/estrogen ratio might be responsible for the downregulated adipogenesis in SAT of adolescent PCOS-like sheep.

Lean women with PCOS have the same degree of insulin resistance as obese PCOS women (527). In our study adolescent PCOS-like sheep had significantly lower expression of *INSR*, *SLC2A4* and *IRS2* in SAT, potentially suggesting perturbed insulin signalling. Functional glucose uptake and metabolism are central for normal adipose tissue function (461). Animal studies showed that deletion of *SLC2A4* from adipose tissue leads to systemic insulin resistance (528). In addition, *SLC2A4* is decreased in SAT of PCOS women (320) and patients with T2DM and their first degree relatives (529,530). Interestingly, *SLC2A4* is also a marker of mature adipocytes, therefore the decreased level of *SLC2A4* supports our finding of

decreased adipocyte differentiation in adolescent PCOS-like sheep. Insulin regulates growth and differentiation of adipose tissue by controlling the expression of PPARG (531). *INSR* is up-regulated during adipogenesis however, lack of *INSR* does not result in selective impairment of the adipocyte differentiation but impacts on adipocyte volume (532,533). Interestingly, acute knockdown of the *INSR* or *IRS1* and *IRS2* in 3T3-L1 adipocytes suppresses adiponectin production (532). As shown in the knockout models of *IRS1* and *IRS2* in deficient embryonic fibroblast cells and 3T3-L1 murine adipocytes, both insulin receptor substrates are required during adipocyte differentiation (532,534). The ability of *IRS1* deficient cells to differentiate into adipocytes was approximately 60% lower, and the ability of *IRS2* deficient was 15% lower than wild type cells, whereas double knockout cells (*IRS-1*^{-/-} and *IRS2*^{-/-}) were unable to differentiate into adipocytes (534). Therefore, reduced insulin signalling in SAT of adolescent PCOS-like sheep can contribute to decreased adipocyte development and reduced adiponectin levels. Though, puberty is associated with physiological reduction in insulin sensitivity, a compensatory increase in insulin secretion, and decreased levels of circulating adiponectin, however, insulin resistance is resolved at the end of pubertal transition (535,536). Our young adult 30 months old PCOS-like sheep have normal expression of *INSR* and *SLC2A4* in SAT and normal levels of circulating adiponectin, yet are still hyperinsulineamic. Likewise, adult PCOS women have reduced insulin sensitivity after pubertal transition, which worsen with age. Therefore, it is possible that combination of decreased insulin sensitivity and increased androgen levels in adolescent PCOS women and sheep, rather than insulin resistance alone, leads to decreased adipogenesis in SAT during puberty resulting in adipocyte hypertrophy in early adulthood. Sequentially this could lead to altered adipokine secretion, IR, increased body weight and visceral adiposity resulting in a deteriorating metabolic profile in future.

In summary, we have shown that altered adipogenesis in the SAT of PCOS-like sheep and decreased levels of beneficial adipokines correlate with the pubertal/adolescent stage and hyperinsulinemia, independent of central adiposity. Decreased adipocyte differentiation in adolescent PCOS-like sheep might result from mutual action of decreased insulin sensitivity and hyperandrogenemia or altered androgen/estrogen ratio. Decreased adipocyte differentiation during adolescence result in hypertrophy and inflammation of adult SAT. This consequently lowers capacity of SAT to safely store fat and potentially explain metabolic perturbations observed in PCOS-like female sheep. These provide better understanding of the pathophysiology of PCOS from puberty to adulthood and give opportunities for early clinical intervention to ameliorate the metabolic phenotype of PCOS.

Chapter 4 The effect of prenatal androgenisation on energy expenditure

4.1 Introduction

Adult, prenatally androgenised sheep had increased body weight when compared with control animals, and trend towards increased total abdominal adiposity, as discussed in chapter 3. In addition, those adult PCOS-like animals had increased insulin levels, both fasting and during 45 min IVGTT. Obesity, increased central adiposity and reduced insulin sensitivity are common characteristics of PCOS. It is estimated that as many as 61% to 80% women with PCOS are overweight or obese, depending on ethnicity and geographical location (537,538). Although, both lean and overweight women can suffer from PCOS, there is evidence showing that women with PCOS have normal lean mass but increased central and global adiposity, independent of BMI (539-542). Obesity plays a negative role in pathophysiology of PCOS, amplifying hyperandrogenism and menstrual disturbances, impacting fertility and worsening insulin resistance and hyperinsulinemia in women with PCOS (440,538). Even modest weight reduction improves menstrual cyclicality, increases ovulation rates and fertility, reduces hyperandrogenism and improves insulin sensitivity in PCOS patients (194,328,543,544). In the view of detrimental role of obesity in PCOS, weight management is a preferable first line treatment in obese patients with PCOS (545), however it seems that women with PCOS find maintaining a healthy weight particularly difficult (546-548). While the mechanisms leading to obesity in PCOS remain uncertain there are a few studies looking at energy expenditure in PCOS. There are contradictory data regarding basal metabolic rate (BMR) in PCOS patients. One study reported decreased BMR in PCOS (211), but others did not support this finding (549,550). Franks and colleagues showed that PCOS subjects, both lean and obese, have a reduced postprandial metabolic rate, as measured by continuous indirect calorimetry, when compared to BMI matched controls (212). These authors also noted that the reduced postprandial thermogenesis (PPT) correlated with decreased insulin sensitivity in PCOS patients (212). However, another study looking at PPT in PCOS patients found no difference between controls and PCOS (551), therefore, the question of whether PCOS patients are predestined to become obese, due to difference in caloric utilisation, or if obesity is only a secondary factor aggravating the condition, is still unanswered.

Obesity, a state of excessive accumulation of TG in adipose tissue, results from increased energy intake and/or reduced energy expenditure, and it is a major risk factor for development of T2DM, atherosclerosis, hypertension, heart disease, stroke, NAFLD, and dyslipidemia (552). It has been shown that even subtle perturbations in energy balance can lead to obesity. A persistent error of only 1% between input and output of energy will lead to a gain or loss of 1 kg per year (553). Basal metabolic rate, adaptive thermogenesis and physical activity are the

three main components of total energy expenditure (554). Adaptive thermogenesis protects the organism from cold exposure (non-shivering thermogenesis) and regulates energy balance by heat production from combustion of food or stored forms of energy, therefore, both environmental temperature and diet impact adaptive thermogenesis (554). It has been shown that acute and chronic cold exposure in rodents can markedly increase adaptive thermogenesis however, since humans have a broader thermoneutral zone, an ability to adjust the amount of clothing and have a much smaller surface to volume ratio than rodents, environmental temperature plays relatively small part in overall energy expenditure (554). On the contrary, diet significantly contributes to human adaptive thermogenesis. It has been shown, that acute feeding, depending on macronutrient content of the meal, can acutely increase metabolic rate by 25-40%, and that overall energy expenditure after food intake (thermic effect of food, TEF; diet induced thermogenesis, DIT; postprandial thermogenesis, PPT) accounts for up to 15% of total energy expenditure (555-557). Thus, when the organism is resting and at thermoneutrality, postprandial thermogenesis can be measured directly as heat production (direct calorimetry), or as the amount of oxygen consumption (indirect calorimetry) (554).

BAT, or brown fat, was first formally described as the 'hibernating gland' in 1551 by Conrad Gessner and over 300 years later, in 1961, identified as the main site of thermoregulatory non-shivering thermogenesis (558). BAT play an important role in adaptive thermogenesis through its capacity to heat production and energy dissipation from glucose and lipids via uncoupling proteins, mainly UCP1 (559). UCP1 is located in the inner mitochondrial membrane and its activation leads to redirection of protons from ATP synthesis, resulting in proton leakage, reduced ATP synthesis but increased energy expenditure. Brown adipocytes are characterised by rich vasculature, and abundant sympathetic nervous system (SNS) innervation, the presence of multilocular lipids droplets and densely packed large mitochondria (560). BAT thermogenesis is mainly regulated by sympathetic nervous system, where noradrenaline released from sympathetic ganglion cell terminals binds to β -adrenergic receptors on brown adipocytes, inducing their proliferation, increasing transcription and activity of *UCP1*, and mitochondrial biogenesis (561). BAT heat production however, can be also affected by other factors, such as FFA uptake and metabolism, substrate availability or oxidative phosphorylation (560). It has been pointed out that *UCP1* mRNA levels do not always reflect UCP1 activity therefore BAT function should be also evaluated by means of other parameters such as respiratory capacity or heat generation (559,562). Until recently it was thought that BAT was exclusively found in neonates, not in adults, but imaging studies using fluorodeoxyglucose-positron emission tomography (F-FDG-PET) together with computed tomography (CT) in adult humans, revealed presence of metabolically active BAT in the

clavicular, neck and sternal regions of the body (563). What is more, there is also growing evidence that there are two types of UCP1 positive thermogenic adipocytes, classical brown and beige or brite (brown in white) adipocytes, that are dispersed in WAT (559). Although sharing its main metabolic role, classical brown and beige adipocytes have distinct developmental origins as well as gene expression patterns. BAT share the same precursor cells expressing *Myf5* with skeletal muscles but BAT divergence from myoblasts is determined by expression of different transcriptional regulators, such as *PRDM16* and *C/EBP β* (564-566). In contrast, beige adipocytes do not originate from cells expressing *Myf5* and although they express the majority of BAT-enriched genes, such as *UCP1*, *PPARGC1A* and *PRDM16*, they also have distinct beige cell markers, such as *TMEM26*, *CITED1* and *TBX1* (567). Beige adipocytes also have a distinct molecular signature when compared to white adipocytes, therefore, the existence of defined beige precursors have been suggested. However, it has been shown that upon stimulation with β 3-ADR or PPAR γ agonists, white adipocytes can become UCP1 positive, hence cellular plasticity between white and beige preadipocytes or mature adipocytes cannot be excluded (568-571). Interestingly, it was recently reported that human BAT isolated from multiple body locations abundantly express beige cell markers suggesting that human BAT may be primarily composed of beige adipocytes (572). BAT activation is mainly stimulated by cold exposure however, diet can also induce BAT thermogenesis. Overfeeding triggers PPT and activates BAT, leading to excessive calorie intake being dissipated as heat, therefore protecting individuals from obesity (573,574). This physiological process is known as *luxuskonsumption* (573). Variability in PPT responses has been proposed as a major factor contributing to large individual variances in weight gain in response to overfeeding (575). Indeed, it has been shown that decreased BAT prevalence and activity correlates with obesity, increased adiposity and reduced insulin sensitivity, suggesting regulatory links between BAT and whole body energy metabolism (576).

Adult prenatally androgenised female sheep have ovarian, hormonal and metabolic characteristics of PCOS. These PCOS-like sheep are obese and insulin resistant. Furthermore, obesity in those animals, like in women with PCOS, is not a consequence of intrauterine growth restriction and catch-up growth, but is likely programmed by their intrauterine environment. In addition, those sheep have comparable body weight, similar surface to volume ratio, and brown and beige adipose tissue distribution as adult women (577). Given the inconsistent data regarding the role of PPT and predisposition to obesity in PCOS and a potential role of BAT in regulating body weight, we aimed to:

1. determine whether differences in PPT, measured as direct calorimetry, predict the propensity for obesity in our adult PCOS-like sheep
2. identify the possible involvement of BAT and other potential molecular mechanisms in regulating PPT

4.2 Methods

4.2.1 Experimental animals

The ovine model, the animals used, their husbandry and treatments have been described previously in Section 2.2. The female animals assessed in this chapter are detailed in Table 4.1.

Treatment	Developmental stage	Sample number (n)
Fetal		
Maternal Injection D62-102	Fetal day 112	C=9, TP=4
Juvenile		
Maternal Injections D62-102	Lambs 11 weeks old	C=8, TP=8
Adolescent		
Maternal Injection D62-102	Ewes 11 months old	C=5, TP=9
Adult		
Maternal Injections D62-102	Ewes 30 months old	C=11, TP=4
Contemporary Injections 2 Weeks		C=5, TP=5

Table 4.1 Treatment regime, age, and corresponding sample numbers of experimental animals discussed in this chapter.

4.2.2 Measuring postprandial thermogenesis

For this experiment, adult ewes prenatally exposed to increased levels of androgens (TP=4) and a subset of lean (CN=4) and naturally obese (CO=4) control animals were selected. Datalogger thermometers were implanted by Prof. Colin Duncan into the interscapular adipose tissue (IAT) under local anaesthesia, with the lead and download point being exteriorised, and the wound sutured. Animals were allowed to recover from surgery before the onset of the experiment. Measurement of PPT was carried during the times when ovaries are quiescent (the non-breeding season) to eliminate potential biases because of known hormonal regulation of temperature (e.g. progesterone increase temperature after ovulation). During the experiment, animals were kept in individual pens allowing them to sit and stand but restricting further movement, to exclude other confounding factors. Ewes were placed on a feeding schedule, with access to feed between 07:00 to 9.30 to entrain a postprandial thermogenic response, food

intake was recorded, and postprandial temperature measurement were logged from 10:00 till 16:00, at 1 min intervals, on 2 separate days.

4.2.3 Gene expression analysis using qRT-PCR.

Extraction of RNA from fetal and postnatal adipose tissue was performed using the combination of TRI reagent and Qiagen RNeasy Mini Kit (Qiagen Ltd., West Sussex, UK), as described in section 2.8.1. Extraction of RNA from muscles was performed using Qiagen RNeasy Fibrous Tissue Mini Kit (Qiagen Ltd., West Sussex, UK), as described in section 2.8.1. Protocols for cDNA synthesis and qRT-PCR are described in section 2.8.3. and 2.8.4, respectively. Forward and reverse primers were designed and validated as stated in section 2.8.6 and primer sequences analysed in this chapter are listed in Table 4.2.

Gene	Forward Sequence	Reverse Sequence	Product Size (bp)
<i>UCP1</i>	AGAGCCATCTCCACGGTCCCA	CCAAAGCCCCGTCAAG	92
<i>UCP2</i>	AAGGCCACCTAATGACAGA	CCCAGGGCAGAGTTCATGT	128
<i>UCP3</i>	AGATGAGCTTCGCCTCCAT	TGAAAGCGGATCTTCACCAC	172
<i>ADRB1</i>	CTTCTTCTGGCCAACGTG	GGGTTGAAGGCCGAGTTG	105
<i>ADRB2</i>	CATGCCCAAACGTCAGTC	TCTTGAGGGCTTTGTGTTCC	100
<i>ADRB3</i>	GCACCCAATACTGCCAACG	GTTGGTCATGGTCTGGAGTCT	159
<i>PPARGC1A</i>	ATGAGTCAGGCCACTGCAGAC	CTCTGCGGTATTCTTCCCTCT	150
<i>PRDM16</i>	GGACAACCACGCACTTTTAGA	GGTGCCATCTAGGTTCTGGA	136
<i>TMEM26</i>	TCCTTATGTTTGTGGGGACAG	TAGCATGCTCCAGGTCCATA	128
<i>SIRT1</i>	GGAAGGAAAACACTTCGCAAC	CCTCGTACAGCTTCACAGTCA	150
<i>TLE3</i>	CTGCAGCAGCACGACTTTAC	GTAGGCGAACTTGAGGGACA	174
<i>RYR1</i>	GGACCTCATCGGCTACTTTG	GACATTTAGGCGGTCAATGC	151
<i>ATP2A1</i>	GACAGGGTAGATGGGGACCT	GTCCAAGGAGGAGTCATTGC	171
<i>ATP2A2</i>	GGTGCTCCTGAAGGTGTCAT	CAGTGGGTTGTCATGAGTGG	168

Table 4.2 Forward and reverse primer sequences and product size for genes analysed in the fetal and postnatal adipose tissue using SYBR Green qRT-PCR.

4.2.4 Immunohistochemistry

Adipose tissue samples from four different anatomical locations per animal were processed and immunohistochemistry was carried out as described in section 2.3, using antibodies to UCP1 and UCP3. Negative controls consisted of omission of the primary antibody and substitution with serum immunoglobulins of equivalent concentrations. Details of primary and secondary antibodies and optimised working concentrations are listed in Table 4.3.

Primary Antibody	Dilution	Secondary Antibody	Dilution
UCP1 Polyclonal Goat (M-17; sc-6529) Santa Cruz Biotechnology	1:100	Rabbit anti Goat Biotinylated (BA-5000) Vector Laboratories	1:500
UCP3 Polyclonal Goat (C-20; sc-7756) Santa Cruz Biotechnology	1:100	Rabbit anti Goat Biotinylated (BA-5000) Vector Laboratories	1:500

Table 4.3 Details of antibodies used for immunohistochemistry in the adult adipose tissue samples. The primary and secondary antibodies suppliers and optimised concentrations are listed.

4.2.5 Noradrenaline ELISA

Noradrenaline level within adipose tissue samples was measured using Noradrenaline Research ELISA (ImmuSmol, BA E-5200, Pessac, France), as per the manufacturer's instruction. A representative sample of adipose tissue was cut on dry ice and transferred into 2ml eppendorf tube containing a metal bead (Qiagen Ltd.) and 300µl of a homogenisation buffer (HCl 0.01N; EDTA 1mM; sodium metabisulfite (Na₂S₂O₅) 4mM), using TissueLyser (Qiagen Ltd.) and homogenised at 25Hz for total of 4 min. The homogenate was transferred into a new eppendorf tube and centrifuged at 1600g at 4°C for 10 min, and the supernatants stored at -20°C. Protein concentration in sample was quantified using the Bradford assay as described in section 2.4.2. A 10µl aliquot of standards, controls and sample supernatants were pipetted into respective wells of the ELISA plate and filled up with distilled water to a final volume of 100µl. Immunoassay absorbance was measured at 450nm, with a reference wavelength of 650nm to control for background, using a ThermoMax Microplate Reader (Molecular Devices, CA, USA) and the concentrations were calculated from standard curve by plotting the known concentration of standard against the absorbance values. All samples were assayed in duplicate. Calculated results were corrected by the total protein content in the sample. The assay sensitivity was 0.1ng/ml intra and inter-assay CVs were <8.4% and <6.9%, respectively.

4.2.6 Statistical analysis

Statistical analysis was performed with GraphPad Prism version 6.0 (GraphPad Software, Inc., San Diego, CA). For comparing means of two treatment groups with equal variances an unpaired, two-tailed Student's t test was used. To compare multiple sets of data a one-way ANOVA was used. Log transformation was used to approximate the normal distribution for parametric analysis when necessary. A P value of <0.05 was considered as statistically significant. Results are presented as mean + S.E.M, where * signifies a P<0.05, ** P<0.01 and *** P<0.001. Area under the curve (AUC) was calculated using the trapezoidal method. Correlation was assessed by calculation of the Pearson r co-efficient. A line of best fit was incorporated only in the figures where correlation was statistically significant.

4.3 Results

4.3.1 PPT is decreased in adult PCOS-like sheep

To investigate the potential role of PPT in the propensity to obesity in PCOS-like sheep, we measured food intake and thermogenic output after standard meal in controls and TP-exposed animals. The thermogenesis experiment was undertaken in adult PCOS-like sheep (TP; n=4) and a subset of adult female control sheep selected based on weight characteristics, normal (CN; n=4) and obese (CO; n=4). CN animals had significantly lower body weight when compared to both CO and TP groups ($P < 0.0001$; Fig. 4.1 A) however, there was no difference in body weight between CO and TP animals (CN: 74.75 ± 0.75 kg; CO: 85.5 ± 1.25 kg; TP: 85.75 ± 0.75 kg). There was also no statistical difference in visceral adiposity among all groups (Fig. 4.1 B) (CN: 1.08 ± 0.2 kg; CO: 1.55 ± 0.22 kg; TP: 1.62 ± 0.23 kg). In addition, fasting insulin and G:I ratio were analysed in those selected animals. PCOS-like animals had significantly increased fasting insulin levels when compared with lean controls (Fig. 4.1 C; $P < 0.05$) however, there was no difference between CO and TP animals. Further, there was no statistical difference in G:I ratio among groups (Fig. 4.1 D).

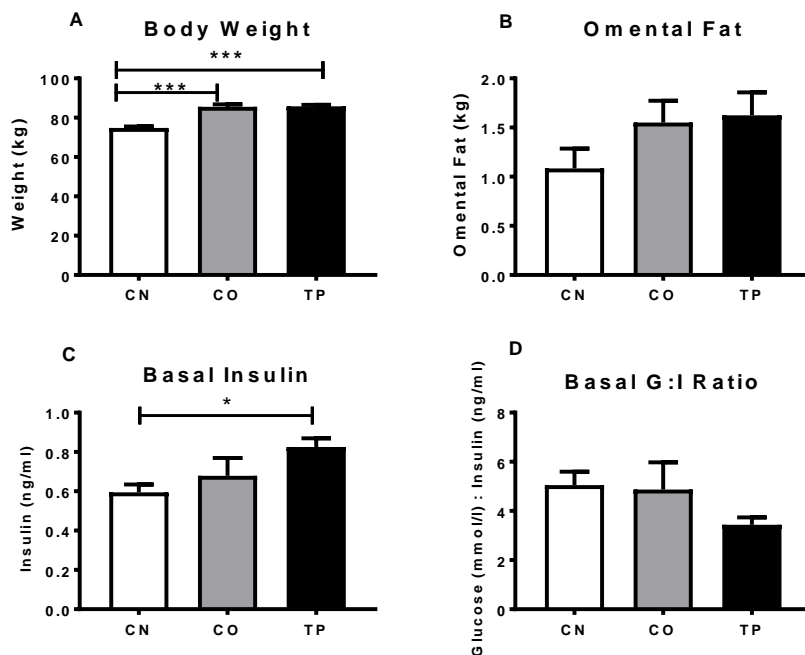


Figure 4.1 Characteristics of animals selected for thermogenesis study. A) Body Weight, B) Omental Fat, C) Fasting Insulin and D) Fasting Glucose to Insulin Ratio in adult lean control (CN), obese control (CO) and prenatally androgenised (TP) animals. P value of < 0.05 was considered as statistically significant. Results are presented as mean + S.E.M, where * signifies a $P < 0.05$, *** $P < 0.001$

Adult PCOS-like sheep had a decreased amplitude of PPT ($P < 0.05$; Fig. 4.2 A), despite consuming the same amount of food and without difference in basal body temperature (Fig. 4.2 C). Decreased change in postprandial temperature was not primarily a function of increased body weight as a difference in PPT was also observed between a subset of matched obese controls (CO) and TP exposed animals ($P < 0.05$; Fig. 4.2B). There was no difference in the duration of the peak postprandial thermogenic response (Fig. 4.2D) however, prenatally androgenised females demonstrated increased latency from commencement of feeding to maximal postprandial temperature when compared with normal (CN) and obese (CO) controls ($P < 0.05$; Fig. 4.2 E and F).

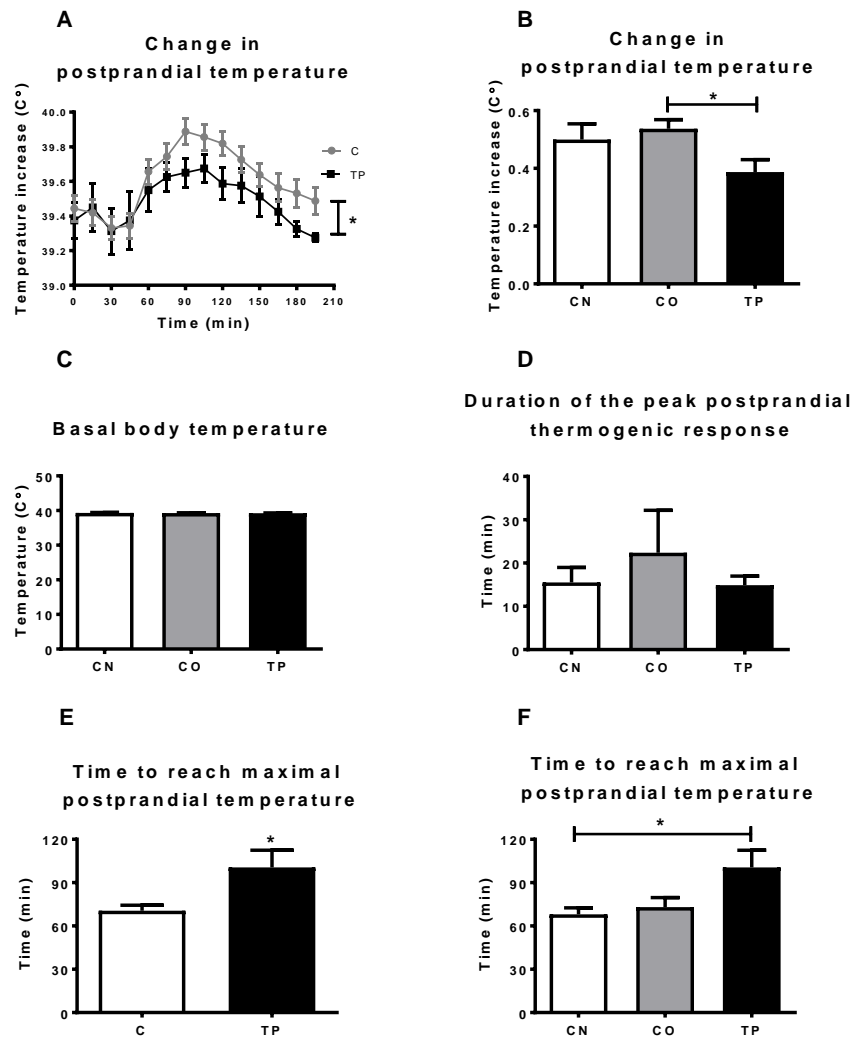


Figure 4.2 A-B) Postprandial thermogenesis; C) Basal body temperature; D) Duration of the peak postprandial thermogenic response; E-F) Time to reach maximal postprandial temperature in adult normal controls (CN), obese controls (CO) and prenatally androgenised (TP) animals. P value of < 0.05 was considered as statistically significant. Results are presented as mean + S.E.M, where * signifies a $P < 0.05$.

4.3.2 Gene expression of uncoupling proteins in adipose tissue depots

Brown and beige adipose tissue are an important site of cold and diet-induced thermogenesis. The primary molecule involved in adaptive thermogenesis is UCP1 and its two homologues, UCP2 and UCP3. In the view of decreased PPT in adult PCOS-like sheep, we next assessed gene expression of uncoupling proteins (UCPs) in four different fat depots: interscapular adipose tissue (IAT), neck adipose tissue (NAT), SAT and VAT. In IAT, near the site where we implanted temperature dataloggers, there was no significant difference in the expression of *UCP1* (Fig. 4.3 A) but expression of *UCP2* and *UCP3* was significantly downregulated in prenatally TP-exposed animals ($P < 0.05$; Fig. 4.3 B and C, respectively). Expression of *UCP1* was significantly decreased in NAT, SAT and VAT of prenatally androgenised adult ewes ($P < 0.05-0.01$; Fig. 4.3 D, G and J, respectively) however, there was no difference of the expression of *UCP2* and *UCP3* in these fat depots (Fig. 4.3 E, F, H, I, K and L).

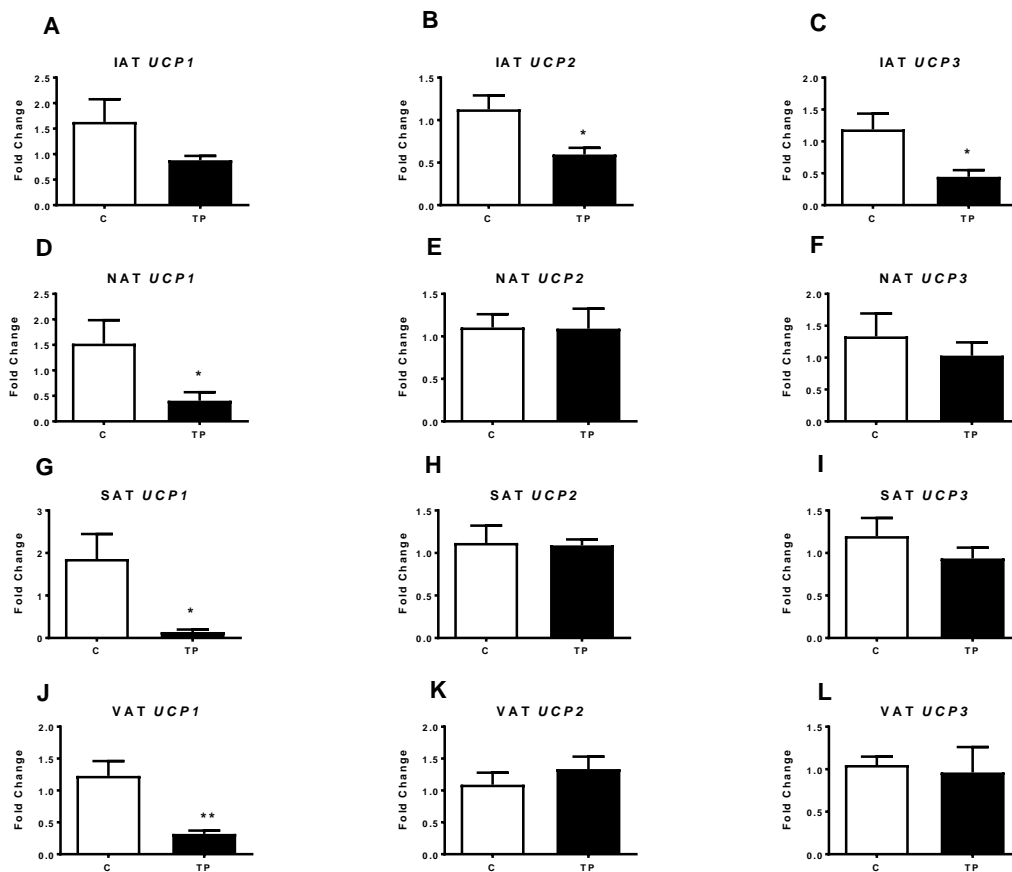


Figure 4.3 Expression of *UCP1*, *UCP2* and *UCP3* in different adipose tissue depots of adult control (C) and prenatally androgenised (TP) animals, as quantified by qRT-PCR. P value of < 0.05 was considered as statistically significant. Results are presented as mean + S.E.M, where * signifies a $P < 0.05$.

Subsequently we evaluated the association of differently expressed UCP mRNA in all selected fat depots with the amplitude of PPT. In IAT there was significant correlation of PPT with expression of *UCP1* ($P < 0.05$; $r = 0.53$; Fig. 4.4 A), *UCP2* ($P < 0.05$; $r = 0.68$; Fig. 4.4 B) and *UCP3* ($P < 0.01$; $r = 0.72$; Fig. 4.4 C). PPT was also correlated with expression of *UCP1* in SAT ($P < 0.05$; $r = 0.66$; Fig. 4.4 E) and VAT ($P < 0.05$; $r = 0.52$; Fig. 4.4 F), but not NAT (Fig. 4.4 D).

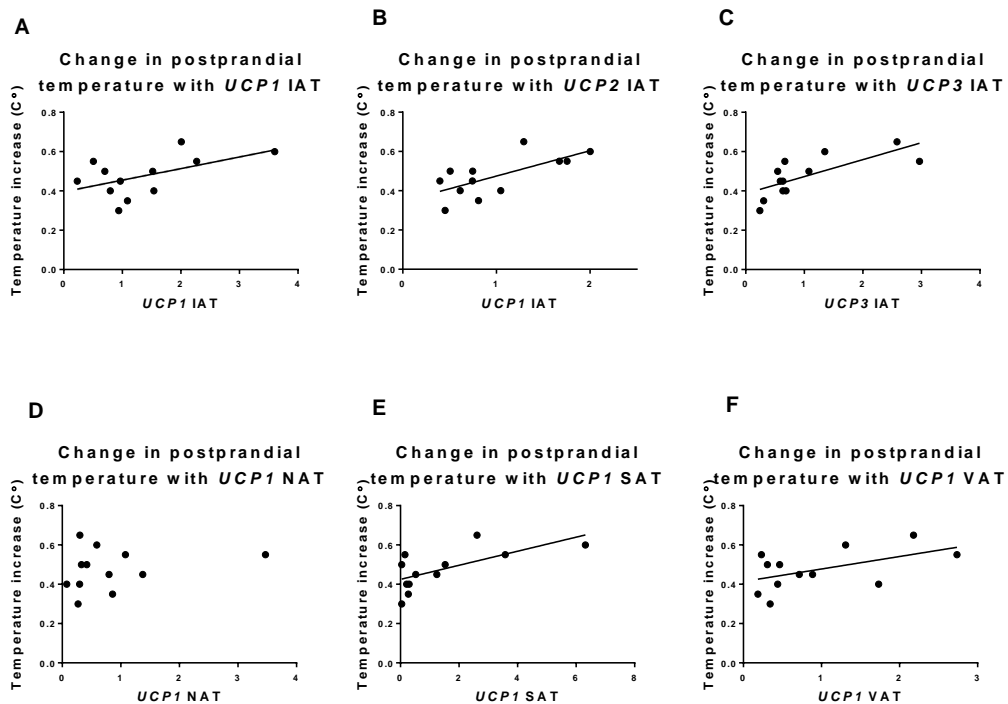


Figure 4.4 Correlation of expression of UCPs mRNA in different fat depots with change in postprandial temperature in adult controls and prenatally androgenised animals.

4.3.3 Immunohistochemical examination of the UCP1 and UCP3 expression in adipose tissue depots.

We next performed histological analysis of adipose tissue from control and TP-exposed animals dissected from four different anatomical locations. In all sections analysed histologically, adipose tissue was composed mainly of adipocytes with unilocular lipid droplets, and no cells with classical multilocular brown adipocyte morphology were identified. However, in controls but not PCOS-like sheep, we observed some UCP3-positive adipocytes in IAT (Fig. 4.5 A), which tended to be smaller than adjacent adipocytes. We also detected some UCP1-positive adipocytes in NAT and SAT of control animals (Fig. 4.5 C and E, respectively), but not prenatally TP-exposed animals (Fig. 4.5 D and F). In VAT, UCP1 was undetectable in section from both controls and TP-exposed animals (Fig. 4.5 G and H, respectively).

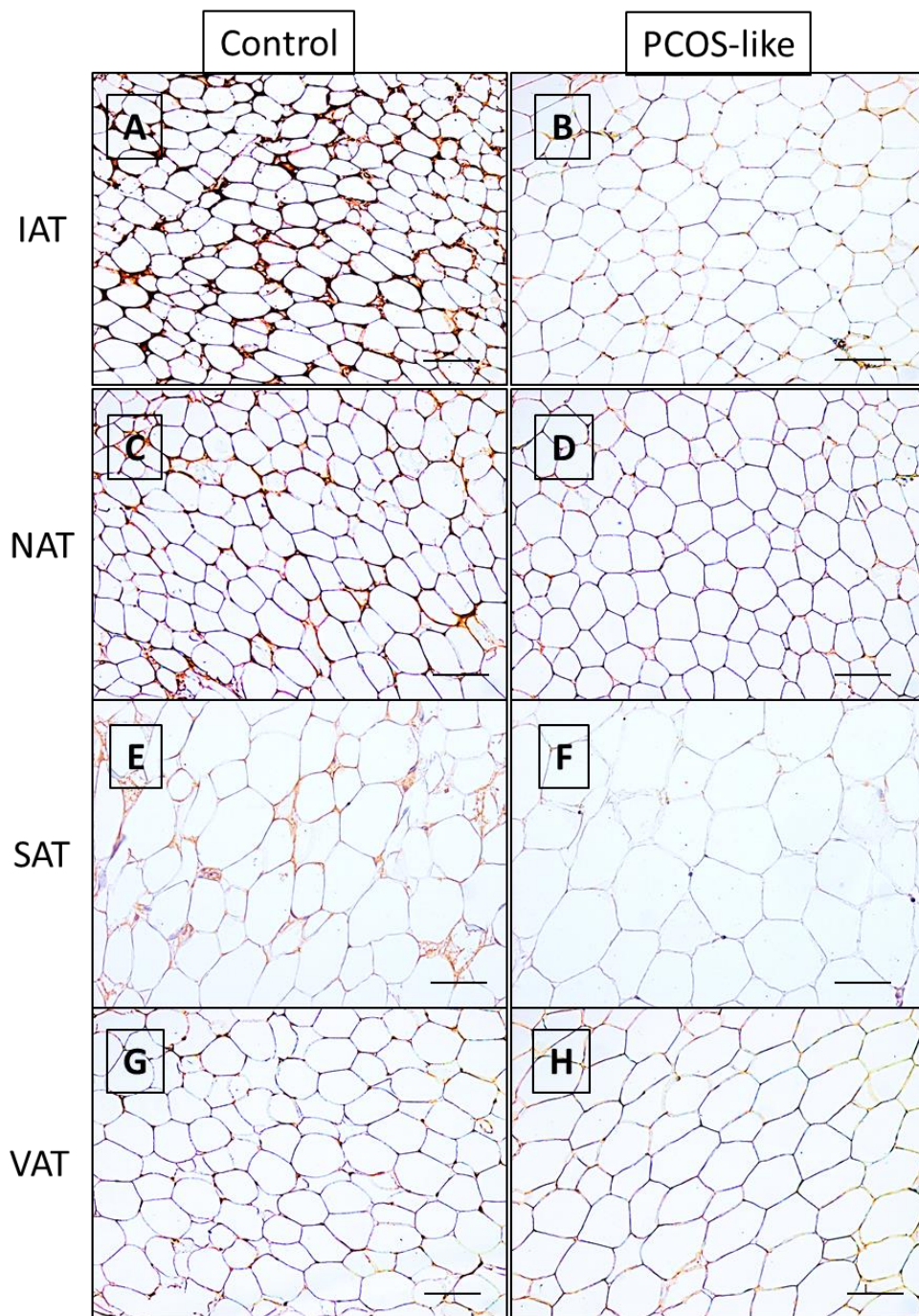


Figure 4.5 Immunohistochemical examination of the UCP1 and UCP3 expression in adipose tissue depots. A-B) Representative images of IAT from control (A) and PCOS-like sheep (B) stained with anti-UCP3. C-D) Representative images of NAT from control (C) and PCOS-like sheep (D) stained with anti-UCP1. E-F) Representative images of SAT from control (E) and PCOS-like sheep (F) stained with anti-UCP1. G-H) Representative images of VAT from control (G) and PCOS-like sheep (H) stained with anti-UCP1. Images are shown at 10X magnification; scale bar 100 μ m.

4.3.4 Insulin resistance in adult PCOS-like sheep correlates with decreased PPT

Female sheep prenatally programmed to develop PCOS-like condition are insulin resistant with increased fasting insulin concentrations and elevated AUC_{insulin} but normal AUC_{glucose} during a 45-min IVGTT as discussed in chapter 3. Since decreased insulin sensitivity is associated with reduced glucose induced thermogenesis (GIT), we performed a correlation analysis to determine the relationship between PPT and fasting levels of insulin. There was negative correlation between the reduction in PPT and increasing levels of fasting insulin ($P < 0.05$; $r = -0.56$; Fig. 4.6 A) while increased time to reach maximal temperature post-feeding correlated positively with increased levels of fasting insulin ($P < 0.05$; $r = 0.56$; Fig. 4.6 B). We also analysed association between fasting insulin levels and gene expression of *UCPI* in fat depots. *UCPI* mRNA levels in NAT, SAT and VAT correlated negatively with fasting insulin ($P < 0.05-0.01$; $r = -0.73$, $r = -0.56$, $r = -0.79$, respectively; Fig. 4.6 D-F), whereas this association was not evident in IAT (Fig. 4.6 C).

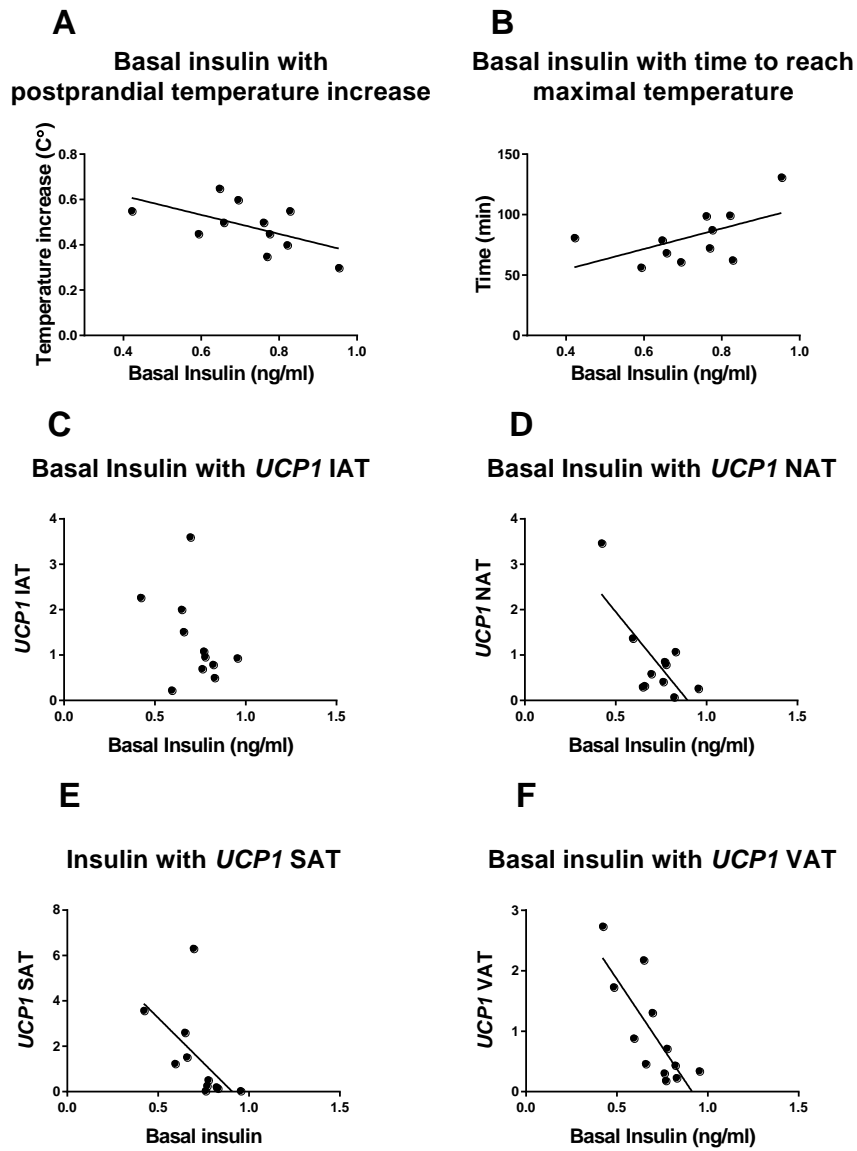


Figure 4.6 The association between A-B) fasting insulin levels and changes in postprandial thermogenesis dynamics; C-F) Relationship between mRNA expression of *UCP1* in different fat depots and fasting insulin levels in adult control and prenatally androgenised animals.

4.3.5 Noradrenaline levels and β -adrenergic receptors expression

Considering the importance of β -adrenergic system in regulation of adaptive thermogenesis we assessed gene expression of three subtypes of β -ADR (β 1-, β 2-, and β 3-ADRs) in all four adipose tissue depots analysed. There was no difference in the expression of *ADRB1*, *ADRB2* or *ADRB3* between control and TP-exposed animals in any of fat depots (Fig. 4.7 A-K). Of note levels of *ADRB3* in SAT were below detectable threshold level.

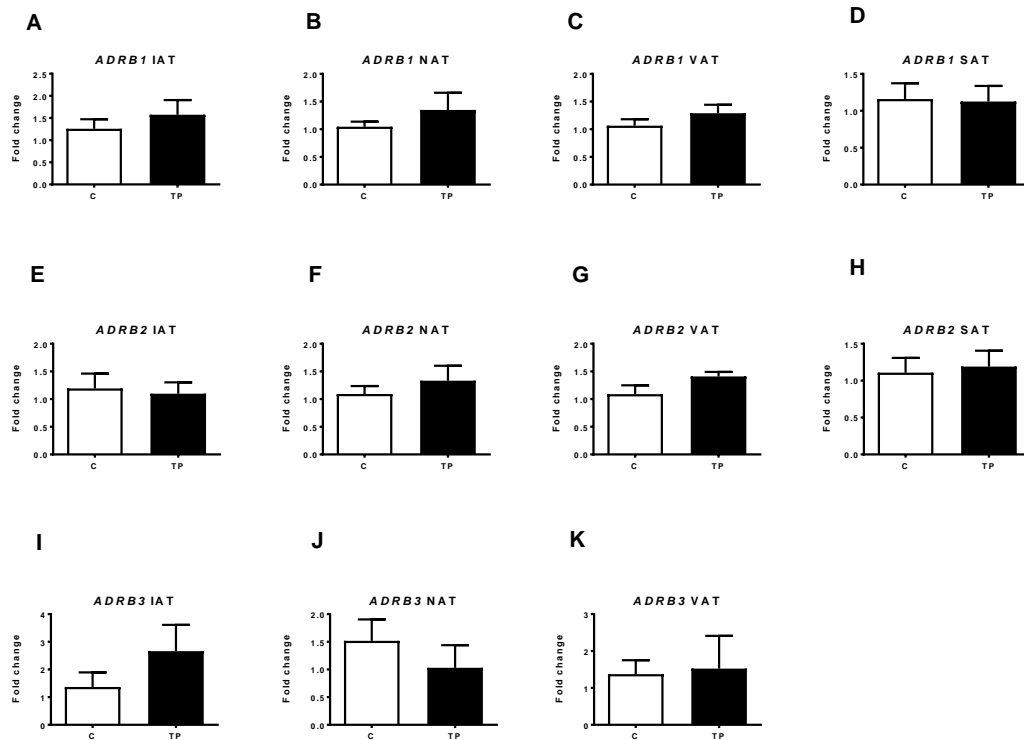


Figure 4.7 Expression of *ADRB1*, *ADRB2* and *ADRB3* in four different adipose tissue depots in adult control (C) and prenatally androgenised (TP) animals, as quantified by qRT-PCR. Results are presented as mean + S.E.M.

We next assessed levels of noradrenaline in adipose tissue from four different anatomical locations. Noradrenaline was measured directly in adipose tissue and its levels were corrected for total amount of proteins. Noradrenaline levels were significantly lower in NAT, SAT and VAT ($P < 0.05$; Fig. 4.8 B-D) but not IAT of PCOS-like sheep when compared to controls (Fig. 4.8 A). Average amount of noradrenaline measured in all fat depots was significantly lower in TP-exposed animals ($P < 0.05$; Fig. 4.8 E) and this decreased concentration could not be solely attributed to increased body weight as a difference in averaged noradrenaline levels was also noticed between a subset of matched obese controls (CO) and TP exposed animals, although

this did not reach statistical significance ($P=0.12$; Fig. 4.8 F). However, there was a negative correlation between body weight and average levels of noradrenaline ($P<0.05$; $r= -0.59$; Fig. 4.8 G). There was also a positive correlation between average levels of noradrenaline in adipose tissue and PPT ($P<0.05$; $r= 0.58$; Fig. 4.8 H).

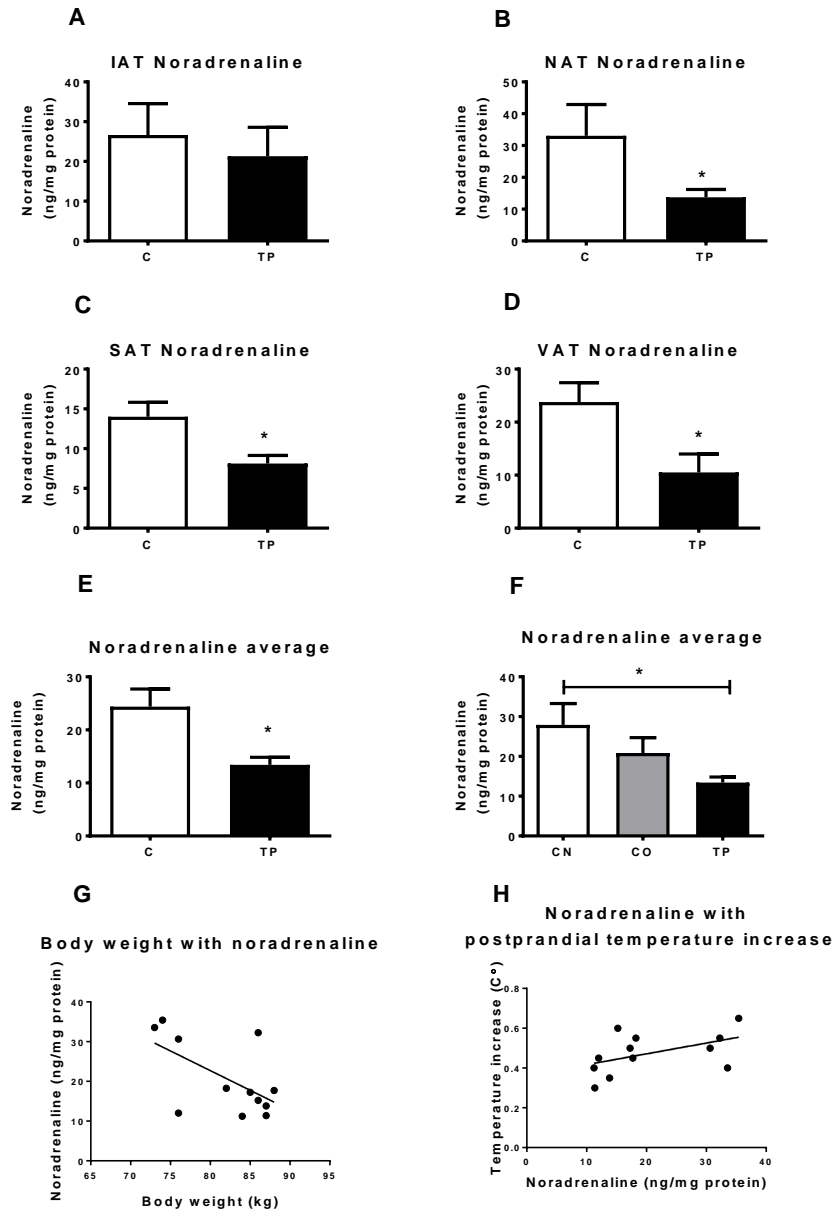


Figure 4.8 Noradrenaline concentrations in A-D) different adipose tissue depots; E) average noradrenaline levels in four different anatomical adipose tissue location in control (C) and prenatally androgenised (TP) animals; F) Average noradrenaline level in four different anatomical location in normal control (CN), obese control (CO) and prenatally androgenised (TP) animals; Correlation of average noradrenaline level in four different anatomical adipose tissue location in control and prenatally androgenised animals with G) body weight and H) postprandial temperature increase. P value of <0.05 was considered as statistically significant. Results are presented as mean + S.E.M, where * signifies a $P<0.05$.

Since FFA are well known activators of UCP1 and BAT thermogenesis, we therefore looked also at association of fasting FFA in circulation with PPT, *UCP1* mRNA levels and average noradrenaline levels from four different adipose tissue depots. There was no correlation between levels of *UCP1* mRNA and FFA (data not shown), but we found that there was a negative correlation between fasting FFA and both PPT ($P < 0.05$; $r = -0.56$; Fig. 4.9 A) and average noradrenaline levels ($P < 0.05$; $r = -0.60$; Fig. 4.9 B).

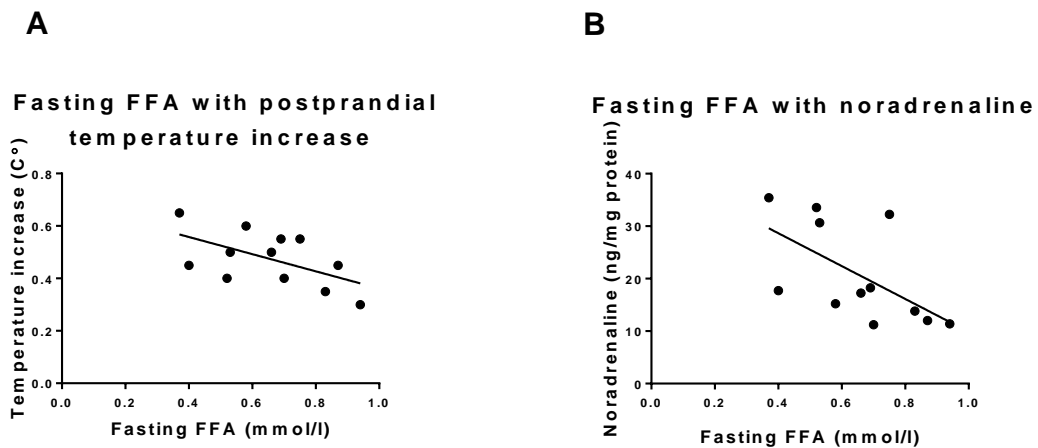


Figure 4.9 Correlation of fasting FFA with A) postprandial temperature change; B) with average noradrenaline level in four different anatomical adipose tissue location in adult control and prenatally androgenised animals.

4.3.6 Expression of beige adipocyte markers is depot specific

Given the white adipose tissue like morphology but propensity toward higher expression of *UCP1* in control animals, we next looked at the expression of selected beige adipocyte markers in adipose tissue dissected from all four different anatomical locations. There was no difference in the expression of selected beige markers in NAT (Fig. 4.10 F-J) and VAT (Fig. 4.10 P-U). In IAT expression of *PPARGC1A* was significantly upregulated in TP-exposed animals ($P < 0.01$; Fig. 4.10 A), but there was no difference in the expression of the remaining beige adipocyte markers (Fig. 4.10 B-E). In contrast, in SAT expression of *PPARGC1A* and *SIRT1* was significantly downregulated in PCOS-like sheep ($P < 0.05$; Fig. 4.10 K and N, respectively), and there was a trend for decreased expression of *TMEM26* ($P = 0.058$; Fig. 4.10 M), however, this did not reach statistical significance. There was no difference in the levels of *PRDM16* and *TLE3* (Fig. 4.10 L and O, respectively).

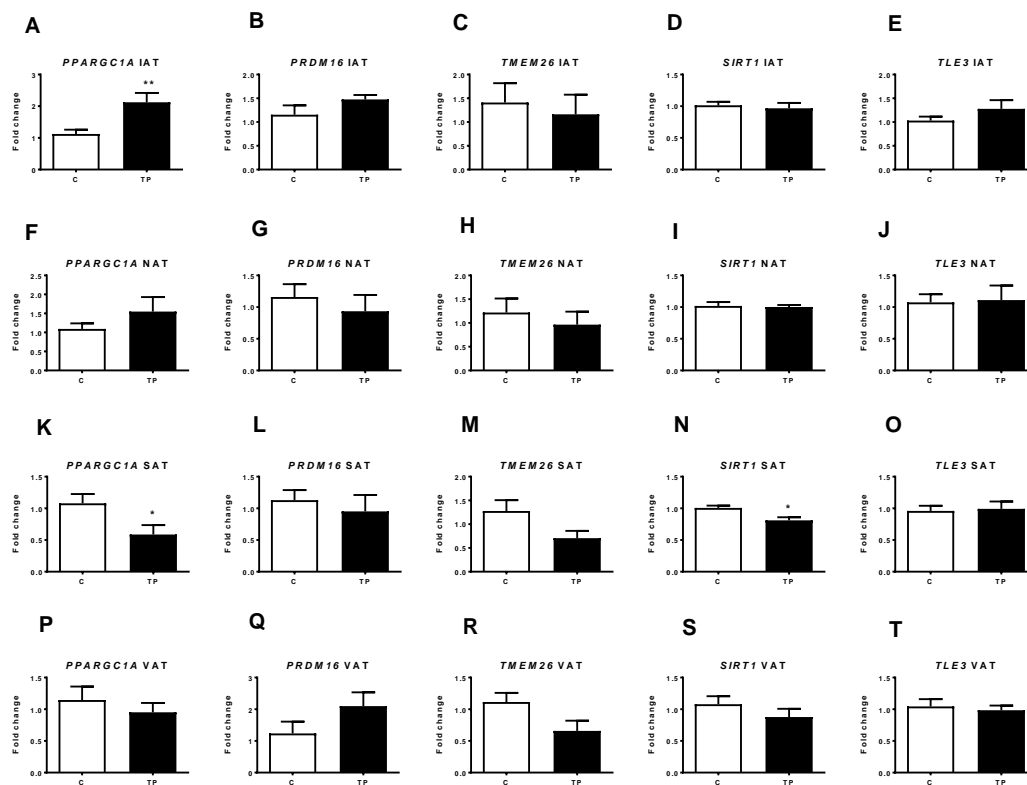


Figure 4.10 Expression of selected beige adipocyte markers in four different adipose tissue locations, A-E IAT; F-J NAT; K-O SAT and P-T VAT, in adult control (C) and prenatally androgenised (TP) animals, as quantified by qRT-PCR. P value of <0.05 was considered as statistically significant. Results are presented as mean + S.E.M, where * signifies $P < 0.05$, ** $P < 0.01$.

4.3.7 Thermogenic potential of skeletal muscles

Thermogenesis primarily takes place in brown and beige adipose tissue however, it has been shown that skeletal muscles also exhibit thermogenic properties. Therefore, we investigated thermogenic potential of skeletal muscles in adult female sheep to assess if muscle thermogenesis could contribute to differences in PPT that we observed between C and TP animals. Although we did not measure postprandial thermogenesis in muscle directly, we looked at the expression levels of genes associated with dissipation of energy through the production of heat in muscle (UCPs) and genes involved in calcium cycling (*RYR1*, *ATP2A1* and *ATP2A2*). There was a trend toward increased expression of *UCP3* in PCOS-like sheep ($P = 0.06$; Fig. 4.11C) however, this did not reach statistical significance and there was no difference in the expression of *UCP1*, *UCP2*, *RyR1*, *ATP2A1* and *ATP2A2* between control and TP-exposed animals (Fig. 4.11 A-B and Fig. 4.11 D-F, respectively).

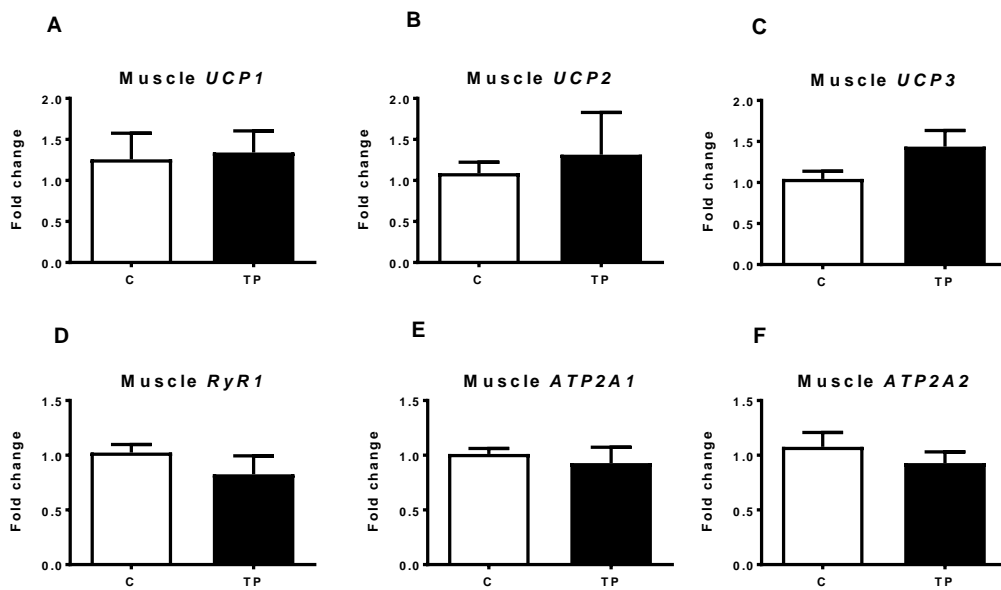


Figure 4.11 Expression of UCPs mRNA and genes involved in calcium cycling in muscles of adult control (C) and prenatally androgenised (TP) animals, as quantified by qRT-PCR. Results are presented as mean + S.E.M.

4.3.8 Expression of thermogenic genes across different developmental stages

To establish the potential timing of reduced expression of UCPs in adipose tissue of TP-exposed animals, we investigated the expression of *UCP1*, *UCP2* and *UCP3* in SAT from D112 fetuses and prepubertal animals. We also looked at the expression of UCPs in SAT from normal ewes treated with androgens for two weeks. Unfortunately, we did not have samples of interscapular or neck adipose tissue from those animals. Altered expression of *UCP1*, *UCP2* or *UCP3* was not observed in fetal life (Fig. 4.12 A-C), prepubertally (Fig. 4.12 D-F) or in animals contemporaneously treated with androgens (Fig. 4.12 G-I).

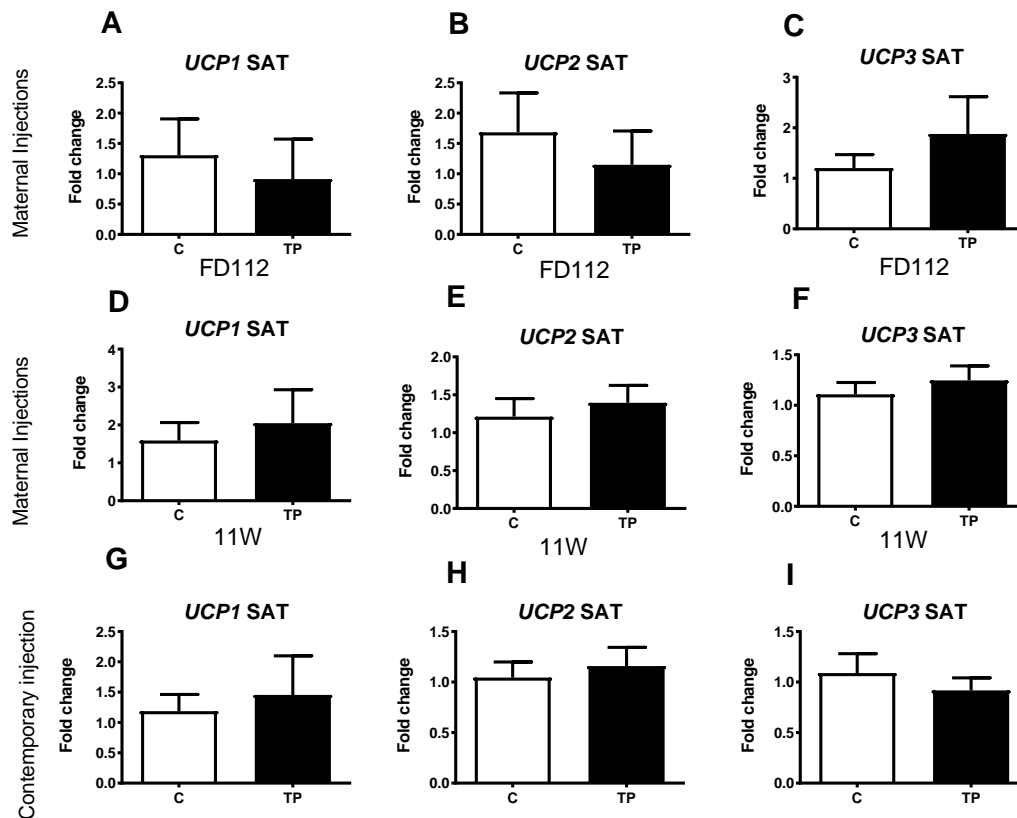


Figure 4.12 Expression of UCP genes in A-C) SAT of fetal day 112 control (C) and prenatally androgenised (TP) animals; D-F) 11 weeks old control (C) and prenatally androgenised (TP) animals; G-I) adolescent controls (C) and animals contemporary treated with testosterone for 2 weeks (TP), as quantified by qRT-PCR. Results are presented as mean + S.E.M.

Finally, we investigated expression of UCPs and selected beige fat markers in adolescent adipose tissue. There was no alteration in the expression of UCPs in VAT (Fig.4.13 A-C) and no difference in the expression of *UCP1* and *UCP2* in SAT (Fig. 4.13 D-E) however, expression of *UCP3* was decreased in prenatally TP-exposed animals ($P < 0.05$; Fig. 4.13 F). In addition, expression of *PRDM16* was downregulated ($P < 0.05$; Fig. 4.13 H), but no difference in expression of other beige fat markers was detected (Fig. 4.13 G and 4.13 I-K).

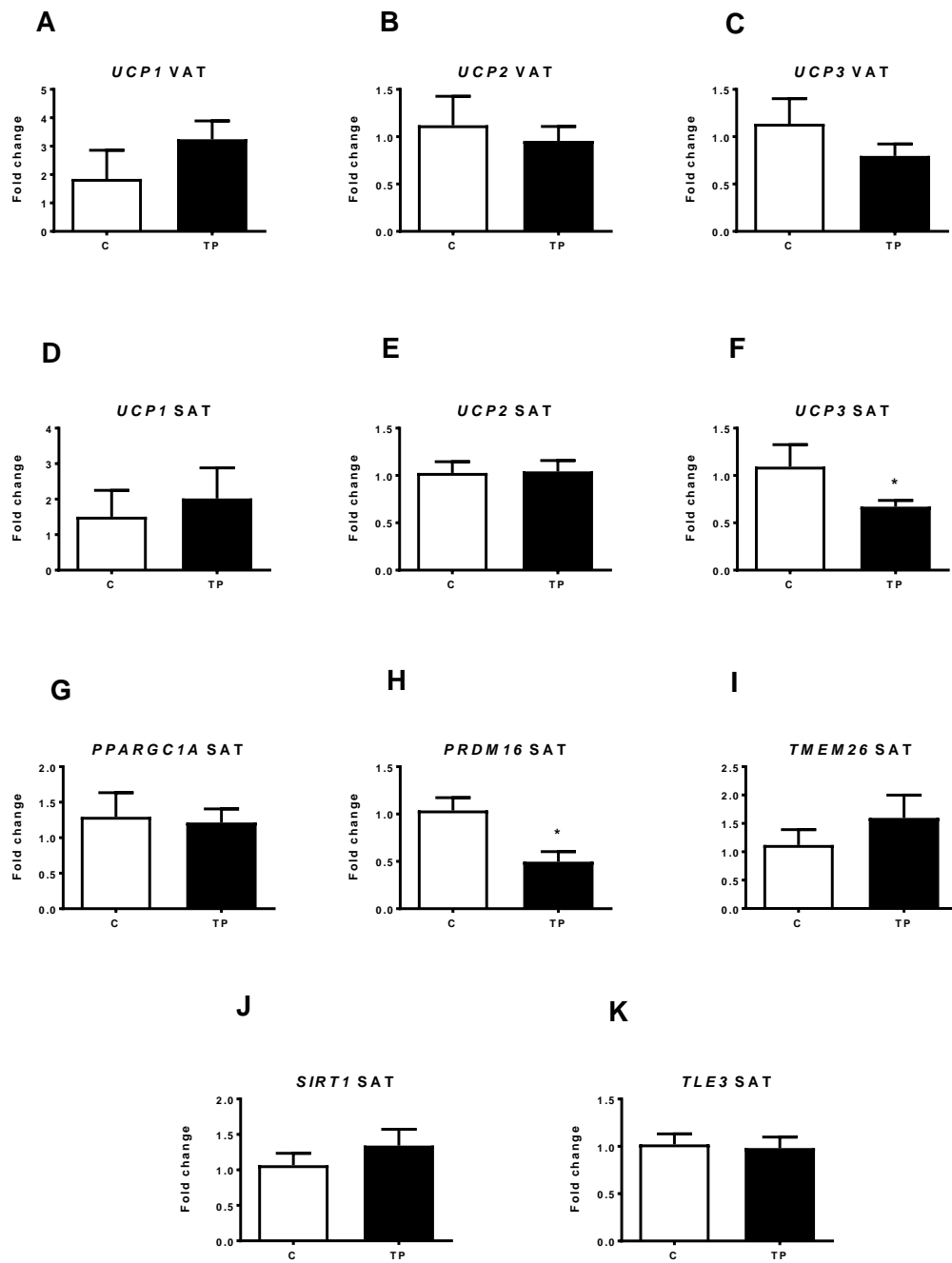


Figure 4.13 Expression of UCP genes in A-C) VAT; D-F) SAT and G-K) expression of selected beige adipocyte markers in SAT of adolescent control (C) and prenatally androgenised (TP) animal, as quantified by qRT-PCR. P value of <math><0.05</math> was considered as statistically significant. Results are presented as mean + S.E.M, where * signifies a

4.4 Discussion

The aim of this study was to assess the potential role of PPT in obesity of female sheep prenatally programmed to develop PCOS-like condition. We found that adult PCOS-like sheep have a decreased amplitude of PPT when compared with controls, measured through direct calorimetry, without a difference in basal body temperature, despite receiving the same caloric intake, and independent of obesity. What is more, we also report that these PCOS-like sheep have increased time to reach their maximal postprandial temperature, again independent of obesity. These findings suggest that prenatally androgenised sheep have reduced capacity for energy expenditure, which may explain propensity for obesity in these animals. Interestingly, it has been shown that obese individuals, with a childhood history of obesity, have lower PPT, before and after weight loss, suggesting that thermogenic defect may be a cause rather than a consequence of obesity (578). In addition, recent work by Henry *et al.* documented that genetically fat sheep have reduced PPT when compared with lean animals, and this is likely a consequence of decreased UCP1 expression in retroperitoneal adipose tissue (579). However, there is a lot of discrepancies regarding the potential role of decreased PPT in obesity, mainly due to varying methodologies applied in different studies (580). To our knowledge this is the first study reporting decreased PPT in an animal model of PCOS, however, analogous findings were reported in women with PCOS (212). A limited number of studies have examined the role of basal metabolic rate in PCOS associated obesity, although reports are inconsistent. Five case-control studies reported no difference in BMR between PCOS and age- and BMI-matched controls, and regardless of insulin resistance status (212,546,549-551). On the contrary, Georgopoulos *et al.* reported that BMR was lower in PCOS women than in age- and BMI-matched controls, and the lowest BMR was found in women with both PCOS and insulin resistance, suggesting that insulin sensitivity can affect overall energy expenditure (211). However, it should be noted that participants in the latter study were younger and had overall lower BMI than subjects in the remaining five studies and this could contribute to the result discrepancies among those reports. Obesity results from increased calorie intake, reduced energy expenditure or a combination of both. We have investigated only one aspect of energy expenditure, PPT, in controlled environment, with set caloric intake and restricted movement in order to exclude possible confounding factors. However, we cannot exclude that increased calorie consumption or decreased physical activity in uncontrolled environment also contribute to increased body weight in those animals. There are several reports looking at other aspects of energy intake and expenditure in patients with PCOS. There is inconsistent data regarding energy intake in PCOS women. Decreased (581), and increased (582,583) dietary

intake have been reported in women with PCOS, however, the majority of the studies found no differences in daily food and nutrient consumption in PCOS women when compared with controls (547,584-587). Wright *et al.* reported that PCOS patients with a normal BMI consumed significantly lower number of calories (≥ 250 kcal/day) than BMI-matched controls, hypothesising that this might be necessary to prevent weight gain in those women (547). They also noted that in higher BMI categories there was no difference in calorie intake between PCOS and BMI-matched controls (547). Studies evaluating physical activity levels in women with and without PCOS have greater result consistency, reporting no difference in overall levels of physical activity (547,582,583,587,588). Therefore, based on the current status of knowledge, it can be implied that the tendency to obesity in PCOS women is unlikely to result from increased calorie intake or decreased physical activity, suggesting that a decreased PPT might play a role. So, what is the possible mechanism programming decreased PPT and obesity in PCOS?

Insulin resistance and compensatory hyperinsulinemia are key factors contributing to pathophysiology of PCOS (589,590). It is estimated that as many as 50-70% PCOS women are insulin resistant, independent of BMI (190,191,591,592). On average, insulin sensitivity is decreased by 35–40% in patients with PCOS when compared to matched controls (590). Some authors suggested that intrinsic pancreatic β -cell dysfunction and hyperinsulinemia may be a key pathogenic determinant in PCOS (193,593-595). In our ovine model of PCOS, lean adolescent (411) and obese adult prenatally androgenised sheep are hyperinsulinemic and have decreased insulin sensitivity. Prenatal androgenisation results in increased number of pancreatic β -cells, which correlates with hyperinsulinemia, in both ovine and nonhuman primate models of PCOS (431,596,597). These findings suggest that hyperinsulinemia might precede insulin resistance, at least in animal models of PCOS. Indeed, some authors suggested that hyperinsulinemia itself might be causing or sustaining insulin resistance (598). We have found a negative correlation between increasing levels of fasting insulin with reduction in PPT and positive association with increasing time to reach maximal temperature post-feeding. Parallel findings were reported by Robinson *et al.* in their study on PPT in PCOS women, showing that decreased PPT is associated with reduced insulin sensitivity in patients with PCOS (212). The link between decreased insulin sensitivity and reduced PPT has been also shown by others although the mechanisms are still not fully understood (599-602). A proposed explanation was that peripheral insulin resistance results in decreased glucose uptake and hence decreased glucose substrate availability (603). However, a study on intranasal insulin administration in healthy men, reported that insulin increased PPT by 17% when compared to placebo, decreased level of circulating insulin and temporarily decreased FFA in serum, thus

showing that efficient brain insulin signalling is necessary for whole-body energy flux (604). Since peripheral insulin resistance and obesity has been shown to be associated with reduced insulin sensitivity in central nervous system (605-607), it can be speculated that prenatally androgenised sheep and women with PCOS might also have decreased central insulin sensitivity, which in turn might be accountable for reduced PPT, although currently there is no data to support this hypothesis. Additionally, it has been demonstrated that direct injections of insulin into the preoptic area of the mice hypothalamus, activated BAT thermogenesis and stimulated increase in core body temperature in dose-dependent manner (608), whereas a study on streptozotocin-induced diabetes in mice showed that the thermogenic capacity of BAT declined progressively with insulin deficiency (609). Recent study in humans demonstrated that BAT is a highly insulin-sensitive tissue, with comparable rate of glucose uptake to that in skeletal muscle (610). Furthermore, a study in rodents demonstrated that increasing BAT mass, by transplantation into the visceral cavity, improved glucose tolerance and insulin sensitivity, decreased body weight and fat mass, in dose-dependent manner (611). In addition, it was also documented that BAT transplantation increased glucose uptake into BAT, WAT and heart muscle, but not skeletal muscle (611). These studies provide a strong evidence for a direct link between insulin, thermogenesis and BAT, therefore, we have also investigated potential role of BAT and/or beige adipocytes in regulating PPT in our ovine model of PCOS. Histological analysis of adipose tissue dissected from four different anatomical locations from control and PCOS-like animals revealed that none of the tissues analysed had a classical multilocular brown adipocyte morphology. Despite that, in control animals but not PCOS-like, some adipose cells, especially from IAT, NAT and SAT depots, expressed low levels of UCP1 and UCP3 proteins, as verified through immunohistochemical examination. Additionally, adipocytes from control animals in IAT and NAT and SAT depots appeared to be smaller than those from TP-exposed animals, although we only quantified this in SAT depot, confirming that PCOS-like animals have hypertrophic adipocytes when compared with controls, as discussed in chapter 3. The above findings suggest that some adipose cells in IAT, NAT and SAT depots might have properties of beige rather than brown adipocytes and that there might be increased number of thermogenic adipocytes in control than in PCOS-like animals.

To further confirm this initial hypothesis, we looked at the expression of selected markers of beige adipocytes in four adipose tissue depots, IAT, NAT, SAT and VAT of controls and prenatally androgenised animals. All selected markers were detectable in adipose tissue depots analysed. We found no difference in the expression of beige markers in NAT and VAT, but to our surprise, there was significant upregulation of *PPARGC1A* in IAT of the TP-exposed animals with no difference in the expression of the remaining markers, namely *PRDM16*,

TMEM26, *SIRT1* and *TLE3*. In contrary, in SAT expression of *PPARGC1A* and *SIRT1* was significantly downregulated in PCOS-like sheep but no difference in the levels of *PRDM16* and *TLE3*. *PPARGC1A* (PPARG coactivator-1 α ; PGC-1 α) is an important regulator of mitochondrial biogenesis and oxidative metabolism (612,613). Gain of function experiments have shown that ectopic expression of *PPARGC1A* in white adipocytes induced characteristics of brown fat cells, including increased expression of mitochondrial and thermogenic genes (614), whereas *PPARGC1A* deficient mice have increased body fat and are unable to maintain core body temperature after cold exposure (615). *SIRT1* (Sirtuin 1) regulates *PPARGC1A* expression and equally plays an important role in brown adipocyte biology and thermogenesis (616-618). *SIRT1* is a protein deacetylase, targeting transcription factors and enzymes with key roles in mitochondrial biogenesis, lipid catabolism, cholesterol homeostasis and gluconeogenesis (619). It has been shown that moderate overexpression of *SIRT1* in mice results in amplified BAT activity and thermogenic potential, increased lipolysis and improved insulin sensitivity due to enhanced transcriptional responses to β 3-adrenergic stimulation (620). What is more, *SIRT1* has been shown to increase browning of WAT (621), and to protect against high-fat diet-induced metabolic damage (622) whereas *SIRT1* deficient mice show increased adiposity, lower thermogenic activity and metabolic dysfunction (623). We also observed trend for decreased expression of *TMEM26* in SAT of PCOS-like sheep. Transmembrane protein 26 (*TMEM26*) was first identified as specific beige adipocyte marker (567,624), however, others have suggested that *TMEM26* might be actually a marker of beige adipocyte precursors in WAT rather than differentiated beige adipocytes (625). Our data indicate depot specific expression of beige adipocyte markers. We do not know how these different adipose tissue depots contribute to overall metabolic status however, it is tempting to speculate that considering the much greater volume of SAT compared with remaining adipose depots, decreased expression of beige fat markers in SAT might contribute to decreased PPT in those animals. As shown by others, beige adipocytes resemble white adipocytes in having unilocular appearance and low basal level of *UCP1* expression, however upon stimulation with cyclic AMP, β -adrenergic or *PPARG* agonists, beige cells show significantly increased *UCP1* expression and high rates of respiration and energy expenditure, comparable to that of brown adipocytes (567). Interestingly, recent studies have provided evidence that in humans, fat depots previously identified as BAT are actually composed mainly of beige adipocytes (567).

Therefore, in order to further evaluate thermogenic potential of adipocytes in our animals, we have studied mRNA expression of three isoforms of UCP proteins (*UCP1*, 2 and 3) in four adipose tissue depots, IAT, NAT, SAT and VAT. We have found that in IAT, near the site where we implanted temperature dataloggers, mRNA expression of *UCP2* and *UCP3* was

significantly decreased in PCOS-like animals as compared with controls, and there was a trend toward decreased expression of *UCP1*, although this did not reach statistical significance. There was also reduced *UCP1* expression in the remaining three adipose tissue depots, NAT, SAT and VAT. Interestingly, similar findings were reported in genetically fat sheep, where significant downregulation of PPT and *UCP1* in retroperitoneal adipose tissue, but not *UCP2* or *UCP3*, was reported (579). Although we did not quantify UCP protein levels, there was a positive correlation between amplitude of PPT increase and expression of *UCP1*, *UCP2* and *UCP3* mRNA in IAT, as well as *UCP1* in SAT and VAT, indicating that mRNA levels of UCP might be also a reliable measure of thermogenic potential. There was also a negative correlation between *UCP1* expression in adipose tissue and fasting insulin level, suggesting that hyperinsulinemia in PCOS-like sheep might contribute to decreased expression of *UCP1* and hence reduced thermogenic potential of BAT and/or beige adipocytes, which in turn might account for the diminished postprandial thermogenic response in those animals. This hypothesis is further supported by existing evidence on the role of BAT and UCPs in diet induced thermogenesis from both rodent and human studies. The first observations that BAT is involved in PPT came from studies in rodents, showing that rats fed with a highly palatable diet, voluntarily overfed however, have an ability to dissipate extra energy from food as heat (575,626) and demonstrate a significant increase of UCP1, both mRNA and protein, in BAT (627,628). In parallel, pair-fed studies of genetically obese mice and their lean siblings showed that the development of obesity is associated with diminished thermogenesis (629,630), and this was further linked to a reduced concentration of UCP1 in BAT (631). Further research demonstrated that these genetically obese rodents have lower sympathetic activity in BAT, at thermoneutral conditions, as shown through noradrenaline turnover assessment (632). However, the final evidence for the central role of BAT and UCPs in PPT came from *UCP1* knockout studies, demonstrating that mice lacking *UCP1* become obese when kept at thermoneutrality even when consuming normal diets (633,634). However, a persisting question was, whether animal data on BAT and its role in PPT and development of obesity, is applicable to humans. Several studies demonstrated decreased BAT activity in obese subjects however, there was a lot of controversy whether diminished BAT activity is a cause rather than a consequence of obesity and to what degree PPT actually contributes to overall energy expenditure (635). However, more recent human studies showed that UCP1 polymorphisms are related to decreased PPT (636) and that BAT recruitment due to cold acclimation at 19°C enhances PPT and insulin sensitivity without muscle shivering (637). In the latter study Lee *et al.* demonstrated that increased BAT volume and activity, with possible enhanced browning of WAT, resulted in increased levels of circulating adiponectin and decreased levels of

circulating leptin, and these changes were mirrored in altered gene expression in adipose tissue, even at thermoneutrality, suggesting that increased BAT/ beige fat proliferation and/or transformation, impacts whole-body metabolism (638). Furthermore, it was reported that humans with active BAT, as evaluated by (F-FDG-PET/CT), have increased PPT by 56 kcal per day and an enhanced rate of fat utilisation as compared to BAT-negative subjects, under free-living and thermoneutral conditions, suggesting that metabolically active BAT can contribute to PPT in humans (639). However, while the role of UCP1 in adaptive thermogenesis is well established, the precise function of UCP2 and UCP3 in cells remains unknown. Since UCP2 and UCP3 have 60% sequence identity with UCP1 and 70% similarity with each other, it has been suggested that these proteins are likely to have also similar biochemical function, however, early studies did not confirm this hypothesis (640). It has been shown that UCP2 and UCP3 are able to catalyse proton conductance of mitochondria but only when specific activators, such as FFA or free radicals, are present (641). The genomic location of human UCP2 and UCP3 is in a chromosomal locus mapped as relevant to obesity and hyperinsulinemia (642,643). Indeed, studies on transgenic animals have demonstrated that rodents overexpressing UCP2/UCP3 have decreased adiposity and are protected from diet-induced obesity (644-646). Human studies looking at polymorphisms of *UCP2* and *UCP3* further support link between differential expression of those genes and obesity (647-649). However, it has been shown that *UCP2* and *UCP3* knockout mice have normal body weight, metabolic rate, and responses to cold, indicating that these proteins are not essential for normal metabolic function, but presence of other compensatory mechanisms cannot be excluded (650,651). What is more, a study on the expression of thermogenesis-related genes in WAT of lean and obese subjects reported that expression of *UCP2* is significantly downregulated, but with no difference in methylation levels, in SAT and VAT of obese individuals, whereas no difference was found in the expression of *UCP1* and *UCP3* (652). The authors concluded that this might indicate that there were no differences in the content of beige adipocytes between lean and obese individuals (652). This finding might appear contradictory to our results, as we report decreased *UCP1* expression in WAT, potentially resulting in decreased content of beige adipocytes in obese PCOS-like sheep. However, as discussed earlier, differences in thermogenic potential between controls and PCOS-like animals in our study do not result from obesity *per se* but most likely is a consequence of prenatally programmed reduced energy expenditure.

In contrast to the expression of *UCP1*, which is restricted to thermogenic adipocytes, the expression of *UCP2* is ubiquitous (including pancreas, muscles, WAT and BAT), whereas the expression of *UCP3* is limited to muscles and BAT (642). The wide distribution of these

proteins has implicated their potential role in FFA transport, the attenuation of reactive oxygen species (ROS) production and protection against oxidative damage, degenerative disease and aging (653). Additionally, *UCP2* has been suggested to decrease insulin secretion in pancreas whereas *UCP3* has been suggested to mediate thermogenesis in muscle (653). Interestingly, it has been demonstrated that mRNA expression of *UCP2* and *UCP3* in rat muscles is increased during starvation and decreased after refeeding, suggesting regulatory role of FFA on expression of *UCP2* and *UCP3* (654). In addition, Bezaire *et al.* has shown that the proteins involved in FFA uptake and oxidation are increased in muscle of transgenic mice overexpressing *UCP3*, supporting a role for *UCP3* in fatty acid metabolism (655). Furthermore, human studies reported that elevated FFA levels, during triglyceride infusion, increased the expression of *UCP3*, but not *UCP2*, in muscles, and that physiological hyperinsulinemia prevents this upregulation of *UCP3*, which again supports potential regulatory role of insulin on the expression of UCPs (656). A study in *UCP1* knockout mice reported that *UCP3* expression increases in skeletal muscle upon cold exposure suggesting interdependence of *UCP1* in BAT and *UCP3* in skeletal muscle (657). In contrast, a recent study has reported that expression of *UCP3* directly correlated with levels of *UCP1* in murine BAT, demonstrating that *UCP3*, but not *UCP2*, is significantly lower in BAT, but not skeletal muscles, of *UCP1* knockout mice (658). Interestingly, the authors also noted that in wild-type mice cold exposure increased *UCP3* expression in BAT, but not skeletal muscles, however, cold acclimation of *UCP1* knockout mice resulted in the lowest *UCP3* levels (658). All above findings indicate that *UCP2* and *UCP3* are not able to overcome the loss of the thermogenic function of *UCP1* in BAT and are more likely to be involved in FFA transport and metabolism. As pointed out by Thompson and Kim in their review on links between FFA and expression of *UCP2* and *UCP3*, in physiological and pathological states leading to significant FFA elevation, there is a trend in the literature showing that in muscles *UCP3* is increased, with no change in *UCP2* levels, and the reverse correlation is present in WAT, whereas in BAT *UCP3* tends to be decreased (659). This is partially in agreement with our results. PCOS-like sheep have elevated fasting FFA, decreased *UCP3* mRNA in IAT and trend for increased *UCP3* mRNA in muscles, however, with no difference in the expression of *UCP2* in WAT. Assuming *UCP2* and *UCP3* have roles as FFA transporters, decreased expression of *UCP2* and *UCP3* in IAT of PCOS-like sheep could indicate that there is lower uptake of FFA into this adipose tissue depot. Interestingly, experiments in both rodents and humans showed that BAT mainly utilises FFA as energy, and that individuals with higher BAT activity have increased fat oxidation under thermoneutral conditions (639,660). Since low fat oxidation predicts future weight gain (661,662), perhaps it can be suggested that subjects with decreased BAT activity

and hence lower fat utilisation are more likely to gain weight and have decreased insulin sensitivity (639). Adolescent and adult PCOS-like sheep have increased fasting FFA in the circulation. Although we did not measure levels of PPT in adolescent prenatally androgenised sheep, we have now found that there is negative correlation between levels of fasting FFA in adult animals and amplitude of PPT, suggesting that decreased PPT and BAT activity in PCOS-like animals might contribute to decreased fat oxidation in BAT resulting in increased FFA in the circulation. Furthermore, there was a negative relationship between average noradrenaline levels in adipose tissue with fasting FFA, again supporting the role of SNS and BAT in the regulation of FFA levels. BAT thermogenesis is controlled by the SNS, where localised release and action of noradrenaline increases the mass, temperature and lipolytic response of BAT through activation of UCP1 (574). This effect is conducted via the β -adrenergic receptors located in thermogenic adipose tissue and deletion of all three isoforms of (ADRB1, ADRB2 and ADRB3) results in an obese phenotype and decreased UCP1 expression (663). It has been demonstrated that noradrenaline concentration is increased after feeding and correlates closely with heat production in response to overfeeding and mild cold exposure (664-667). Although we did not measure the circulating noradrenaline concentration during the postprandial period in our animals, we have investigated noradrenaline levels and mRNA expression of β -adrenergic receptors in four adipose tissue depots after 15 minutes of a IVGTT test. There were no differences in the expression of adrenergic receptors, however, noradrenaline concentrations were significantly lower in NAT, SAT and VAT, but not IAT of PCOS-like animals when compared to controls. Interestingly, the IAT adipose tissue depot was also the only depot where *UCP1* expression was not significantly decreased as in the remaining adipose depots of TP-exposed animals, therefore it is likely that the relatively increased levels of noradrenaline in that depot may have a contributory role. In addition, the total average level of noradrenaline from those four adipose tissue depots was significantly lower in prenatally androgenised animals, and this was independent of obesity. Furthermore, there was a positive correlation between average level of noradrenaline and PPT amplitude, but not individual mRNA UCPs levels in adipose tissue depots. These findings suggest that the SNS might contribute towards decreased PPT in PCOS-like animals due to decreased sympathetic activity, but not sensitivity, however, this should be further investigated. Interestingly, since noradrenaline action in BAT results also in hydrolysis of TG in lipid droplets (559), the decreased level of noradrenaline in adipose tissue depots of PCOS-like animals could also contribute to the increased adipocyte size observed in those animals. To our knowledge, there is no study available looking directly at noradrenaline levels in adipose tissue of PCOS women however, there are reports showing a generally increased sympathetic

tone (668) but decreased adrenergic responsiveness and consequently reduced lipolysis in adipose tissue in PCOS women (231,669). In addition, Backstrom *et al.* reported that, in response to hypoglycaemia, peripheral serum noradrenaline levels, which originate from both the sympathetic nervous system and the adrenal medulla, were lower in the obese women with PCOS than in the BMI matched controls as well as in lean women with and without PCOS (670). The authors also noted that decreased noradrenaline concentrations correlated inversely with increased fasting insulin levels in obese women with PCOS (670). Insulin is an important regulator of sympathetic activity and it has been shown that intracerebroventricular injection of insulin increases sympathetic activation in animal studies (671) however, the stimulatory actions of insulin on the sympathetic outflow may be reduced in obesity and the metabolic syndrome (672). Therefore, it is possible that the decreased noradrenaline levels observed in adipose tissue of PCOS-like animals is a secondary to the potential peripheral and central insulin resistance in those animals.

It has been suggested that skeletal muscle also play a role in adaptive thermogenesis (673,674). Skeletal muscles express all three UCP proteins, with UCP3 being the most abundant. Initial *in vitro* studies in isolated mitochondria hinted that UCP3 has uncoupling potential however, *in vivo* studies indicated that UCP3 levels typically mirror peripheral FFA (640,659,675). Some authors, however, indicated that brown adipocytes interspersed among muscle fibres might be the actual source of thermogenic potential of skeletal muscles (676). We did not find any difference in the expression of *UCP1*, *UCP2*, and *UCP3* in skeletal muscles of control and PCOS-like sheep although there was non-statistically significant trend towards increased expression of UCP3 in TP-exposed animals, which, as mentioned earlier, might reflect increased levels of fasting FFA in those animals. In addition to mitochondrial uncoupling, cellular pathways such as the futile calcium cycling and myosin-ATP turnover have also been indicated to underpin thermogenesis in skeletal muscle (673). Calcium cycling occurs across the sarcoplasmic reticulum membrane in skeletal muscle and involves the ryanodine type 1 receptor (RYR1) and the sarcoendoplasmic reticulum calcium-dependent ATPases (ATP2A1 and ATP2A2) (673). Studies in sheep demonstrated that feeding increases muscle temperature and expression of RYR1 and ATP2A1 (677,678). There were no differences in the expression of elements of the futile calcium cycling pathway in skeletal muscle between control and prenatally androgenised sheep after 15 min of an IVGTT test. However, since we did not measure postprandial temperature directly in muscle, we cannot answer if and to what extent skeletal muscle contributes to decreased postprandial thermogenesis observed in PCOS-like animals.

We also aimed to establish the potential timing of reduced expression of thermogenic genes in adipose tissue of prenatally androgenised animals. There were no differences in the expression of UCPs in SAT of fetal and juvenile sheep however, due to limited tissue availability we only assessed expression of those genes in one adipose tissue depot in those animals. Interestingly, adolescent PCOS-like animals had significantly decreased expression of *UCP3* and *PRDM16* in SAT but there was no difference in the expression of any of the thermogenic associated genes in VAT. Again, we did not have samples of IAT or NAT from this age cohort. *PRDM16* is an enriched factor of both beige and brown adipocytes and plays a pivotal role in regulating brown/beige fat cell fate and function (679). It has been demonstrated that *PRDM16* is essential to induce full molecular programming of brown adipose cells, including the expression of thermogenic genes, mitochondrial components and increased cellular respiration in cell culture models, and to promote browning of VAT under β -adrenergic stimulation (680). *PRDM16* also represses white adipose tissue-specific genes (681). In addition, depletion of *PRDM16* in brown fat cells causes a near total loss of the brown characteristics, and in subcutaneous adipocytes decreases the recruitment of beige adipocytes in WAT in response to a PPAR γ agonist (564,569,680). Rodents with ablated beige fat function, due to a mutation in the *PRDM16* gene, develop obesity, insulin resistance, hepatic steatosis as well as enlarged subcutaneous adipocytes with virtually no UCP1 expression, and increased level of inflammatory markers in that depot, when exposed to high-fat diet (HFD) (682). *PRDM16* evokes its function through coactivating PGC-1 α , PPAR γ and C/EBPs (559). It has been demonstrated that *PRDM16* forms a complex with C/EBP β to induce the expression of brown-fat specific genes, loss of C/EBP β results in impaired thermogenesis, while increased levels of C/EBP β lead to browning of WAT, and *PRDM16*-C/EBP β -PPAR γ interaction is indicated as central pathway in brown and beige adipose cell development (559,566,683-685). Assuming that beige adipocytes differentiate from defined precursor cells rather than pre-existing adipocytes (624), this finding suggest that reduced expression of *PRDM16* in adolescent SAT might program decreased brown/beige development in that depot, which presumably explains decreased expression of *UCP1* and beige cell markers in adult SAT of PCOS-like animals. Interestingly, in chapter 3 we had reported previously decreased expression of *PPARG*, *CEBPA* and *CEBPB* associated with decreased adipogenesis in SAT of those adolescent prenatally androgenised sheep. We hypothesise that prenatal androgen exposure could underline those changes. Is there evidence for a role of sex hormones in programming brown and beige adipose tissue function?

Sex hormones play an important role in the regulation of energy balance and determination the distribution and function of WAT. However, the potential mechanisms underpinning the

link between sex hormones and energy homeostasis in beige/brown adipocytes is not well understood. Sex differences in BAT thermogenic capacity have been reported suggesting a potential link between sex hormones and BAT. Women have higher BAT prevalence, mass and activity than men (146,147,576,686). In addition, lower incidence of BAT has been linked to increased visceral adiposity in men rather than in women (686). Parallel results were also reported in rodents. Female rats were found to have 2-fold higher UCP1 content and higher energy expenditure than males (149), and when exposed to high fat diet, male rats were described to gain more body weight than females (687). In addition, the authors reported that mitochondria in female BAT were larger and had greater amount of cristae than males, suggesting that this might account for increased thermogenic potential in females (149). Furthermore, higher AR mRNA expression in male rodent BAT was reported (688). While *in vitro* studies on the effect of sex hormones on differentiated brown adipocytes found that testosterone treatment resulted in dose-dependent inhibition of UCP1 mRNA expression in noradrenaline stimulated adipocytes and this was reversed when adipocytes were co-treated with flutamide, an androgen antagonist (689). The authors also reported that progesterone treatment caused increased expression of UCP1 whereas no effect was found in 17 β -estradiol treated cells (689). Testosterone has also been reported to decrease the expression of PGC-1 α in cell-cultured brown adipocytes (690). There is also evidence that estrogens impact energy expenditure and stimulate BAT activity, mainly through interaction with melanocortin and leptinergic systems (691-693). It was shown that UCP1 expression in BAT of ovariectomised, estrogen-deficient rats, was significantly lower (694) whereas estrogen receptor-alpha knockout mice had increased body weight and decreased energy expenditure by 11% when compared with control animals (695). A role for sex hormones in regulating BAT activity might be further supported by the evidence that physiological states characterised by changes in sex steroid levels, such as pregnancy and lactation, result in altered BAT function. It has been demonstrated that pregnancy and lactation in rodents is associated with BAT atrophy, decreased levels of UCP1 and reduced noradrenaline turnover in BAT, most likely to preserve energy (696,697). In addition, it has been suggested that age related decreases in BAT activity might be due to declining levels of sex steroids (698,699). The α 2A/ β 3 adrenoreceptor ratio has been indicated as an important regulatory factor in lipolysis and thermogenesis, with a lower ratio resulting in greater thermogenic activity (700). Interestingly, *in vitro* studies also demonstrated that testosterone treatment of brown adipocytes leads to increased expression of α 2A-adrenergic receptors, whereas progesterone and 17 β -estradiol have an opposite effect, resulting in a lower α 2A/ β 3 ratio (700). Lower ratios were also reported in female rats when compared to males, further supporting the fact that sex hormones might drive higher

thermogenic capacity in females (149). Unfortunately, we did not investigate gene and protein expression of ADRA2A, therefore we are unable to define the ratio in our animals. However, since one of the main features of PCOS is increased antenatal and postnatal androgen levels it is very likely that increased testosterone levels might be responsible for the decreased BAT/beige fat thermogenic potential in PCOS-like sheep and women with PCOS. Interestingly, a recent study in a DHEA-induced rat model of PCOS demonstrated that PCOS-like rats have significantly reduced BAT activity with decreased UCP1 and PGC-1 α expression, and lower thermogenic capacity (701). Transplantation of BAT from age- and sex-matched donors not only improved metabolic profile but also reversed anovulation, hyperandrogenism, polycystic ovaries and improved fertility in this animal model of PCOS (701). Furthermore, the authors also reported that BAT transplantation activated endogenous BAT and increased levels of circulating adiponectin, an insulin sensitising adipokine, which is often reported to be lower in PCOS patients (701).

In summary, obesity and increased adiposity are highly prevalent in PCOS patients and decreased energy expenditure has been documented in women with PCOS, however, to date there was a limited evidence that women with PCOS might be predisposed to obesity. Using clinically realistic ovine model of PCOS we have demonstrated that adult PCOS-like sheep have a decreased amplitude of PPT when compared with controls, without differences in basal body temperature, despite receiving the same caloric intake, and independent of obesity. These findings suggest that prenatally androgenised female sheep as adults have reduced capacity for energy expenditure, which is mirrored in women with PCOS. This reduced capacity for postprandial thermogenesis is correlated to hyperinsulinemia and decreased noradrenaline rather than obesity, and might result from reduced thermogenic potential of BAT and/or beige adipocytes. This suggests that women with PCOS might be prenatally programmed to become obese.

Chapter 5 The effect of prenatal androgens on hepatic phenotype

5.1 Introduction

As stated in previous chapters, prenatally androgenised adolescent sheep had evidence of fatty liver, as examined through histological analysis, but without changes in serum determinants of liver function, and independent of body weight or central adiposity (411). NAFLD is a term describing a spectrum of liver pathologies, from simple hepatic steatosis, characterized by more than 5% fat infiltration on imaging or histology, and a benign prognosis, to non-alcoholic steatohepatitis (NASH) (702). It is estimated that about 15% of patients with simple steatosis will eventually develop NASH, a combination of hepatocellular injury, inflammation, and an increased risk of liver fibrosis, which might result in cirrhosis and hepatocellular carcinoma (252,703).

NAFLD is the most common cause of chronic liver disease in western countries and a major public and clinical health burden (702,703). NAFLD is highly prevalent, it is estimated that in general population 30-40% of men and 15-20% of women are affected, with occurrence significantly increasing to 60%-70% in overweight people and subjects with T2DM, and over 90% in morbidly obese patients (252,704,705). In addition, NAFLD is the most prevalent chronic liver disease in paediatric population, with up to 17.3% of adolescents, aged 15 to 19 years, affected (706). A recent meta-analysis reported that mean prevalence of NAFLD in children from general population was 7.6% however, in children with obesity occurrence increased to 34.2% (707). There was also evidence that the prevalence was higher in males compared with females, and increased proportionally with BMI (707).

The majority of patients with NAFLD are asymptomatic until the late stage of disease (708). The disease can be diagnosed through ultrasonography, although liver biopsy is still considered a gold standard for diagnosing NASH and to assess degree of fibrosis (708). In addition, liver function tests (LFTs) measuring alanine transaminase (ALT) and aspartate transaminase (AST) in blood samples can be used, however, it has been demonstrated that biochemical tests are not reliable markers for assessing NAFLD severity, since patients with normal transaminases may still have NASH (252,709). NAFLD is considered a hepatic manifestation of metabolic syndrome and a risk factor for developing IR and T2DM, dyslipidaemia and hypertension, obesity and PCOS (710,711). NAFLD is therefore a multisystem disease, affecting a several extra-hepatic organs and regulatory pathways (703). However, it was also postulated that NAFLD precedes the development of the metabolic syndrome, which indicates that resolution of NAFLD could prevent the development of the metabolic syndrome and its cardiovascular consequences (712). Currently, there are no

pharmacological therapies approved for treating NAFLD, therefore therapeutic approaches centre on treating associated comorbidities, such as obesity, insulin resistance, dyslipidaemia and inflammation (713). Lifestyle modifications and weight management, through diet improvements and increased physical activity, remain the cornerstone approach to improving, or at least delaying progression of the disease (713). In addition, pharmacological treatment with TZDs, PPAR γ agonists, has been shown to have some potential benefits, promoting fatty acid oxidation, decreasing hepatic lipogenesis, and reducing inflammation, resulting in decreased hepatic TG accumulation in patients with NAFLD (714,715).

The mechanisms underlying aetiology and pathophysiology of NAFLD are not fully understood. It was demonstrated that NAFLD shows some familial clustering, suggesting a possible genetic predisposition (716). In addition, obesity and T2DM are known risk factors for development of NAFLD. However, since numerous subjects with NAFLD are lean and not diabetic it has been postulated that insulin resistance might be the main risk factor (717). Indeed, a decline in whole-body, hepatic, and adipose tissue insulin sensitivity was documented in NAFLD (717).

Insulin is crucial for the regulation of carbohydrate and lipid homeostasis. In response to increased postprandial glucose levels insulin is secreted by pancreatic β cells. A large proportion of glucose is instantly transported to the liver, which converts it into glycogen. However, when glycogen saturation occurs, any additional glucose transported into liver is shunted into pathways synthesising fatty acids, which will be further esterified into TG. In addition, in a fed state, insulin inhibits FFA release from adipose tissue, reduces hepatic glucose production, through decreased gluconeogenesis and glycogenolysis, and increases the rate of glucose uptake, primarily into skeletal muscle and adipose tissue. Consequently, decreased insulin sensitivity results in elevated postprandial levels of insulin and insufficiently suppressed lipolysis in adipose tissue, increased FFA in circulation, independent of nutritional status, and increased flux of FFA to the liver. In turn, fatty acids in the liver can promote hepatic lipotoxicity by stimulating TNF α expression and reactive oxygen species (ROS) formation, which can further exaggerate inflammation and apoptosis, subsequently resulting in progression to NASH and fibrogenesis (718,719). In addition, hyperinsulinemia may lead to increased *de novo* lipogenesis, while hepatic insulin resistance may also lead to inadequately suppressed gluconeogenesis. Overall this may result in increased hepatic lipid accumulation, dyslipidaemia and progressive insulin resistance. The onset of NAFLD is associated with progressive accumulation of lipids in the liver. The liver has a crucial role in lipid metabolism, through importing FFA, manufacturing, storing and exporting lipids and thus dysregulation of

any of those processes can lead to development of NAFLD (702). The mechanisms leading to accumulation of lipids in the liver include increased delivery of FFA to the liver, decreased fatty acid oxidation, and amplified *de novo* lipogenesis (717). However, it has been demonstrated that NAFLD results mainly from increased transport of FFA to the liver and enhanced *de novo* lipogenesis, whereas removal, by mitochondrial fatty acid oxidation and lipid export are only moderately affected (702,720). Of the total hepatic triglyceride content in patients with NAFLD, 60% resulted from adipose-derived NEFA, 10% from the diet, and 30% came from *de novo* lipogenesis (720).

Hepatic FFA uptake is facilitated by FFA transporters and depends on FFA concentration in the plasma, hepatocellular capacity, and number and activity of those transporters. The main plasma transporters for FFA are the fatty acid transporter proteins (FATP), of which FATP2 and FATP5 are the major ones, caveolins (1-3), the fatty acid binding proteins (FABP), of which FABP2 and FABP5 have been demonstrated to play an important role in normal hepatic physiology and pathophysiology, and fatty acid translocase (FAT)/CD36 (702).

De novo lipogenesis, the mechanism in which liver synthesises endogenous FAs from glucose is a complex process, regulated by insulin and glucose levels, in which acetyl-CoA carboxylase (ACC1), FA synthase (FAS) and sterol CoA desaturase 1 (SCD1) play a crucial role. The rate of *de novo* lipogenesis is regulated primarily at transcriptional level by several nuclear transcription factors among which are sterol regulatory element-binding protein 1C (SREBP1c), regulated by insulin, and carbohydrate-responsive element binding protein (ChREBP), regulated by glucose, are among the main ones.

Fatty acid oxidation takes place mainly in mitochondria although, it can also occur in peroxisomes and endoplasmic reticulum (ER). It is suppressed in a fed state and upregulated during fasting. The rate of oxidation is mainly regulated by insulin and peroxisome proliferator receptor alpha (PPARA). PPARA controls the expression of several genes related to mitochondrial FA oxidation and therefore activation of PPARA prevents lipid accumulation in the liver and leads to decreased hepatic fat storage. Conversely, inefficient activation of PPARA may lead to hepatic steatosis.

Hepatic gluconeogenesis occurs during prolonged fasting by the induction of pyruvate carboxylase in an abundance of acetyl-CoA and is further regulated by transcriptional activation of phosphoenolpyruvate carboxykinase (PEPCK) and glucose-6-phosphatase (G6PC). Insulin normally suppresses gluconeogenesis however, this inhibitory function of insulin might be impaired in insulin resistance. In addition, ChREBP and forkhead box O1

(FOXO1) further regulate rate of hepatic glucose formation, through activating PEPCK and G6PC.

Women with PCOS are at increased risk of developing NAFLD, and these women are more likely to have the more severe forms of NAFLD (708,721,722). Moreover, it was noted that PCOS is diagnosed frequently in female patients with biopsy-confirmed NAFLD (723). The estimated prevalence of NAFLD in women with PCOS varies between 35 to 70 %, compared to 20 to 30 % in the control population. (256,708,724-727). In addition, as demonstrated in some studies, this might be independent of age, BMI, waist circumference and associated comorbidities, however, it should be noted that majority of the studies on assessing the risk of NAFLD in PCOS, included only the overweight/obese population with PCOS. Furthermore, it was demonstrated that NAFLD was more prevalent in adolescent girls with PCOS than girls without PCOS, 37.5% vs 15.1% respectively, and that degree of steatosis in girls with both NAFLD and PCOS was greater than in those with NAFLD but without PCOS (728). Insulin resistance is a central factor contributing to pathophysiology of both PCOS and NAFLD, and both conditions are now considered as manifestations of metabolic syndrome (722). In addition, it has been documented that the prevalence of PCOS and NAFLD rise proportionally to the degree of insulin resistance. Moreover, it was demonstrated that decreased SHBG and increased androgens were associated with the incidence of NAFLD in women with PCOS (729,730). However, it was also shown that among women with PCOS, patients with NAFLD and PCOS demonstrate greater insulin resistance, but have similar circulating androgen levels, when compared with those with PCOS alone (731). Interestingly, NAFLD is an early predictor of metabolic disorders, particularly in the normal weigh population (711). Moreover, it was found that young, lean subjects with insulin resistance in skeletal muscle, have redirected energy derived from carbohydrates into hepatic *de novo* lipogenesis, also have increased hepatic triglyceride synthesis, as compared with healthy controls (732,733). Given, than young lean PCOS women often present with insulin resistance (734), and insulin resistance is central in the aetiology and pathophysiology of NAFLD, it is likely that lean PCOS women might be at higher risk of developing NAFLD than age- and BMI-matched controls.

Adolescent PCOS-like sheep were hyperinsulinemic, but normoglycemic, and had evidence of subclinical hepatic steatosis, but without changes in plasma ALT and AST, and independent of body weight and central adiposity (411). Further, it was demonstrated that these prenatally androgenised 11 months old sheep had normal levels of circulating testosterone but increased expression of hepatic AR, when compared with controls (411). In addition, in chapter 3, it was reported that that these adolescent PCOS-like sheep had evidence of decreased adipogenesis in SAT and impaired expression of genes associated with insulin signalling in that adipose depot. Further, these animals had also increased fasting FFA concentrations, likely due to decreased adipose tissue storage.

The aims of this chapter were to:

1. establish molecular mechanisms underlying fatty liver in adolescent PCOS-like sheep
2. evaluate hepatic liver fat content in adult control and PCOS-like animals
3. investigate gene expression associated with hepatic lipid and glucose metabolism in the adult cohort of PCOS-like sheep

5.2 Methods

5.2.1 Experimental animals

The ovine model, the animals used, their husbandry and treatments have been described previously in Section 2.2. The female animals assessed in this chapter are detailed in Table 5.1.

Treatment	Developmental stage	Sample number (n)
Adolescent		
Maternal Injection D62-102	Ewes 11 months old	C=5, TP=9
Adult		
Maternal Injections D62-102	Ewes 30 months old	C=11, TP=4

Table 5.1 Treatment regime, age and corresponding sample numbers of experimental animals discussed in this chapter.

5.2.2 Gene expression analysis using qRT-PCR.

Extraction of RNA from liver tissue was performed using Qiagen RNeasy Mini Kit (Qiagen Ltd., West Sussex, UK), as described in section 2.8.1. Protocols for cDNA synthesis and qRT-PCR are described in section 2.8.3. and 2.8.4, respectively. Forward and reverse primers were designed and validated as stated in section 2.8.6 and primer sequences analysed in this chapter are listed in Table 5.2.

Gene	Forward Sequence	Reverse Sequence	Product Size (bp)
<i>SLC27A2</i>	GTGGAAAGGGGAAAATGTGG	TCAAATTCATGGTCTGCCTTC	156
<i>SLC27A5</i>	CGGACATCAAGTTGCGAAG	ATCCCTGATACCTGCAGCAC	109
<i>CAVI</i>	CATCTCTACACTGTTCCCATCC	ACGTCGTCGTTGAGATGCTT	155
<i>CAV2</i>	CCACAGCAGCGTCGATTAC	CACTGGCTCTGCAATCACAT	121
<i>FABP4</i>	TGTAAATGGGGATGTGGTCA	CAGCACCAGCTTATCATCCA	217
<i>FABP5</i>	TTCAGCAGCTGGTAGGAAGA	GCACCTACTTTTCGCAGAGC	100
<i>SREBF1</i>	CAATGTGTGAGAAGGCCAGT	AGGAGCAGGTCACACAGGAG	106
<i>ACACA</i>	CTCGCCAGCAGAATTTGTTA	CGGATGGATCTCATGCATTT	105
<i>FASN</i>	CATGGCGTTCCACTCCTATT	GGACTCGGGGATGGAAGT	124
<i>PPARA</i>	CACAAGTGCCTTTCCGTTGG	ATGACGAAGGGCGGATTGTT	248
<i>MLXIPL</i>	CTCTGACACGCTCTTCACCA	GTCAGGTCTGGCTGGATCAT	105
<i>FOXO1</i>	CCAGCTCGAACGCTAGTACC	GGGGTTACTGATCTCGGACA	155
<i>PEPCK</i>	AAAGAGATACGGTGCCCATC	ATGCCAATCTTGGACAGAGG	178
<i>G6PC</i>	GAATGTCTGCCTGTCACGAA	ATCCAATGGCGAAACTGAAC	179
<i>GHR</i>	CGTCTCTGCTGGTGAAAACA	AGGATGTCGGCATGAATCTC	204
<i>STAT5A</i>	CTTGTTGCGCTTTAGCGACT	GTGTGGTGAATGGCTTCAGA	101
<i>STAT5B</i>	GTCAGCATTTCCCATTTGAG	TGGGTGGCCTTAATGTTCTC	109

Table 5.2 Forward and reverse primer sequences and product size for genes analysed in the postnatal liver tissue using SYBR Green qRT-PCR.

5.2.3 Oil Red O Lipid Staining and Analysis

Oil Red O (ORO) lipid staining on the liver samples was performed and analysed as per protocol published in Nature Protocols for imaging of neutral lipids (735). Liver samples were embedded in OCT (VWR International, Leicestershire, UK), as described in section 2.2.5. Four frozen 10µm sections per animal, 40µm apart, were cut on a cryostat (Leica Cryostat Microtome 1900, Leica Biosystems, Germany) at -20°C, mounted onto glass slides and air-dried. The ORO stock solution was prepared by dissolving 2.5g ORO in 400ml 99% (vol/vol) isopropanol, and the ORO working solution by mixing 1.5 part of stock solution with 1 part of distilled water. The working solution was filtered through 45µm filter to remove precipitates and used immediately. Sections were immersed in the ORO solution for 5 min at room temperature and rinsed under running tap water for 30 min, taking care that sections were not damaged during this process. Slides were mounted in Aqua-Mount media (Fisher Scientific Ltd.). On the same day, to prevent precipitation of the ORO dye, sections were visualised with light microscope at x20 magnification with and two representative images (frames) per section were captured. Lipid accumulation was quantified via the amount of ORO staining with ImageJ, as per the published protocol.

5.2.4 Measurement of plasma analytes

Measurement of plasma analytes was performed by Dr Forbes Howie. To measure the concentration of ALT, AST, albumin, cholesterol, LDL and HDL, commercial assay kits were employed (Alpha Laboratories Ltd., Eastleigh, UK) as per the manufacturer's protocols, using a Cobas Fara centrifugal analyser (Roche Diagnostics Ltd.) to obtain analyte concentration. Assay sensitivities for ALT, AST, albumin, cholesterol, LDL and HDL were 2U/l, 2U/l, 0.5g/l, 0.1mmol/l, 0.02mmol/l and 0.02mmol/l, respectively, and the overall CVs were all <3%.

5.2.5 Statistical analysis

Statistical analysis was performed with GraphPad Prism version 6.0 (GraphPad Software, Inc., San Diego, CA). For comparing means of two treatment groups with equal variances an unpaired, two-tailed Student's t test was used. To compare multiple sets of data a one-way ANOVA was used. Log transformation was used to approximate the normal distribution for parametric analysis when necessary. A P value of <0.05 was considered as statistically significant. Results are presented as mean + S.E.M, where * signifies a P<0.05, ** P<0.01 and *** P<0.001. Area under the curve was calculated using the trapezoidal method. Correlation was assessed by calculation of the Pearson r co-efficient. A line of best fit was incorporated only in the figures where correlation was statistically significant.

5.3 Results

5.3.1 Hepatic FA uptake in adolescent animals

Considering the evidence of hepatic steatosis and increased fasting FFA in the circulation of 11 months old PCOS-like animals, we assessed hepatic fatty acid uptake potential in adolescent animals. Adolescent prenatally androgenised animals had significantly upregulated expression of *SLC27A2* and *SLC27A5*, encoding FATP2 and FATP5 respectively ($P < 0.05$; Fig. 5.1 A and B). In addition, adolescent PCOS-like sheep had a significantly elevated expression hepatic *CAV2* ($P < 0.05$; Fig. 5.1D) and trend for increased *FABP4* expression ($P = 0.06$; Fig. 5.1 E) however, this did not reach statistical significance.. There was no difference in the expression of *CAV1* and *FABP5* between control and prenatally TP-exposed animals (Fig. 5.1 C and F).

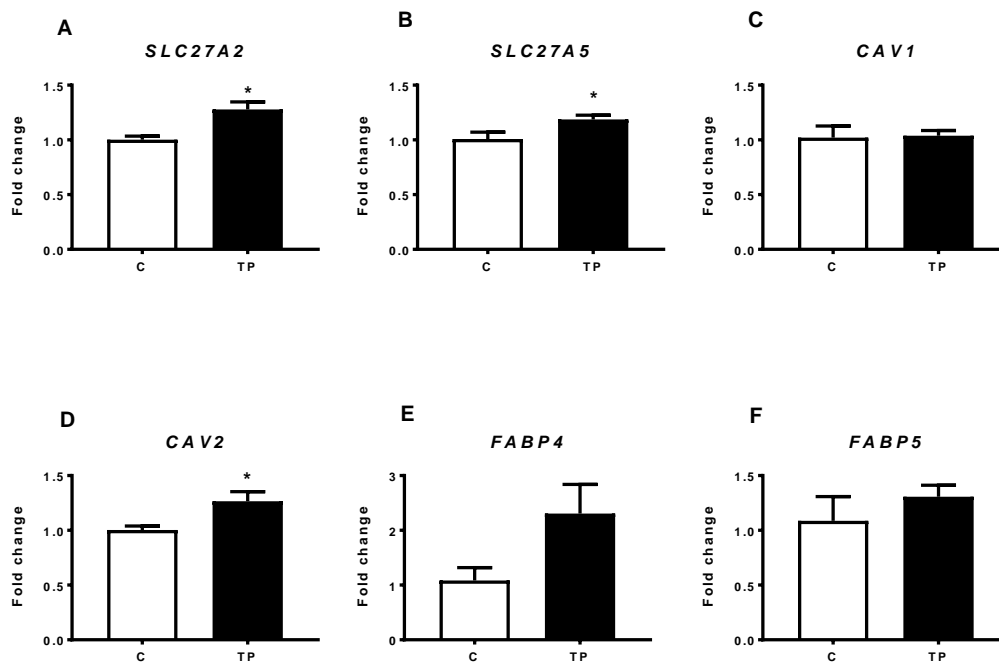


Figure 5.1 Hepatic expression of genes associated with FA uptake in adolescent controls (C) and prenatally androgenised (TP) animals, as quantified by qRT-PCR. P value of < 0.05 was considered as statistically significant. Results are presented as mean + S.E.M, where * signifies a $P < 0.05$.

5.3.2 Hepatic *de novo* lipogenesis in livers of 11 months old animals.

Next, we investigated a possible role of *de novo* lipogenesis in hepatic phenotype of adolescent PCOS-like sheep. Adolescent prenatally androgenised animals had significantly elevated mRNA expression of *ACACA*, encoding ACC1, and *FASN*, encoding FAS ($P < 0.05$; Fig. 5.2 B and C, respectively), and a trend towards increased expression of *SREBF1*, encoding SREBP1c ($P = 0.07$; Fig. 5.2 A) however, this did not reach statistical significance.

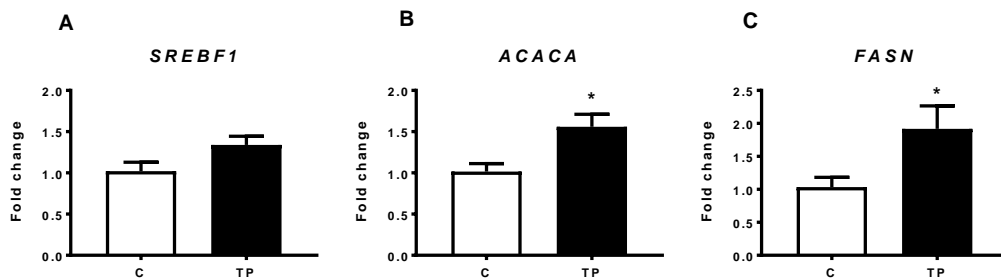


Figure 5.2 Hepatic expression of genes involved in *de novo* lipogenesis in adolescent control (C) and prenatally androgenised (TP) animals, as quantified by qRT-PCR. P value of < 0.05 was considered as statistically significant. Results are presented as mean + S.E.M, where * signifies a $P < 0.05$.

5.3.3 Hepatic fatty acid utilisation and storage in adolescent animals

Subsequently, we evaluated gene expression associated with fatty acid utilisation and storage. There was no difference in the expression of *PPARA*, regulating FA oxidation, and *PPARG*, promoting lipid storage, between control and PCOS-like animals (Fig. 5.3 A and B, respectively). However, there was trend towards decreased expression of *PPARGC1A*, a transcriptional co-activator regulating fatty acid oxidation, mitochondrial biology and energy homeostasis, in prenatally androgenised animals ($P = 0.06$; Fig. 5.3 C), but this did not reach statistical significance.

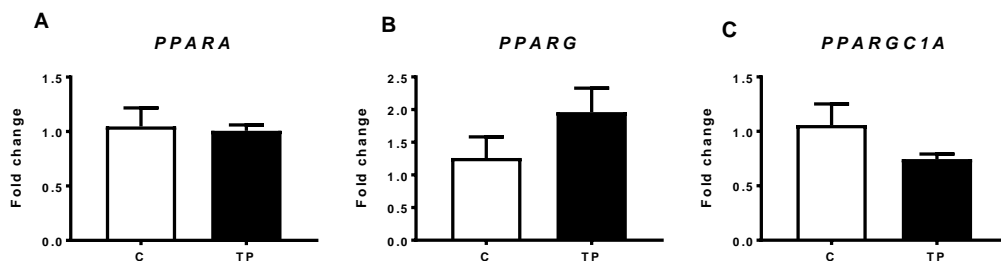


Figure 5.3 Hepatic expression of genes associated with FA utilisation and storage in adolescent control (C) and prenatally androgenised (TP) animals, as quantified by qRT-PCR. Results are presented as mean + S.E.M.

5.3.4 Gluconeogenesis in adolescent PCOS-like animals

In the view of hyperinsulinemic normoglycaemia in adolescent PCOS-like animals we further investigated expression of main molecular components of the hepatic gluconeogenic pathway. Adolescent PCOS-like animals had a trend towards decreased expression of *MLXIPL*, encoding ChREBP (P=0.09; Fig. 5.4 A) however, this did not reach statistical significance. There was no difference in the expression of *FOXO1*, as well as *PEPCK* and *G6PC*, a downstream component of gluconeogenesis between control and prenatally TP-exposed animals (Fig. 5.4 B-D).

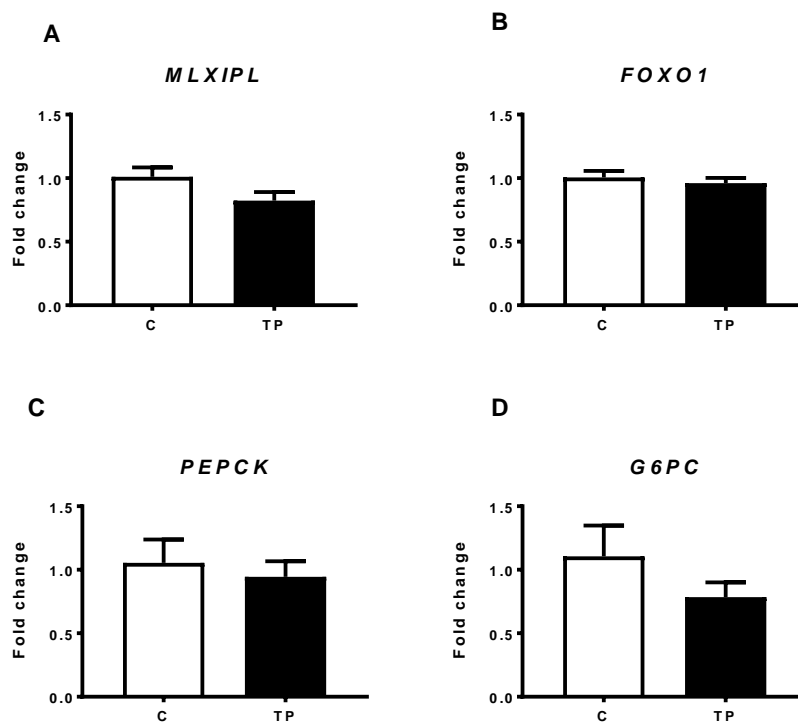


Figure 5.4 Hepatic expression of genes associated with gluconeogenesis in adolescent control (C) and prenatally androgenised (TP) animals, as quantified by qRT-PCR. Results are presented as mean + S.E.M.

5.3.5 Hepatic expression of insulin and growth hormone receptors

Considering the normal expression of genes involved in gluconeogenic pathway we next evaluated expression of *INSR* and *GHR*, and components of its downstream signalling pathway (*STAT5A* and *STAT5B*). There was no difference in the expression of *INSR*, *GHR* and *STAT5A* between controls and PCOS-like animals (Fig. 4.5 A-C) however, there was a trend towards decreased expression of *STAT5B* in TP-exposed animals ($P=0.08$; Fig. 4.5 D) but this did not reach statistical significance.

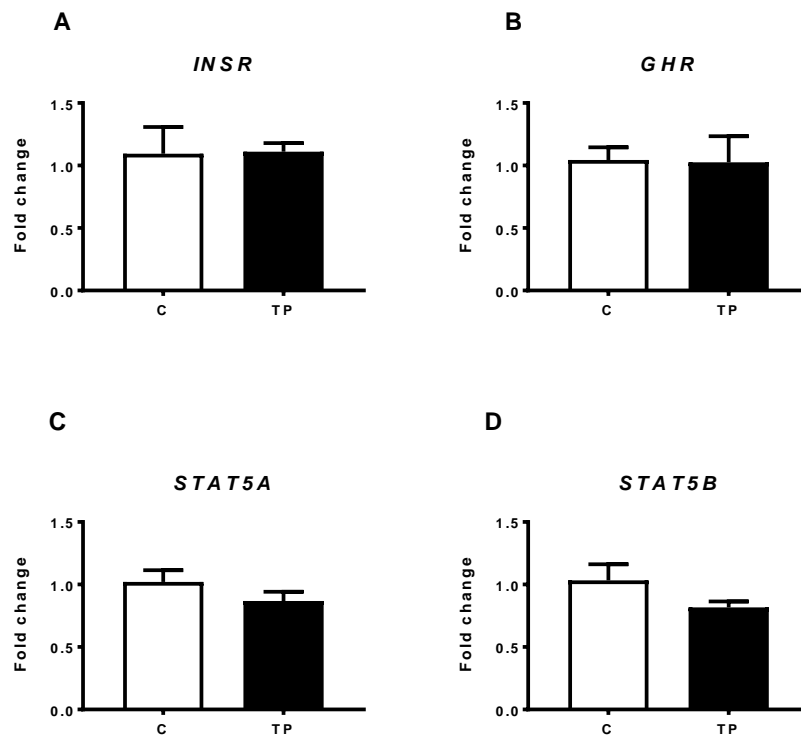


Figure 5.5 Hepatic expression of insulin and growth hormone receptors, *STAT5A* and *STAT5B* in adolescent control (C) and prenatally androgenised (TP) animals, as quantified by qRT-PCR. Results are presented as mean + S.E.M.

5.3.6 Correlation of insulin with selected hepatic gene expression

In view of importance of insulin in regulation of *de novo* lipogenesis and gluconeogenesis we next examined any potential correlation of insulin levels in blood samples collected after 15 min of IVGTT test with hepatic expression of *INSR*, *SREBF1* and *PEPCK* and *G6PC*. In adolescence, there was no correlation between level of insulin with hepatic expression of *INSR*, *PEPCK* and *G6PC* (Fig. 5.6A, C and D, respectively) however, there was a significant correlation between insulin and hepatic *SREBF1* expression ($P < 0.01$; $r = 0.68$; Fig. 5.6 B).

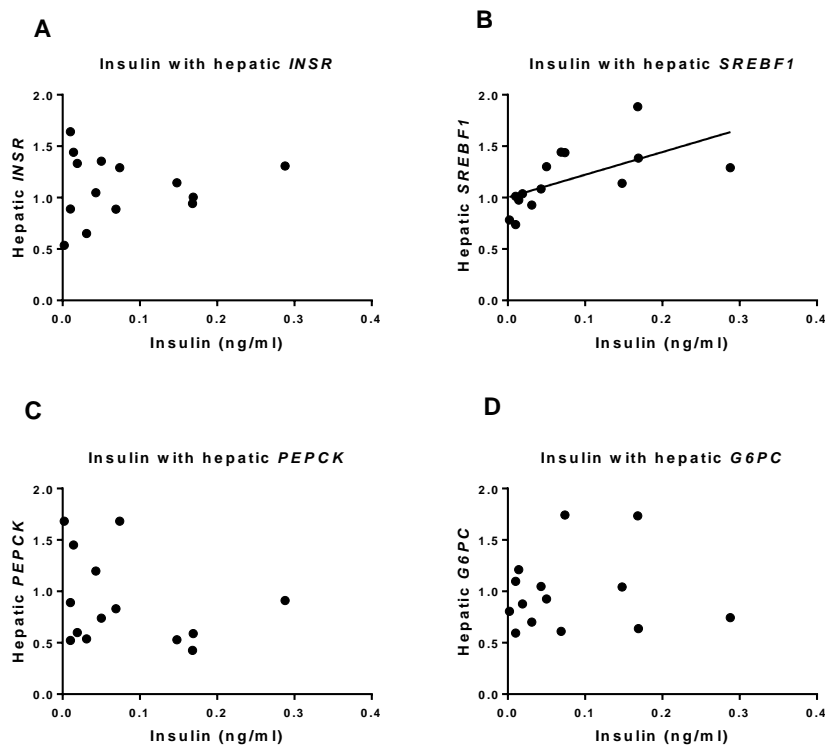


Figure 5.6 Correlation of insulin level at 15min of IVGTT with hepatic expression of *INSR*, *SREBF1*, *PEPCK* and *G6PC* in adolescent control (C) and prenatally androgenised animals (TP).

5.3.7 Liver lipid content in adult animals

To determine hepatic lipid content in adult animals, four frozen sections of liver tissue from each animal were stained with an ORO histological lipid stain, and analysed using image J. This analysis revealed that there was no difference in the amount of hepatic fat between adult control and PCOS-like animals (Fig. 5.7 B). Subsequently, we evaluated the determinants of liver function. There was no difference in the levels of ALT, AST and Albumin between control and PCOS-like animals (Fig. 5.7 C-E). In addition, we assessed the levels of circulating total cholesterol, LDL and HDL. Again, there was no difference in level of total cholesterol, LDL and HDL between control and PCOS-like animals (Fig. 5.7 F-H).

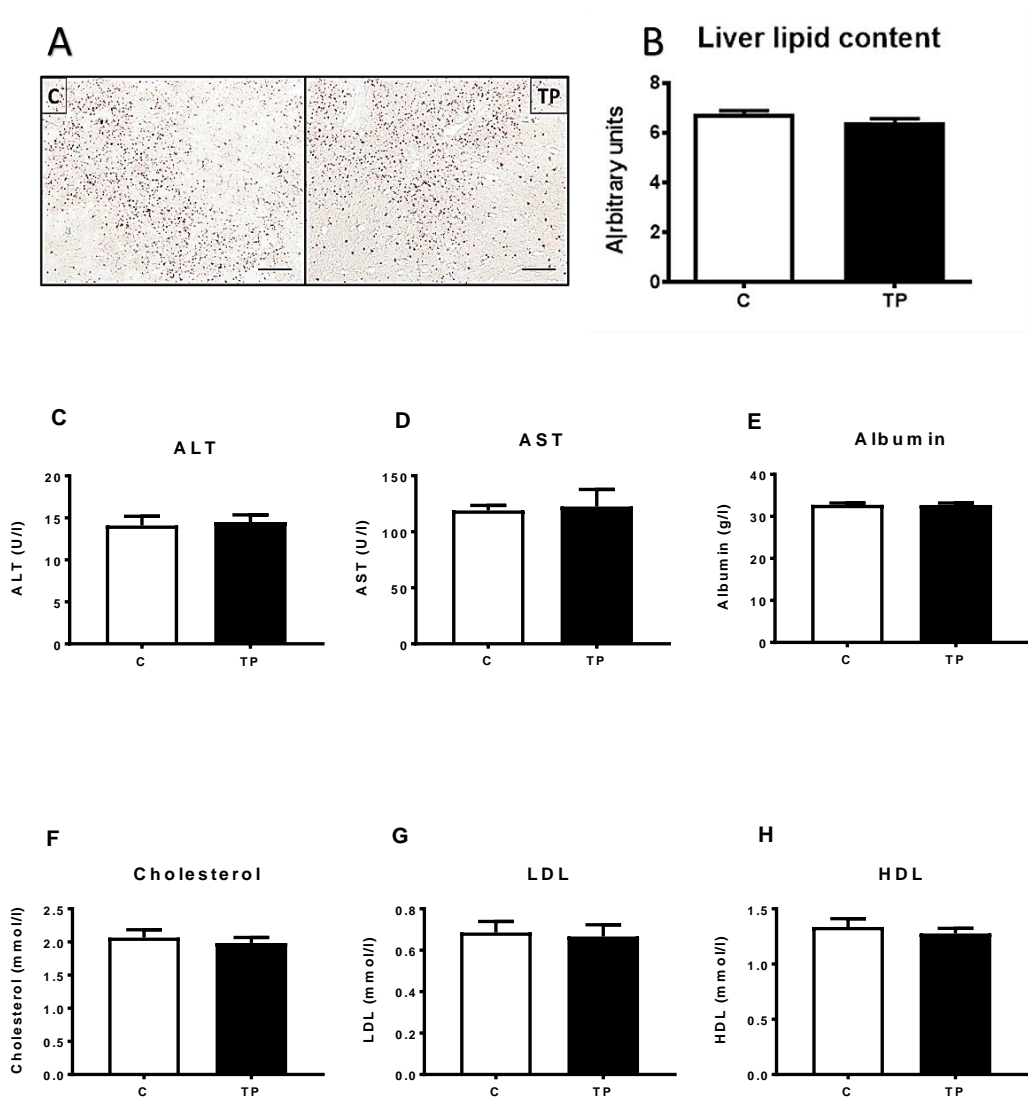


Figure 5.7 Liver lipid content, plasma liver analytes and cholesterol level in adult animals. A) representative Oil red O histological stain for lipids in adult liver sections of control (C) and prenatally androgenised (TP) animals; scale bars = 100 μ m; B) quantification of liver lipid content using Image J; C-E) plasma liver analytes; F-H) plasma cholesterol level. Results are presented as mean + S.E.M.

5.3.8 Hepatic FA uptake in adult old animals.

In adulthood, there was a trend towards decreased expression of *SLC27A2* ($P=0.08$; Fig. 5.8 A), *SLC27A5* ($P=0.11$; Fig. 5.8 B) and *FABP4* ($P=0.15$; Fig. 5.8 E) in PCOS-like animals, but this did not reach statistical significance. Conversely, there was a trend for increased expression of *CAV1* and *CAV2* in TP-exposed animals ($P=0.14$ and $P=0.16$; Fig. 5.8 C and D, respectively). There was no difference in the expression of *FABP5* between control and PCOS-like animals (Fig. 5.8 F).

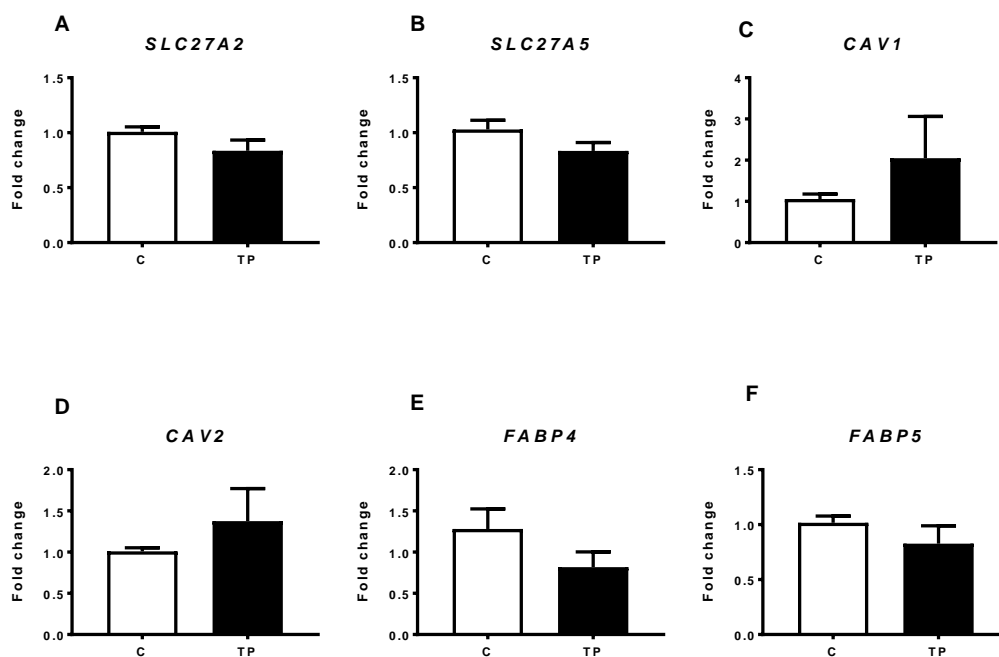


Figure 5.8 Hepatic expression of genes associated with FA uptake in adult controls (C) and prenatally androgenised (TP) animals, as quantified by qRT-PCR. Results are presented as mean + S.E.M.

5.3.9 Hepatic *de novo* lipogenesis in adult animals.

Next, we assessed expression of genes involved in *de novo* lipogenesis. There was no difference in the expression of *SREBF*, *ACACA* and *FASN* between adult control and PCOS-like animals (Fig. 5.9 A-C).

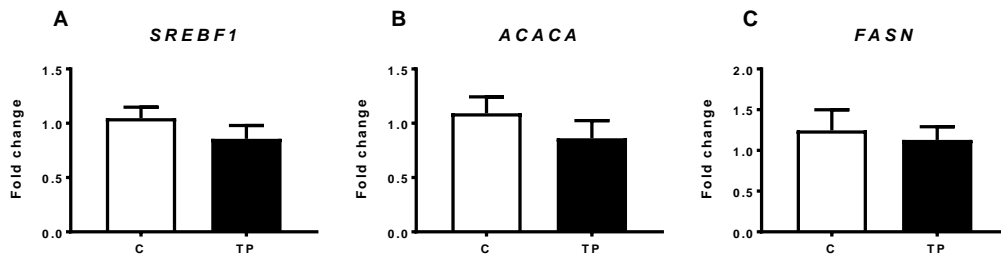


Figure 5.9 Hepatic expression of genes associated with *de novo* lipogenesis in adult control (C) and prenatally androgenised (TP) animals, as quantified by qRTR-PCR. Results are presented as mean + S.E.M

5.3.10 Hepatic fatty acid utilisation and storage in adult animals.

There was no difference in the expression of *PPARA* and *PPARG* between control and PCOS-like animals (Fig. 5.10 A and B; respectively). There was a trend towards increased expression of *PPARGC1A* in prenatally androgenised animals however, this did not reach statistical significance ($P=0.09$; Fig. 5.10 C).

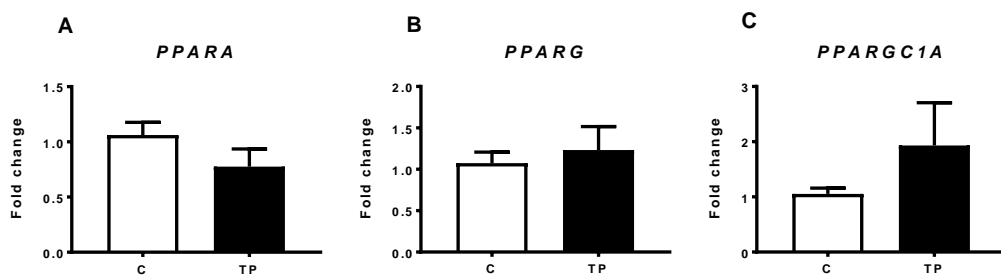


Figure 5.10 Hepatic expression of genes associated with fatty acid utilisation and storage in adult control (C) and prenatally androgenised (TP) animals, as quantified by qRT-PCR. Results are presented as mean + S.E.M.

5.3.11 Gluconeogenesis regulation in adult animals.

Analysis of the expression of genes involved in hepatic gluconeogenesis revealed that there was no difference in the expression of *MLXIPL*, *FOXO1*, *PEPCK* and *G6PC* between adult control and TP-exposed animals (Fig. 5.11 A-D).

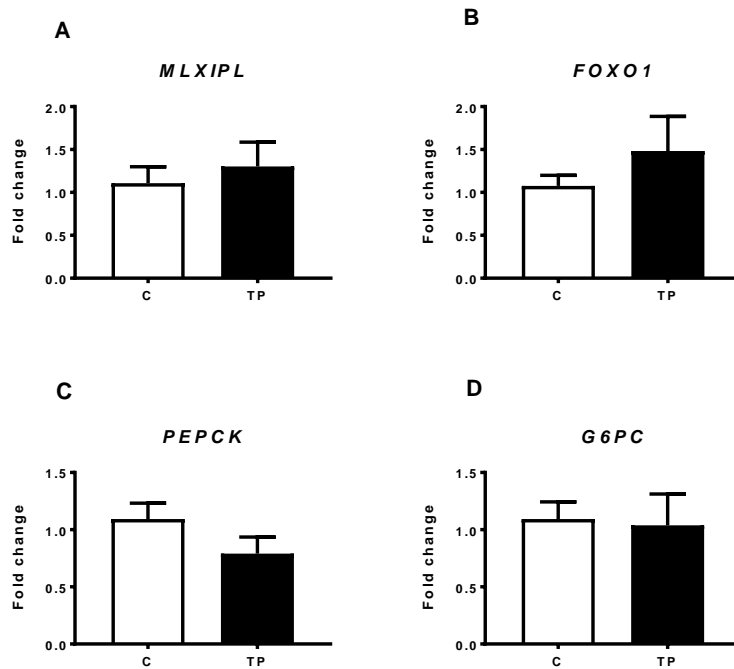


Figure 5.11 Hepatic expression of genes associated with gluconeogenesis in adult control (C) and prenatally androgenised (TP) animals, as quantified by qRT-PCR. Results are presented as mean + S.E.M.

5.3.12 Hepatic expression of insulin and growth hormone receptors

In adult PCOS-like animals there was a trend towards decreased expression of *INSR* ($P=0.08$; Fig. 5.12 A) however, this did not reach statistical significance. There was no difference in the expression of *GHR*, *STAT5A* and *STAT5B* between controls and PCOS-like animals (Fig. 5.12 B-D).

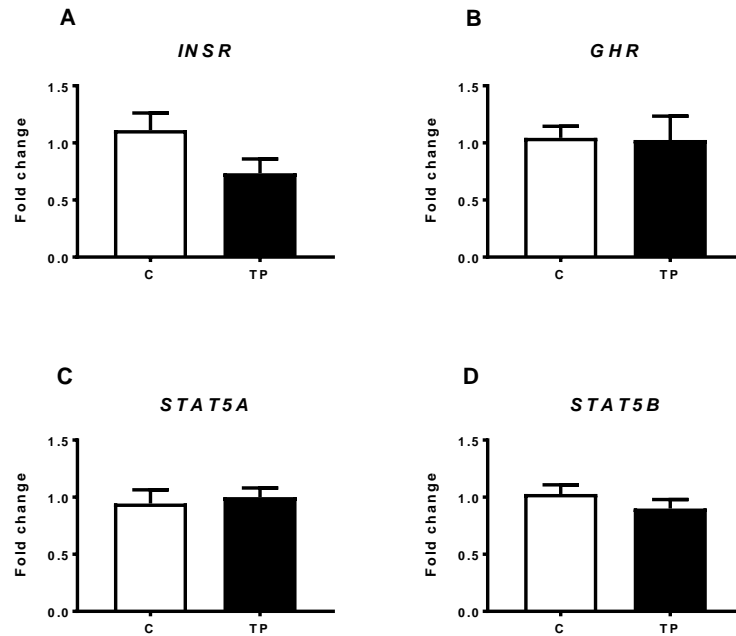


Figure 5.12 Hepatic expression of insulin and growth hormone receptors, *STAT5A* and *STAT5B* in adolescent control (C) and prenatally androgenised (TP) animals, as quantified by qRT-PCR. Results are presented as mean + S.E.M

5.3.13 Correlation of insulin with selected hepatic gene expression

In adulthood, there was a positive correlation between levels of circulating insulin in blood samples collected after 15 min of IVGTT and hepatic *INSR* expression ($P < 0.05$; $r = -0.051$; Fig. 5.13 A) however, there was no correlation between insulin and *SREBF1*, *PEPCK* and *G6PC* (Fig. 5.12 B-D).

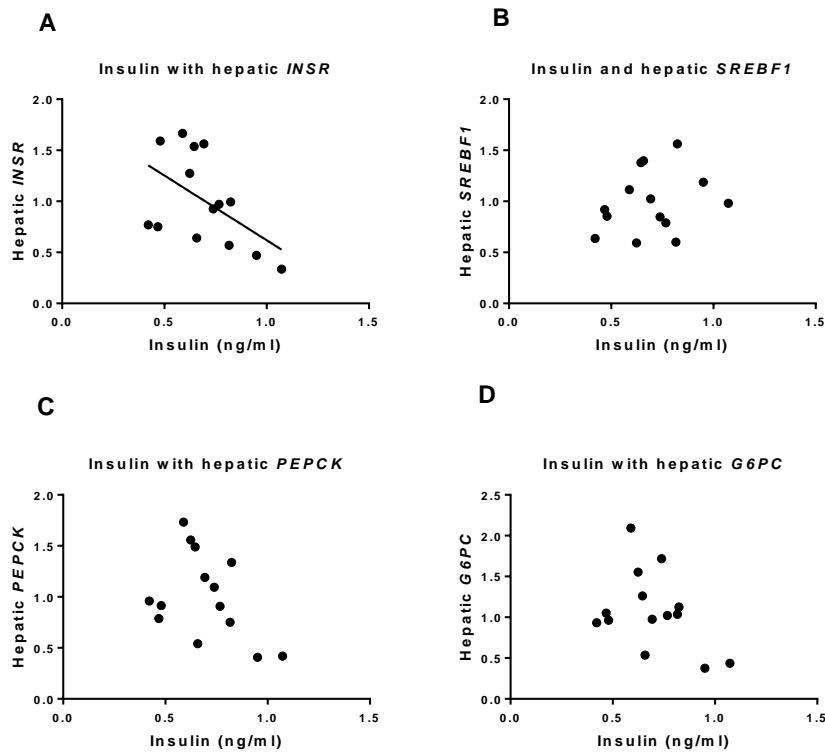


Figure 5.13 Correlation of insulin level at 15min of IVGTT with hepatic expression of *INSR*, *SREBF1*, *PEPCK* and *G6PC* in adult control (C) and prenatally androgenised animals (TP).

5.4 Discussion

Previous research has demonstrated that adolescent PCOS-like sheep had evidence of subclinical hepatic steatosis (411). Furthermore, in chapter 3, it was reported that these adolescent prenatally androgenised animals had increased circulating fasting FFA, most likely due to decreased adipogenesis and perturbed insulin signalling in SAT, but independent of body weight and central adiposity. Since, it was established that circulating FFA comprise majority of hepatic lipids in NAFLD, we aimed to investigate the potential role of increased fasting FFA in hepatic phenotype of adolescent PCOS-like animals. Here, we provide evidence that these adolescent PCOS-like sheep had upregulated expression of genes involved in hepatic FA uptake and *de novo* lipogenesis, but normal expression of genes associated with FA oxidation, which might elucidate the mechanisms involved in increased lipid accumulation in those animals.

The mRNA expression of *SLC27A2* (FATP2) and *SLC27A5* (FATP5) was significantly upregulated in livers of adolescent PCOS-like animals. Although, there are 6 FATP isoforms that have been identified in mammalian cells, FATP2 and FATP5 are utilised as the major FATPs in liver (736,737). It was demonstrated that mice with liver specific *FATP2* deficiency, when fed a high fat diet, had reduced liver TG levels and decreased fasting glucose and insulin levels, when compared with control mice (738). Correspondingly, mice with hepatic *FATP5* knockdown had reduced FA uptake and were protected from NAFLD (739). In addition, authors found that induced *FATP5* deficiency in mice liver can reverse already established NAFLD, resulting in significantly improved whole-body glucose homeostasis (739). Moreover, human studies shown that hepatic *FATP5* mRNA is upregulated in patients with steatosis (740), and *FATP5* promoter polymorphism is associated with features of the metabolic syndrome and steatosis (741)

Our results also demonstrated that expression of hepatic *CAV2*, but not *CAV1*, was significantly upregulated in livers of adolescent PCOS-like animals. Caveolins are fatty acid and cholesterol binding proteins and main structural components of caveolae, which are plasma membrane pits implicated in endocytosis, cholesterol homeostasis and signal transduction (742,743). It was demonstrated that *CAV1* and *CAV2* have the same tissue distribution, as *CAV1* usually forms oligomers with *CAV2*, and are mainly localised to the plasma membrane compartment, but also mitochondria, lipid droplets, and liver peroxisomes (744). However, whereas much is known about potential role of *CAV1* in pathophysiology of NAFLD (745,746), reports on the role of *CAV2* are scarce (747). Hepatic overexpression of

CAV1 or *CAV2* increased bile flow (748). In addition, the same study demonstrated that overexpression of *CAV1*, but not *CAV2*, induced increase in plasma HDL cholesterol levels and hepatic free cholesterol content (748). Several mouse models have shown that global *CAV1* deficiency prevents fat accumulation within hepatocytes, and therefore prevents steatosis, however *CAV1* overexpression does not appear to cause liver steatosis. Therefore, based on the current knowledge we are unable to draw any definite conclusions regarding potential role of increased *CAV2* in the livers of adolescent PCOS-like animals.

In addition, our results showed that 11 months old prenatally androgenised sheep had trend for upregulated expression of *FABP4*. Cytoplasmic FABPs actively regulate FA trafficking to specific organelles in the cell for lipid oxidation storage as lipid droplets in the cytoplasm (749). It was demonstrated that hepatic *FABP4* expression is upregulated in patients with NAFLD and that levels of *FABP4* positively correlate with liver fat content (750,751).

Overall, these results provided strong evidence that upregulated expression of hepatic FA transporters likely contribute to hepatic steatosis in adolescent prenatally androgenised animals. Interestingly, we found a positive correlation between levels of fasting FFA with expression of *FATP2* and *FABP4*, suggesting that circulating FFA might directly regulate expression of those transporters in liver. Indeed, based on experimental data it was proposed that FFA can upregulate expression of hepatic transporters when existing ones become saturated (752). Consequently, increased FFA in adolescent PCOS-like animals could directly upregulate specific hepatic FA transporters in those animals. However, to explore other potential mechanisms contributing to increased hepatic lipid content, the expression of genes indicated in *de novo* lipogenesis, a process in which the liver synthesises endogenous FAs from glucose, was also investigated.

Our result demonstrated that *ACACA* (*ACC1*) and *FASN* (*FAS*) were significantly overexpressed, together with a trend for increased expression of *SREBF1* (*SREBP1C*) in adolescent PCOS-like animals. In the process of FA synthesis, *ACC1* converts acetyl-CoA, an essential substrate of fatty acids, to malonyl-CoA. *FAS* then utilises both acetyl-CoA and malonyl-CoA to form palmitic acid (702). *SCD1* catalyses the synthesis of monounsaturated FAs. Both *ACC1* and *FAS* are highly regulated by the transcriptional factor *SREBP1c*, which could be reflected in the positive correlation in the expression of *SREBP1c* with *ACC1* and *FAS*, as demonstrated in adolescent animals. In turn, expression of *SREBF1* is directly regulated by insulin (753-755), which again was mirrored in positive correlation between levels of insulin after 15 min of IVGTT and hepatic mRNA expression of *SREBF1* in

adolescent animals. Hepatic expression of ACC1, FAS and SREB1C have been shown to be upregulated in patients with NAFLD (740,756,757). FAS catalyses the last step in FA biosynthesis therefore, it is considered a main determinant of the maximal hepatic capacity to generate *de novo* fatty acids (757). Furthermore, results from animal studies provide additional information about importance of ACC in the pathogenesis of NAFLD. It was demonstrated that mice with hepatic ablation of ACC1 accumulated 40% less TG than control mice (758), whereas in rats with NAFLD, suppression of ACC1 and ACC2 resulted in decreased hepatic lipids content and improved hepatic insulin sensitivity (759). In summary, it is likely that hepatic steatosis in adolescent PCOS-like animals might result from combination of elevated circulating FFA and subsequent increased transport of FFA into liver as well as hyperinsulinemia and amplified *de novo* lipogenesis in those animals.

We also assessed the hepatic expression of *PPARA* and *PPARG* and found no difference in the expression those genes between control and prenatally androgenised animals. *PPARA* plays a central role in fatty acid metabolism by controlling expression of numerous genes involved in mitochondrial and peroxisome fatty acid oxidation, therefore, activation of *PPARA* can prevent or at least decrease hepatic lipid content (702). It was demonstrated that mice with hepatocyte specific *PPARA* deletion had impaired fatty acid homeostasis and developed NAFLD (760), whereas treatment of mice with spontaneous hepatic steatosis with a *PPARA* agonist, fenofibrate, decreased hepatic lipid content by activating expression of genes involved in fatty acid turnover (761). Therefore, comparable expression of *PPARA* between control and PCOS-like animals indicate that increased uptake of FAs and *de novo* lipogenesis is not countered by increased oxidation. Interestingly, *PPARA* activity and FA oxidation are also directly influenced by adiponectin (108). Treatment with recombinant adiponectin of mice with induced steatosis has been shown to reduced steatosis and inflammation, due to enhanced hepatic FA oxidation and decreased activity of ACC1 and FAS (762). Moreover, it was reported that patients with NAFLD have decreased levels of circulating adiponectin, independent of BMI and adiposity (763,764), suggesting that adiponectin can be a potential therapeutic agent for NAFLD (765). Thus, decreased level of circulating adiponectin in adolescent PCOS-like animals could also contribute to increased hepatic steatosis in those animals.

PPARG, in opposite to *PPARA* function, promotes lipid storage. It was found that expression of *PPARG* was elevated in a murine model of steatosis (766), and some researchers (750,767), but not others (768), reported increased expression of *PPARG* in NAFLD patients. In addition, it was shown that mice with liver specific *PPARG* knockdown had reduced hepatic TG content

(769,770). It was proposed that steatosis promoting the activity of hepatic PPARG is due to the upregulation of genes involved in lipogenesis, TG synthesis and lipid droplet formation (771). However, in contrast to these studies presenting potential adverse effects of PPARG on NAFLD, adenovirus-mediated overexpression of PPARG in the liver was shown to decrease hepatic steatosis, inflammation and fibrosis (772). Moreover, treatment with PPARG agonists have been shown to reduce liver steatosis in a mouse model of induced NAFLD (773) and humans with steatosis (774). PPARG could modulate NAFLD through several mechanisms. First, numerous studies documented that PPARG agonists improve insulin sensitivity in peripheral tissues, leading to enhanced uptake of FFA in skeletal muscle and adipose tissue, thus decreased FFA flux to the liver. In addition, since PPARG stimulates adipogenesis, it increases capacity of adipose tissue to buffer FFA in the circulation, thus again shunting them from liver. Finally, treatment with PPARG agonists increase circulating adiponectin, which in turn, increase insulin sensitivity, decrease hepatic steatosis and inflammation (775).

We also found a trend towards decreased hepatic expression of *PPARGC1A* ($PGC1\alpha$) in adolescent PCOS-like animals. In liver $PGC1\alpha$ regulates mitochondrial biogenesis, oxidative metabolism, and a complex program of metabolic changes that occur during the transition from fasted to fed state, including gluconeogenesis and fatty acid oxidation (776). Moreover, it was reported that activity of $PGC1\alpha$ was decreased in rodent model of steatosis, which was further paralleled by reduced mitochondrial biogenesis (777). Similarly, it was found that insulin resistant patients with NAFLD had decreased mitochondrial DNA content and higher *PPARGC1A* promoter methylation levels which was further associated with decreased *PPARGC1A* mRNA levels showing that DNA methylation of the promoter silenced gene expression (778). Furthermore, the authors demonstrated that the abundance of liver *PPARGC1A* mRNA inversely correlated with fasting plasma insulin levels and homeostasis model assessment of insulin resistance (HOMA-IR), indicating that peripheral insulin resistance and the transcriptional activity of *PPARGC1A* in the liver might be interrelated (778). Likewise, we also found a negative correlation between fasting insulin and hepatic *PPARGC1A* expression, suggesting that high insulin levels in PCOS-like animals suppress expression of *PPARGC1A* in livers of those animals. Interestingly, $PGC1\alpha$ has also been indicated in regulating hepatic insulin sensitivity and gluconeogenesis (779). Recently, it was found that women with PCOS have increased *PPARGC1A* promoter methylation and decreased mitochondrial content in leukocytes (780). Furthermore, a positive correlation was found between the *PPARGC1A* promoter methylation ratio and the FAI in women with PCOS, suggesting that *PPARGC1A* promoter hypermethylation can be induced by androgens (780). Therefore, it is likely that reduced hepatic *PPARGC1A* in adolescent prenatally androgenised

animals could result from early epigenetic programming. However, PGC1 α expression was upregulated in a mouse models of diabetes where it promoted constitutive activation of gluconeogenesis (779). In addition, it was demonstrated that PGC1 α expression, like gluconeogenesis, is suppressed by insulin and the action of the INSR (779) and that PGC1 α directly stimulate FOXO1, which in turn regulates gluconeogenesis (781). Mice with hepatic deletion of *PPARGCIA* had an increased TG content and diminished expression of genes involved in β -oxidation in their livers, but also reduced fasting glucose levels and decreased expression of *PEPCK* and *G6PC* (782). However, PCOS-like animals had normal fasting glucose levels and comparable hepatic expression of *PEPCK* and *G6PC* despite downregulated expression of *PPARGCIA*. Moreover, our result showed that these animals had normal expression of other hepatic genes controlling gluconeogenesis, *MLXIPL* (ChREBP) and *FOXO1*, as well as *INSR*. However, considering increased circulating insulin in adolescent PCOS-like animals, both fasting and during glucose load, the predicted expression of genes associated with gluconeogenesis should be lower than in control animals. In addition, there was no correlation between levels of insulin and hepatic expression of *PEPCK* and *G6PC*. Therefore, these results might indicate potentially perturbed hepatic insulin signalling in prenatally androgenised animals. Interestingly, comparable mRNA levels of *MLXIPL* support similar levels of circulating glucose after 15 minutes of glucose load in control and PCOS-like sheep, as ChREBP is directly stimulated by glucose (783). However, since ChREBP regulates gluconeogenesis and lipogenesis (784), it seems that increased *de novo* lipogenesis in PCOS-like animals is independent of glucose levels.

Finally, we assessed growth hormone signalling. There was no difference in the expression of *GHR* and *STAT5A* between control and PCOS-like animals however there was a trend towards reduced expression of hepatic *STAT5B* in prenatally androgenised animals. Growth hormone (GH) plays an important role in regulating hepatic biology (785). GH action is facilitated via the GH receptor (GHR) and downstream hepatic GH signalling is mediated by *STAT5A* and *STAT5B*, which in turn control hepatic lipid metabolism. It was demonstrated that diminished GH-*STAT5* signalling predisposes mice and humans to early development of hepatic steatosis (786-790). Further, it was found that reduced hepatic *STAT5* signalling was paralleled by increased expression of *SREBP1c* and fatty acid transporters in the liver (790). GH also has significant roles in regulating hepatic glucose homeostasis. Increased GH is linked with impaired glucose tolerance, insulin resistance and compensatory hyperinsulinemia, whereas GH deficiency is associated with increased insulin sensitivity, decreased fasting glucose levels, decreased insulin secretion, and lowered hepatic glucose production (791). However, hepatic *STAT5* deficient mice have impaired insulin signalling and are affected by

hyperinsulinemia and insulin resistance (791). Interestingly, GH, through different patterns of pulsatility, with more frequent pituitary GH secretion in females than in males, and therefore more continuous pattern of plasma GH in females, has an important role in regulating sex-dependent hepatic gene expression (792,793). Hence, *STAT5B*, a downstream effector of GH signalling, is considered a key regulator of sexually dimorphic gene expression in the liver (794). Females, due to the persistence of plasma GH stimulation display partial desensitisation and consequently have decreased expression of *STAT5B* as compared to males (793,794). Since, decreased *STAT5B* is associated with NAFLD, and males present more frequently with hepatic steatosis than females, it was proposed that “feminisation” of the male liver leads to accumulation of hepatic triglycerides (793). It was demonstrated that castrated mice had reversed gene expression pattern, comparable to intact male *STAT5B*-null mice, which could mostly be restored by treatment with DHT (793). Furthermore, female mice treated with DHT presented with that the male-like expression pattern of the *STAT5B*, however, ovariectomy did not have significant impact on gene expression pattern, nor does treatment of ovariectomised females with estradiol, suggesting that *STAT5B* might be more of an androgen-driven than an estrogen-driven sexually dimorphic gene (793). Considering, a possibly reduced expression of *STAT5B* in adolescent PCOS-like sheep, it could be speculated that these females, due to prenatal androgen exposure, are born with somewhat male-like liver gene expression pattern, which is being altered - feminised during puberty, leading to decreased *STAT5B* expression and hepatic steatosis. Although, we did not investigate GH pulsatility in prenatally androgenised sheep, studies on androgenised mice revealed that early androgen exposure in females reprograms partially GHRH-GH system and defeminises hepatic-steroid-metabolising enzymes (795).

Interestingly, adult PCOS-like sheep had comparable levels of hepatic fat content with control animals, similar levels of hepatic analytes and cholesterol levels in blood. Further, there was no statistically significant difference in the expression of hepatic genes involved in fatty acid uptake, *de novo* lipogenesis, fatty acid utilisation and gluconeogenesis, despite increased body weight, elevated FFA and hyperinsulinemia. Adult PCOS-like sheep did however display a trend towards increased expression of *PPARGC1A* and decreased expression of hepatic *INSR* which further negatively correlated with insulin levels. Increased expression of *PPARGC1A* in adult PCOS-like animals could indicate induced hepatic fatty acid oxidation and mitochondrial biogenesis (796), which in turn, could contribute to normalised, as compared with control animals, levels of liver fat content in those animals. Further, it could be speculated that considering the hyperinsulinemia in PCOS-like animals, decreased hepatic *INSR* mRNA expression, likely due to chronically elevated insulin levels, might be beneficial and serve as

a limiting factor preventing hyperinsulinemic drive for increased *de novo* lipogenesis. In addition, changes in hepatic fat content in PCOS-like animals could be attributed to hypertrophic expansion of SAT and normalised leptin levels, as described in Chapter 4, which could increase adipose tissue capacity for FFA storage, hence redirecting FFA from liver to adipose tissue. This observation is reinforced by normal expression of hepatic fatty acid transporters, despite increased circulating FFA concentrations in prenatally androgenised animals. Moreover, this hypothesis is further supported by findings from studies on partial lipodystrophy, in humans and experimental animal models, demonstrating strong association between lipodystrophy with NAFLD, presumably due to decreased adipose tissue capacity (797-800). In addition, treatment of lipodystrophic patients with leptin or TZDs, can reverse or at least decrease hepatic steatosis, due to reduction in lipoatrophy and lipotoxicity, improved insulin sensitivity (95,800,801). Interestingly, a very similar metabolic and hepatic phenotype to adolescent PCOS-like sheep was reported in lipodystrophic mice (797), and prenatally androgenised pubertal female rats (802). Although, we are unable to verify if the normalised level of hepatic fat in PCOS-like animals is due to increased hepatic fat accumulation in control animals or due to hepatic changes in PCOS-like animals, it seems that combination of relatively increased fatty acid utilisation, decreased fatty acid uptake and *de novo* lipogenesis, as compared with adolescent PCOS-like animals, might underlie that change.

In summary, adolescent PCOS-like animals display a more perturbed hepatic phenotype than adult PCOS-like sheep. Adolescent prenatally androgenised animals have increased hepatic steatosis and display a mixed pattern of hepatic insulin sensitivity and resistance. Considering the presence of hyperinsulinemia in those animals, insulin resistance is demonstrated by disproportionately normal gluconeogenesis whereas sensitivity by upregulated *de novo* lipogenesis. Furthermore, adolescent PCOS-like animals had increased hepatic uptake of fatty acids, likely due to decreased buffering capacity of adipose tissue. Adult prenatally androgenised sheep have normalised hepatic fat content, which is paralleled by normal levels of FFA uptake, likely due to SAT hypertrophy. In addition, paradoxically, decreased expression of *INSR* in adult PCOS-like animal might protect these animals from increased *de novo* lipogenesis, as observed in adolescent animals. However, it can be speculated that once the capacity of adipose tissue is saturated fatty acids might be shunt back to the liver, resulting in NAFLD once again.

Chapter 6 Role of FGF21 and irisin in the metabolic phenotype of PCOS-like sheep.

6.1 Introduction

Fibroblast growth factor 21 (FGF21) and irisin are recently identified novel metabolic regulators with ability to regulate glucose metabolism, insulin sensitivity, lipid homeostasis and energy balance. As described in previous chapters, adolescent and adult prenatally androgenised sheep display various metabolic perturbations, including obesity, decreased PPT and reduced thermogenic potential of BAT/beige adipocytes, hyperinsulinemia, increased circulating FFA and fatty liver, decreased adipogenesis and SAT hypertrophy. Therefore, this chapter aimed to assess potential role of FGF21 and irisin in metabolic phenotype of adolescent and adult PCOS-like ewes.

Mammalian FGF21 belongs to the FGF superfamily comprising of 22 structurally related factors with diverse biological functions, including cell growth and differentiation, embryonic development, and metabolism (803). However, abnormal FGF signalling has been also indicated in pathological conditions, such as cancer and metabolic disease (804,805). FGFs propagate their signal through binding to four different plasma membrane tyrosine kinase receptors (FGFR1-4) (805). FGFs are further divided into 7 subgroups, with FGF21 belonging to hormonal subfamily, together with FGF19 and FGF23 (803). These hormonal FGFs are unique, as they require an additional co-receptor for signalling, klotho for FGF23 and β -klotho (KLB) for FGF19 and FGF21 (803,806). FGF21 is conserved in mammals, with only one amino acid difference between human and gorillas and 80% homology between human and rodents (807). The physiology of FGF21 is complex. It is synthesised in multiple organs, although mainly secreted from liver, it can be also expressed in pancreas, muscle and adipose tissue (807,808). FGF21 also act on multiple target tissue, such as hypothalamus, heart, pancreas and liver, in endocrine, paracrine and autocrine fashions. Adipose tissue however, is the primary target of FGF21 action, in which it preferentially binds to FGFR1 linked to KLB co-receptors (809). It has been shown that both WAT and BAT express high levels of KLB co-receptors and are sensitive to exogenous FGF21 stimulation (810).

The first reports on FGF21 action documented that it stimulates glucose uptake, in insulin independent manner, in mouse and human adipocytes *in vitro* (811). Furthermore, it has been shown that transgenic animals overexpressing hepatic FGF21 have improved insulin sensitivity, reduced TG levels and are resistant to diet-induced obesity whereas mice lacking FGF21 have increased body weight, hypertrophic adipocytes with decreased lipolysis rates, and accumulated hepatic TG (812). What is more, FGF21 infusions were shown to reduce serum glucose and lipids, and improve insulin sensitivity in genetic murine models of obesity,

Zucker diabetic fatty rats and diabetic rhesus monkeys (813,814). Interestingly, it was also reported that during carbohydrate intake FGF21 is an inducible factor, which functions in a feed-forward loop in adipose tissue to regulate the activity of PPARG, a master transcriptional regulator of adipogenesis (812). FGF21 deficient mice have defects in PPARG signalling and decreased body fat (812). These data suggest that FGF21 might act as regulator of the adipose tissue storage capacity. FGF21 treatment was also shown to increase serum adiponectin levels, a potent insulin sensitising adipokine, while adiponectin knockout mice were refractory to therapeutic benefits of FGF21 (815,816). In addition, it was reported that FGF21 treatment of obese mice resulted in weight loss through increased energy expenditure and fat utilisation (817). In line with these findings further reports demonstrated that FGF21 regulates also adaptive thermogenesis through upregulating UCP1 and PGC1 α as well as browning WAT, while FGF21-knockout mice have impaired response to cold (818). Interestingly, mild cold exposure has been shown to also induce circulating FGF21 levels in humans, which further correlates with increased energy exposure and lipolysis (819). Paradoxically, however, it has been shown, in both mice and humans, that obesity also results in increased serum FGF21 levels suggesting that obesity is an FGF21-resistant state (820,821). Indeed, there are reports showing a reduced expression of KLB in adipose tissue of obese mice and humans (822,823). Interestingly, increased FGF21 concentrations were also documented in various pathological conditions such as anorexia nervosa (824), metabolic syndrome (825), mitochondrial diseases (826), autophagy deficiency (827), and nephropathy (828,829). Not much is known about the regulation of FGF21 expression. It has been demonstrated that hepatic FGF21 level is induced directly in response to fasting as well as a protein insufficiency, by the corresponding actions of PPARA and activating transcription factor 4 (ATF4) (830,831). In mice, fasting for 24 hours, increased hepatic and plasma FGF21 levels however, in humans increased circulating FGF21 levels were only observed after a prolonged, seven day, fast (832,833). Interestingly, FGF21 deficient mice, in response to a ketogenic diet, gain weight and develop hepatosteatosis (834). However, hepatic FGF21 is upregulated not only by nutrient deficiency but also by nutrient excess. In humans, five days of high-fat feeding resulted in significantly increase in plasma FGF21 concentrations (835). It has been shown that in states of calorie excess, FGF21 is upregulated through carbohydrate response element binding protein (836,837). Therefore, it has been suggested recently that FGF21 is a stress hormone, protecting tissue from the oxidative environment seen during various pathological conditions (838,839) .

Irisin is a novel hormone-like polypeptide, proposed to mediate the beneficial effects of exercise on metabolism, recently identified in both mice and human. Irisin is encoded by the *FNDC5* gene, cleaved and secreted part of the transmembrane protein FNDC5 (fibronectin

type III domain containing 5) (840). It was firstly discovered by the research group of Spiegelman from Harvard University in 2012 and described as muscle-derived factor (myokine) induced by exercise downstream of PGC1 α , with the potential to stimulate browning of the white adipose tissue and thermogenesis, both *in vitro* and *in vivo* (840). The paper from this group also reported that mildly increased blood levels of irisin, through viral-delivery, in a high fat diet induced mouse model of obesity resulted in increased energy expenditure, caused small, but statistically significant weight loss and improved glucose homeostasis (840). Interestingly, as the secreted portion of FNDC5 is highly conserved among species it was speculated that irisin evolved as a muscle secreted hormone that was stimulated as result of muscle contraction during shivering, which in turn activated adipose thermogenesis as a defence against hypothermia (840). Indeed, Lee *et al.* found that induction of irisin secretion was proportional to shivering intensity, in magnitude similar to exercise-stimulated secretion (841). Further reports supported the original discovery showing that irisin levels are upregulated in response to exercise, enhancing browning of WAT and energy expenditure, and mediating some of the beneficial effects of exercise, in both rodents and humans (841-846). What is more, it was found that diabetic patients have decreased levels of circulating irisin, and that the expression of *FNDC5* in both skeletal muscle and white adipose tissue is reduced and negatively correlated with obesity, insulin resistance and liver fat content (847-852). This evidence made irisin a potential new target for the treatment of metabolic disease. However, some researchers have raised doubts regarding the physiological function of irisin in humans, reporting no association between levels of irisin and exercise training, and no effect on the browning of WAT (853-856). In addition, controversy has arisen regarding the molecular weight of the soluble portion of irisin, mechanisms of its secretion, and lack of identified receptor (857). Further, a positive correlation of circulating irisin with BMI, insulin resistance (843,848,858) and metabolic syndrome (859), was also reported. Huh *et al.* noted that weight-loss was linked to diminished levels of circulating irisin and that there was a positive correlation between muscle mass and circulating irisin concentrations (843). These data suggest that the positive association of irisin with BMI might be partially explained by a decrease in muscle mass. Although the first reports documented the expression of irisin in skeletal muscle only, further investigations reported its expression, but to a lesser extent, in adipose tissue, liver, brain, bone, pancreas, kidney and ovary (850,860). Several studies reported a positive association of circulating irisin with fat mass in human (850,861,862). Interestingly, some researchers postulated that irisin might also be an adipokine, regulated by exercise and nutritional status (863). Therefore, a positive correlation between BMI and irisin could be also attributed to both muscle and adipose tissue mass and their differential

contributions to circulating irisin levels in different physiological and pathological states (857). Alternatively, increased irisin levels in obesity might be a compensatory mechanism trying to counteract metabolic disturbances associated with obesity by increasing browning of WAT and energy expenditure.

In view of metabolic perturbations present in adolescent and adult prenatally androgenised sheep, which were described in previous chapters of this thesis, this chapter aimed to:

1. Investigate the potential role of FGF21 in adolescent and adult phenotype of PCOS-like sheep
2. Determine the possible involvement of irisin into the metabolic pathophysiology of adolescent and adult TP-exposed sheep

6.2 Methods

6.2.1 Experimental animals

The ovine model, the animals used, their husbandry and treatments have been described previously (section 2.2). The female animals assessed in this chapter are detailed in Table 6.1.

Treatment	Developmental stage	Sample number (n)
Fetal		
Maternal Injection D62-collection	Fetal day 70	C=3, TP=6
Maternal Injection D62-collection	Fetal day 90	C= 6, TP=6
Maternal Injection D62-102	Fetal day 112	C=9, TP=4
Juvenile		
Maternal Injections D62-102	Lambs 11 weeks old	C=8, TP=8
Adolescent		
Maternal Injection D62-102	Ewes 11 months old	C=5, TP=9
Adult		
Maternal Injections D62-102	Ewes 30 months old	C=11, TP=4

Table 6.1 Treatment regime, age, and corresponding sample numbers of experimental animals discussed in this chapter.

6.2.2 Measuring gene expression using qRT-PCR

Extraction of RNA from fetal and postnatal adipose tissue was performed using the combination of TRI reagent and Qiagen RNeasy Mini Kit (Qiagen Ltd., West Sussex, UK), as described in section 2.8.1. Extraction of RNA from liver was performed using Qiagen RNeasy Mini Kit (Qiagen Ltd., West Sussex, UK), and from skeletal muscles using Qiagen RNeasy Fibrous Tissue Mini Kit (Qiagen Ltd., West Sussex, UK), as described in section 2.8.1. Protocols for cDNA synthesis and qRT-PCR are described in section 2.8.3 and 2.8.4, respectively. Forward and reverse primers were designed and validated as stated in section 2.8.6 and primer sequences analysed in this chapter are listed in Table 6.2.

Gene	Forward Sequence	Reverse Sequence	Product Size (bp)
<i>FGF21</i>	ATGATGCCCAGGAGACAGAG	TCAAAGTGCAGCGATCCATA	196
<i>KLB</i>	CAGAGGATACCACAGCCATCT	CCAGGCTGTGTAACCAAACA	101
<i>FGFR1</i>	TCAGAGACCCACCTTCAAGC	GAAGCTGGGGGAGTATTGGT	115
<i>FGFR2</i>	GCTGAAAAACGGGAAGGAAT	GTCAGACGGGACCACACTTT	103
<i>FGFR3</i>	ACCCTGGGCAAGCCTCTT	ATCTCCATCTCGGACACCAG	167
<i>FGFR4</i>	GGCTGAAGCACATCGTCAT	CCTCCACCTCTGAGCTATTGA	102
<i>ATF4</i>	TCTCCTGCGACAAGGCTAAG	CTCCACCATCCAATCTGTCC	116
<i>ATF6</i>	ACTTGGATTTGATGCCTTGG	CTTGAGGAGGCTGGTGAAAG	109
<i>XBP1</i>	AGACTGCCAGAGACCGAAAG	GGCCATGAGTTTTCTCTCGT	123
<i>SLC2A1</i>	TGCTGAGCGTCATCTTCATC	GGCTCTCCTCCTTCATCTCC	180
<i>EIF2AK3</i>	TTCAATGCTTGGTTGGAAGC	CCATGGGACTAGGAGAGCTG	109
<i>ERN1</i>	CAACAACCTGCCCAAACAC	CGGAGAAACCGTGGTAGGT	121
<i>FNDC5</i>	GTAAGCTGGGACGTCTTGGGA	GTGGTGTTACCTCCTGGAT	104

Table 6.2 Forward and reverse primer sequences and product size for genes analysed in the postnatal liver tissue using SYBR Green qRT-PCR.

6.2.3 FGF21 ELISA

Plasma FGF21 was measured using the Abcam Human FGF21 ELISA kit (ab125966; Abcam Cambridge, UK) as per the manufacturer's instructions. Immunoassay absorbance was measured at 450nm using a ThermoMax Microplate Reader (Molecular Devices, CA, USA) and the concentrations were calculated from four-parameter logistic curve. All samples were assayed in duplicate. The assay sensitivity was 0.03 ng/ml intra and inter-assay CVs were 4.7% and 7.2%, respectively.

6.2.4 Irisin ELISA

Plasma Irisin was measured using the Recombinant Irisin (Human, Mouse, Rat, Canine) ELISA kit (EK-067-29; Phoenix Pharmaceuticals, Karlsruhe, Germany) as per the manufacturer's instructions. Immunoassay absorbance was measured at 450nm using a ThermoMax Microplate Reader (Molecular Devices, CA, USA) and the concentrations were calculated from four-parameter logistic curve. All samples were assayed in duplicate. The assay sensitivity was 0.1 ng/ml intra and inter-assay CVs were <10% and <15%, respectively.

6.2.5 Statistical analysis

Statistical analysis was performed with GraphPad Prism version 6.0 (GraphPad Software, Inc., San Diego, CA). For comparing means of two treatment groups with equal variances an unpaired, two-tailed Student's t test was used. To compare multiple sets of data a one-way ANOVA was used. Log transformation was used to approximate the normal distribution for parametric analysis when necessary. A P value of <0.05 was considered as statistically significant. Results are presented as mean + S.E.M, where * signifies a P<0.05, ** P<0.01 and *** P<0.001. AUC was calculated using the trapezoidal method. Correlation was assessed by calculation of the Pearson r co-efficient. A line of best fit was incorporated only in the figures where correlation was statistically significant.

6.3 Results

6.3.1 FGF21 expression in adolescents and adult PCOS-like sheep

To determine whether metabolic disturbances present in prenatally androgenised sheep might be associated with altered levels of FGF21, circulating and hepatic expression of FGF21 were assessed in serum samples from adolescent and adult animals. In addition, we had serum samples from the adult cohort animals, which were taken from those animals at 22 months of age. Adolescent and young adult (11 and 22 months of age, respectively), but not adult (30 months of age) PCOS-like sheep had decreased levels of circulating FGF21 ($P < 0.05$; Fig. 6.1 A). Correspondingly, there was decreased hepatic expression of *FGF21* in adolescent (11M), but not adult (30M) prenatally androgenised animals ($P < 0.05$; Fig. 6.1 B). Therefore, to establish the onset of the altered expression of hepatic *FGF21*, gene expression was further evaluated in fetal (D70, F90 and D112 of gestation) and juvenile (11 weeks of age) livers. Hepatic expression of *FGF21* was very low during all stages of fetal life (D70, D90 and D112) and increased sharply (~20 fold) after birth (11W), however there was no difference in the expression of *FGF21* between control and PCOS-like sheep during early-life (Fig. 6.1 C). Although both hepatic and circulating levels of FGF21 were decreased in adolescence, there was no direct correlation between hepatic expression and levels of circulating FGF21, in both 11 months old and adult animals (Fig. 6.1 E-F), suggesting an additional source of circulating FGF21. Therefore, the expression of *FGF21* in SAT, VAT and muscle tissue were investigated. The expression levels in both adipose tissue depots were undetectable, whereas the expression of *FGF21* in muscle tissue, although still very low, was elevated in adult PCOS-like sheep, with no difference during adolescence ($P < 0.05$; Fig. 6.1 D). However, there was no correlation between muscle *FGF21* and circulating levels of FGF21 in both adolescent and adult animals (Fig. 6.1 G-H).

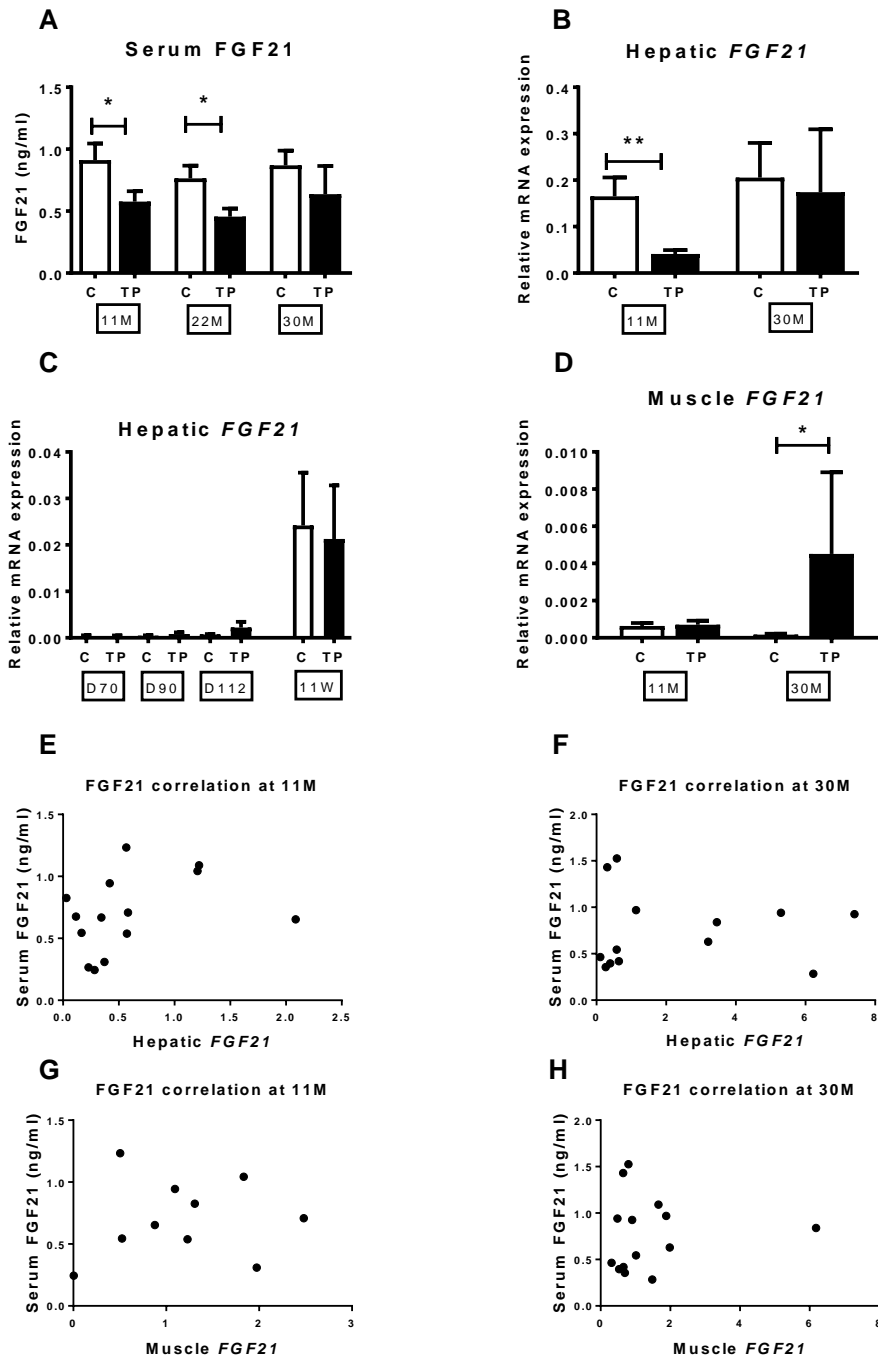


Figure 6.1 FGF21 levels in control (C) and prenatally androgenised (TP) animals. A) serum FGF21 levels in adolescent and adult animals; B) Hepatic *FGF21* expression in adolescent and adult sheep; C) Hepatic expression of *FGF21* in fetal and juvenile animals; D) Muscle *FGF21* expression in adolescent and adult animals; E-F) Correlation of hepatic *FGF21* expression with circulating FGF21 in adolescent and adult animals; G-H) Correlation of muscle *FGF21* expression with circulating FGF21 in adolescent and adult animals. P value of <0.05 was considered as statistically significant. Results are presented as mean + S.E.M, where * signifies a $P < 0.05$.

6.3.2 Potential regulatory mechanisms underlying altered levels of FGF21

We next investigated the potential regulatory mechanisms underlying decreased levels of FGF21 in adolescent PCOS-like sheep. The nuclear fatty acid receptor, PPARA, is suggested to be a main regulator of hepatic *FGF21* expression during fasting, however, there was no difference at the expression of *PPARA* between control and prenatally TP-exposed animals in adolescent (chapter 5, Fig. 5.3 A) and adult animals (chapter 5, Fig. 5.10 A). Furthermore, there was no correlation between expression of hepatic *FGF21* and *PPARA* at 11M (Fig. 6.2 A) and at 30M of age (Fig. 6.2 B), suggesting other regulatory mechanisms. PGC-1 α was also showed as a potential regulator of FGF21 action therefore the hepatic expression of *PPARGC1A* was also investigated. There was a trend towards decreased hepatic *PPARGC1A* expression (chapter 5, Fig. 5.3 C) and positive correlation between hepatic *PPARGC1A* and *FGF21* expression ($P < 0.001$; $r = 0.72$; Fig. 6.2 C) in adolescent PCOS-like sheep. At 30 months of age there was a trend towards increased expression of *PPARGC1A* in prenatally androgenised sheep (chapter 5; Fig. 5.10 C) however, there was no correlation between hepatic expression of *PPARGC1A* and *FGF21* (Fig. 6.2 D).

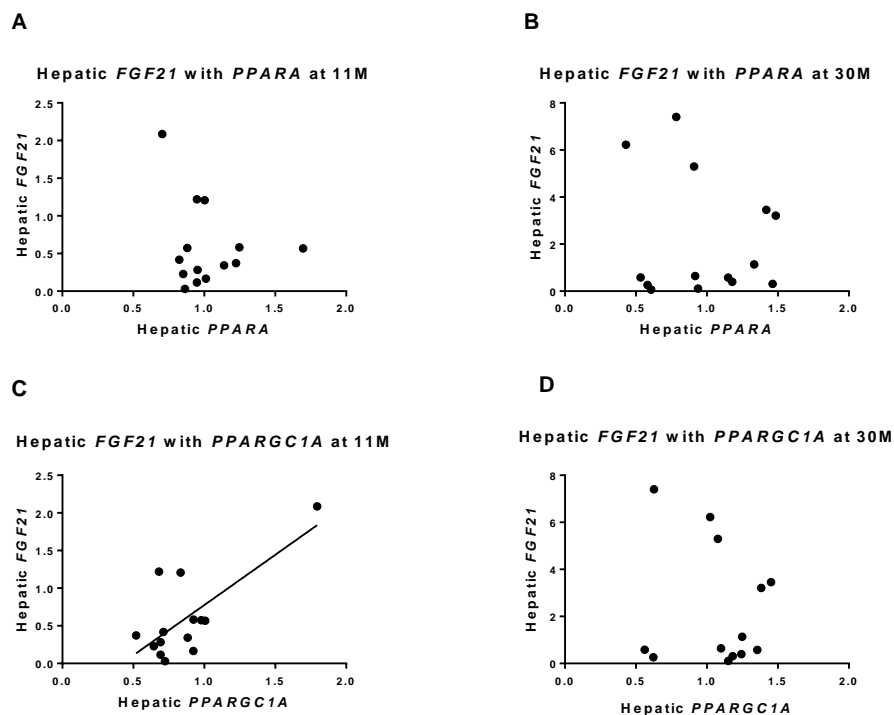


Figure 6.2 Correlation of hepatic *FGF21* expression A-B) with hepatic *PPARA* expression and C-D) hepatic *PPARGC1A* expression in adolescent and adult control and prenatally androgenised animals.

6.3.3 Autocrine regulation of FGF21 expression

FGF21 has been also shown to act directly on the liver and expression of hepatic fibroblast growth factor receptor isoforms and β -klotho coreceptor has been postulated to be the regulatory factor for FGF21 signalling within this tissue. Therefore, hepatic expression of FGF receptors and β -klotho coreceptor in adolescent and adult sheep liver was determined. There was no difference in the expression of hepatic *KLB*, *FGFR2*, *FGFR3* and *FGFR4* in adolescent animals (Fig. 6.3 A, E, G and I, respectively). There was a trend towards decreased hepatic expression of *FGFR1* in those animals ($P=0.059$; Fig. 6.3 C) however, this did not reach statistical significance. In adulthood, there was no difference in the hepatic expression of *KLB*, *FGFR1*, *FGFR2*, *FGFR3* and *FGFR4* (Fig. 6.3 B, D, F, H and J, respectively).

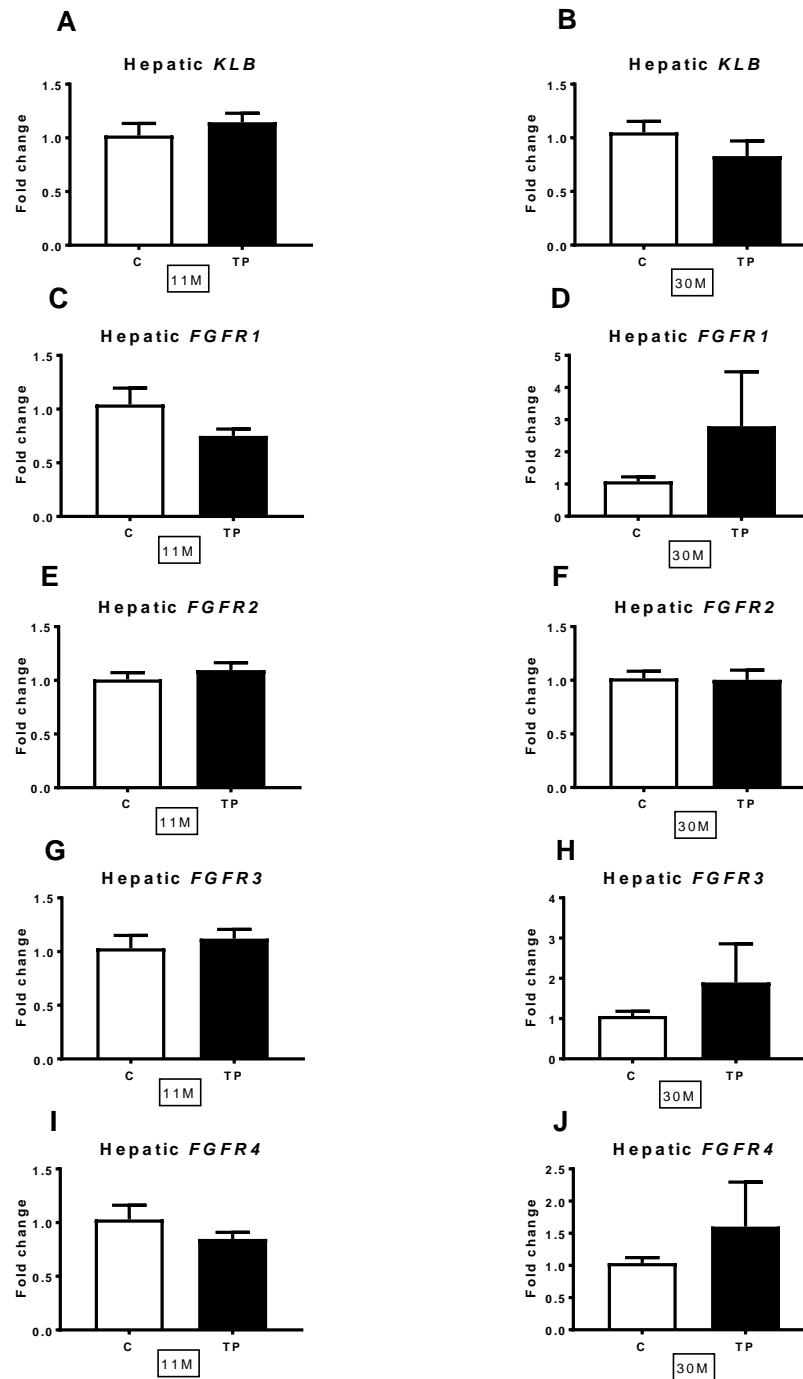


Figure 6.3 Hepatic expression of *KLB* and FGF receptors in adolescent and adult control (C) and prenatally androgenised (TP) animals, as quantified by qRT-PCR. Results are presented as mean + S.E.M.

6.3.4 FGF21 and endoplasmic reticulum stress

FGF21 has been suggested to also act a stress-responsive hormone, and the *FGF21* gene promoter has been shown to have specific response elements that are stimulated by ATF4. Therefore, the expression of selected endoplasmic reticulum stress markers, ATF4, the activating transcription factor 6 (ATF6) and the X-box-binding protein 1 (XBP1), were investigated in livers of adolescent and adult animals. There was no difference in the expression of *ATF4*, *ATF6* and *XBP1* in adolescent (Fig. 6.4 A, C and E, respectively) and adult animals (Fig. 6.4 B, D and F, respectively).

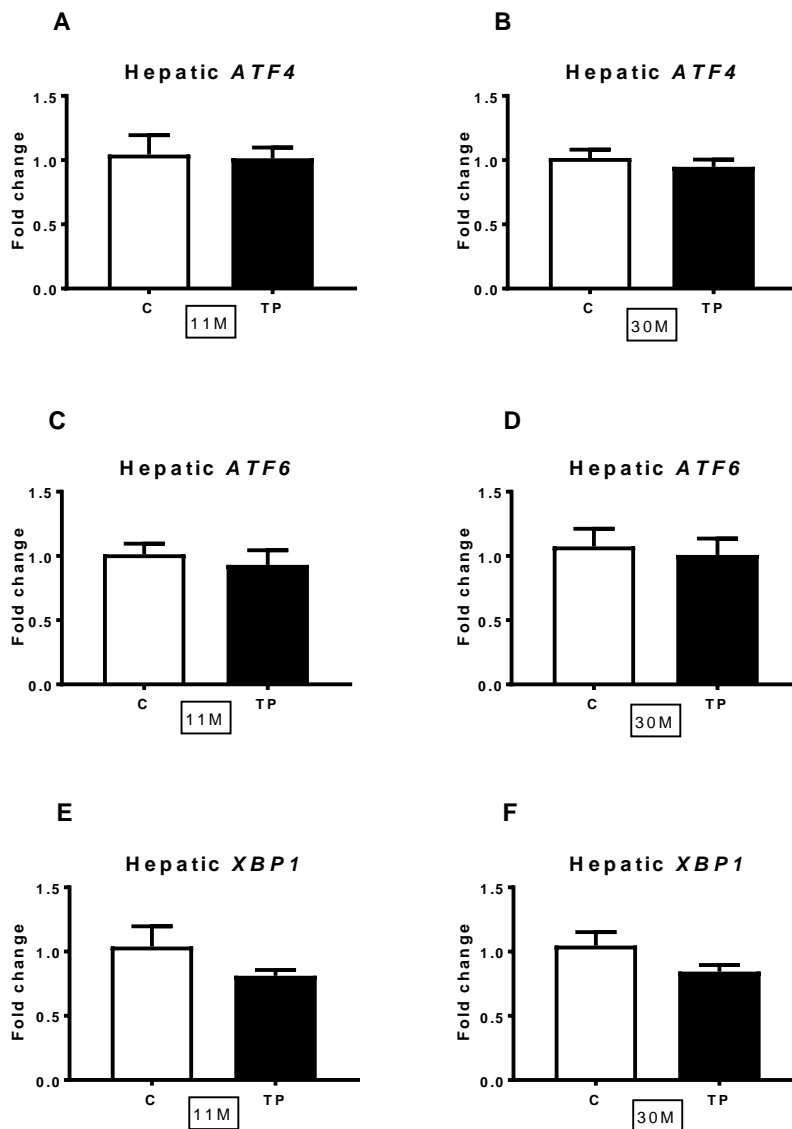


Figure 6.4 Hepatic expression of endoplasmic reticulum stress markers in adolescent and adult control (C) and prenatally androgenised (TP) animals, as quantified by qRT-PCR. Results are presented as mean + S.E.M.

6.3.5 Association between FGF21 and metabolic parameters

FGF21 is known as a metabolic regulator, therefore we have investigated the relationship between FGF21 and selected metabolic parameters at 11 and 30 months of age. In adolescence, there was a positive correlation between serum leptin levels with circulating FGF21 ($P < 0.05$; $r = 0.56$; Fig. 6.5 A) and hepatic expression of *FGF21* ($P < 0.05$; $r = 0.64$; Fig. 6.5 B). Furthermore, circulating levels of FGF21 correlated positively with the volume of omental fat ($P < 0.01$; $r = 0.68$; Fig. 6.5 C), and negatively with levels of circulating FFA ($P < 0.05$; $r = -0.59$; Fig. 6.5 D). However, there was no correlation between FGF21 and levels of fasting insulin or adiponectin (Fig. 5.6 E and F, respectively).

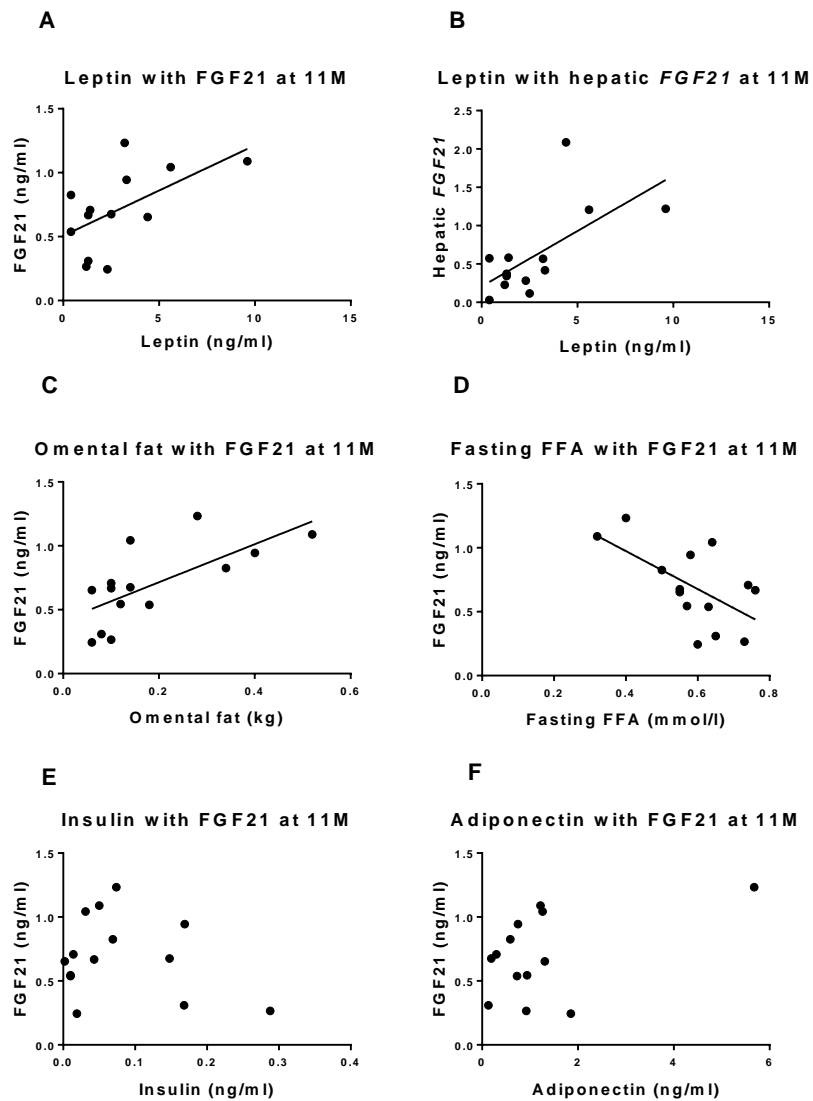


Figure 6.5 Correlation of FGF21 with metabolic parameters in adolescent animals in control and prenatally androgenised animals.

In adult animals, there was a weak positive relationship between serum leptin levels and circulating FGF21 although this did not reach statistical significance ($P=0.059$; $r=0.56$; Fig. 6.6 A) however, there was no association with hepatic expression of *FGF21* with leptin at 30 months of age (Fig. 6.6 B). Circulating FGF21 levels correlated negatively with volume of omental fat ($P<0.05$; $r=-0.61$; Fig. 6.6 C) but there was no relationship between FGF21 and serum levels of FFA, fasting insulin and adiponectin at 30M (Fig. 6.6 D, E and F, respectively).

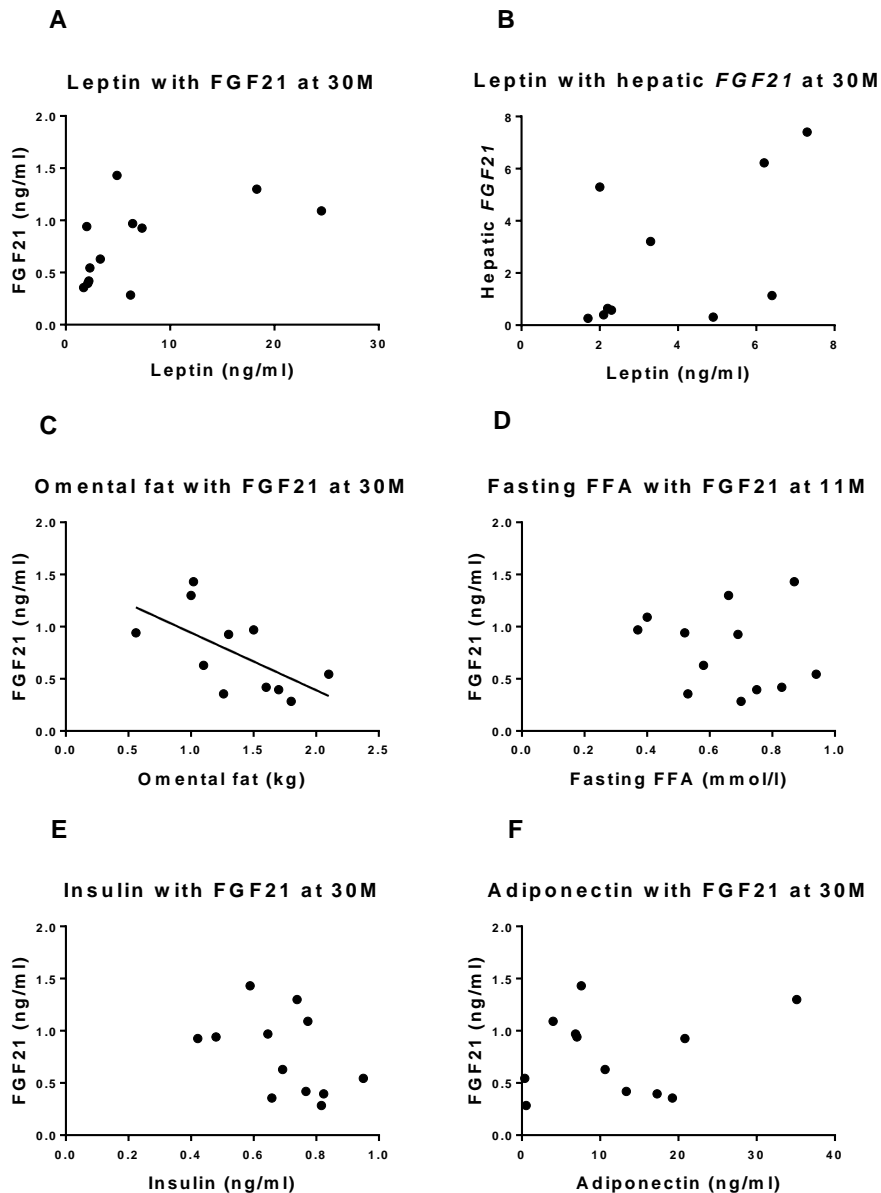


Figure 6.6 Correlation of FGF21 with metabolic parameters in adult animals in control and prenatally androgenised animals.

6.3.6 FGF21 signalling in adipose tissue

We next investigated FGF21 signalling in adipose tissue in adolescent and adult animals. Expression of *KLB* was significantly downregulated in SAT of 11 months old PCOS-like sheep ($P < 0.05$; Fig. 6.7 A), whereas expression levels of *FGFR1* in SAT as well as *KLB* and *FGFR1* in VAT at 11 months did not differ between control and prenatally TP-exposed animals (Fig. 6.7 C, E and H, respectively). In adult 30 months old animals, there were no difference in the expression of *KLB* and *FGFR1* in SAT (Fig. 6.7 B and D) however, in VAT both *KLB* and *FGFR1* were significantly upregulated ($P < 0.05$; Fig. 6.7 F and G, respectively).

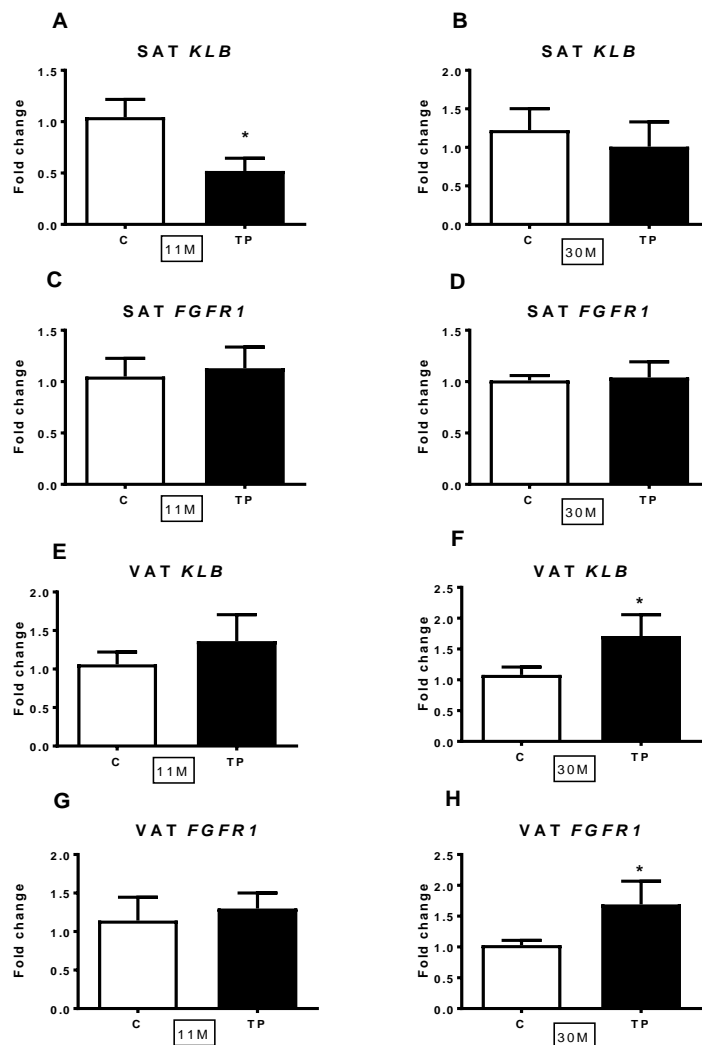


Figure 6.7 FGF21 signalling in subcutaneous (SAT) and visceral adipose tissue (VAT) in adolescent and adult control (C) and prenatally androgenised (TP) animals, as quantified by qRT-PCR. P value of < 0.05 was considered as statistically significant. Results are presented as mean + S.E.M, where * signifies $P < 0.05$.

6.3.7 Downstream FGF signalling in adipose tissue

In adipose tissue FGF21 regulates the activity of PPARG, the master regulator of adipogenesis, and adiponectin is a downstream effector of FGF21 signalling. We have previously shown that both *PPARG* and *ADIPOQ* are significantly downregulated in SAT of adolescent PCOS-like sheep (chapter 3, Fig. 3.2 A and F, respectively). Subsequently the correlation between expression of *KLB*, *PPARG* and *ADIPOQ* in SAT and VAT was investigated. There was a strong positive correlation between expression of *KLB* and *PPARG* in SAT at 11M ($P<0.0001$; $r=0.94$; Fig. 6.8 A) and at 30M ($P<0.0001$; $r=0.85$; Fig. 6.8 C). In addition, there was a positive association between expression of *KLB* and *PPARG* in VAT at 11M ($P<0.0001$; $r=0.90$; Fig. 6.8 E) and at 30M ($P<0.001$; $r=0.73$; Fig. 6.8 G). Likewise, the expression of *ADIPOQ* was also strongly correlated with *KLB* expression at 11M in SAT ($P<0.001$; $r=0.79$; Fig. 6.8 B) and in VAT ($P<0.01$; $r=0.7$; Fig. 6.8 F). Similarly, at 30M there was a strong correlation of between *KLB* and *ADIPOQ* in SAT ($P<0.001$; $r=0.77$; Fig. 6.8 D) and in VAT ($P<0.0001$; $r=0.92$; Fig. 6.8 H).

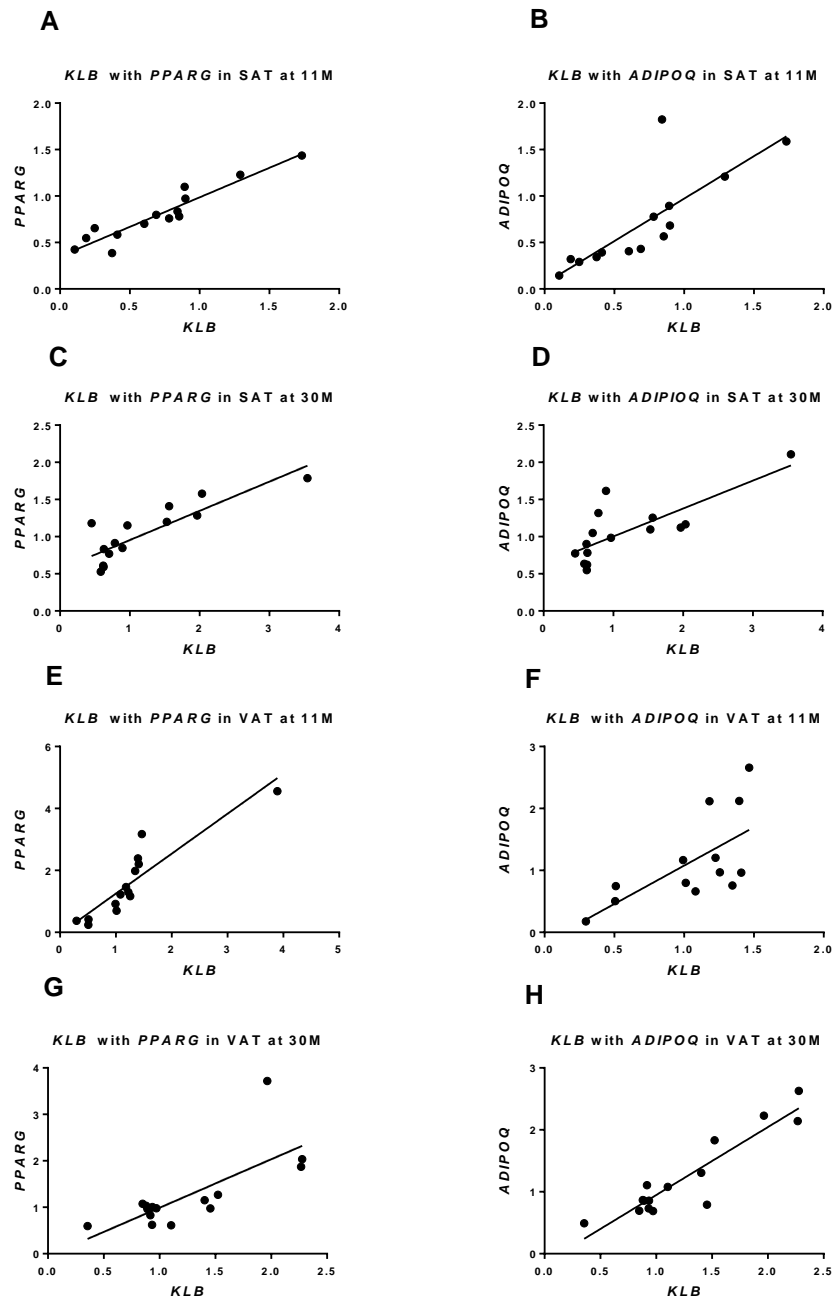


Figure 6.8 Correlation of *KLB* expression with *PPARG* and *ADIPOQ* in subcutaneous and visceral adipose tissue in adolescent and adult control and prenatally androgenised animals.

To further investigate FGF21 action in adipose tissue, levels of *SLC2A1*, encoding GLUT1 was assessed through qRT-PCR. FGF21 has been shown to induce glucose uptake in adipocytes through activation and up-regulation of the glucose transporter GLUT1. However, our result showed that there were no differences in the expression of *SLC2A1* in SAT and VAT of adolescent animals (Fig. 6.9 A and B), and in SAT and VAT of adult animals (Fig. 6.9 C and D).

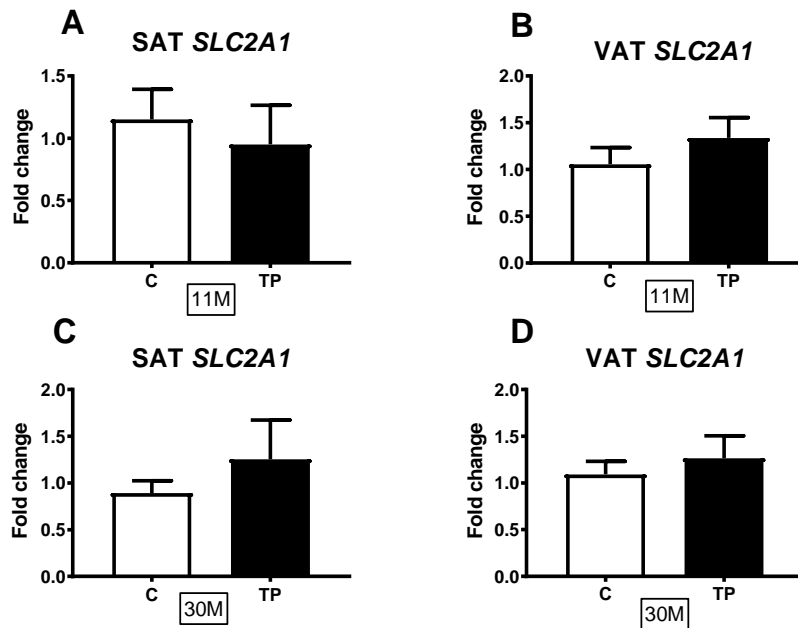


Figure 6.9 Expression of *SLC2A1* in subcutaneous and visceral adipose tissue of adolescent and adult control (C) and prenatally androgenised (TP) animals, as quantified by qRT-PCR. Results are presented as mean + S.E.M.

6.3.8 FGF21 signalling in muscle tissue

We next investigated FGF21 signalling in skeletal muscles. At 11 months of age there was a trend towards a decreased expression of *KLB* ($P=0.79$; Fig. 6.10 A) and *FGFR1* ($P=0.63$; Fig. 6.10 B) in skeletal muscles of PCOS-like sheep, however this did not reach statistical significance. Nevertheless, there was decreased expression of *PPARG* in adolescent TP-exposed sheep ($P<0.05$; Fig. 6.10 C), and levels of *PPARG* positively correlated with levels of *KLB* expression ($P<0.05$; $r=0.57$; Fig. 6.10 D). In adult animals, there was upregulated expression of *FGFR1* in TP-exposed animals ($P<0.05$; Fig. 6.10 F) however, there was no difference in the expression of *KLB* (Fig. 6.10 E). There was a trend towards decreased expression of *PPARG*, however this did not reach statistical significance ($P=0.075$; Fig. 6.10 G) and there was no association between levels of *KLB* and *PPARG* (Fig. 6.10 H).

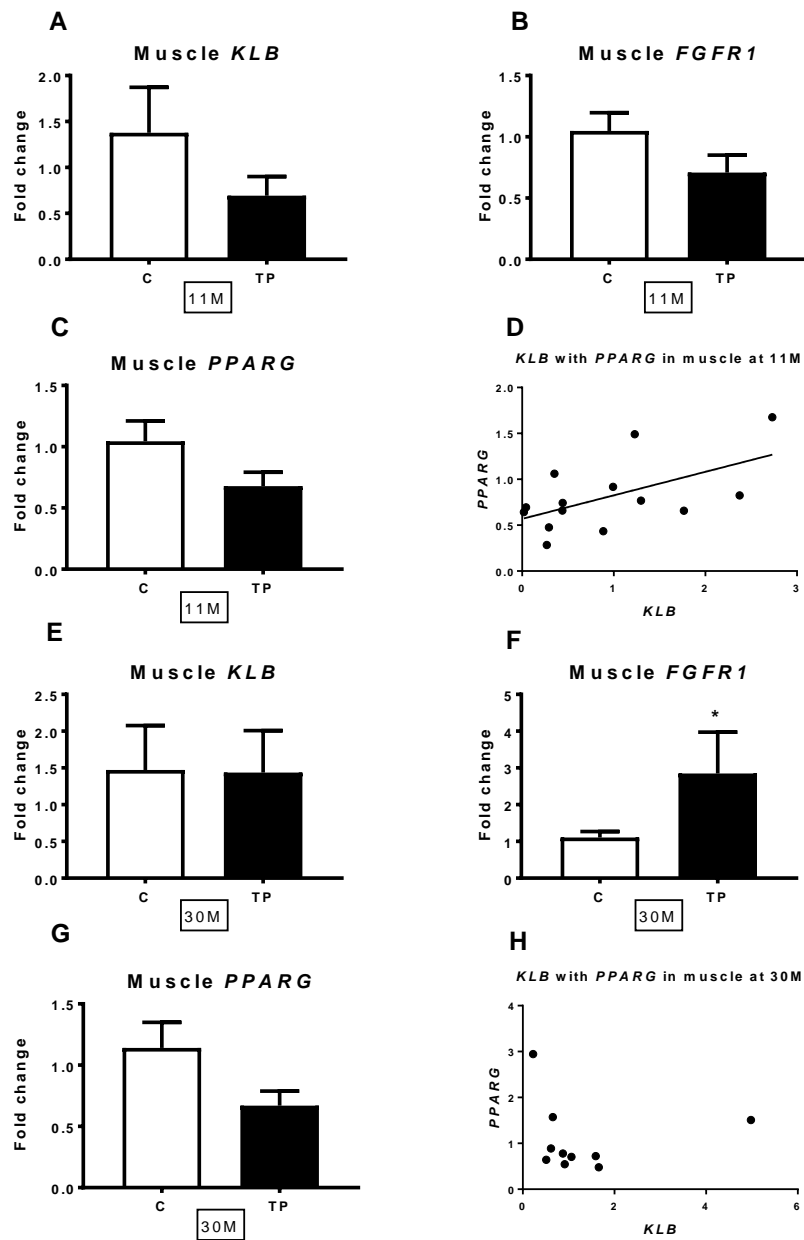


Figure 6.10 Expression of *KLB*, *FGFR1* and *PPARG* in skeletal muscle of adolescent (A-C) and adult (E-G) control (C) and prenatally androgenised (TP) animals, as quantified by qRT-PCR. Correlation of *PPARG* with *KLB* expression in skeletal muscle in adolescent (D) and adult (H) animals. P value of <0.05 was considered as statistically significant. Results are presented as mean + S.E.M, where * signifies a P<0.05.

6.3.9 Insulin and adiponectin signalling in muscle tissue

Subsequently we have assessed insulin and adiponectin signalling in skeletal muscles. There was no difference in the expression of *INSR*, *IRS1* and *IRS2* in skeletal muscles of 11 months old sheep (Fig. 6.11 A, C and E, respectively) and 30 months old (Fig. 6.11 B, D and F, respectively). Likewise, the expression levels of adiponectin receptors *ADIPOR1* and *ADIPOR2* in skeletal muscles of adolescent and adult animals were similar between control and PCOS-like sheep (Fig. 6.11 G-J).

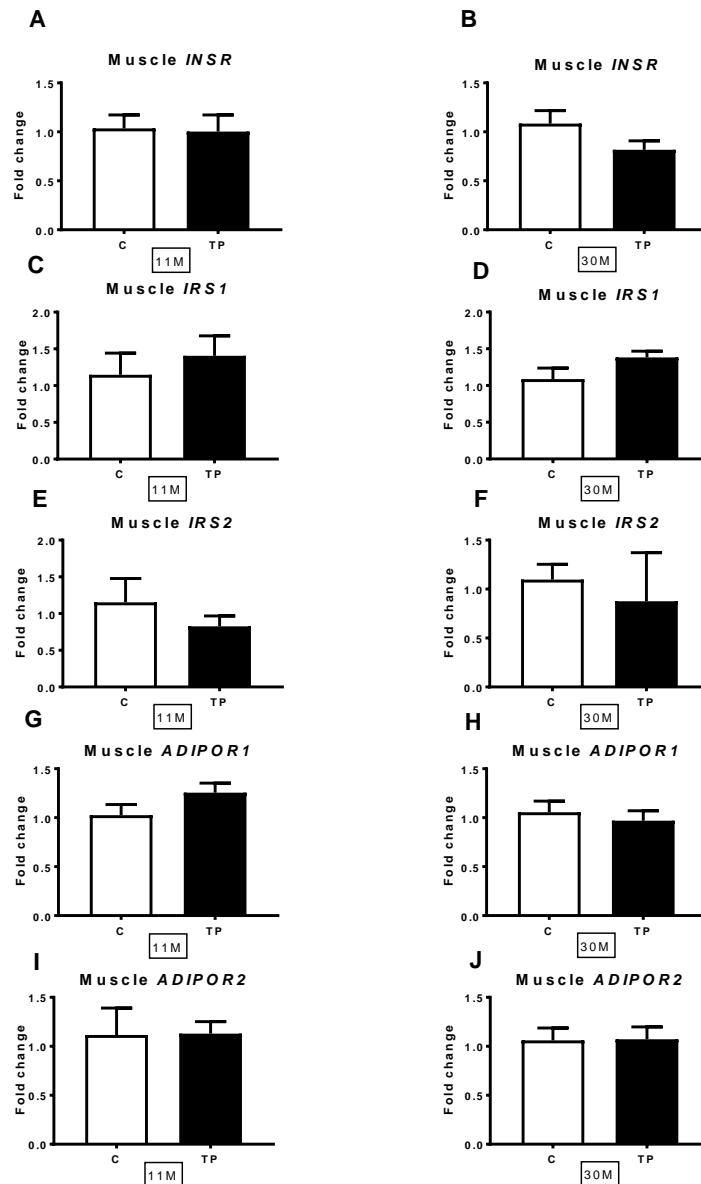


Figure 6.11 Expression of *INSR*, *IRS1*, *IRS2*, *ADIPOR1* and *ADIPOR2* in skeletal muscle of adolescent and adult control (C) and prenatally androgenised (TP) animals, as quantified by qRT-PCR. Results are presented as mean + S.E.M.

6.3.10 Expression of ER stress markers in muscle tissue

Considering the importance of ER stress in the regulation of FGF21 and overall muscle function, the expression of selected markers of ER stress was determined. There were no differences in the expression of *ATF4*, *ATF6*, *EIF2AK3* and *ERN1* in muscles of 11 months (Fig. 6.12 A, C, E and G, respectively) and 30 months old sheep (Fig. 6.12 B, D, F and H, respectively).

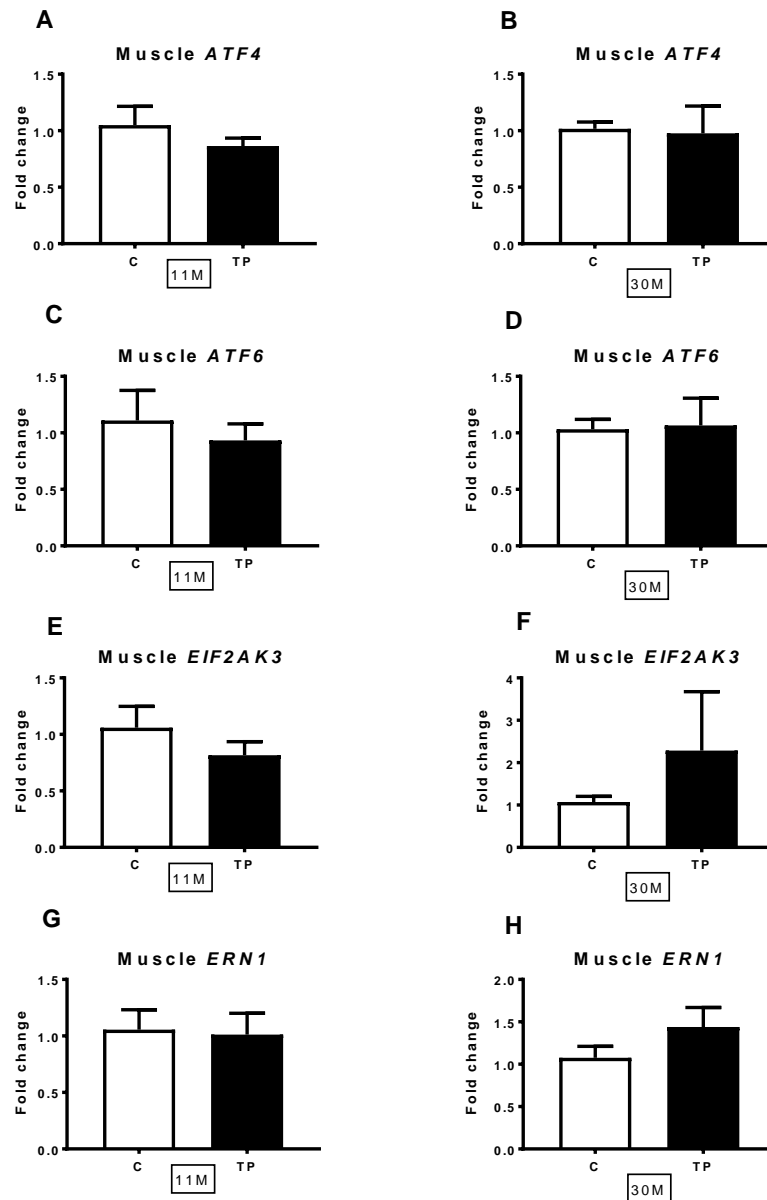


Figure 6.12 Expression of selected ER stress markers in skeletal muscle of adolescent and adult control (C) and prenatally androgenised (TP) animals, as quantified by qRT-PCR. Results are presented as mean + S.E.M.

6.3.11 Prenatal androgenisation does not affect levels of irisin

Considering that irisin is a regulator of insulin sensitivity and energy metabolism we aimed to assess the levels of circulating irisin and expression of muscle *FNDC5* in adolescent and adult animals. There was no difference in the expression of *FNDC5* in muscles between control and TP-exposed animals at 11 months and 30 months (Fig. 6.13 A). Correspondingly, there was no difference in circulating levels of irisin between control and TP-exposed animals at 11 months and 30 months of age however, there was a significant increase in levels of circulating irisin in adult PCOS-like animals as compared with adolescent PCOS-like sheep, but this difference was not observed in control animals (Fig. 6.13 B). In addition, there was no correlation between muscles expression of *FNDC5* and serum irisin level in both adolescent and adult animals (Fig. 6.13 C and D, respectively).

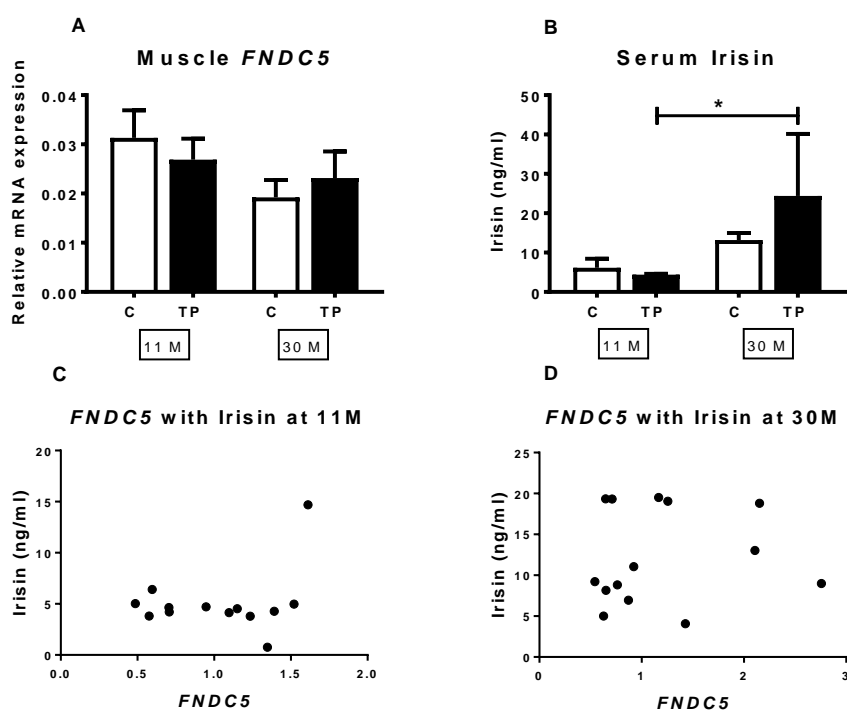


Figure 6.13 A-B) Expression of *FNDC5* in skeletal muscles and level of circulating irisin in adolescent and adult control (C) and prenatally androgenised (TP) animals. C-D) Correlation of *FNDC5* expression in skeletal muscle with circulating levels of irisin in adolescent and adult control and TP-exposed animals. P value of <0.05 was considered as statistically significant. Results are presented as mean + S.E.M, where * signifies a P<0.05.

6.3.12 Correlation of irisin with metabolic parameters

Finally, the association of irisin with selected metabolic parameters was assessed in both adolescent and adult animals. There were no associations between levels of circulating irisin and fasting insulin in both adolescent and adult animals (Fig. 6.14 A and E, respectively). Nevertheless, there was a positive correlation between circulating irisin and omental fat ($P<0.01$; $r=0.72$; Fig. 6.14 B) and leptin ($P<0.05$; $r=0.59$; Fig. 6.14 C) in adolescent, but not in adult sheep (Fig. 6.14 F and G, respectively). In addition, there was a negative correlation between circulating irisin and FFA in adolescent ewes however, this did not reach statistical significance ($P=0.052$; $r= -0.55$; Fig. 6.14 D). The potential association between plasma irisin and FFA was not present in adult animals (Fig. 6.14 H).

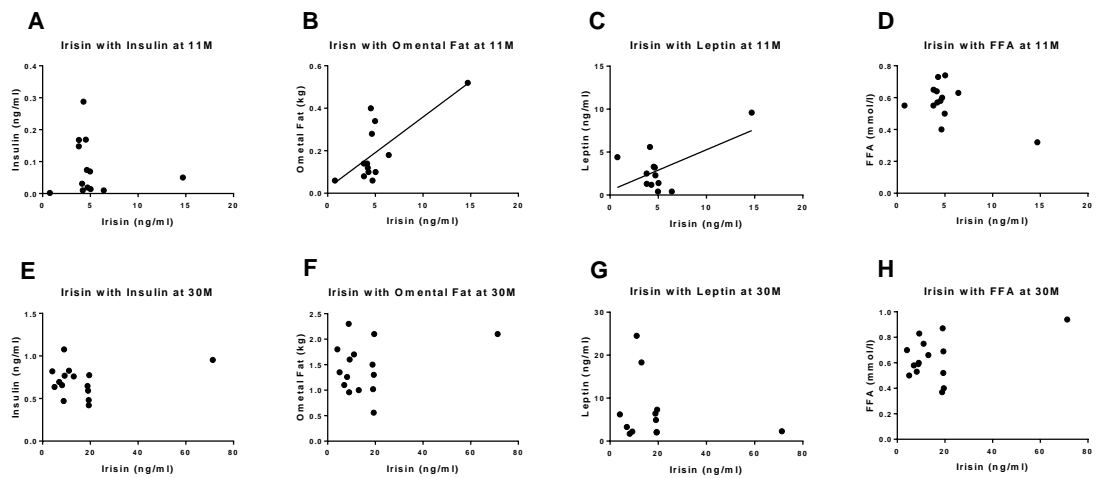


Figure 6.14 Association of circulating irisin with selected metabolic parameters in adolescent and adult control and prenatally androgenised animals

6.4 Discussion

Adolescent prenatally androgenised sheep were hyperinsulinemic, and had early fatty-liver changes without difference in body weight and non-significant reduction in adiposity (411). These 11 months old sheep also had altered pancreas structure and function, with increased β -cell number (431,596). In addition, these adolescent PCOS-like animals had decreased adipocyte differentiation in SAT, decreased plasma levels of leptin and adiponectin, and elevated FFA, as described in chapter 3. In adulthood (30M), PCOS-like sheep become obese, had adipose tissue hypertrophy in SAT, hyperinsulinemia and lipodystrophy, however, at this age, there was no difference in hepatic TG content between control and PCOS-like animals, as discussed in chapter 5. Furthermore, these adult prenatally androgenised sheep had a decreased amplitude of PPT, independent of obesity, which was paralleled by diminished noradrenaline levels and reduced expression of thermogenic genes in adipose tissue, as demonstrated in chapter 4. This chapter provides evidence that hepatic and circulating levels of FGF21 are decreased in prenatally androgenised sheep in puberty (11M) and during the transition from adolescents to adulthood (22M) however, there is no difference in the FGF21 level between adult (30M) PCOS-like sheep and controls. FGF21 is a hormone primarily secreted from the liver, which regulates glucose metabolism, insulin sensitivity, lipid homeostasis and energy balance. Therefore, it is likely that changes in its expression might contribute to the perturbed metabolic phenotype, as observed in adolescent and adult prenatally androgenised sheep.

Indeed, experimental animals with a complete absence of FGF21, FGF21 knockout (FGF21-KO) mice, had a comparable metabolic profile to adolescent PCOS-like sheep. FGF21-KO mice were normoglycemic, hyperinsulinemic and insulin resistant, and displayed pancreatic islet hyperplasia and increased β -cell proliferation (864). In addition, FGF21-KO mice were prone to delayed weight gain, displaying mild obesity with increased volume of adipose tissue, after 24 weeks on standard diet (834). Interestingly, it was demonstrated that weight gain in FGF21-KO mice was attributed to increased caloric intake and decreased energy expenditure (834). FGF21-KO mice have also been shown to have increased fat content in their livers when compared with wild type (WT) mice, when fed a methionine- and choline- deficient diet, a known inducer of murine non-alcoholic liver steatohepatitis, or a ketogenic diet (833,834,865). However, treatment with exogenous FGF21 has been shown to reverse hepatic steatosis in diet-induced obesity (DIO) mice (866). In addition, FGF21 deficient mice had decreased expression of hepatic PGC1 α , a gene involved in fatty acid β -oxidation, which was independent of PPARA levels (834). Likewise, our results show that adolescent PCOS-like

sheep have an increased hepatic TG content, but normal hepatic *PPARA* expression and trend towards decreased expression of *PPARGC1A*, as demonstrated in chapter 5, which further positively correlated with hepatic FGF21 levels. Interestingly, wild type mice with alcohol or diet induced fatty liver were shown to have elevated hepatic and serum FGF21 levels (865,867). However, it was demonstrated that FGF21-KO mice had more pronounced hepatic fat accumulation and inflammation, and a more pronounced decrease in PGC1 α activity, when compared with wild type mice with alcoholic liver disease, independent of food and alcohol intake (867). Likewise, some studies described that adult humans with alcoholic fatty liver disease, NAFLD or NASH had higher levels of circulating FGF21 (868-870). Moreover, a study by Yan *et al.* reported that although serum FGF21 increased progressively with the increase of hepatic fat content in adults with mild to moderate hepatic steatosis, when hepatic fat content increased significantly, FGF21 levels started to decline (870). Similar findings were described in study by Dushay *et al.*, where hepatic *FGF21* mRNA expression was significantly elevated in NAFLD but not in NASH (820). Confounding findings were reported in the paediatric population, where no differences in *FGF21* were reported in children with NAFLD (871-873). A study in obese adolescents with NAFLD, with average age 14-15 years and BMI 34-35, found increased levels of *FGF21* (871), whereas no association was found in children with average age 12-13, and BMI of 28 (874). Interestingly, in study of children with biopsy-proven NAFLD, with a median age 10-11, and BMI of 25, *FGF21* and hepatic *KLB* expression were inversely correlated with NAFLD progression and fibrosis (872). These findings indicate that FGF21 might be differentially expressed in paediatric and adult populations with NAFLD. In addition, it is likely that link between FGF21 and NAFLD in children might be modified by age and BMI. It has been suggested that FGF21 might participate in the defence against hepatic steatosis and hepatotoxicity, and that increased levels of FGF21 in alcoholic liver disease, NAFLD and NASH might be an adaptive response against lipid dysregulation and ER stress, through increased FGF21 dependent lipid oxidation (834,867). Correspondingly, it was demonstrated that treatment with recombinant FGF21 in mice attenuated hepatic fat accumulation and inflammation, and upregulated the expression of hepatic *PPARGC1A* (875,876). These findings could suggest that decreased FGF21 levels in adolescent PCOS-like sheep might be a primary rather than secondary factor contributing to hepatic TG accumulation.

Adolescent, prenatally androgenised sheep had normal body weights but a non-significant reduction in omental fat when compared with control animals (411). In addition, in chapter 3, we demonstrated that these 11 months old PCOS-like sheep had a diminished mRNA expression of genes regulating adipogenesis in SAT, with decreased leptin mRNA, which was

further paralleled by reduced circulating leptin levels. We have now established that there is a positive correlation between circulating leptin levels with hepatic and plasma FGF21 levels in adolescent sheep. Furthermore, there was a positive association between omental fat and circulating FGF21 in 11 months old sheep. Leptin is an adipokine, which correlates with body fat, and maintains homeostatic control of body weight, adipose tissue mass and energy balance through a negative feedback on hypothalamus, protecting individuals from the risks associated with having too little or too much adipose tissue (877). In addition, leptin plays an important role in glucose and lipid regulation, reproduction, inflammation and tissue remodelling (878). Mutations in leptin or its receptor, cause massive obesity in mice and humans, and leptin can effectively treat obesity in leptin-deficient patients (877). In addition, patients with lipodystrophy syndromes and anorexia nervosa display leptin deficiency (878). Numerous studies demonstrated that body weight and body fat mass correlate with plasma FGF21 in anorexic, lean, overweight and obese adult subjects (879-881). Similar findings were reported in the paediatric population, showing that in both lean and obese children, circulating FGF21 is correlated to BMI and leptin levels (874). In addition, it was reported that weight loss in obese children and adults resulted in a corresponding decrease in FGF21 concentrations (873,882). Furthermore, it was found that leptin can directly regulate FGF21 levels, both *in vitro* and *in vivo* (883). However, it was also documented that mice with induced lipodystrophy, and patients with congenital or acquired lipodystrophy, who are characterised by nearly complete absence of adipose tissue and negligible leptin levels, insulin resistance, lipodystrophy and hepatic steatosis, have increased circulating FGF21 levels (884,885). This might at first be counterintuitive, however both lipodystrophy and obesity are characterised by diminished leptin action and comparable metabolic complications. Thus, increased circulating levels of FGF21 in both pathological conditions might be a physiological mechanism trying to restore metabolic homeostasis. In support of this view is the finding by Veniant *et al.*, demonstrating that lipodystrophic mice were refractory to the effects of recombinant FGF21 treatment however, treatment with leptin, or transplantation of adipose tissue, fully restored FGF21 responsiveness in those lipodystrophic mice (886). Therefore, these results indicate that leptin potentiates the action of FGF21, and that fully functional adipose tissue is a requirement for FGF21 efficacy. Adolescent PCOS-like sheep had only mildly decreased adiposity and clearly did not display as severe metabolic phenotype as subjects with lipodystrophy, it is therefore possible, that decreased circulating leptin levels, which corresponded with low volume of omental fat and diminished adipogenesis in SAT, underlined decreased hepatic and circulating FGF21 levels in those animals.

FGF21 plays an important role in adipose tissue biology. It has been shown that FGF21 binds preferentially to FGFR1 and its β -klotho co-receptor, which are abundantly expressed in WAT, and regulate variety of metabolic processes including lipogenesis, lipolysis, and fatty acid oxidation (817,887). In addition, detectable expression of FGF21 in murine and human adipocyte cultures were reported, and further shown to be induced by *in vitro* treatment with TZDs (812,825,888). The TZDs, rosiglitazone and pioglitazone, represent a class of insulin-sensitising drugs that activate PPAR γ , a master regulator of adipocyte differentiation (889). However, it was demonstrated that treatment of mice with rosiglitazone upregulated FGF21 mRNA and protein expression in WAT, but it did not result in a corresponding increase in circulating FGF21, whereas treatment with a PPAR α agonist, induced hepatic expression of FGF21 with a corresponding increase in plasma levels, suggesting an autocrine and paracrine role of FGF21 in WAT and an endocrine role for hepatic FGF21 (812). Here, we report undetectable levels of FGF21 in ovine WAT. Likewise, some studies have reported that there is no detectable expression of *FGF21* in human WAT samples (820,823). Considering that FGF21 expression in murine WAT has been found to be maximal four hours after feeding, as opposite to hepatic FGF21, which is highest during the fasting state, these discrepancies could be attributed to different nutritional status of subjects during sample dissection (812). Subsequently, our ovine adipose tissue samples were excised after overnight fast followed by 15 min of a IVGGT test, which could potentially explain why FGF21 expression in WAT was undetectable. Alternatively, these results might suggest that WAT plays an insignificant role in contributing to circulating FGF21 levels in humans and sheep. However, WAT has been demonstrated to be an important target of FGF21 action in both, mice and humans. Mice with reduced body fat, unlike wild-type mice, are refractory to anti-diabetic treatment with recombinant murine FGF21, while transplantation of WAT into these lipodystrophic mice restores FGF21 responsiveness, thus confirming a significant role of WAT in FGF21 biology (886). It was reported that FGF21-KO mice had increased adipocyte size in subcutaneous and epididymal WAT, increased lipid stores in BAT, accompanied by decreased mRNA expression of the lipolytic enzymes, ATGL and HSL (834,890). In addition, there was reduced mRNA expression of *PLIN1*, *PPARA*, *PPARD*, *PPARG*, *PPARGC1A* and *PPARGC1B* in WAT of FGF21-KO mice (834). Correspondingly, FGF21 transgenic mice have reduced adipocyte size and increased mRNA expression of lipolytic enzymes ATGL and HSL (891). However, conflicting results were reported by Dutchak *et al.*, where lean FGF21-KO mice were described to have mild lipodystrophy with a significant decrease of total fat mass and reduced amounts of epididymal, subcutaneous, mesenteric, retroperitoneal and interscapular WAT as well as BAT, independent of body mass and calorie intake (812). The authors reported

that decreased adiposity in those FGF21-KO mice was a consequence of decreased adipocyte size rather than a reduction in number of adipocyte (812). Interestingly, Dutchak *et al.* examined the differentiation of preadipocytes derived from FGF21-KO mice and found that there was no difference in the expression of *CEBPB*, *CEBPD* and *FGFR1* however, *PPARG*, *CEBPA* and *KLB* mRNA levels were significantly decreased in adipocytes from FGF21-KO mice (812). The results from this study matches our findings, where adolescent PCOS-like sheep had reduced hepatic and circulating FGF21 levels, diminished mRNA expression of FGF21 co-receptor *KLB*, as well as decreased *PPARG*, *CEBPA* and *CEBPB* expression, with no difference in the expression of *FGFR1* and *CEBPD*, in SAT. *KLB* has been found to be a crucial component of FGF21 signalling, as when fed a high fat diet, mice with total knockout of β -klotho (*KLB*-KO) are refractory to exogenous FGF21 treatment, and show no changes in energy homeostasis, glucose and lipid control, as opposite to control mice (806). Ding *et al.* demonstrated that a selective reduction of *KLB* mRNA in adipose tissue by 70% resulted in a corresponding decrease in the *KLB* protein and complete absence of FGF21-stimulated insulin-sensitising effect in obese mice (892). Correspondingly, overexpression of β -klotho in adipose tissue in mice sensitised those animals to endogenous FGF21 treatment, reduced plasma FFA and provided protection from diet-induced obesity (893). In addition, it was demonstrated that overexpression of β -klotho in adipose tissue, resulted in upregulated expression of *SLC2A4*, *PPARGC1A*, *DIO2* and *UCP1* in BAT, and after treatment with exogenous FGF21, mice overexpressing *KLB* in adipose tissue, had increased magnitude of caloric expenditure and increased expression of genes associated with enhanced thermogenic capacity (*COX7A*, *COX7B* and *UCP1*) in WAT, when compared with control mice (893). Interestingly, it was demonstrated that TNF- α inhibited β -klotho expression, but did not impact *FGFR1* expression, *in vitro* in murine and human adipocytes, and impaired FGF21 action (894). Therefore, the increased *TNF* mRNA expression in SAT of adolescent PCOS-like sheep, as reported in chapter 3, could potentially result in decreased *KLB* expression. This in turn, could indicate that decreased circulating FGF21 levels, together with reduced signalling in SAT, due to decreased expression of *KLB*, in 11 months old prenatally androgenised sheep, might further contribute to decreased adipogenesis in SAT, as reported in chapter 3. In support of this hypothesis are the findings by Dutchak and colleagues, who reported that *PPARG* and *KLB* mRNA in adipocytes from FGF21-KO mice were restored by the addition of recombinant FGF21 in the differentiation medium *in vitro*. Furthermore, it was demonstrated that lipid accumulation, together with the expression of fatty acid binding protein, aP2, and various lipogenic proteins, were reduced in FGF21-KO adipocytes, and again partially restored when treated with FGF21 (812). In addition, *in vitro* and *in vivo* experiments demonstrated that

FGF21 increases PPARG transcriptional activity by suppressing its sumoylation, a type of post-translational modification (812). Interestingly however, when those FGF21-KO mice were fed a 10 week high-fat diet, they had significantly elevated levels of plasma FFA, increased hepatic TG and increased adipocyte size when compared with control mice fed the same high-fat diet (812). This indicates that FGF21-KO mice might have a decreased capacity for storage in adipose tissue, and as a consequence, when fed a high fat diet, develop adipocyte hypertrophy and dyslipidaemia. This metabolic phenotype parallels our ovine model of PCOS, where adolescent sheep have decreased FGF21 levels with decreased adipogenesis in SAT, whereas adult prenatally androgenised sheep, despite being on normal diet, present with obesity, increased FFA and adipocyte hypertrophy in SAT. Therefore, this notion supports a potential role of FGF21 in the metabolic dysregulation of the ovine model of PCOS.

In chapter 3, we provided evidence that in adolescent PCOS-like sheep, *ADIPOQ* mRNA expression was significantly decreased in SAT, which was further reflected in low circulating level of adiponectin. Adiponectin, like FGF21, regulates glucose and lipid metabolism, and insulin sensitivity, however, while the liver is the main source of serum FGF21, adiponectin is produced and secreted entirely by adipose tissue, but acts mostly on liver and muscles (895). Interestingly, adiponectin is also a downstream effector of PPARG and is crucial in mediating some of the therapeutic benefits of TZDs (896,897). In addition, *in vitro* studies demonstrated that human and murine adipocyte treatment with FGF21 results in increased *ADIPOQ* mRNA expression and adiponectin secretion however, pre-treatment with PPARG antagonists partially reduced FGF21-induced adiponectin secretion (815). Correspondingly, the circulating levels of adiponectin were lower in FGF21 KO mice, and treatment with recombinant FGF21 resulted in a significant increase in serum adiponectin (815), while rosiglitazone administration induced adiponectin levels in control mice but this response was significantly attenuated in FGF21-KO mice (812). In addition, it was shown that a single administration of recombinant FGF21 acutely reduced circulating glucose, insulin and triglyceride levels in diet induced obese mice and db/db diabetic mice however, in adiponectin knockout mice (ADNKO), the magnitude of the beneficial effects of FGF21 treatment was significantly reduced (815,816). Holland *et al.* demonstrated that one week of FGF21 treatment is able to promote weight loss in both control and ADNKO mice, however ADNKO mice, lost significantly less body weight than control mice, with 39% of fat mass in control mice versus 6.7% in ADNKO mice (816). These differences in fat mass reduction were accompanied by decreased energy expenditure in ADNKO mice (816). In addition, in contrast to control mice with high fat diet-induced hepatic steatosis, ADNKO mice were refractory to chronic FGF21 treatment and showed no improvement in hepatic steatosis, no decrease of

hepatic inflammation, and no reduction in the expression of genes involved in lipogenesis (815). Similarly, chronic administration of FGF21 decreased intramuscular TG accumulation and increased insulin sensitivity in muscles in control mice, however these muscular effects of FGF21 treatment were abrogated in ADNKO mice (815). The link between FGF21 and adiponectin is further emphasised by a randomised, double-blinded clinical trial, where administration of a FGF21 analogue, to overweight and obese patients and non-human primates with T2DM, resulted in significantly increased circulating adiponectin levels in dose-dependent manner (898,899). Moreover, it has been demonstrated that *KLB*-KO mice, when treated with exogenous FGF21, show no increase in plasma adiponectin as opposite to control mice (806). In addition, we have found a strong correlation between expression of *KLB* with *PPARG* and *ADIPOQ* in WAT of both adolescent and adult animals. Surprisingly, despite a comparable expression pattern of FGF21 and adiponectin in adolescent and adult animals, we did not find a direct correlation between circulating FGF21 and adiponectin levels. However, regardless of the plausible genetic and pharmacological evidence supporting the strong metabolic link between FGF21 and adiponectin, the interrelationship between these two metabolic regulators under pathological conditions is less straightforward. As documented in numerous studies, in overweight and obese subjects, and in metabolic syndrome, adiponectin levels are decreased while FGF21 increased (101,820,823,880,900,901). Few potential mechanisms can be proposed to explain this discrepancy. Adiponectin expression is suppressed by inflammation, oxidative and ER stress, which are elevated during the progression of obesity (902,903). In contrast, FGF21 has been shown to be upregulated during metabolic stress, however, the protective mechanism induced by FGF21 might be insufficient to counteract the suppressive factors on adiponectin synthesis, such as increased local inflammation in adipose tissue (838). In addition, obesity has been found to be a FGF21 resistant state, with decreased β -klotho expression in WAT documented in diet-induced obese rodents, non-human primates and obese humans (822,823,894,904). Therefore, this could potentially explain why synthesis of adiponectin is diminished despite increased levels of FGF21 in obesity.

Circulating FGF21 levels were reported to be increased in patients with hyperinsulinemia and insulin-resistant states, such as impaired glucose tolerance (IGT) and T2DM, and to correlate inversely with whole-body insulin sensitivity (905-909). Numerous studies reported that FGF21 is detectable in murine and human muscles and might be directly regulated by insulin (907,909,910), and that *FGF21* mRNA is increased in skeletal muscles of IGT and T2DM patients (908). It was shown that *FGF21* mRNA expression in muscle biopsies significantly increased after four hours of insulin infusion in healthy young men during hyperinsulinemic-

euglycemic clamp studies, and that there was a positive relationship between fasting insulin and muscle FGF21 levels (907). In addition, some authors reported that FGF21 secreted from muscles might be a source of increased plasma FGF21 in states of insulin resistance. Although we detected *FGF21* mRNA expression in ovine muscles, levels were low and there was no difference in the expression of muscle FGF21 between adolescent control and PCOS-like animals, despite evident hyperinsulinemia in prenatally androgenised sheep. Similar results were reported by Mashili *et al.* showing that expression of *FGF21* mRNA in muscles were low and there was no difference in mRNA levels between normoglycemic subjects and patients with T2DM, suggesting that elevated plasma FGF21 in insulin resistant humans is unrelated to skeletal muscle expression (909). In addition, the authors demonstrated that BMI was the strongest independent variable that was positively correlated with plasma FGF21 levels in patients with T2DM (909). We did not find a correlation between fasting insulin and plasma FGF21 in adolescent and adult animals, which indicates that adiposity might be the strongest predictor of levels of circulating FGF21 in the ovine model of PCOS. In addition, there was no correlation between muscle FGF21 and plasma FGF21 levels. Similar results were reported by Hojman *et al.*, who suggested that FGF21 expression in muscles is more likely to have a paracrine role (907). It was demonstrated that FGF21 treatment of cultured myotubes resulted in glucose uptake and increased mRNA expression protein abundance of *SLC2A1*, but not *SLC2A4*, and that insulin and FGF21 treatment had additive effects on glucose transport in myotubes *in vitro* (909). These results suggest that FGF21 resistance, even with normal insulin signalling could contribute to decreased insulin sensitivity in muscles, therefore we also investigated insulin and FGF21 receptivity in muscle tissue and found that there was no difference in the expression of *INSR*, but both *KLB* and *FGFR1* tended to be lower in 11 months old PCOS-like sheep, although this did not reach statistical significance. Interestingly, impaired FGF21 signalling in muscles of patients with impaired glucose tolerance and T2DM was reported (908). In addition, similar findings were confirmed in muscle biopsies from DIO mice, including decreased β -klotho and phosphorylated FGFR levels (908). We also noticed that expression of *PPARG* was significantly downregulated and, as in WAT, there was a significant positive correlation between *KLB* and *PPARG* expression in adolescent animals. Furthermore, there was no difference in the expression of *IRS1* and *IRS2* and selected ER stress markers, potentially suggesting that insulin signalling is not disturbed in muscles of adolescent prenatally androgenised animals however, this should be further investigated at protein level. Nevertheless, decreased *PPARG* expression might indicate a degree of insulin resistance, since *PPARG* has an important role in the maintenance of skeletal muscle insulin action, despite overall low *PPARG* expression in that tissue (911).

It was demonstrated that mice with a targeted deletion of *PPARG* in skeletal muscle developed glucose intolerance and progressive insulin resistance, with secondary insulin resistance in liver and adipose tissue (912,913). In addition, mice with disrupted muscle *PPARG* expression had impaired glucose uptake with altered IRS1 and protein kinase B (PKB) phosphorylation, but normal gene and protein expression of IRS1, PKB and GLUT4 (913).

It was demonstrated that FGF21 can act directly on liver, and regulate hepatic oxidation of fatty acids and gluconeogenesis in an autocrine and paracrine manner (810). It was reported that expression of hepatic *KLB* in children with NAFLD was decreased, and this was directly correlated with circulating levels of FGF21. Therefore, expression of FGF21 receptors in a liver might be a limiting factor for FGF21 expression. Mice treated with exogenous FGF21 had increased hepatic phosphorylation of MAPK1/3 and fibroblast growth factor receptor substrate 2 (FRS2) (810). In addition, it was found that in the liver FGF21 treatment induced expression of genes regulating gluconeogenesis and fatty acid oxidation, *G6PC*, *PEPCK* and *PPARGC1A* and reduced levels of circulating insulin and FFA however, only at pharmacological doses, whereas low doses of FGF21 had only effect on expression of PGC1- α and plasma FFA (810). Therefore, to further investigate the potential causes and consequences of decreased hepatic and circulating FGF21 in adolescent PCOS-like sheep, we have studied hepatic expression of the four isoforms of FGFR receptors (FGFR1-4) and the β -klotho co-receptor. No differences in the expression of *KLB*, *FGFR2*, *FGFR3* and *FGFR4* were found, however, there was a trend towards decreased expression of *FGFR1* in the liver of adolescent prenatally androgenised sheep. Interestingly, it was postulated that decreased expression of *FGFR1* in the liver is the limiting factor for the FGF21 signalling within this tissue (822). It was found that, DIO mice had normal expression of *KLB*, *FGFR2*, *FGFR3* and *FGFR4* but decreased expression of hepatic *FGFR1*, and this was associated with impaired response to low-dose FGF21 treatment and diminished MAPK1/3 phosphorylation (822). Although, we did not investigate phosphorylation of MAPK1/3, we found no difference in the expression of *G6PC* and *PEPCK* in the livers of adolescent PCOS-like sheep however, there was a non-significant decrease in *PPARGC1A* expression indicating that there might be limited FGF21 signalling within liver of adolescent PCOS-like animals. Based on our results we are unable to determine whether potentially decreased expression of *FGFR1* in liver of adolescent PCOS-like sheep is a cause or the consequence of diminished hepatic and circulating FGF21, but it remains possible that decreased expression of hepatic FGFR1 might contribute to decreased expression of FGF21. Nevertheless, decreased expression of *FGFR1* in the liver and *KLB* in SAT might indicate some degree of FGF21 resistance in adolescent PCOS-like sheep. This is a noteworthy finding as studies in mice fed a high-fat diet for 4 weeks demonstrated

that FGF21 resistance precedes obesity and FGF21 overexpression (822), whereas FGF21 KO mice fed a normal chow diet displayed mild late-onset obesity. Taken together, these results indicate that decreased FGF21 levels in adolescent PCOS-like sheep, together with potential FGF21 resistance in liver, muscle and SAT might contribute to the onset of obesity and metabolic phenotype in adult PCOS-like sheep.

There is a lot of confounding data regarding FGF21 expression in paediatric population. Some studies reported that, as in adults, in children and adolescents, FGF21 correlated with BMI, adiposity and leptin levels (871,874,914), but others did not (915,916). Interestingly, the largest study to date, evaluating the role of FGF21 in nearly 20,000 school children aged 6-18, found that FGF21 levels were reduced in association with obesity and correlated negatively with insulin resistance, HOMA-IR scores and components of metabolic syndrome, and positively with adiponectin levels, independent of BMI, age and gender (917). In addition, the authors reported that children with increased FGF21 had a healthier metabolic profile, including lower systolic pressure, fasting insulin and HOMA-IR scores, and higher HDL cholesterol, whereas children with diminished FGF21 had highest proportion of insulin resistance and metabolic syndrome (917). These results suggest that in the paediatric population, a relative FGF21 deficiency, rather than resistance, may play a role in the pathogenesis of insulin resistance, components of metabolic syndrome and low levels of adiponectin, independent of obesity (917). This is in agreement with study by Alisi *et al.* showing that paediatric NAFLD is associated with FGF21 deficiency, independent of BMI (872). Moreover, it was demonstrated that FGF21 levels differed by gender in puberty, with circulating FGF21 levels declining during puberty in boys, but not girls, and being lower than in girls throughout puberty (917). Corresponding results were reported in the study on FGF21 expression in Danish children and adolescents, showing that boys had significantly decreased levels of circulating FGF21 (915), and in the study by Reinehr *et al.*, although the difference in FGF21 levels between boys and girls did not reach statistical significance in this report (874). Moreover, similar findings were reported in adults, showing that females have increased circulating FGF21, when compared to males (918). Therefore, it is possible that sex hormones might have a role in regulation of FGF21 expression. However, to our knowledge, there are no investigations directly addressing the effect of sex hormones on FGF21 expression or potential sexual dimorphism in FGF21 concentration in either adults or children. To date only one study has investigated the role of FGF21 in reproduction. It was reported that female, but not male, transgenic mice overexpressing FGF21 were infertile (891). Further investigation revealed that FGF21 overexpression in female mice resulted in delayed puberty, anovulatory hypogonadism with normal FSH and decreased LH levels, suggesting that abnormal FGF21

levels might contribute to reproductive aberrations (919). Unfortunately, there are no studies investigating FGF21 levels in adolescent girls with PCOS. The only comparable study was conducted on lean adolescent girls with hyperinsulinemic androgen excess and reported that those girls have normal levels of circulating FGF21 as compared to BMI- and age- matched controls (920). Interestingly, the authors also reported that plasma FGF21 inversely correlated with BMI and adiposity in those girls (920), again demonstrating that association between FGF21 and body composition might be different in paediatric and adult populations. Adult women with PCOS were reported to have comparable FGF21 levels with BMI-matched controls (921,922). However, one study noted that although lean PCOS had comparable circulating FGF21 levels to BMI-matched controls, obese patients with PCOS had elevated plasma FGF21 as compared with obese controls (923). Nonetheless, the same study also reported that plasma FGF21 levels were correlated with BMI, body fat mass and percentage, waist circumference and plasma insulin but did not with estradiol and FAI (923). Therefore, authors concluded that increased plasma FGF21 levels, as observed in obese women with PCOS were associated with metabolic but not hormonal disturbances (923).

Interestingly, comparable to women with PCOS, in adulthood, there was no statistical difference in the levels of hepatic and circulating FGF21 between controls and PCOS-like sheep. However, whereas levels of FGF21 in control animals remained stable across adolescence and adulthood, there was an increase in hepatic and serum FGF21 in adult PCOS-like animals as compared with levels during puberty, although this was not statistically significant. These changes perhaps reflect more rapid changes in body mass and adiposity in PCOS-like animals as compared with controls, during the transition from adolescence to adulthood. As stated earlier, adult PCOS-like sheep were obese with a non-significant increase in omental fat when compared with controls. However, since we investigated the levels of FGF21 at the early onset of obesity in adult PCOS-like animals, based on the published data regarding FGF21 and obesity, it can be speculated that with the predicted progress of obesity in those sheep there would be a corresponding increase in FGF21 levels, potentially resulting in FGF21 resistance. Although, there was no correlation between levels of circulating leptin with hepatic and plasma FGF21, as observed in adolescent animals, there was a negative relationship between volume of omental fat and circulating FGF21, indicating that animals with the lowest levels of FGF21 had the highest levels of omental fat, and suggesting that that decreased levels of FGF21 in adolescent might predispose to obesity in adulthood. Alternatively, the increase in FGF21 level in adult PCOS-like sheep could be a homeostatic response to progressing metabolic distress observed in those animals. Interestingly, we have not found evidence of FGF21 resistance in adult prenatally androgenised sheep, despite

obesity, again supporting the hypothesis that this might be a transition window with an early stage of obesity. In contrast to adolescent PCOS-like animals, adult sheep had normal levels of *KLB* and *FGFR1* expression in SAT, inguinal and neck adipose tissue, and significantly increased expression in VAT. In addition, as described in chapter 3, adult prenatally androgenised sheep, had comparable levels of *PPARG* and *ADIPOQ* expression in both SAT and VAT. However, like in adolescent animals, there was still a significant correlation in expression of *KLB* with *PPARG* and *ADIPOQ*, indicating a potential regulatory feed forward loop in expression of those genes.

Normalised plasma FGF21 levels together with improved FGF21 sensitivity in the adipose tissue of adult PCOS-like animals was an unexpected finding. Especially considering the obesity and decreased expression of thermogenic genes in adipose tissue, reported in chapter 4. Several studies reported that FGF21 plays an important role in the regulation of thermogenesis and expression of thermogenic genes, and that treatment with FGF21 can induce browning of WAT *in vitro* and *in vivo* (818,841,918,924). It was found that circulating FGF21 correlated positively with cold-induced non-shivering thermogenesis and BAT activity in humans (819,918). In addition, it was demonstrated that thermogenic activation induces FGF21 expression and release in BAT (925). However, the majority of those studies were conducted during cold exposure, whereas our study was conducted at thermoneutrality. Notably, Hanssen *et al.* reported that adult females had a trend toward increased circulating FGF21 compared to males at thermoneutrality, however, this difference become statistically significant during cold exposure (918). In addition, a study by Veniant *et al.* documented that FGF21 induced weight loss only in lean mice, but not in DIO obese mice, kept at standard housing temperatures, however, it was inefficient at thermoneutrality and was independent of WAT browning and UCP1, suggesting that FGF21 may only play a significant role at lower temperatures (926). The authors also noted that the beneficial effects of FGF21 treatment on body weight and energy expenditure were related to significant induction of *PPARGC1A* (926). This finding was also reported by others, showing that FGF21 regulates energy metabolism by activating the AMPK-SIRT1-PPARGC1A pathway, and that the role of FGF21 during cold exposure is to enhance PGC-1 α protein levels within thermogenically active fat depots (818,927,928). Interestingly, in chapter 4, it was reported that in IAT of adult PCOS-like animals there was decreased expression of *UCP1*, *UCP2* and *UCP3* but significantly increased expression of *PPARGC1A* and normal *SIRT1*, which could be a compensatory mechanism stimulated by FGF21. However, in SAT of adult prenatally androgenised sheep there was decreased expression of *UCP1* together with *PPARGC1A* and *SIRT1*, which could suggest that this depot might be less sensitive to FGF21 action. Alternatively, since we did not

investigate expression of FGF21 in IAT, it is possible that that FGF21 was expressed and secreted from that fat depot, which might subsequently stimulate thermogenic genes in a paracrine fashion. Interestingly, it was reported that the expression of FGF21 in BAT is stimulated by noradrenaline (925), and in the *in vitro* study of human neck adipocytes it was demonstrated that FGF21 can induce heat production only after noradrenaline exposure (841). In chapter 4, we provided evidence that noradrenaline levels were significantly decreased in all fat depots studied, apart from IAT, where noradrenaline levels were comparable between controls and adult PCOS-like animals. This cross-talk of noradrenaline and FGF21, could perhaps explain why adult PCOS-like animals have decreased postprandial thermogenesis and decreased expression of thermogenic genes despite normal FGF21 levels and sensitivity. Of note, more recent studies reported that FGF21 acts centrally to induce energy expenditure and that signalling to adipose tissue is not required to decrease body weight, therefore, to fully understand the role of FGF21 in thermogenesis FGF21 signalling in the brain should be also investigated (929,930).

In the liver of adult PCOS-like animals, there were no significant differences in the expression of *KLB* and FGF receptors when compared with controls, although a trend for increased expression of *FGFR1*, *FGFR4* together with *PPARGC1A* (chapter 5) was observed, however, likely due to large variation and small number of PCOS-animals, this did not reach statistical significance. Interestingly, it has been demonstrated that FGF21 induces the expression of *PPARGC1A* and causes corresponding increases in FFA oxidation and gluconeogenesis (931). This association of FGF21, *PPARGC1A* and FFA oxidation could contribute to increased levels of hepatic triglycerides in adolescent PCOS-like animals, but comparable levels of hepatic fat with control animals in adult PCOS-like sheep, as demonstrated in chapter 5.

Interestingly, in muscles there was increased expression of both *FGF21* and *FGFR1*, together with trend for increased *PPARG* expression. Since, FGF21 in skeletal muscles has been shown to be upregulated by insulin, and to be elevated in humans with hyperinsulinaemia (907), it is possible that persistent hyperinsulinaemia in PCOS-like animals, might be a driving factor for increased expression of FGF21 in muscles of adult prenatally androgenised sheep. Moreover, increased FGF21 in skeletal muscles was documented in patients with IR and T2DM (908), however, there was normal expression of *INSR*, *IRS1* and *IRS2*, together with trend for increased expression of *PPARG* in skeletal muscle of adult PCOS-like animals. These results could indicate normal insulin sensitivity in that tissue although this should be further investigated at a protein level. In addition, it seems that compared to adolescent PCOS-like animals, adult sheep have improved insulin and FGF21 sensitivity in skeletal muscle.

Paradoxically, this could be attributed to increased body weight and adiposity in those adult PCOS-like animals. It is possible that, in adolescent PCOS-like animals, due to decreased storage capacity in SAT, there was increased concentration of TG in skeletal muscles and hence decreased insulin sensitivity, but hypertrophic expansion of SAT and increasing volume of omental fat in adult animals could lead to redistribution of intramuscular fat back to adipose tissue, and as a consequence, improved insulin sensitivity. Unfortunately, we did not examine distribution of intramuscular triglycerides in adolescent or adult animals and this requires further investigation. Alternatively, since *PPARG* in skeletal muscles mediates upregulation of lipid use in skeletal muscle (912), the trend towards increased expression of *PPARG* in skeletal muscle of PCOS-like animals could indicate an improved use of fatty acids in skeletal muscles, and subsequently this could lead to improved insulin and FGF21 sensitivity. Interestingly, it was demonstrated that mice with muscle specific *PPARG* deficiency were insulin resistant and developed increased adiposity (912). Therefore, it is possible that decreased *PPARG* expression in adolescent PCOS-like sheep, resulting in lower utilisation of FFA, could promote insulin resistance in adolescent animals, and in addition, could contribute to increased adiposity in adult animals. This in turn, could restore insulin sensitivity in skeletal muscles and as a consequence lead to increased expression of *PPARG*, as observed in adult PCOS-like animals. Overall, these data provide evidence that adult PCOS-like sheep, in contrast to adolescent prenatally androgenised animals, have an increased sensitivity for FGF21. This might be a homeostatic mechanism in response to obesity, hyperinsulinemia and increased FFA in those animals. However, there were no correlations in the levels of circulating FGF21 with FFA, insulin or adiponectin. In summary, adolescent PCOS-like sheep have decreased plasma FGF21 together with decreased sensitivity for this hepatokine in SAT, liver and muscle, whereas adult prenatally androgenised sheep have opposite profile, with normalised levels of circulating FGF21 and increased sensitivity for this hormone in VAT, muscles and liver, which might be physiologic response trying to reverse deteriorating metabolic phenotype in those animals.

In this chapter, we also analysed the role of irisin in metabolic profile of adolescent and adult sheep. Irisin, a myokine, is a cleaved and secreted product of the *FNDC5* protein, induced by physical exercise, that was recently implicated in regulating browning of WAT, increasing thermogenesis, reducing insulin resistance and improving glucose homeostasis (840,841,850). In DIO mice, *FNDC5* overexpression in skeletal muscle and increased circulating irisin levels enhanced energy expenditure, increased weight loss, improved insulin sensitivity and reduced hyperlipidaemia, hyperglycaemia and blood pressure (840,932). Overexpression of *FNDC5* in skeletal muscles, significantly increased *UCP1* and *PPARGC1A* levels and reduced adipocyte

diameter in the SAT, but not in the VAT or BAT, in both control and DIO mice, perhaps indicating a adipose depot-specific sensitivity to the metabolic action of irisin (932). However, it was also reported that *FNDC5* mRNA, *FNDC5* protein and irisin levels in skeletal muscle, but not in the circulation, were higher in obese mice than those in control mice (932). In addition, results in humans are inconsistent concerning the potential beneficial role of irisin in metabolism and energy expenditure. Circulating irisin levels were reported to be higher (859,933), and lower (850,852), in subjects with metabolic syndrome and patients with insulin resistance and T2DM. Furthermore, similar level of circulating irisin were found in people with active and non-active BAT (934). Our results showed that there were no differences in the expression of *FNDC5* in skeletal muscle or circulating irisin between control and PCOS-like sheep, in adolescence and adulthood. This finding could simply indicate that control and PCOS-like animals had same level of activity, since majority of the studies confirmed that irisin is an exercise stimulated myokine (933,935,936). However, there was a significant increase in levels of circulating irisin, but not the expression of *FNDC5* in skeletal muscle, in adult PCOS-like animals when compared with adolescent prenatally androgenised sheep, and this change was not present in control animals. This sharp increase in levels of irisin in PCOS-like animals could reflect increasing adiposity associated with significantly increased body weight in those animals, since adipose tissue might be an additional source of irisin, which could also explain why irisin correlates with BMI, adipose tissue mass, and is elevated in obesity (858,861,862,937). Alternatively, this could be a homeostatic response to counteract obesity, as irisin was also demonstrated to increase energy expenditure and browning of WAT, and to enhance lipolysis and correct glucose and lipid metabolic derangements associated with obesity (840,932). However, it should be noted that irisin plays important role in shivering induced thermogenesis as it is secreted from muscles during cold exposure (841). Therefore, the potential role of irisin in postprandial thermogenesis of adult animals, investigated in this thesis, might not be relevant. Conversely, comparable levels of circulating irisin in control and PCOS-like animals might indicate that animals were exposed to the same environmental temperatures. Nevertheless, it was demonstrated that irisin induced glucose and FFA uptake, and *SLC2A4* expression in adipocytes and myocytes (938), therefore, a significant change in circulating irisin may well be an adaptive response in an attempt to improve insulin sensitivity in adult PCOS-like animals. However, we did not find a correlation between levels of fasting insulin and irisin, in adolescent and adult animals. This was a surprising finding since, majority of previous studies reported positive correlation between irisin and fasting insulin, HOMA-IR and other parameters of the metabolic syndrome, indicating a regulatory feedback mechanism or possibly suggesting a degree of irisin resistance (938-940).

We also did not find a correlation between mRNA expression of *FNDC5* in skeletal muscles and circulating irisin. This could be due post-translational modification and proteolytic cleavage of *FNDC5* protein before releasing it into circulation therefore, as noted by some researchers, *FNDC5* mRNA does not always correlate with levels of irisin and mRNA expression alone should be interpreted very cautiously (857). Alternatively, difference in the expression in muscle *FNDC5* mRNA and circulating irisin could be attributed to other tissues secreting this factor. As reported by others, adipose tissue might also secrete irisin. Interestingly, it was demonstrated that in rats irisin is released from mature adipocytes mainly in SAT, and to lesser extent in VAT, but not BAT (863). Therefore, the increased irisin levels in adult PCOS-like animals, compared with adolescents, could reflect decreased number of mature adipocytes in SAT in adolescent sheep and the progressive hypertrophy in SAT in adult animals. Unfortunately, we did not investigate expression of *FNDC5* in adipose tissue. Nevertheless, we found a positive correlation between levels of circulating irisin with omental fat and leptin, but only in adolescent, not adult animals. Perhaps this observation could be attributed to dysfunctional adipose tissue in obesity, or this could suggest that irisin levels are modified by additional factors in adult animals. Similar findings were reported by Sanchis-Gomar *et al.*, where no correlation of irisin with BMI, or other metabolic parameters in obese and diabetic patients were found (941). We also found a negative relationship of irisin with fasting FFA in adolescent, but not in adult animals. Comparable findings were reported by Volzke *et al.*, showing that there was a negative correlation of irisin with LDL cholesterol and TG in general population (942). Interestingly, it was recently reported that *FNDC5* mRNA was expressed in the brain and in the reproductive neuroendocrine axis, and that circulating irisin could be modified by diet and hormonal status (943). In addition, a sexual dimorphism in the concentrations of irisin in children, adolescents and adults was reported, with females having higher levels than men (844,944,945). It was therefore suggested that sex hormones may play a role in regulating irisin concentration (844).

In women with PCOS, just like in general population, the findings regarding levels of circulating irisin are inconsistent. Serum irisin has been demonstrated to be increased (946-949), decreased (950), or no difference was found (951,952). In addition, some reported an association of irisin in patients with PCOS with BMI, obesity and hyperinsulinemia (946,947,951,953), whereas others found no association with these metabolic factors (950,952). In addition, few studies documented association of irisin with hormonal status of women with PCOS, including hyperandrogenemia and levels of LH (946,947,950,953). Evidently there are a lot of discrepancies between the above studies. It is likely that differences in clinical characteristics of study cohort, such as age, BMI, degree of insulin resistance, and

variations in sex hormones, may explain some of them. Furthermore, medication commonly prescribed to women with PCOS could also alter the results. For example, it was demonstrated that metformin promotes irisin release from skeletal muscles (954). In addition, as recently reviewed by Perakakis *et al.* some of the ELISA kits used for the measurement of irisin concentrations had low accuracy with cross-reactivity with non-specific serum proteins (938). Therefore, further research is needed to provide comprehensive understanding of the potential role of irisin in PCOS.

In summary, our study provide evidence that there is no difference in the concentration of irisin between control and PCOS-like animals in adolescence and adulthood, it is therefore unlikely that irisin might play an important role in metabolic profile of the ovine model of PCOS. However, it should be noted, that due to small number of animals and large result variation, our results might not be fully representative.

Chapter 7 General Discussion

Prenatal programming can be defined as the ability of the intrauterine environment to induce phenotypic alterations in the developing fetus. Hormonal imbalance during this crucial developmental window may programme permanent changes in the differentiating tissues of the individual that will determine further development but also its reproductive and metabolic capacity as well as predisposition for health and disease. It has been proposed that the adult PCOS phenotype is likely to be programmed by exposure of female fetuses to increased androgens *in utero*. Results documented in this thesis present further evidence to support this hypothesis and provide better understanding into some of the mechanisms underlying the metabolic problems associated with the syndrome

It has been documented that some aspects of metabolism are sexually dimorphic. Differences between males and females in glucose and lipid metabolism, peripheral insulin sensitivity and liver metabolism have been described (955-957). Furthermore, males have been reported to have increased prevalence of dyslipidaemia (958), NAFLD (959), IR (960), T2DM (961), CVD (962), and lower concentration of adiponectin than females (499). Body fat distribution patterns are also sexually dimorphic. In general, women are characterised by a higher body fat percentage than men, with a greater proportion of adipose tissue in gluteal and femoral regions, while men tend to have more adipose tissue accumulated in the VAT and decreased volume of SAT (125,142). Since visceral obesity is considered a significant risk for metabolic complications (123,124) while preferential gynoid fat distribution is believed to be protective, those differences in adipose tissue distribution have been postulated as one of the main causes underlying those sex-specific differences in aforementioned metabolic problems (960,961).

What induces adipose tissue differences between males and females? Sex hormones play an important role in the regulation of body fat distribution. This may be particularly important with regards to androgens, which inhibit preadipocyte differentiation, modulate adipocyte function and affect the size and distribution of adipose tissue (142). Women with PCOS have been reported to have increased central and decreased gynoidal adipose tissue, thus displaying an android pattern of adipose tissue distribution (145,963). In addition, adipose tissue dysfunction, independent of obesity, have been described in PCOS (964). Furthermore, there is evidence showing link between partial lipodystrophy and PCOS (221-226). Moreover, women with PCOS have been found to have higher prevalence of IR, T2DM, NAFLD, dyslipidaemia, and lower concentration of adiponectin than BMI-matched women in general population. These observations raise several questions: are women with PCOS programmed to have male-like adipose tissue distribution and function and therefore increased prevalence

of male-like metabolic problems? If so, what are potential mechanisms underlying this? When do these changes occur? Is this an androgenic effect?

Animal models of PCOS provide great opportunity to answer some of those questions. Numerous studies documented that exposure of ovine female fetuses to increased levels of androgens *in utero* result in many reproductive, neuroendocrine and metabolic characteristics that mirror those of PCOS women. Previous data generated in our lab demonstrated that adolescent prenatally androgenised sheep display some of the PCOS features, including enhanced capacity for androgen synthesis in theca cells and adrenal glands, accompanied by global upregulation of steroidogenic genes, fatty liver, hyperinsulinemia, however, without confounding factors such as hyperandrogenemia or obesity. Likewise, pre-pubertal and early-pubertal daughters of PCOS mothers have been shown to have some of metabolic characteristic of adult PCOS, including hyperinsulinemia and decreased adiponectin however, independent of obesity and without increased androgen levels, therefore indicating that metabolic changes might precede development of hyperandrogenism (286,965).

Our results demonstrate that adolescent sheep that were exposed to increased androgens *in utero* through maternal injections had decreased expression of markers of adipogenesis in SAT. Further, we provide evidence that perturbed adipogenesis in SAT is likely to be a consequence of prenatal androgen exposure, as in the model of direct fetal injections with steroids, only adolescent sheep that were exposed to androgens in fetal life, but not those treated with estrogen or glucocorticoids, displayed perturbed adipogenesis in SAT. Moreover, we show that altered adipogenesis correlates with onset of puberty, as changes in expression of adipogenic markers were not evident during fetal and early life, neither in adulthood. So why these changes are only apparent during puberty?

Studies demonstrated that throughout life there are two main waves of adipocyte differentiation, fetal life and puberty. Adipocyte proliferation tends to decline by the end of the gestation, and adiposity is increased primarily by filling of predetermined adipocytes until puberty, after which another intensified proliferation and maturation of adipocytes occurs (68). Therefore, the total number of adipocytes that the individual will have as an adult is set during puberty, although, the differentiation potential of preadipocytes into mature adipocytes is present throughout life, and depends on the body energy status and the storage needs. However, in adult life, the capacity of preadipocytes to become fully functional mature adipocytes declines (69,70). Consequently, diminished adipogenesis results in decreased storage capacity of adipose tissue, which might cause accumulation of lipids in non-adipose

tissues, such as liver and muscles, and subsequently leads to lipotoxicity, insulin resistance and metabolic perturbations (72,73). Therefore, inability of an individual to increase adipose cell number results in the development of hypertrophic adipocytes, which might increase risk of metabolic diseases (74). And although, adipogenesis in PCOS patients has not been investigated, there is growing evidence of decreased adipogenesis in SAT from insulin resistant individuals and subjects with abdominal obesity (473-475). Therefore, what are the potential mechanisms underlying decreased adipogenesis in adolescent PCOS-like sheep?

Insulin and androgens, both suggested to be important contributors to the PCOS phenotype, affect adipose tissue function, however, insulin and androgens have opposing regulatory effects on the differentiation of preadipocytes to adipocytes. There is evidence that insulin stimulate adipogenesis (227), while androgens inhibit preadipocyte differentiation (228), thus hormonal and metabolic derangements are likely to play an important role in adipose tissue function in PCOS. However, since adolescent prenatally androgenised sheep were not hyperandrogenemic, this raises a question whether androgens prime SAT in fetal life to be a male-like and whether there are any additional factors contributing to that? Wang *et al.* documented that in subcutaneous adipocytes from PCOS patients, expression of testosterone synthesising enzymes was higher, while expression of aromatase was decreased, suggesting increased local androgen action (229). In addition, PCOS women and daughters of women with PCOS were reported to have increased 5 α -reductase activity (966,967), therefore there is possibility that adolescent PCOS-like sheep might have increased peripheral androgen metabolism. In addition, as discussed throughout this thesis adolescent PCOS-like sheep were hyperinsulinemic with some features of insulin resistance and had decreased gene expression of proteins associated with insulin signalling in SAT, although insulin sensitivity was not assessed in those animals. Nevertheless, puberty is associated with decreased insulin sensitivity (968). Insulin has a stimulatory effect on adipogenesis, therefore it is likely that mixture of androgenic programming combined with a degree of insulin resistance, so prevalent in PCOS girls and adult women might lead to decreased adipogenesis in SAT. Furthermore, adolescent PCOS sheep, like adolescent and adult women with PCOS had decreased adiponectin, which as discussed in chapter 3 is likely due to dysfunctional SAT. In turn, low levels of adiponectin, an insulin sensitising adipokine might lead to further deterioration of insulin sensitivity. Therefore, what are the potential consequences of decreased adipogenesis in SAT during puberty?

Decreased adipogenesis indicates lower capacity of SAT to safely store fat. Adolescent prenatally androgenised animals had increased circulating fasting FFA, most likely due to decreased adipogenesis and perturbed insulin signalling in SAT, but independent of body weight and central adiposity, as reviewed in chapter 3. Circulating FFA comprise majority of hepatic lipids in NAFLD. Chapter 5 provide evidence that these adolescent PCOS-like sheep had upregulated expression of genes involved in hepatic FA uptake and *de novo* lipogenesis, but normal expression of genes associated with FA oxidation, which might elucidate the mechanisms involved in increased hepatic lipid accumulation in those animals and perhaps explaining increased prevalence of NAFLD in adolescent and adult women with PCOS, which is again independent of obesity. Moreover, since increased FFA have been demonstrated to directly stimulate pancreatic insulin secretion (269), this delivers an additional link between perturbed adipogenesis in SAT and hyperinsulinemia PCOS-like animals and potentially women with PCOS. Further, as discussed in chapter 3, SAT represents about 80% of total body adipose tissue and given set adipocyte number in adulthood, decreased SAT adipogenesis in adolescents would result in decreased storage capacity in adulthood and increased lipid storage in already developed adipocytes, resulting in hypertrophy. Indeed, adult PCOS-like sheep have decreased total number of adipocytes in SAT with a corresponding increase in large, hypertrophic adipocytes. Enlarged adipocytes are less insulin sensitive and individuals with hypertrophic adipocytes in SAT are more insulin resistant than people with comparable adiposity but smaller adipocytes (469-471). Moreover, there are reports documenting adipocyte hypertrophy in women with PCOS (230), thus potentially explaining high prevalence of insulin resistance, independent of obesity (189). Conversely, adipocyte hypertrophy is not only strongly associated with increased release of lipid content and insulin resistance but also with increased inflammation, which might further impair insulin sensitivity and dysregulate adipokine secretion. Again, results documented in chapter 3, show increased expression of pro-inflammatory genes in that fat depot. In addition, it can be speculated that due to the combination of diminished storage capacity and adipocyte hypertrophy in SAT of adult PCOS-like sheep, there is a physiological response to increase buffering capacity of other adipose tissue depots, represented by increased omental fat volume in those animals, although not statistically significant, as discussed in chapter 3. This in turn however, might explain normalised hepatic fat content in those adult PCOS-like ewes, which was paralleled by normal levels of hepatic FA uptake, as demonstrated in chapter 5, suggesting that fat from the liver might be redirected back to adipose tissue. In addition, the early increase in volume of VAT, likely paralleled by increased adipokines secretion, might contribute to normalised levels of leptin and adiponectin in those young adult sheep, as demonstrated in chapter 3. Although it

is tempting to speculate that once the capacity of visceral adipose tissue would become saturated, there would be an increase in inflammation in that depot paralleled by dysregulated adipokine secretion, while FA would be shunt back to the liver, resulting in NAFLD once again. This in turn would result in progressive deterioration of insulin sensitivity and overall metabolic profile, as it is normally observed in adult women with PCOS. In addition, due to decreased capacity of SAT, even normal caloric intake could be relatively excessive, resulting in SAT hypertrophy, subsequent increase in central obesity and insulin resistance.

Decreased adiponectin and leptin in adolescent prenatally androgenised sheep are likely to be additional consequences of decreased adipogenesis in SAT. As discussed throughout this thesis, these adipokines regulate broad spectrum of metabolic aspects, including insulin sensitivity, FFA oxidation, energy expenditure and appetite, therefore dysregulated secretion of those adipokines is likely to contribute to perturbed metabolic profile in adolescent PCOS-sheep. In addition, there is evidence showing that adiponectin can suppress theca cell androgen synthesis, and therefore decreased levels of adiponectin in PCOS may contribute to enhanced capacity of ovarian androgen production, as previously demonstrated in our ovine model of PCOS and typically seen in women with PCOS.

Moreover, decreased leptin levels in adolescent prenatally androgenised sheep might, at least partially, be responsible for decreased expression of hepatic FGF21 in those animals, as discussed in chapter 6. FGF21 regulates a broad spectrum of metabolism, including insulin sensitivity, lipid homeostasis and energy balance. Therefore, it is likely that changes in its expression might contribute to the perturbed metabolic phenotype, as observed in adolescent prenatally androgenised sheep. In addition, adolescent PCOS-like sheep displayed decreased FGF21 sensitivity in SAT and liver, which could in turn, contribute to decreased adipogenesis paralleled by reduced adiponectin, and decreased FA oxidation, respectively. Conversely, adult prenatally androgenised sheep display an opposite FGF21 profile, with normalised levels of circulating FGF21 and increased sensitivity for this hormone in VAT, muscles and liver, which might represent a homeostatic mechanism trying to reverse deteriorating metabolic phenotype in those adult animals.

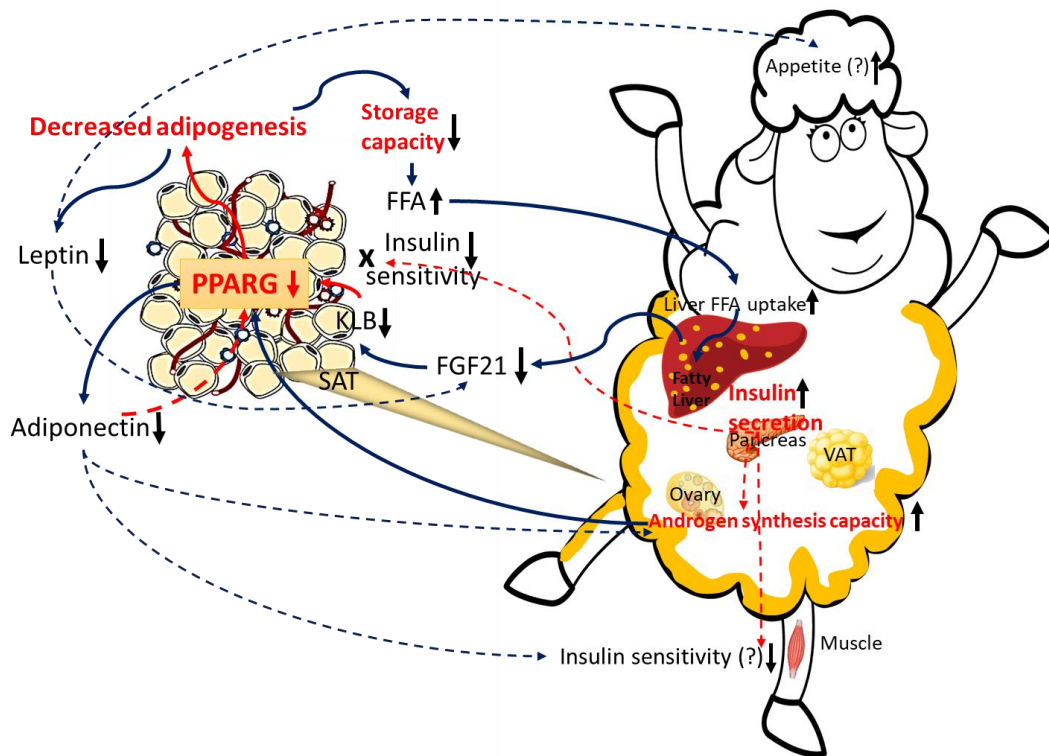


Figure 7.1 An adolescent PCOS-like model of prenatally androgenized sheep. Adolescent PCOS-like sheep have decreased adipogenesis in SAT, likely due to combination of increased androgens and insulin resistance, accompanied by decreased circulating concentrations of leptin and adiponectin. Decreased storage capacity of SAT results in increased concentration of FFA in circulation, which is countered by increased FFA uptake into liver resulting in hepatic fat accumulation. In addition, adolescent prenatally androgenized sheep have decreased concentration of FGF21, likely due to decreased leptin levels, and decreased expression of *KLB* in SAT further augmenting expression of *PPARG* and adiponectin. Decreased adiponectin levels might result in decreased insulin sensitivity and increased ovarian androgen synthesis while reduced leptin concentration might lead to increased appetite resulting in an increased body weight in future.

Does perturbed adipogenesis only affect white adipose tissue? In chapter 3, we provide evidence of reduced expression of *PRDM16* in adolescent SAT, which is associated with programming of brown/beige adipocyte development. Further, in chapter 4 we show that there is significantly reduced thermogenic potential of adipocytes in three different adipose tissue depots of adult PCOS-like animals, further paralleled by decreased noradrenaline concentration. Is there evidence for a role of sex hormones in programming brown and beige adipose tissue function?

Besides the well-known impact of sex hormones on WAT distribution, there is some evidence that there is also sexual dimorphism in distribution and function of BAT. Women have been found to have greater volume of BAT, than men (146,147). Further, studies on rodents demonstrated that, there is sex-specific composition of lipids in BAT (148), mitochondrial function and sensitivity of BAT to adrenergic stimulation (149). Female mice are more responsive to browning of WAT during β -adrenergic stimulation than males (150), and have higher UCP1 expression in BAT (151).

What are potential consequences of diminished thermogenic potential of brown/beige adipocytes in an ovine model of PCOS? Epidemiological studies provide a clear evidence for the close link between PCOS and obesity, showing that 38%–88% women with PCOS are overweight or obese (207), and conversely, that the prevalence of PCOS is high in unselected obese female population, with up to 28% of all cases (208,209). Therefore, considering the high prevalence of obesity in PCOS, some authors postulated that women with PCOS might have a unique predisposition to obesity, and that these women might face additional barriers to effective weight management (210). Indeed, decreased basal BMR (211) and postprandial thermogenesis (212) have been reported in women with PCOS. In addition, Wright *et al.* reported that PCOS patients with a normal BMI consumed significantly lower number of calories (≥ 250 kcal/day) than BMI-matched controls, hypothesising that this might be necessary to prevent weight gain in those women (547). Moreover, obesity exacerbates symptoms of PCOS. It has been demonstrated that obesity can further increase prevalence of irregular menstrual cycles, amplify androgen concentrations and elevate risk for pregnancy complications (213). Obesity is also linked to a reduced response to infertility treatment (213). Conversely, even modest weight loss in obese PCOS women can significantly improve reproductive and metabolic characteristics of the syndrome (207).

What are the potential mechanism underlying increased prevalence of obesity in women with PCOS? In chapter 5 we have provided evidence that adult PCOS-like sheep have a decreased amplitude of PPT when compared with controls, measured through direct calorimetry, without a difference in basal body temperature, despite receiving the same caloric intake, and independent of obesity. What is more, we also reported that these PCOS-like sheep have increased time to reach their maximal postprandial temperature, again independent of obesity. These findings suggest that prenatally androgenised sheep have reduced capacity for energy expenditure, which may explain propensity for obesity in these animals, and potentially PCOS women. Interestingly, it has been shown that obese individuals, with a childhood history of obesity, have lower PPT, before and after weight loss, suggesting that thermogenic defect may be a cause rather than a consequence of obesity (578).

Is decreased thermogenic potential of adipose tissue solely responsible for decreased PPT in adult PCOS-like sheep? This is unlikely. As discussed in chapter 5, there are possible additional factors, including potential peripheral, and/or central insulin resistance. As reviewed in chapter 5, a study on intranasal insulin administration reported that administration of intranasal insulin increased PPT by 17% when compared to placebo, thus showing that efficient brain insulin signalling is necessary for whole-body energy flux (604). Since peripheral insulin resistance and obesity has been shown to be associated with reduced insulin sensitivity in central nervous system (605-607), it can be speculated that prenatally androgenised sheep and women with PCOS might also have decreased central insulin sensitivity, which in turn might be accountable for reduced sympathetic outflow, decreased noradrenaline and consequently diminished PPT, although currently there is no data to support this hypothesis.

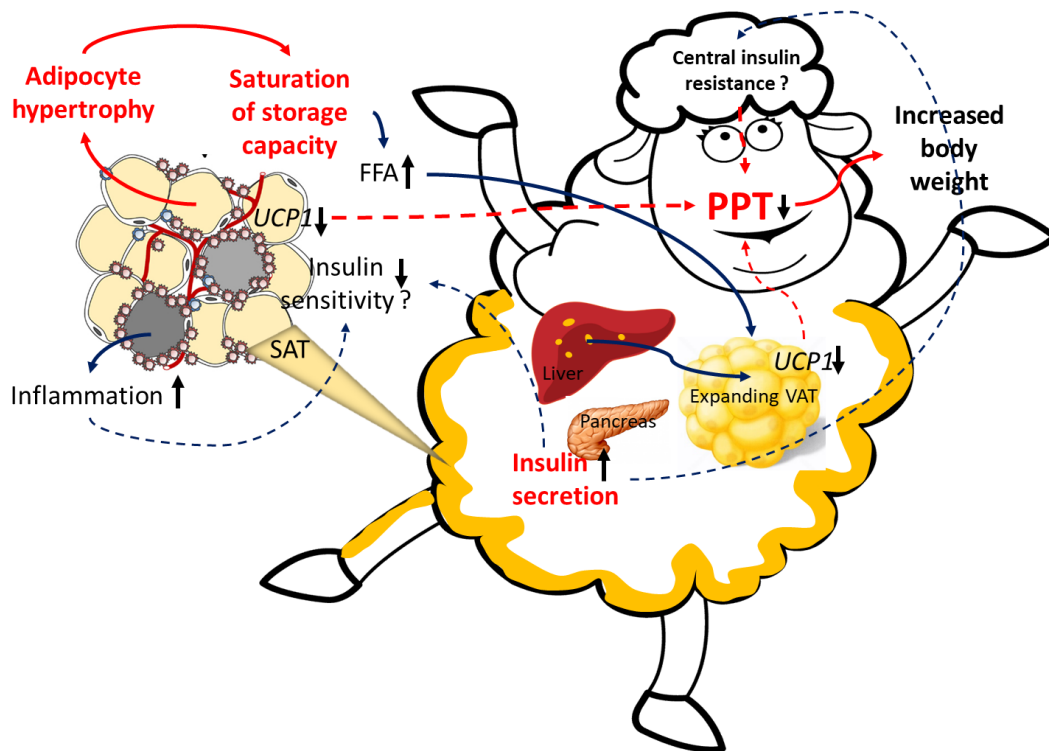


Figure 7.2 An adult PCOS-like model of prenatally androgenized sheep. Adult PCOS-like sheep have increased body weight, adipocyte hypertrophy in SAT, which is further associated with increased expression of inflammatory markers and elevated concentration of circulating FFA, likely due to saturation of SAT storage capacity. Further, due to combination of reduced SAT storage capacity and adipocyte hypertrophy there is a physiological response to increase buffering capacity of VAT volume, potentially explaining normalised hepatic fat content in those adult PCOS-like animals. Adult prenatally androgenized animals have decreased PPT independent of obesity and further associated with hyperinsulinemia and decreased thermogenic potential of brown/beige adipocytes represented by diminished expression of *UCP1*.

Are there any advantages of decreased subcutaneous and increased visceral adiposity, as well as diminished energy expenditure in women with PCOS? It is highly speculative however, some authors postulated that women with PCOS might have reproductive advantage during the times of food deprivation. It has been suggested, that although women with PCOS have increased likelihood of being obese and anovulatory during times of normal or excess food availability however, they start to ovulate after body weight loss, therefore displaying a selective advantage by being able to reproduce during periods of food shortage when other women become anovulatory (969,970). Therefore, considering this hypothesis, it can be suggested, that since adipocytes in the VAT depot exhibit increased rate of lipolysis during adrenergic stimulation, thus being more metabolically active, having increased visceral adiposity during times of food deprivation would provide more accessible energy stores, while decreased PPT would offer improved energy utilisation during those adverse conditions.

Can we potentially prevent some of the metabolic problems associated with PCOS? As discussed, pre-puberty or early puberty in girls at high risk of developing PCOS, such as daughters of PCOS mothers, would be an ideal time for early clinical intervention to ameliorate the metabolic phenotype of adult PCOS. Adiponectin could be used as an early marker of metabolic perturbations while treatment with FGF21 analogs or TZDs could be used as preventative measure. Although, FGF21 therapeutics represents an attractive opportunity for novel drug development treating metabolic disorders, these drugs are still under scrutiny (971), while TZDs, a class of antidiabetic drugs, which are also potent stimulators of adipose tissue differentiation, have been already successfully used as therapeutic measure in adult women with PCOS (972), therefore suggesting a more realistic approach.

Can findings described in this thesis be extrapolated to our understanding of PCOS in human? As discussed throughout this thesis, midgestational exposure of fetal sheep to increased levels of androgens results in clinically realistic model of PCOS. In sheep, fetal development, metabolism, thermogenesis, histological location of WAT and BAT as well as adult body weight parallel humans. Adolescent daughters of PCOS mothers have increased levels of insulin and reduced levels of adiponectin as compared with age and BMI-matched controls (482). Moreover, it was found that metabolic perturbations often precede reproductive complications in adolescent PCOS (448). Further, adult women with PCOS were reported to have hypertrophic adipocytes in SAT (472), increased insulin and decreased adiponectin levels, independent of obesity when compared with control women (489). In addition, women with PCOS are often overweight or obese, and were reported to have reduced PPT, which further correlated with insulin resistance. We now provide further evidence that ovine model

of PCOS mirrors metabolic complications of adolescent and adult women with PCOS, including increased insulin, decreased adiponectin and hepatic fat accumulation that precede obesity and reproductive problems in adolescents as well as obesity, decreased PPT and adipose tissue dysfunction in adulthood. Moreover, we deliver mechanistic understanding into the aforementioned metabolic pathophysiology of PCOS from puberty to adulthood and therefore, we believe that findings documented in this thesis can be extrapolated to our understanding of PCOS in human.

7.1 Future work

The studies demonstrated in this thesis investigated the effects of prenatal androgens on metabolism of adolescent and adult PCOS-like sheep. However, to fully understand and characterise an adult ovine model of PCOS further studies are required. Especially, a reproductive phenotype of those adult PCOS sheep should be studied, including ovarian morphology, but also hormonal profile. Although, we have undertaken a several attempts to measure androgens in those animals, these were unsuccessful, due to very low concentration of those hormones in adult ewes.

Further, to fully characterise metabolic profile in adolescent and adult sheep, a study of insulin signalling on protein and phosphorylation level should be carried, especially in muscle, liver and adipose tissue. In addition, performing a hyperinsulinemic-euglycemic clamp to assess overall insulin sensitivity in those animals would be highly recommended. Moreover, to fully understand consequences of perturbed adipogenesis, quantification a fat deposits in skeletal muscle should be performed. Preferably, morphological analysis of SAT and VAT should be also conducted in future. Finally, to fully understand impact of steroids on adipogenesis a peripheral steroid metabolism should be assessed, through analysis of gene and protein expression of steroidogenic enzymes in WAT.

Regarding postprandial thermogenesis study, a protein expression of brown/beige adipocyte markers in different adipose tissue depots should be validated by western blotting. In addition, an impact of muscle thermogenesis on overall energy expenditure should be assessed in our model. Finally, an effect of intranasal insulin administration on energy expenditure in adult control and PCOS-like animals should be studied.

Lastly, since a period of possible intervention has been established, this could be utilised to study an effect of potential treatments, FGF21 analogs and TZDs, on adolescent PCOS-like sheep and consequences of those treatments during puberty on adult PCOS-like phenotype.

References

1. Hossain A, Saunders GF. The human sex-determining gene SRY is a direct target of WT1. *J Biol Chem*. 2001;276(20):16817–16823.
2. Hacker A, Capel B, Goodfellow P, Lovell-Badge R. Expression of Sry, the mouse sex determining gene. *Development*. 1995;121(6):1603–1614.
3. Brennan J, Capel B. One tissue, two fates: molecular genetic events that underlie testis versus ovary development. *Nat Rev Genet*. 2004;5(7):509–521.
4. Koopman P, Gubbay J, Vivian N, Goodfellow P, Lovell-Badge R. Male development of chromosomally female mice transgenic for Sry. *Nature*. 1991;351(6322):117–121.
5. Hiort O. The differential role of androgens in early human sex development. *BMC Med*. 2013;11:152.
6. Sobel V, Zhu YS, Imperato-McGinley J. Fetal hormones and sexual differentiation. *Obstet Gynecol Clin North Am*. 2004;31(4):837–856.
7. Fujimoto T, Miyayama Y, Fuyuta M. The origin, migration and fine morphology of human primordial germ cells. *The Anatomical Record*. 1977;188(3):315–330.
8. Wylie CC. The biology of primordial germ cells. *Eur Urol*. 1993;23(1):62–66.
9. Satoh M. Histogenesis and organogenesis of the gonad in human embryos. *J Anat*. 1991;177:85–107.
10. Sarraj MA, Drummond AE. Mammalian foetal ovarian development: consequences for health and disease. *Reproduction*. 2012;143(2):151–163.
11. Skinner MK. Regulation of primordial follicle assembly and development. *Hum Reprod Update*. 2005;11(5):461–471.
12. McNatty KP, Fidler AE, Juengel JL, Quirke LD, Smith PR, Heath DA, et al. Growth and paracrine factors regulating follicular formation and cellular function. *Mol Cell Endocrinol*. 2000;163(1-2):11–30.
13. Meyts ER-D, Jørgensen N, Graem N, Müller J, Cate RL, Skakkebaek NE. Expression of anti-Müllerian hormone during normal and pathological gonadal development: association with differentiation of Sertoli and granulosa cells. *J Clin Endocrinol Metab*. 1999;84(10):3836–3844.
14. Capel B. The battle of the sexes. *Mechanisms of Development*. 2000;92(1):89–103.
15. Zachmann M, Tassinari D, Prader A. Clinical and biochemical variability of congenital adrenal hyperplasia due to 11 beta-hydroxylase deficiency. A study of 25 patients. *J Clin Endocrinol Metab*. 1983;56(2):222–229.

References

16. Khattab A, Haider S, Kumar A, Dhawan S, Alam D, Romero R, et al. Clinical, genetic, and structural basis of congenital adrenal hyperplasia due to 11 β -hydroxylase deficiency. *Proc Nat Acad Sci USA*. 2017;114(10):1933–1940.
17. Johnson MH, Everitt BJ. *Essential Reproduction*. 6th ed. Oxford: Blackwell Publishing; 2007.
18. Lehman MN, Coolen LM, Goodman RL. Minireview: kisspeptin/neurokinin B/dynorphin (KNDy) cells of the arcuate nucleus: a central node in the control of gonadotropin-releasing hormone secretion. *Endocrinology*. 2010;151(8):3479–3489.
19. Skorupskaite K, George JT, Anderson RA. The kisspeptin-GnRH pathway in human reproductive health and disease. *Hum Reprod Update*. 2014;20(4):485–500.
20. Skorupskaite K, George JT, Veldhuis JD, Millar RP, Anderson RA. Interactions between neurokinin B and kisspeptin in mediating estrogen feedback in healthy women. *J Clin Endocrinol Metab*. 2016;101(12):4628–4636.
21. Scaramuzzi RJ, Baird DT, Campbell BK, Driancourt MA, Dupont J, Fortune JE, et al. Regulation of folliculogenesis and the determination of ovulation rate in ruminants. *Reprod Fertil Dev*. 2011;23(3):444–467.
22. Baker TG. A Quantitive and cytological study of germ cells in human ovaries. *Proc R Soc Lond, B, Biol Sci*. 1963;158:417–433.
23. Maheshwari A, Fowler PA. Primordial follicular assembly in humans - revisited. *Zygote*. 2008;16(4):285–296.
24. McGee EA, Hsueh A. Initial and cyclic recruitment of ovarian follicles. *Endocrine Reviews*. 2000;21(2):200–214.
25. White YAR, Woods DC, Takai Y, Ishihara O, Seki H, Tilly JL. Oocyte formation by mitotically active germ cells purified from ovaries of reproductive-age women. *Nat Med*. 2012;18(3):413–421.
26. Johnson J, Canning J, Kaneko T, Pru JK, Tilly JL. Germline stem cells and follicular renewal in the postnatal mammalian ovary. *Nature*. 2004;428(6979):145–150.
27. Gougeon A. Dynamics of follicular growth in the human: a model from preliminary results. *Hum Reprod*. 1986;1(2):81–87.
28. McGee EA, Raj RS. Regulators of ovarian preantral follicle development. *Semin Reprod Med*. 2015;33(3):179–184.
29. Richards JS, Midgley AR. Protein hormone action: a key to understanding ovarian follicular and luteal cell development. *Biol Reprod*. 1976;14(1):82–94.
30. Hillier SG, Whitelaw PF, Smyth CD. Follicular oestrogen synthesis: the "two-cell, two-gonadotrophin" model revisited. *Mol Cell Endocrinol*. 1994;100(1-2):51–54.

References

31. Fortune JE, Armstrong DT. Androgen production by theca and granulosa isolated from proestrous rat follicles. *Endocrinology*. 1977;100(5):1341–1347.
32. Lux-Lantos V, Catalano PN, Desimone MF, Alvarez GS, Libertun C, Diaz LE, et al. Sol-gel immobilized ovarian follicles: Collaboration between two different cell types in hormone production and secretion. *Journal of Materials Chemistry*. 2012;22(23):11681–11687.
33. Ebling F. The neuroendocrine timing of puberty. *Reproduction*. 2005;129(6):675–683.
34. Frisch RE, McArthur JW. Menstrual cycles: Fatness as a determinant of minimum weight for height necessary for their maintenance or onset. *Science*. 1974;185(4155):949–951.
35. Frisch RE. Weight at menarche: similarity for well-nourished and undernourished girls at differing ages, and evidence for historical constancy. *Pediatrics*. 1972;50(3):445–450.
36. Clayton PE, Trueman JA. Leptin and puberty. *Arch Dis Child*. 2000;83(1):1-4.
37. Bakos O, Lundkvist O, Wide L, Bergh T. Ultrasonographical and hormonal description of the normal ovulatory menstrual cycle. *Acta Obstet Gynecol Scand*. 1994;73(10):790–796.
38. Mihm M, Gangooly S, Muttukrishna S. The normal menstrual cycle in women. *Anim Reprod Sci*. 2011;124(3):229–236.
39. Waller K, Swan SH, Windham GC, Fenster L, Elkin EP, Lasley BL. Use of urine biomarkers to evaluate menstrual function in healthy premenopausal women. *Am J Epidemiol*. 1998;147(11):1071–1080.
40. Miro F, Aspinall LJ. The onset of the initial rise in follicle-stimulating hormone during the human menstrual cycle. *Hum Reprod*. 2005;20(1):96–100.
41. Jamnongjit M, Hammes SR. Ovarian steroids: the good, the bad, and the signals that raise them. *Cell Cycle*. 2006;5(11):1178–1183.
42. Payne AH, Hales DB. Overview of steroidogenic enzymes in the pathway from cholesterol to active steroid hormones. *Endocrine Reviews*. 2004;25(6):947–970.
43. Burger HG. Androgen production in women. *Fertility and Sterility*. 2002;77:S3–5.
44. Enea C, Boisseau N, Diaz V, Dugué B. Biological factors and the determination of androgens in female subjects. *Steroids*. 2008;73(12):1203-1216.
45. Zumoff B, Strain GW, Miller LK. Twenty-four-hour mean plasma testosterone concentration declines with age in normal premenopausal women. *J Clin Endocrinol Metab*. 1995;80(4):1429-1430.
47. Abraham GE. Ovarian and adrenal contribution to peripheral androgens during the menstrual cycle. *J Clin Endocrinol Metab*. 1974;39(2):340–346.

References

46. Burger HG, Dudley EC, Cui J. A prospective longitudinal study of serum testosterone, dehydroepiandrosterone sulfate, and sex hormone-binding globulin levels through the menopause transition. *J Clin Endocrinol Metab.* 2000;85(8):2832-2838.
48. Labrie F, Van Luu-The, Labrie C, Bélanger A, Simard J, Lin S-X, et al. Endocrine and intracrine sources of androgens in women: inhibition of breast cancer and other roles of androgens and their precursor dehydroepiandrosterone. *Endocrine Reviews.* 2003;24(2):152–182.
49. Davison SL, Davis SR. Androgens in women. *J Steroid Biochem Mol Biol.* 2003;85(2-5):363-366.
50. Martel C, Melner MH, Gagné D, Simard J, Labrie F. Widespread tissue distribution of steroid sulfatase, 3 β -hydroxysteroid dehydrogenase/ Δ 5- Δ 4 isomerase (3 β -HSD), 17 β -HSD 5 α -reductase and aromatase activities in the rhesus monkey. *Mol Cell Endocrinol.* 1994;104:103–111.
51. Parker CR. Androgens throughout the life of women. In: Azziz R, Nestler JE, Dewailly D, editors. *Androgen excess disorders in women. Polycystic ovary syndrome and other disorders.* Human Press; 2006. pp. 35–47.
52. Goodman RL, Inskoop EK. Control of the ovarian cycle of the sheep. In: Plant T, Zeleznik A, editors. *Knobil and Neill's Physiology of Reproduction.* 2015. pp. 1259–1305.
53. Convey E, Hansel W. Physiology of the estrous cycle. *J Anim Sci.* 1983;57(4):404–424.
54. Evans AC. Ovarian follicle growth and consequences for fertility in sheep. *Anim Reprod Sci.* 2003;78(3):289–306.
55. McHugh N, Berry DP, Pabiou T. Risk factors associated with lambing traits. *Animal.* 2015;10(1):89–95.
56. Gardner DS, Buttery PJ, Daniel Z, Symonds ME. Factors affecting birth weight in sheep: maternal environment. *Reproduction.* 2007;133(1):297–307.
57. Foster DL, Hileman SM. Puberty in the Sheep. In: Plant T, Zeleznik A, editors. *Knobil and Neill's Physiology of Reproduction.* 2014. pp. 1441–1485.
58. Morrison CD, Wood R, McFadin EL, Whitley NC, Keisler DH. Effect of intravenous infusion of recombinant ovine leptin on feed intake and serum concentrations of GH, LH, insulin, IGF-1, cortisol, and thyroxine in growing prepubertal ewe lambs. *Domestic Animal Endocrinology.* 2002;22(2):103–112.
59. Morrison CD, Daniel JA, Holmberg BJ, Djiane J, Raver N, Gertler A, et al. Central infusion of leptin into well-fed and undernourished ewe lambs: effects on feed intake and serum concentrations of growth hormone and luteinizing hormone. *J Endocrinol.* 2001;168(2):317–324.

References

60. Shen W, Wang Z, Punyanita M, Lei J, Sinav A, Kral JG, et al. Adipose tissue quantification by imaging methods: a proposed classification. *Obes Res.* 2003;11(1):5–16.
61. Kershaw EE, Flier JS. Adipose tissue as an endocrine organ. *JCEM.* 2004;89(6):2548-2556.
62. Lee M-J, Wu Y, Fried SK. Adipose tissue heterogeneity: Implication of depot differences in adipose tissue for obesity complications. *Mol Aspects Med.* 2013;34(1):1–11.
63. Bloor I, Symonds M. Sexual dimorphism in white and brown adipose tissue with obesity and inflammation. *Horm Behav.* 2014;66(1):95–103.
64. Tchkonina T, Tchoukalova YD, Giorgadze N, Pirtskhalava T, Karagiannides I, Forse RA, et al. Abundance of two human preadipocyte subtypes with distinct capacities for replication, adipogenesis, and apoptosis varies among fat depots. *Am J Physiol Endocrinol Metab.* 2004;288(1):E267–277.
65. Poissonnet CM, Burdi AR, Bookstein FL. Growth and development of human adipose tissue during early gestation. *Early Hum Dev.* 1983;8(1):1–11.
66. Wensvoort P. The development of adipose tissue in sheep fetuses. *Pathologia Veterinaria.* 1967;4(1):69–78.
67. Koh GY, Kim H, Han J, Chang SI, Shibuya M, Oh N, et al. The spatiotemporal development of adipose tissue. *Development.* 2011;138(22):5027-5037.
68. Rosen ED, Spiegelman BM. What we talk about when we talk about fat. *Cell.* 2014;156(1-2):20–44.
69. Karagiannides I, Tchkonina T, Dobson DE, Steppan CM, Cummins P, Chan G, et al. Altered expression of C/EBP family members results in decreased adipogenesis with aging. *Am J Physiol Regul Integr Comp Physiol.* 2001;280(6):1772–1780.
70. Tchkonina T, Morbeck DE, Zglinicki von T, van Deursen J, Lustgarten J, Scrbale H, et al. Fat tissue, aging, and cellular senescence. *Aging Cell.* 2010;9(5):667–684.
71. Schipper BM, Marra KG, Zhang W, Donnenberg AD, Rubin JP. Regional anatomic and age effects on cell function of human adipose-derived stem cells. *Ann Plast Surg.* 2008;60(5):538–544.
72. Slawik M, Vidal-Puig AJ. Lipotoxicity, overnutrition and energy metabolism in aging. *Ageing Res Rev.* 2006;5(2):144–164.
73. Vázquez-Vela MEF, Torres N, Tovar AR. White adipose tissue as endocrine organ and its role in obesity. *Arch Med Res.* 2008;39(8):715–728.
74. Dubois SG, Heilbronn LK, Smith SR, Albu JB, Kelley DE, Ravussin E. Decreased expression of adipogenic genes in obese subjects with type 2 diabetes. *Obesity.* 2006;14(9):1543–1552.

References

75. Lafontan M, Sengenès C, Galitzky J. Recent developments on lipolysis regulation in humans and discovery of a new lipolytic pathway. *Int J Obesity*. 2000;24:47–52.
76. Zhang Y, Proença R, Maffei M, Barone M, Leopold L, Friedman JM. Positional cloning of the mouse obese gene and its human homologue. *Nature*. 1994;372(6521):425–432.
77. Kelesidis T, Kelesidis I, Chou S, Mantzoros CS. Narrative review: the role of leptin in human physiology: emerging clinical applications. *Ann Intern Med*. 2010;152(2):93–100.
78. Considine RV, Sinha MK, Heiman ML, Kriauciunas A, Stephens TW, Nyce MR, et al. Serum immunoreactive-leptin concentrations in normal-weight and obese humans. *N Engl J Med*. 1996;334(5):292–295.
79. Boden G, Chen X, Mozzoli M, Ryan I. Effect of fasting on serum leptin in normal human subjects. *J Clin Endocrinol Metab*. 1996;81(9):3419–3423.
80. Haynes WG, Morgan DA, Walsh SA, Mark AL, Sivitz WI. Receptor-mediated regional sympathetic nerve activation by leptin. *J Clin Invest*. 1997;100(2):270–278.
81. Scarpace PJ, Matheny M, Pollock BH, Tümer N. Leptin increases uncoupling protein expression and energy expenditure. *Endocrinology*. 1997;273(1):226–230.
82. Welt CK, Chan JL, Bullen J, Murphy R, Smith P, DePaoli AM, et al. Recombinant human leptin in women with hypothalamic amenorrhea. *N Engl J Med*. 2004;351(10):987–997.
83. Vázquez MJ, Romero-Ruiz A, Tena-Sempere M. Roles of leptin in reproduction, pregnancy and polycystic ovary syndrome: Consensus knowledge and recent developments. *Metabolism*. 2015;64(1):79–91.
84. Kendall NR, Gutierrez CG, Scaramuzzi RJ, Baird DT, Webb R, Campbell BK. Direct in vivo effects of leptin on ovarian steroidogenesis in sheep. *Reproduction*. 2004;128(6):757–765.
85. Ghizzoni L, Barreca A, Mastorakos G, Furlini M, Vottero A, Ferrari B, et al. Leptin inhibits steroid biosynthesis by human granulosa-lutein cells. *Horm Metab Res*. 2003;33(6):323–328.
86. Duggal PS, Van Der Hoek KH, Milner CR, Ryan NK, Armstrong DT, Magoffin DA, et al. The in vivo and in vitro effects of exogenous leptin on ovulation in the rat. *Endocrinology*. 2000;141(6):1971–1976.
87. Margetic S, Gazzola C, Pegg GG, Hill RA. Leptin: a review of its peripheral actions and interactions. *Int J Obes*. 2002;26(11):1407–1433.
88. Bates SH, Stearns WH, Dundon TA, Schubert M, Tso AWK, Wang Y, et al. STAT3 signalling is required for leptin regulation of energy balance but not reproduction. *Nature*. 2003;421(6925):856–859.

References

89. Niswender KD, Morton GJ, Stearns WH, Rhodes CJ, Myers MG, Schwartz MW. Intracellular signalling. Key enzyme in leptin-induced anorexia. *Nature*. 2001;413(6858):794–795.
90. Strobel A, Issad T, Camoin L, Ozata M, Strosberg AD. A leptin missense mutation associated with hypogonadism and morbid obesity. *Nature*. 1998;18(3):213–215.
91. Farooqi IS, Wangensteen T, Collins S, Kimber W, Matarese G, Keogh JM, et al. Clinical and molecular genetic spectrum of congenital deficiency of the leptin receptor. *N Engl J Med*. 2007;356(3):237–247.
92. Farooqi IS, Bullmore E, Keogh J, Gillard J, O’Rahilly S, Fletcher PC. Leptin regulates striatal regions and human eating behavior. *Science*. 2007;317(5843):1355–1358.
93. Farooqi IS, Jebb SA, Langmack G. Effects of recombinant leptin therapy in a child with congenital leptin deficiency. *N Engl J Med*. 1999;341(12):879–884.
94. Javor ED, Cochran EK, Musso C, Young JR, DePaoli AM, Gorden P. Long-term efficacy of leptin replacement in patients with generalized lipodystrophy. *Diabetes*. 2005;54(7):1994–2002.
95. Petersen KF, Oral EA, Dufour S, Befroy D, Ariyan C, Yu C, et al. Leptin reverses insulin resistance and hepatic steatosis in patients with severe lipodystrophy. *J Clin Invest*. 2002;109(10):1345–1350.
96. Musso C, Cochran E, Javor E, Young J, DePaoli AM, Gorden P. The long-term effect of recombinant methionyl human leptin therapy on hyperandrogenism and menstrual function in female and pituitary function in male and female hypoleptinemic lipodystrophic patients. *Metabolism*. 2005;54(2):255–263.
97. Myers MG, Cowley MA, Muenzberg H. Mechanisms of leptin action and leptin resistance. *Annu Rev Physiol*. 2008;70(1):537–556.
98. Scherer PE, Williams S, Fogliano M, Baldini G, Lodish HF. A novel serum protein similar to C1q, produced exclusively in adipocytes. *J Biol Chem*. 1995;270(45):26746–26749.
99. Yamauchi T, Kadowaki T. Physiological and pathophysiological roles of adiponectin and adiponectin receptors in the integrated regulation of metabolic and cardiovascular diseases. *Int J Obes*. 2009;32:13–18.
100. Yamauchi T, Iwabu M, Okada-Iwabu M, Kadowaki T. Adiponectin receptors: A review of their structure, function and how they work. *Best Pract Res Clin Endocrinol Metab*. 2014;28(1):15–23.
101. Arita Y, Kihara S, Ouchi N, Takahashi M, Maeda K, Miyagawa J, et al. Paradoxical decrease of an adipose-specific protein, adiponectin, in obesity. *Biochem Biophys Res Commun*. 1999;257(1):79–83.
102. Hu E, Liang P, Spiegelman BM. AdipoQ is a novel adipose-specific gene dysregulated in obesity. *J Biol Chem*. 1996;271(18):10697–10703.

References

103. Tomas E, Tsao TS, Saha AK, Murrey HE, Zhang CC, Itani SI, et al. Enhanced muscle fat oxidation and glucose transport by ACRP30 globular domain: acetyl-CoA carboxylase inhibition and AMP-activated protein kinase activation. *Proc Natl Acad Sci USA*. 2002;99(25):16309–16313.
104. Fruebis J, Tsao TS, Javorschi S, Ebbets-Reed D, Erickson MR, Yen FT, et al. Proteolytic cleavage product of 30-kDa adipocyte complement-related protein increases fatty acid oxidation in muscle and causes weight loss in mice. *Proc Natl Acad Sci USA*. 2001;98(4):2005–2010.
105. Yamauchi T, Kamon J, Waki H, Terauchi Y, Kubota N, Hara K, et al. The fat-derived hormone adiponectin reverses insulin resistance associated with both lipoatrophy and obesity. *Nat Med*. 2001;7(8):941–946.
106. Combs TP, Berg AH, Obici S, Scherer PE, Rossetti L. Endogenous glucose production is inhibited by the adipose-derived protein Acrp30. *J Clin Invest*. 2001;108(12):1875–1881.
107. Wu X, Motoshima H, Mahadev K, Stalker TJ, Scalia R, Goldstein BJ. Involvement of AMP-activated protein kinase in glucose uptake stimulated by the globular domain of adiponectin in primary rat adipocytes. *Diabetes*. 2003;52(6):1355–1363.
108. Yamauchi T, Kamon J, Minokoshi Y, Ito Y, Waki H, Uchida S, et al. Adiponectin stimulates glucose utilization and fatty-acid oxidation by activating AMP-activated protein kinase. *Nat Med*. 2002;8(11):1288–1295.
109. Hug C, Lodish HF. The role of the adipocyte hormone adiponectin in cardiovascular disease. *Curr Opin Pharmacol*. 2005;5(2):129–134.
110. Wen J-P, Lv W-S, Yang J, Nie A-F, Cheng X-B, Yang Y, et al. Globular adiponectin inhibits GnRH secretion from GT1-7 hypothalamic GnRH neurons by induction of hyperpolarization of membrane potential. *Biochem Biophys Res Commun*. 2008;371(4):756–761.
111. Psilopanagioti A, Papadaki H, Kranioti EF, Alexandrides TK, Varakis JN. Expression of adiponectin and adiponectin receptors in human pituitary gland and brain. *Neuroendocrinology*. 2008;89(1):38–47.
112. Lu M, Tang Q, Olefsky JM, Mellon PL. Adiponectin activates adenosine monophosphate-activated protein kinase and decreases luteinizing hormone secretion in LβT2 gonadotropes. *Mol Endocrinol*. 2008;22(3):760–771.
113. Ledoux S, Campos DB, Lopes FL, Dobias-Goff M, Palin M-F, Murphy BD. Adiponectin induces periovulatory changes in ovarian follicular cells. *Endocrinology*. 2006;147(11):5178–5186.
114. Campos DB, Palin M-F, Bordignon V, Murphy BD. The “beneficial” adipokines in reproduction and fertility. *Int J Obes*. 2007;32(2):223–231.
115. Xu A, Chan KW, Hoo RLC, Wang Y, Tan KCB, Zhang J, et al. Testosterone selectively reduces the high molecular weight form of adiponectin by inhibiting its secretion from adipocytes. *J Biol Chem*. 2005;280(18):18073–18080.

References

116. Michalakis KG, Segars JH. The role of adiponectin in reproduction: from polycystic ovary syndrome to assisted reproduction. *Fertil Steril*. 2010;94(6):1949–1957.
117. Tchkonina T, Thomou T, Zhu Y, Karagiannides I, Pothoulakis C, Jensen MD, et al. Mechanisms and metabolic implications of regional differences among fat depots. *Cell Metabolism*. 2013;17(5):644–656.
118. Macotela Y, Emanuelli B, Mori MA, Gesta S. Intrinsic differences in adipocyte precursor cells from different white fat depots. *Diabetes*. 2012;61(7):1691–1699.
119. Tran TT, Kahn CR. Transplantation of adipose tissue and stem cells: role in metabolism and disease. *Nat Rev Endocrinol*. 2010;6(4):195–213.
120. Ibrahim MM. Subcutaneous and visceral adipose tissue: structural and functional differences. *Obesity Reviews*. 2010;11(1):11–18.
121. Weisberg SP, McCann D, Desai M, Rosenbaum M, Leibel RL, Ferrante AW Jr. Obesity is associated with macrophage accumulation in adipose tissue. *J Clin Invest*. 2003;112(12):1796–1808.
122. Bruun JM, Lihn AS, Pedersen SB, Richelsen B. Monocyte chemoattractant protein-1 release is higher in visceral than subcutaneous human adipose tissue (AT): implication of macrophages resident in the AT. *J Clin Endocrinol Metab*. 2005;90(4):2282–2289.
123. Misra A, Vikram NK. Clinical and pathophysiological consequences of abdominal adiposity and abdominal adipose tissue depots. *Nutrition*. 2003;19(5):457–466.
124. Smith SR, Lovejoy JC, Greenway F, Ryan D, deJonge L, la Bretonne de J, et al. Contributions of total body fat, abdominal subcutaneous adipose tissue compartments, and visceral adipose tissue to the metabolic complications of obesity. *Metabolism*. 2001;50(4):425–435.
125. Krotkiewski M, Björntorp P, Sjöström L. Impact of obesity on metabolism in men and women. Importance of regional adipose tissue distribution. *J Clin Invest*. 1983;72(3):1150–1162.
126. Salans LB, Horton ES, Sims EA. Experimental obesity in man: cellular character of the adipose tissue. *J Clin Invest*. 1971;50(5):1005–1011.
127. Tchoukalova YD, Votruba SB, Tchkonina T, Giorgadze N, Kirkland JL, Jensen MD. Regional differences in cellular mechanisms of adipose tissue gain with overfeeding. *Proc Natl Acad Sci USA*. 2010;107(42):18226–18231.
128. Björntorp P, Carlgren G, Isaksson B, Krotkiewski M, Larsson B, Sjöström L. Effect of an energy-reduced dietary regimen in relation to adipose tissue cellularity in obese women. *Am J Clin Nutr*. 1975;28(5):445–452.
129. Krishnan J, Danzer C, Simka T, Ukropec J, Walter KM, Kumpf S, et al. Dietary obesity-associated Hif1 α activation in adipocytes restricts fatty acid oxidation and energy expenditure via suppression of the Sirt2-NAD⁺ system. *Genes Dev*. 2012;26(3):259–270.

References

130. Neels JG, Olefsky JM. Inflamed fat: what starts the fire? *J Clin Invest.* 2006;116(1):33–35.
131. Gaelic S, Oakhill JS, Steinberg GR. Adipose tissue as an endocrine organ. *Mol Cell Endocrinol.* 2009;316(2):129–139.
132. Choe SS, Huh JY, Hwang IJ, Kim JI, Kim JB. Adipose tissue remodeling: its role in energy metabolism and metabolic disorders. *Front Endocrinol.* 2016;7:1–16.
133. Lee Y-H, Jung Y-S, Choi D. Recent advance in brown adipose physiology and its therapeutic potential. *Exp Mol Med.* 2014;46:78.
134. Nedergaard J, Bengtsson T, Cannon B. Unexpected evidence for active brown adipose tissue in adult humans. *Am J Physiol Endocrinol Metab.* 2007;293(2):444–452.
135. Villarroya J, Cereijo R, Villarroya F. An endocrine role for brown adipose tissue? *Am J Physiol Endocrinol Metab.* 2013;305(5):567–572.
136. Vijgen G, van Marken Lichtenbelt W. Brown adipose tissue: clinical impact of a re-discovered thermogenic organ. *Frontiers in Bioscience.* 2013;5(3):823–833.
137. Lee YH, Mottillo EP, Granneman JG. Adipose tissue plasticity from WAT to BAT and in between. *Biochim Biophys Acta.* 2014;1842(3):358–369.
138. Vegiopoulos A, Muller-Decker K, Strzoda D, Schmitt I, Chichelnitskiy E, Ostertag A, et al. Cyclooxygenase-2 controls energy homeostasis in mice by de novo recruitment of brown adipocytes. *Science.* 2010;328(5982):1158–1161.
139. Peirce V, Carobbio S, Vidal-Puig A. The different shades of fat. *Nature.* 2014;510(7503):76–83.
140. Blouin K, Veilleux A, Van Luu-The, Tchernof A. Androgen metabolism in adipose tissue: recent advances. *Mol Cell Endocrinol.* 2008;301(1-2):97–103.
141. Després JP, Moorjani S, Lupien PJ, Tremblay A, Nadeau A, Bouchard C. Regional distribution of body fat, plasma lipoproteins, and cardiovascular disease. *Arteriosclerosis.* 1990;10:497–511.
142. Blouin K, Boivin A, Tchernof A. Androgens and body fat distribution. *J Steroid Biochem Mol Biol.* 2007;108(3-5):272–280.
143. Haffner SM, Karhapää P, Mykkänen L, Laakso M. Insulin resistance, body fat distribution, and sex hormones in men. *Diabetes.* 1994;43(2):212–219.
144. Gooren LJG, Giltay EJ. Review of studies of androgen treatment of female-to-male transsexuals: effects and risks of administration of androgens to females. *J Sex Med.* 2008;5(4):765–776.
145. Horejsi R, Moller R, Rackl S, Giuliani A. Android subcutaneous adipose tissue topography in lean and obese women suffering from PCOS: comparison with type 2 diabetic women. *Am J Phys Anthropol.* 2004;124(3):275–281.

References

146. Pfannenbergh C, Werner MK, Ripkens S, Stef I, Deckert A, Schmadl M, et al. Impact of age on the relationships of brown adipose tissue with sex and adiposity in humans. *Diabetes*. 2010;59(7):1789–1793.
147. Cypess AM, Lehman S, Williams G, Tal I, Rodman D, Goldfine AB, et al. Identification and importance of brown adipose tissue in adult humans. *N Engl J Med*. 2009;360(15):1509–1517.
148. Hoene M, Li J, Häring H-U, Weigert C, Xu G, Lehmann R. The lipid profile of brown adipose tissue is sex-specific in mice. *Biochim Biophys Acta*. 2014;1841(10):1563-1570.
149. Rodriguez-Cuenca S, Pujol E, Justo R, Frontera M, Oliver J, Gianotti M, et al. Sex-dependent thermogenesis, differences in mitochondrial morphology and function, and adrenergic response in brown adipose tissue. *J Biol Chem*. 2002;277(45):42958–42963.
150. Kim S-N, Jung Y-S, Kwon H-J, Seong JK, Granneman JG, Lee Y-H. Sex differences in sympathetic innervation and browning of white adipose tissue of mice. *Biol Sex Differ*. 2016;7:67.
151. Valle A, Català-Niell A, Colom B, García-Palmer FJ, Oliver J, Roca P. Sex-related differences in energy balance in response to caloric restriction. *AJP: Endocrinol Metab*. 2005;289(1):15–22.
152. Stein IF, Leventhal ML. Amenorrhea associated with bilateral polycystic ovaries. *Am J Obstet Gynecol*. 1935;29(2):181–191.
153. Azziz R, Adashi EY. Stein and Leventhal: 80 years on. *Am J Obstet Gynecol*. 2015;214(2):247–247.
154. Rotterdam ESHRE/ASRM-sponsored PCOS consensus workshop group. Revised 2003 consensus on diagnostic criteria and long-term health risks related to polycystic ovary syndrome (PCOS). *Hum Reprod*. 2004;19(1):41–47.
155. Azziz R, Carmina E, Dewailly D, Diamanti-Kandarakis E, Escobar-Morreale HF, Futterweit W, et al. Criteria for defining polycystic ovary syndrome as a predominantly hyperandrogenic syndrome: An Androgen Excess Society guideline. *J Clin Endocrinol Metab*. 2006;91(11):4237–4245.
156. Polson DW, Adams J, Wadsworth J, Franks S. Polycystic ovaries - a common finding in normal women. *The Lancet*. 1988;1(8590):870–872.
157. Balen AH, Conway GS, Kaltsas G, Techatrasak K, Manning PJ, West C, et al. Polycystic ovary syndrome: the spectrum of the disorder in 1741 patients. *Hum Reprod*. 1995;10(8):2107–2111.
158. Azziz R, Sanchez LA, Knochenhauer ES, Moran C, Lazenby J, Stephens KC, et al. Androgen excess in women: experience with over 1000 consecutive patients. *J Clin Endocrinol Metab*. 2004;89(2):453–462.

References

159. Afifi L, Saeed L, Pasch LA, Huddleston HG, Cedars MI, Zane LT, et al. Association of ethnicity, Fitzpatrick skin type, and hirsutism: A retrospective cross-sectional study of women with polycystic ovarian syndrome. *Int J Womens Dermatol*. 2017;3(1):37-43.
160. Fauser BCJM, Tarlatzis BC, Rebar RW, Legro RS, Balen AH, Lobo R, et al. Consensus on women's health aspects of polycystic ovary syndrome (PCOS): the Amsterdam ESHRE/ASRM-Sponsored 3rd PCOS Consensus Workshop Group. *Fertility and Sterility*. 2011;97(1):28–38.
161. Quinn M, Pasch L, Shinkai K, Kuzmich L, Cedars M, Huddleston H. Prevalence of androgenic alopecia (AGA) in patients with polycystic ovarian syndrome (PCOS) and characterization of associated clinical and biochemical features. *Fertility and Sterility*. 2014;101(4):1129-1134.
162. Timpatanapong P, Rojanasakul A. Hormonal profiles and prevalence of polycystic ovary syndrome in women with acne. *J Dermatol*. 1997;24(4):223–229.
163. Balen A. The pathophysiology of polycystic ovary syndrome: trying to understand PCOS and its endocrinology. *Best PractRes Clin Obstet Gynaecol*. 2004;18(5):685–706.
164. van Santbrink EJ, Hop WC, Fauser BC. Classification of normogonadotropic infertility: polycystic ovaries diagnosed by ultrasound versus endocrine characteristics of polycystic ovary syndrome. *Fertility and Sterility*. 1997;67(3):452–458.
165. Teede H, Deeks A, Moran L. Polycystic ovary syndrome: a complex condition with psychological, reproductive and metabolic manifestations that impacts on health across the lifespan. *BMC Med*. 2010;8:41.
166. Zawadzki JK, Dunaif A. Diagnostic criteria for polycystic ovary syndrome: towards a rational approach. In: Dunaif A, Givens JR, Haseltine FP, Merriam GR, editors. *Polycystic ovary syndrome*. Boston: Blackwell Scientific Publications; 1992. pp. 377–84.
167. Lizneva D, Suturina L, Walker W, Brakta S, Gavrilova-Jordan L, Azziz R. Criteria, prevalence, and phenotypes of polycystic ovary syndrome. *Fertility and Sterility*. 2016;106(1):6–15.
168. Clark NM, Podolski AJ, Brooks ED, Chizen DR, Pierson RA, Lehotay DC, et al. Prevalence of polycystic ovary syndrome phenotypes using updated criteria for polycystic ovarian morphology: an assessment of over 100 consecutive women self-reporting features of polycystic ovary syndrome. *Reproductive Sciences*. 2014;21(8):1034–1043.
169. Lizneva D, Kirubakaran R, Mykhalchenko K, Suturina L, Chernukha G, Diamond MP, et al. Phenotypes and body mass in women with polycystic ovary syndrome identified in referral versus unselected populations: systematic review and meta-analysis. *Fertility and Sterility*. 2016;106(6):1510–1520.

References

170. Johnson T, Kaplan L, Ouyang P, Rizza R. National Institutes of Health. Evidence-based methodology workshop on polycystic ovary syndrome (PCOS). <https://prevention.nih.gov/docs/programs/pcos/FinalReport.pdf>. 2012.
171. Azziz R, Carmina E, Dewailly D, Diamanti-Kandarakis E, Escobar-Morreale HF, Futterweit W, et al. The Androgen Excess and PCOS Society criteria for the polycystic ovary syndrome: the complete task force report. *Fertility and Sterility*. 2008;91(2):456–488.
172. Elting MW, Korsen TJ, Rekers-Mombarg LT, Schoemaker J. Women with polycystic ovary syndrome gain regular menstrual cycles when ageing. *Hum Reprod*. 1999;15(1):24–28.
173. Alsamarai S, Adams JM, Murphy MK, Post MD, Hayden DL, Hall JE, et al. Criteria for polycystic ovarian morphology in polycystic ovary syndrome as a function of age. *J Clin Endocrinol Metab*. 2009;94(12):4961–4970.
174. Elting MW, Kwee J, Korsen TJM, Rekers-Mombarg LTM, Schoemaker J. Aging women with polycystic ovary syndrome who achieve regular menstrual cycles have a smaller follicle cohort than those who continue to have irregular cycles. *Fertility and Sterility*. 2003;79(5):1154–1560.
175. Pinola P, Piltonen TT, Puurunen J, Vanky E, Sundstrom-Poromaa I, Stener-Victorin E, et al. Androgen profile through life in women with polycystic ovary syndrome: A Nordic Multicenter Collaboration Study. *J Clin Endocrinol Metab*. 2015;100(9):3400–407.
176. Blank SK, Helm KD, McCartney CR, Marshall JC. Polycystic ovary syndrome in adolescence. *Ann N Y Acad Sci*. 2008;1135(1):76–84.
177. Codner E, Villarroel C, Eyzaguirre FC, López P, Merino PM, Pérez-Bravo F, et al. Polycystic ovarian morphology in postmenarchal adolescents. *Fertility and Sterility*. 2011;95(2):702–706.
178. Rosenfield RL. Identifying children at risk for polycystic ovary syndrome. *J Clin Endocrinol Metab*. 2007;92(3):787–796.
179. Lazar L, Kauli R, Bruchis C, Nordenberg J, Galatzer A, Pertzalan A. Early polycystic ovary-like syndrome in girls with central precocious puberty and exaggerated adrenal response. *Eur J Endocrinol*. 1995;133(4):403–406.
180. Ibáñez L, Potau N, Virdis R, Zampolli M, Terzi C, Gussinye M, et al. Postpubertal outcome in girls diagnosed of premature pubarche during childhood: increased frequency of functional ovarian hyperandrogenism. *J Clin Endocrinol Metab*. 1993;76(6):1599–1603.
181. King M, Dorosz J, Patel SS, Kinney GL, Cree-Green M, Wang H, et al. Obese adolescents with polycystic ovarian syndrome have elevated cardiovascular disease risk markers. *Vascular Medicine*. 2017;22(2):85–95.
182. Bozdag G, Mumusoglu S, Zengin D, Karabulut E, Yildiz BO. The prevalence and phenotypic features of polycystic ovary syndrome: a systematic review and meta-analysis. *Hum Reprod*. 2016;31(12):2841–2855.

References

183. Hickey M, Doherty DA, Atkinson H, Sloboda DM, Franks S, Norman RJ, et al. Clinical, ultrasound and biochemical features of polycystic ovary syndrome in adolescents: implications for diagnosis. *Hum Reprod.* 2011;26(6):1469–1477.
184. Hashemipour M, Faghihimani S, Zolfaghary B, Hovsepian S, Ahmadi F, Haghighi S. Prevalence of polycystic ovary syndrome in girls aged 14-18 years in Isfahan, Iran. *Horm Res Paediatr.* 2004;62(6):278–282.
185. Christensen SB, Black MH, Smith N, Martinez MM, Jacobsen SJ, Porter AH, et al. Prevalence of polycystic ovary syndrome in adolescents. *Fertility and Sterility.* 2013;100(2):470–477.
186. Lo JC, Feigenbaum SL, Yang JR, Pressman AR, Selby JV, Go AS. Epidemiology and adverse cardiovascular risk profile of diagnosed polycystic ovary syndrome. *J Clin Endocrinol Metab.* 2006;91(4):1357–1363.
187. Azziz R, Marin C, Hoq L, Badamgarav E, Song P. Health care-related economic burden of the polycystic ovary syndrome during the reproductive life span. *J Clin Endocrinol Metab.* 2005;90(8):4650–4658.
188. Wilcox G. Insulin and insulin resistance. *Clin Biochem Rev.* 2005;26:19–39.
189. Cassar S, Misso ML, Hopkins WG, Shaw CS, Teede HJ, Stepto NK. Insulin resistance in polycystic ovary syndrome: a systematic review and meta-analysis of euglycaemic-hyperinsulinaemic clamp studies. *Hum Reprod.* 2016;31(11):2619–31.
190. Legro RS, Castracane VD, Kauffman RP. Detecting insulin resistance in polycystic ovary syndrome: purposes and pitfalls. *Obstet Gynecol Surv.* 2004;59(2):141–54.
191. Stepto NK, Cassar S, Joham AE, Hutchison SK, Harrison CL, Goldstein RF, et al. Women with polycystic ovary syndrome have intrinsic insulin resistance on euglycaemic-hyperinsulinaemic clamp. *Hum Reprod.* 2013;28(3):777–784.
192. Vrbikova J, Bendlova B, Hill M, Vankova M, Vondra K, Starka L. Insulin sensitivity and beta-cell function in women with polycystic ovary syndrome. *Diabetes Care.* 2002;25(7):1217–1222.
193. Ciampelli M, Fulghesu AM, Murgia F, Guido M, Cucinelli F, Apa R, et al. Acute insulin response to intravenous glucagon in polycystic ovary syndrome. *Hum Reprod.* 1998;13(4):847–851.
194. Holte J, Bergh T, Berne C, Wide L, Lithell H. Restored insulin sensitivity but persistently increased early insulin secretion after weight loss in obese women with polycystic ovary syndrome. *J Clin Endocrinol Metab.* 1995;80(9):2586–2593.
195. O'Meara NM, Blackman JD, Ehrmann DA, Barnes RB, Jaspan JB, Rosenfield RL, et al. Defects in beta-cell function in functional ovarian hyperandrogenism. *J Clin Endocrinol Metab.* 1993;76(5):1241–1247.
196. Nolan CJ, Damm P, Prentki M. Type 2 diabetes across generations: From pathophysiology to prevention and management. *The Lancet.* 2011;378(9786):169–181.

References

197. Ehrmann DA, Barnes RB, Rosenfield RL, Cavaghan MK, Imperial J. Prevalence of impaired glucose tolerance and diabetes in women with polycystic ovary syndrome. *Obstet Gynecol.* 1999;22(1):141–146.
198. Norman RJ, Masters L, Milner CR, Wang JX, Davies MJ. Relative risk of conversion from normoglycaemia to impaired glucose tolerance or non-insulin dependent diabetes mellitus in polycystic ovarian syndrome. *Hum Reprod.* 2001;16(9):1995–1998.
199. Alberti KGMM, Zimmet P, Shaw J. International Diabetes Federation: a consensus on type 2 diabetes prevention. *Diabet Med.* 2007;24(5):451–463.
200. Legro RS. Type 2 diabetes and polycystic ovary syndrome. *Fertility and Sterility.* 2006;86:16–17.
201. Boomsma CM, Eijkemans MJC, Hughes EG, Visser GHA, Fauser BCJM, Macklon NS. A meta-analysis of pregnancy outcomes in women with polycystic ovary syndrome. *Hum Reprod Update.* 2006;12(6):673–683.
202. Ashrafi M, Sheikhan F, Arabipour A, Hosseini R, Nourbakhsh F, Zolfaghari Z. Gestational diabetes mellitus risk factors in women with polycystic ovary syndrome (PCOS). *Eur J Obstet Gynecol Reprod Biol.* 2014;181:195-199.
203. de Wilde MA, Veltman-Verhulst SM, Goverde AJ, Lambalk CB, Laven JSE, Franx A, et al. Preconception predictors of gestational diabetes: a multicentre prospective cohort study on the predominant complication of pregnancy in polycystic ovary syndrome. *Hum Reprod.* 2014;29(6):1327–1336.
204. Minoee S, Tehrani FR, Rahmati M, Mansournia MA, Azizi F. Diabetes incidence and influencing factors in women with and without gestational diabetes mellitus: A 15 year population-based follow-up cohort study. *Diabetes Res Clin Pract.* 2017;128:24–31.
205. Metzger BE, Buchanan TA, Coustan DR. Summary and recommendations of the fifth international workshop-conference on gestational diabetes mellitus. *Diabetes Care.* 2007;30:251.
206. Noctor E, Dunne FP. Type 2 diabetes after gestational diabetes: The influence of changing diagnostic criteria. *WJD.* 2015;6(2):234–244.
207. Barber TM, McCarthy MI, Wass JAH, Franks S. Obesity and polycystic ovary syndrome. *Clin Endocrinol.* 2006;65(2):137–145.
208. Yildiz BO, Knochenhauer ES, Azziz R. Impact of obesity on the risk for polycystic ovary syndrome. *J Clin Endocrinol Metab.* 2008;93(1):162–168.
209. Alvarez-Blasco F, Botella-Carretero JI, Millán JLS, Escobar-Morreale HF. Prevalence and characteristics of the polycystic ovary syndrome in overweight and obese women. *Obstet Gynecol.* 2006;166(19):2081–2086.
210. Hoeger KM, Oberfield SE. Do women with PCOS have a unique predisposition to obesity? *Fertility and Sterility.* 2011;97(1):13–17.

References

211. Georgopoulos NA, Saltamavros AD, Vervita V, Karkoulas K, Adonakis G, Decavalas G, et al. Basal metabolic rate is decreased in women with polycystic ovary syndrome and biochemical hyperandrogenemia and is associated with insulin resistance. *Fertility and Sterility*. 2009;92(1):250–255.
212. Robinson S, Chan SP, Spacey S, Anyaoku V, Johnston DG, Franks S. Postprandial thermogenesis is reduced in polycystic ovary syndrome and is associated with increased insulin resistance. *Clinical Endocrinology*. 1992;36(6):537–543.
213. Pasquali R, Gambineri A, Pagotto U. The impact of obesity on reproduction in women with polycystic ovary syndrome. *BJOG*. 2006;113(10):1148–1159.
214. Rytka JM, Wueest S, Schoenle EJ, Konrad D. The portal theory supported by venous drainage–selective fat transplantation. *Diabetes*. 2011;60(1):56–63.
215. Banerji MA, Faridi N, Atluri R. Body composition, visceral fat, leptin, and insulin resistance in Asian Indian men. *J Clin Endocrinol Metab*. 1999;84(1):137–144.
216. Yildirim B, Sabir N, Sabir, Kaleli B. Relation of intra-abdominal fat distribution to metabolic disorders in nonobese patients with polycystic ovary syndrome. *Fertility and Sterility*. 2003;79(6):1358–1364.
217. Puder JJ, Varga S, Kraenzlin M. Central fat excess in polycystic ovary syndrome: relation to low-grade inflammation and insulin resistance. *J Clin Endocrinol Metab*. 2005;90(11):6014–6021.
218. Escobar-Morreale HF, Millán JLS. Abdominal adiposity and the polycystic ovary syndrome. *Trends Endocrinol Metab*. 2007;18(7):266–272.
219. Barber TM, Golding SJ, Alvey C, Wass JAH, Karpe F, Franks S, et al. Global adiposity rather than abnormal regional fat distribution characterizes women with polycystic ovary syndrome. *J Clin Endocrinol Metab*. 2008;93(3):999–1004.
220. Dolfing JG, Stassen CM, van Haard PMM, Wolffenbuttel BHR, Schweitzer DH. Comparison of MRI-assessed body fat content between lean women with polycystic ovary syndrome (PCOS) and matched controls: less visceral fat with PCOS. *Hum Reprod*. 2011;26(6):1495–1500.
221. Blackwell VC, Salis P, Groves RW. Partial lipodystrophy, polycystic ovary syndrome and proteinuria: a common link to insulin resistance? *J R Soc Med*. 2001;94:238–240.
222. Pahuja I, De P, Sharma N, Kulshreshtha B. Polycystic ovarian syndrome in patients with lipodystrophy: Report of 2 cases with review of literature. *Indian J Endocrinol Metab*. 2012;16(6):1022–1025.
223. Penney LL, Ruangwit U, Miles PA. Congenital lipodystrophy and polycystic ovarian disease. *Endocrinol Metab Clin North Am*. 1981;26(3):142–148.
224. Joy TR, Hegele RA. Prevalence of reproductive abnormalities among women with familial partial lipodystrophy. *Endocr Pract*. 2009;14(9):1126–1132.

References

225. Lungu AO, Zadeh ES, Goodling A, Cochran E, Gorden P. Insulin resistance is a sufficient basis for hyperandrogenism in lipodystrophic women with polycystic ovarian syndrome. *J Clin Endocrinol Metab.* 2011;97(2):563–567.
226. Lewandowski KC, Lewiński A, Dąbrowska K, Jakubowski L, Gach A. Familial partial lipodystrophy as differential diagnosis of polycystic ovary syndrome. *Endokrynologia Polska.* 2015;66(6):550–554.
227. Klemm DJ, Leitner JW, Watson P, Nesterova A, Reusch J, Goalstone ML, et al. Insulin-induced adipocyte differentiation - Activation of CREB rescues adipogenesis from the arrest caused by inhibition of prenylation. *J Biol Chem.* 2001;276(30):28430–28435.
228. Chazenbalk G, Singh P, Irge D, Shah A, Abbott DH, Dumesic DA. Androgens inhibit adipogenesis during human adipose stem cell commitment to preadipocyte formation. *Steroids.* 2013;78(9):920–926.
229. Wang L, Li S, Zhao A, Tao T, Mao X, Zhang P, et al. The expression of sex steroid synthesis and inactivation enzymes in subcutaneous adipose tissue of PCOS patients. *J Steroid Biochem Mol Biol.* 2012;132(1-2):120–126.
230. Manneras-Holm L, Leonhardt H, Jennische E, Kullberg J, Oden A, Holm G, et al. Adipose tissue has aberrant morphology and function in PCOS: enlarged adipocytes and low serum adiponectin, but not circulating sex steroids, are strongly associated with insulin resistance. *J Clin Endocrinol Metab.* 2010;96(2):304–311.
231. Faulds G, Ryden M, Ek I. Mechanisms behind lipolytic catecholamine resistance of subcutaneous fat cells in the polycystic ovarian syndrome. *J Clin Endocrinol Metab.* 2003;88(5):2269–2273.
232. Arner P. Effects of testosterone on fat cell lipolysis. Species differences and possible role in polycystic ovarian syndrome. *Biochimie.* 2005;87(1):39–43.
233. Seow KM, Tsai YL, Hwang JL, Hsu WY, Ho LT, Juan CC. Omental adipose tissue overexpression of fatty acid transporter CD36 and decreased expression of hormone-sensitive lipase in insulin-resistant women with polycystic ovary syndrome. *Hum Reprod.* 2009;24(8):1982–1988.
234. Toulis KA, Goulis DG, Farmakiotis D. Adiponectin levels in women with polycystic ovary syndrome: a systematic review and a meta-analysis. *Hum Reprod Update.* 2009;15(3):297–307.
235. Carmina E, Orio F, Palomba S, Cascella T, Longo RA, Colao AM, et al. Evidence for altered adipocyte function in polycystic ovary syndrome. *Eur J Endocrinol.* 2005;152(3):389–394.
236. Li S, Huang X, Zhong H, Peng Q, Chen S, Xie Y, et al. Low circulating adiponectin levels in women with polycystic ovary syndrome: an updated meta-analysis. *Tumour Biol.* 2014;35(5):3961–3973.
237. Lagaly DV, Aad PY, Grado-Ahuir JA, Hulsey LB, Spicer LJ. Role of adiponectin in regulating ovarian theca and granulosa cell function. *Mol Cell Endocrinol.* 2008;284(1-2):38–45.

References

238. Gonzalez F. Inflammation in polycystic ovary syndrome: Underpinning of insulin resistance and ovarian dysfunction. *Steroids*. 2012;77(4):300–305.
239. Eckel RH, Grundy SM, Zimmet PZ. The metabolic syndrome. *The Lancet*. 2005;365(9468):1415–1428.
240. Alberti KGMM, Eckel RH, Grundy SM, Zimmet PZ, Cleeman JI, Donato KA, et al. Harmonizing the metabolic syndrome: a joint interim statement of the International Diabetes Federation Task Force on Epidemiology and Prevention; National Heart, Lung, and Blood Institute; American Heart Association; World Heart Federation; International Atherosclerosis Society; and International Association for the Study of Obesity. *Circulation*. 2009;120(16):1640–1645.
241. Kahn SE, Prigeon RL, Schwartz RS, Fujimoto WY, Knopp RH, Brunzell JD, et al. Obesity, body fat distribution, insulin sensitivity and Islet beta-cell function as explanations for metabolic diversity. *J Nutr. American Society for Nutrition*; 2001;131(2):354–360.
242. Vural B, Caliskan E, Turkoz E, Kilic T, Demirci A. Evaluation of metabolic syndrome frequency and premature carotid atherosclerosis in young women with polycystic ovary syndrome. *Hum Reprod*. 2005;20(9):2409–2413.
243. Azziz R. How prevalent is metabolic syndrome in women with polycystic ovary syndrome? *Nat Rev Endocrinol*. 2006;2(3):132–133.
244. Glueck CJ, Papanna R, Wang P, Goldenberg N, Sieve-Smith L. Incidence and treatment of metabolic syndrome in newly referred women with confirmed polycystic ovarian syndrome. *Metabolism*. 2003;52(7):908–915.
245. Apridonidze T, Essah PA, Iuorno MJ, Nestler JE. Prevalence and characteristics of the metabolic syndrome in women with polycystic ovary syndrome. *J Clin Endocrinol Metab*. 2004;90(4):1929–1935.
246. Ehrmann DA, Liljenquist DR, Kasza K. Prevalence and predictors of the metabolic syndrome in women with polycystic ovary syndrome. *J Clin Endocrinol Metab*. 2006;91(1):48-53.
247. Ford ES, Giles WH, Dietz WH. Prevalence of the metabolic syndrome among US adults: findings from the third National Health and Nutrition Examination Survey. *Jama*. 2002;287(3):356-359.
248. Sam S, Dunaif A. Polycystic ovary syndrome: Syndrome XX? *Trends Endocrinol Metab*. 2003;14(8):365–370.
249. Korhonen S, Hippeläinen M, Vanhala M, Heinonen S, Niskanen L. The androgenic sex hormone profile is an essential feature of metabolic syndrome in premenopausal women: a controlled community-based study. *Fertility and Sterility*. 2003;79(6):1327–1334.
250. Sam S, Legro RS, Bentley-Lewis R, Dunaif A. Dyslipidemia and metabolic syndrome in the sisters of women with polycystic ovary syndrome. *J Clin Endocrinol Metab*. 2005;90(8):4797–4802.

References

251. Ruukonen A, Glintborg D, Puurunen J, Stener-Victorin E, Tapanainen JS, Sundstrom-Poromaa I, et al. Normo- and hyperandrogenic women with polycystic ovary syndrome exhibit an adverse metabolic profile through life. *Fertility and Sterility*. 2017;107(3):788-795.
252. Fazel Y, Koenig AB, Sayiner M, Goodman ZD, Younossi ZM. Epidemiology and natural history of non-alcoholic fatty liver disease. *Metabolism*. 2016;65(8):1017–1025.
253. Younossi ZM, Diehl AM, Ong JP. Nonalcoholic fatty liver disease: an agenda for clinical research. *Hepatology*. 2002;35(4):746–752.
254. Dixon JB, Bhathal PS, O'Brien PE. Nonalcoholic fatty liver disease: predictors of nonalcoholic steatohepatitis and liver fibrosis in the severely obese. *Eur J Gastroenterol Hepatol*. 2001;121(1):91–100.
255. Hamaguchi M, Kojima T, Takeda N, Nakagawa T, Taniguchi H, Fujii K, et al. The metabolic syndrome as a predictor of nonalcoholic fatty liver disease. *AnnIntern Med*. 2005;143(10):722–728.
256. Gambarin-Gelwan M, Kinkhabwala SV, Schiano TD, Bodian C, Yeh H-C, Futterweit W. Prevalence of nonalcoholic fatty liver disease in women with polycystic ovary syndrome. *Clin Gastroenterol Hepatol*. 2007;5(4):496–501.
257. Makri E, Tziomalos K. Prevalence, etiology and management of non-alcoholic fatty liver disease in patients with polycystic ovary syndrome. *Minerva Endocrinol*. 2016;42(2):122–131.
258. Kaur J. A Comprehensive review on metabolic syndrome. *Cardiol Res Pract*. 2014;2014:1–21.
259. Wild RA, Rizzo M, Clifton S, Carmina E. Lipid levels in polycystic ovary syndrome: systematic review and meta-analysis. *Fertility and Sterility*. 2011;95(3):1073-1079.
260. Wild RA, Bartholomew MJ. The influence of body weight on lipoprotein lipids in patients with polycystic ovary syndrome. *Am J Obstet Gynecol*. 1988;159(2):423–427.
261. Talbott E, Clerici A, Berga SL, Kuller L, Guzick D, Detre K, et al. Adverse lipid and coronary heart disease risk profiles in young women with polycystic ovary syndrome: results of a case-control study. *J Clin Epidemiol*. 1998;51(5):415–422.
262. Diamanti-Kandarakis E, Papavassiliou AG, Kandarakis SA, Chrousos GP. Pathophysiology and types of dyslipidemia in PCOS. *Trends Endocrinol Metab*. 2007;18(7):280-285.
263. Holte J, Bergh T, Berne C, Lithell H. Serum lipoprotein lipid profile in women with the polycystic ovary syndrome: relation to anthropometric, endocrine and metabolic variables. *Clin Endocrinol*. 1994;41(4):463-471.

References

264. Wu Y, Zhang J, Wen Y, Wang H, Zhang M, Cianflone K. Increased acylation-stimulating protein, C-reactive protein, and lipid levels in young women with polycystic ovary syndrome. *Fertility and Sterility*. 2008;91(1):213–219.
265. Wild RA. Dyslipidemia in PCOS. *Steroids*. 2011;77(4):295–299.
266. Mai K, Bobbert T, Kullmann V, Andres J. Free fatty acids increase androgen precursors in vivo. *J Clin Endocrinol Metab*. 2006;91(4):1501-1507.
267. Belfort R, Mandarino L, Kashyap S, Wirfel K, Pratipanawatr T, Berria R, et al. Dose-response effect of elevated plasma free fatty acid on insulin signaling. *Diabetes*. 2005;54(6):1640–1648.
268. Wilding JPH. The importance of free fatty acids in the development of type 2 diabetes. *Diabet Med*. 2007;24(9):934–945.
269. Crespin SR, Greenough WB, Steinberg D. Stimulation of insulin secretion by long-chain free fatty acids. A direct pancreatic effect. *J Clin Invest*. 1973;52(8):1979–1984.
270. Gunning MN, Fauser BCJM. Are women with polycystic ovary syndrome at increased cardiovascular disease risk later in life? *Climacteric*. 2017;20(3):222-227.
271. Roth GA, Johnson C, Abajobir A, Abd-Allah F, Abera SF, Abyu G, et al. Global, regional, and national burden of cardiovascular diseases for 10 causes, 1990 to 2015. *J Am Coll Cardiol*. 2017;70(1):1-25.
272. Toulis KA, Goulis DG, Mintziori G, Kintiraki E, Eukarpidis E, Mouratoglou S-A, et al. Meta-analysis of cardiovascular disease risk markers in women with polycystic ovary syndrome. *Hum Reprod Update*. 2011;17(6):741–460.
273. Orio F, Palomba S, Cascella T, Di Biase S, Manguso F, Tauchmanova L, et al. The increase of leukocytes as a new putative marker of low-grade chronic inflammation and early cardiovascular risk in polycystic ovary syndrome. *J Clin Endocrinol Metab*. 2005;90(1):2–5.
274. Okoroh EM, Boulet SL, George MG, Hooper WC. Assessing the intersection of cardiovascular disease, venous thromboembolism, and polycystic ovary syndrome. *Thromb Res*. 2015;136(6):1165-1668.
275. Hart R, Doherty DA. The potential implications of a PCOS diagnosis on a woman's long-term health using data linkage. *J Clin Endocrinol Metab*. 2014;100(3):911–919.
276. Ouyang P, Vaidya D, Dobs A, Golden SH, Szklo M, Heckbert SR, et al. Sex hormone levels and subclinical atherosclerosis in postmenopausal women: The Multi-Ethnic Study of Atherosclerosis. *Atherosclerosis*. 2009;204(1):255–261.
277. Laughlin GA, Goodell V, Barrett-Connor E. Extremes of endogenous testosterone are associated with increased risk of incident coronary events in older women. *J Clin Endocrinol Metab*. 2009;95(2):740–747.

References

278. Macut D, Antić IB, Bjekić-Macut J. Cardiovascular risk factors and events in women with androgen excess. *J Endocrinol Invest.* 2014;38(3):295–301.
279. Marshall JC, Dunaif A. Should all women with PCOS be treated for insulin resistance? *Fertility and Sterility.* 2011;97(1):18–22.
280. Palmert MR, Gordon CM, Kartashov AI, Legro RS, Emans SJ, Dunaif A. Screening for abnormal glucose tolerance in adolescents with polycystic ovary syndrome. *J Clin Endocrinol Metab.* 2002;87(3):1017–1023.
281. Flannery CA, Rackow B, Cong X, Duran E, Selen DJ, Burgert TS. Polycystic ovary syndrome in adolescence: impaired glucose tolerance occurs across the spectrum of BMI. *Pediatr Diabetes.* 2012;14(1):42–49.
282. Diamanti-Kandarakis E. PCOS in adolescents. *Best Pract Res Clin Obstet Gynaecol.* 2010;24:173-183.
283. Bhattacharya SM, Ghosh M. Insulin resistance and adolescent girls with polycystic ovary syndrome. *J Pediatr Adolesc Gynecol.* 2010;23(3):158–161.
284. Lewy VD, Danadian K, Witchel SF, Arslanian S. Early metabolic abnormalities in adolescent girls with polycystic ovarian syndrome. *J Pediatr.* 2001;138(1):38–44.
285. Kent SC, Gnatuk CL, Kunselman AR, Demers LM, Lee PA, Legro RS. Hyperandrogenism and hyperinsulinism in children of women with polycystic ovary syndrome: a controlled study. *J Clin Endocrinol Metab.* 2008;93(5):1662–1669.
286. Sir-Petermann T, Maliqueo M, Codner E, Echiburú B, Crisosto N, Pérez V, et al. Early metabolic derangements in daughters of women with polycystic ovary syndrome. *J Clin Endocrinol Metab.* 2007;92(12):4637–4642.
287. Ollila M-ME, Piltonen T, Puukka K, Ruukonen A, Järvelin M-R, Tapanainen JS, et al. Weight gain and dyslipidemia in early adulthood associate with polycystic ovary syndrome: prospective cohort study. *J Clin Endocrinol Metab.* 2016;101(2):739–747.
288. Laitinen J, Taponen S, Martikainen H, Pouta A, Millwood I, Hartikainen AL, et al. Body size from birth to adulthood as a predictor of self-reported polycystic ovary syndrome symptoms. *Int J Obes Relat Metab Disord.* 2003;27(6):710–715.
289. Reinehr T, de Sousa G, Roth CL, Andler W. Androgens before and after weight loss in obese children. *J Clin Endocrinol Metab.* 2005;90(10):5588–5595.
290. McCartney CR, Blank SK, Prendergast KA, Chhabra S, Eagleson CA, Helm KD, et al. Obesity and sex steroid changes across puberty: evidence for marked hyperandrogenemia in pre- and early pubertal obese girls. *J Clin Endocrinol Metab.* 2006;92(2):430–436.
291. Cook S. The metabolic syndrome: Antecedent of adult cardiovascular disease in pediatrics. *J Pediatr.* 2004;145(4):427–430.

References

292. Berenson GS, Srinivasan SR, Bao W, Newman WP, Tracy RE, Wattigney WA. Association between multiple cardiovascular risk factors and atherosclerosis in children and young adults. The Bogalusa Heart Study. *N Engl J Med*. 1998;338(23):1650–1656.
293. Reilly JJ, Kelly J. Long-term impact of overweight and obesity in childhood and adolescence on morbidity and premature mortality in adulthood: systematic review. *Int J Obes*. 2011;35(7):891–898.
294. Coviello AD, Legro RS, Dunaif A. Adolescent girls with polycystic ovary syndrome have an increased risk of metabolic syndrome associated with increasing androgen levels independent of obesity and insulin resistance. *J Clin Endocrinol Metab*. 2006;91(2):492-497.
295. Hart R, Doherty DA, Mori T, Huang R-C, Norman RJ, Franks S, et al. Extent of metabolic risk in adolescent girls with features of polycystic ovary syndrome. *Fertility and Sterility*. 2011;95(7):2347–2353.
296. Bhattacharya SM, Jha A. Prevalence and risk of metabolic syndrome in adolescent Indian girls with polycystic ovary syndrome using the 2009 'joint interim criteria'. *J of Obstet Gynaecol Res*. 2011;37(10):1303–1307.
297. Roe AH, Prochaska E, Smith M, Sammel M, Dokras A. Using the Androgen Excess–PCOS Society criteria to diagnose polycystic ovary syndrome and the risk of metabolic syndrome in adolescents. *J Pediatr*. 2013;162(5):937–941.
298. Huang J, Ni R, Chen X, Huang L, Mo Y, Yang D. Metabolic abnormalities in adolescents with polycystic ovary syndrome in south China. *Reprod Biol Endocrinol*. 2010;8:142.
299. Ayonrinde OT, Adams LA, Doherty DA, Mori TA. Adverse metabolic phenotype of adolescent girls with non-alcoholic fatty liver disease plus polycystic ovary syndrome compared with other girls and boys. *J Gastroenterol Hepatol*, 2016;31(5):980-987.
300. Alemzadeh R, Kichler J, Calhoun M. Spectrum of metabolic dysfunction in relationship with hyperandrogenemia in obese adolescent girls with polycystic ovary syndrome. *Eur J Endocrinol*. 2010;162(6):1093–1099.
301. Johnson T, Kaplan L, Ouyang P. Final report of National Institutes of Health evidence-based methodology workshop on polycystic ovary syndrome (PCOS). National Institutes of Health Workshop. 2012:1–14.
302. Duncan WC. A guide to understanding polycystic ovary syndrome (PCOS). *J Fam Plann Reprod Health Care*. 2014;40(3):217–225.
303. Taylor AE, McCourt B, Martin KA, Anderson EJ, Adams JM, Schoenfeld D, et al. Determinants of abnormal gonadotropin secretion in clinically defined women with polycystic ovary syndrome. *J Clin Endocrinol Metab*. 1997;82(7):2248–2256.

References

304. García-Rudaz MC, Ropelato MG, Escobar ME, Veldhuis JD, Barontini M. Augmented frequency and mass of LH discharged per burst are accompanied by marked disorderliness of LH secretion in adolescents with polycystic ovary syndrome. *Eur J Endocrinol.* 1999;139(6):621–630.
305. Nelson VL, Legro RS, Strauss JF, McAllister JM. Augmented androgen production is a stable steroidogenic phenotype of propagated theca cells from polycystic ovaries. *Mol Endocrinol.* 1999;13(6):946–957.
306. Gilling-Smith C, Story H, Rogers V, Franks S. Evidence for a primary abnormality of thecal cell steroidogenesis in the polycystic ovary syndrome. *Clin Endocrinol.* 1997;47(1):93–99.
307. Wood JR, Ho CK, Nelson-Degrave VL, McAllister JM, Strauss JF. The molecular signature of polycystic ovary syndrome (PCOS) theca cells defined by gene expression profiling. *J Reprod Immunol.* 2004;63(1):51–60.
308. McCartney CR, Eagleson CA, Marshall JC. Regulation of gonadotropin secretion: implication for polycystic ovary syndrome. *Semin Reprod Med.* 2002;20(4):317–326.
309. Lockwood GM. The role of inhibin in polycystic ovary syndrome. *Hum Fertil.* 2002;3(2):86–92.
310. Anderson RA, Groome NP, Baird DT. Inhibin A and inhibin B in women with polycystic ovarian syndrome during treatment with FSH to induce mono-ovulation. *Clin Endocrinol.* 1998;48(5):577–584.
311. Jonard S, Dewailly D. The follicular excess in polycystic ovaries, due to intra-ovarian hyperandrogenism, may be the main culprit for the follicular arrest. *Hum Reprod Update.* 2004;10(2):107–117.
312. Maciel GA, Baracat EC, Benda JA, Markham SM, Hensinger K, Chang RJ, et al. Stockpiling of transitional and classic primary follicles in ovaries of women with polycystic ovary syndrome. *J Clin Endocrinol Metab.* 2004;89(11):5321–5327.
313. Moran C, Arriaga M, Arechavaleta-Velasco F, Moran S. Adrenal androgen excess and body mass index in polycystic ovary syndrome. *J Clin Endocrinol Metab.* 2014;100(3):942–950.
314. Azziz R, Black V, Hines GA, Fox LM, Boots LR. Adrenal androgen excess in the polycystic ovary syndrome: Sensitivity and responsivity of the hypothalamic-pituitary-adrenal axis. *J Clin Endocrinol Metab.* 1998;83(7):2317–2323.
315. Horrocks PM, London DR, Kandeel FR. ACTH function in women with the polycystic ovarian syndrome. *Clin Endocrinol.* 1983;19(2):143–150.
316. Nestler JE, Strauss JF. Insulin as an effector of human ovarian and adrenal steroid metabolism. *Endocrinol Metab Clin North Am.* 1991;20(4):807–823.

References

317. Moghetti P, Castello R, Negri C, Tosi F, Spiazzi GG, Brun E, et al. Insulin infusion amplifies 17 alpha-hydroxycorticosteroid intermediates response to adrenocorticotropin in hyperandrogenic women: apparent relative impairment of 17,20-lyase activity. *J Clin Endocrinol Metab.* 1996;81(3):881–886.
318. Cusi K, Maezono K, Osman A, Pendergrass M, Patti ME, Pratipanawat T, et al. Insulin resistance differentially affects the PI 3-kinase- and MAP kinase-mediated signaling in human muscle. *J Clin Invest.* 2000;105(3):311–320.
319. Diamanti-Kandarakis E and Dunaif A. Insulin resistance and polycystic ovary syndrome revisited: an update on mechanisms and implications. *Endocr Rev.* 2012;33(6): 981-1030.
320. Rosenbaum D, Haber RS, Dunaif A. Insulin resistance in polycystic ovary syndrome: Decreased expression of GLUT-4 glucose transporters in adipocytes. *Am J Physiol Endocrinol Metab.* 1993;264:197-202.
321. Escobar-Morreale HF, Villuendas G, Botella-Carretero JI, Álvarez-Blasco F, Sanchón R, Luque-Ramírez M, et al. Adiponectin and resistin in PCOS: a clinical, biochemical and molecular genetic study. *Hum Reprod.* 2006;21(9):2257–2265.
322. Sepilian V, Nagamani M. Adiponectin levels in women with polycystic ovary syndrome and severe insulin resistance. *J Soc Gynecol Investig.* 2005;12(2):129–134.
323. Hoeger KM. Role of lifestyle modification in the management of polycystic ovary syndrome. *Best Prac Res Clin Endocrinol Metab.* 2006;20(2):293-310.
324. Farshchi H, Rane A, Love A, Kennedy RL. Diet and nutrition in polycystic ovary syndrome (PCOS): Pointers for nutritional management. *J Obstet Gynaecol.* 2007;27(8):762–773.
325. Clark AM, Ledger W, Galletly C, Tomlinson L, Blaney F, Wang X, et al. Weight loss results in significant improvement in pregnancy and ovulation rates in anovulatory obese women. *Hum Reprod.* 1995;10(10):2705–2712.
326. Norman RJ, Noakes M, Wu R, Davies MJ, Moran L, Wang JX. Improving reproductive performance in overweight/obese women with effective weight management. *Hum Reprod Update.* 2004;10(3):267–280.
327. Moran LJ, Noakes M, Clifton PM, Tomlinson L, Galletly C, Norman RJ. Dietary composition in restoring reproductive and metabolic physiology in overweight women with polycystic ovary syndrome. *J Clin Endocrinol Metab.* 2003;88(2):812–819.
328. Marzouk TM, Ahmed WAS. Effect of dietary weight loss on menstrual regularity in obese young adult women with polycystic ovary syndrome. *J Pedia Adolesc Gynecol.* 2015;28(6):457-461.
329. Tang T, Lord JM, Lord JM, Norman RJ, Yasmin E, Yasmin E, et al. Insulin-sensitising drugs (metformin, rosiglitazone, pioglitazone, D-chiro-inositol) for women with polycystic ovary syndrome, oligo amenorrhoea and subfertility. *Cochrane Database Syst Rev.* 2012;(5):1–113.

References

330. Palomba S, Falbo A, Zullo F, Orio F. Evidence-based and potential benefits of metformin in the polycystic ovary syndrome: a comprehensive review. *Endocrine Reviews*. 2008;30(1):1–50.
331. Moll E, van der Veen F, van Wely M. The role of metformin in polycystic ovary syndrome: a systematic review. *Hum Reprod Update*. 2007;13(6):527–537.
332. Li XJ, Yu YX, Liu CQ, Zhang W, Zhang HJ, Yan B, et al. Metformin vs thiazolidinediones for treatment of clinical, hormonal and metabolic characteristics of polycystic ovary syndrome: a meta-analysis. *Clin Endocrinol*. 2010;74(3):332–339.
333. Sirmans SM, Pate KA. Epidemiology, diagnosis, and management of polycystic ovary syndrome. *Clinical Epidemiology*. 2014;6:1–13.
334. Sepilian V, Nagamani M. Effects of rosiglitazone in obese women with polycystic ovary syndrome and severe insulin resistance. *J Clin Endocrinol Metab*. 2004;90(1):60–65.
335. Yildiz BO, Yarali H, Oguz H, Bayraktar M. Glucose intolerance, insulin resistance, and hyperandrogenemia in first degree relatives of women with polycystic ovary syndrome. *J Clin Endocrinol Metab*. 2003;88(5):2031–2036.
336. Norman RJ, Masters S, Hague W. Hyperinsulinemia is common in family members of women with polycystic ovary syndrome. *Fertility and Sterility*. 1996;66(6):942–947.
337. Lunde O, Magnus P, Sandvik L, Høglo S. Familial clustering in the polycystic ovarian syndrome. *Gynecol Obstet Invest*. 1989;28(1):23–30.
338. Hague WM, Adams J, Reeders ST, Peto TEA, Jacobs HS. Familial polycystic ovaries: a genetic disease? *Clin Endocrinol*. 1988;29(6):593–605.
339. Givens JR. Familial polycystic ovarian disease. *Endocrinol Metab Clin North Am*. 1988;17(4):771–783.
340. Ferriman D, Purdie AW. The inheritance of polycystic ovarian disease and a possible relationship to premature balding. *Clin Endocrinol*. 1979;11(3):291–300.
341. Legro RS, Driscoll D, Strauss JF, Fox J, Dunaif A. Evidence for a genetic basis for hyperandrogenemia in polycystic ovary syndrome. *Proc Natl Acad Sci USA*. 1998;95(25):14956–14960.
342. Sam S, Sung Y-A, Legro RS, Dunaif A. Evidence for pancreatic β -cell dysfunction in brothers of women with polycystic ovary syndrome. *Metabolism*. 2008;57(1):84–89.
343. Sam S, Coviello AD, Sung Y-A, Legro RS, Dunaif A. Metabolic phenotype in the brothers of women with polycystic ovary syndrome. *Diabetes Care*. 2008;31(6):1237–1241.

References

344. Legro RS, Kunselman AR, Demers L, Wang SC, Bentley-Lewis R, Dunaif A. Elevated dehydroepiandrosterone sulfate levels as the reproductive phenotype in the brothers of women with polycystic ovary syndrome. *J Clin Endocrinol Metab.* 2002;87(5):2134–2138.
345. Liu DM, Torchen LC, Sung Y, Papanicolaou R, Legro RS, Grebe SK, et al. Evidence for gonadotrophin secretory and steroidogenic abnormalities in brothers of women with polycystic ovary syndrome. *Hum Reprod.* 2014;29(12):2764–2772.
346. Recabarren SE, Smith R, Rios R, Maliqueo M, Echiburú B, Codner E, et al. Metabolic profile in sons of women with polycystic ovary syndrome. *J Clin Endocrinol Metab.* 2008;93(5):1820–1826.
347. Vink JM, Sadrzadeh S, Lambalk CB, Boomsma DI. Heritability of polycystic ovary syndrome in a Dutch twin-family study. *J Clin Endocrinol Metab.* 2005;91(6):2100–2104.
348. Schaid DJ, Sommer SS. Genotype relative risks: methods for design and analysis of candidate-gene association studies. *Am J Hum Genet.* 1993;53(5):1114–1126.
349. Manolio TA. Genomewide association studies and assessment of the risk of disease. *N Engl J Med.* 2010;363(2):166–176.
350. Carey AH, Waterworth D, Patel K, White D, Little J, Novelli P, et al. Polycystic ovaries and premature male pattern baldness are associated with one allele of the steroid metabolism gene CYP17. *Hum Mol Genet.* 1994;3(10):1873–1876.
351. Gharani N, Waterworth DM, Batty S, White D, Gilling-Smith C, Conway GS, et al. Association of the steroid synthesis gene CYP11a with polycystic ovary syndrome and hyperandrogenism. *Hum Mol Genet.* 1997;6(3):397–402.
352. Pusalkar M, Meherji P, Gokral J, Chinnaraj S, Maitra A. CYP11A1 and CYP17 promoter polymorphisms associate with hyperandrogenemia in polycystic ovary syndrome. *Fertility and Sterility.* 2008;92(2):653–659.
353. Techatraisak K, Conway GS, Rumsby G. Frequency of a polymorphism in the regulatory region of the 17 alpha-hydroxylase-17,20-lyase (CYP17) gene in hyperandrogenic states. *Clin Endocrinol.* 1997;46(2):131–134.
354. Echiburú B, Pérez-Bravo F, Maliqueo M, Sánchez F, Crisosto N, Sir-Petermann T. Polymorphism T → C (-34 base pairs) of gene CYP17 promoter in women with polycystic ovary syndrome is associated with increased body weight and insulin resistance: a preliminary study. *Metabolism.* 2008;57(12):1765–1771.
355. Gaasenbeek M, Powell BL, Sovio U, Haddad L, Gharani N, Bennett A, et al. Large-scale analysis of the relationship between CYP11A promoter variation, polycystic ovarian syndrome, and serum testosterone. *J Clin Endocrinol Metab.* 2004;89(5):2408–2413.
356. Daneshmand S, Weitsman SR, Navab A, Jakimiuk AJ, Magoffin DA. Overexpression of theca-cell messenger RNA in polycystic ovary syndrome does not correlate with polymorphisms in the cholesterol side-chain cleavage and 17 α -hydroxylase/C17-20 lyase promoters. *Fertility and Sterility.* 2002;77(2):274–280.

References

357. Millán JLS, Sancho J, Calvo RM, Escobar-Morreale HF. Role of the pentanucleotide (tttta)(n) polymorphism in the promoter of the CYP11a gene in the pathogenesis of hirsutism. *Fertility and Sterility*. 2001;75(4):797–802.
358. Ibáñez L, Ong KK, Mongan N, Jääskeläinen J, Marcos MV, Hughes IA, et al. Androgen receptor gene CAG repeat polymorphism in the development of ovarian hyperandrogenism. *J Clin Endocrinol Metab*. 2003;88(7):3333–3338.
359. Peng CY, Xie HJ, Guo ZF, Nie YL, Chen J, Zhou JM, et al. The association between androgen receptor gene CAG polymorphism and polycystic ovary syndrome: a case-control study and meta-analysis. *J Assist Reprod Genet*. 2014;31(9):1211–1219.
360. Dasgupta S, Sirisha PVS, Neelaveni K, Anuradha K, Reddy AG, Thangaraj K, et al. Androgen receptor CAG repeat polymorphism and epigenetic influence among the south Indian women with polycystic ovary syndrome. *PLoS ONE*. 2010;5(8):12401.
361. Skrgatic L, Baldani DP, Cerne JZ, Ferik P, Gersak K. CAG repeat polymorphism in androgen receptor gene is not directly associated with polycystic ovary syndrome but influences serum testosterone levels. *J Steroid Biochem Mol Biol*. 2012;128(3):107–112.
362. Ferik P, Perme MP, Teran N, Gersak K. Androgen receptor gene (CAG)(n) polymorphism in patients with polycystic ovary syndrome. *Fertility and Sterility*. 2008;90(3):860–863.
363. Kim JJ, Choung SH, Choi YM, Yoon SH, Kim SH, Moon SY. Androgen receptor gene CAG repeat polymorphism in women with polycystic ovary syndrome. *Fertility and Sterility*. 2008;90(6):2318–2323.
364. Du J, Wang J, Sun X, Xu X, Zhang F, Bin Wang, et al. Family-based analysis of INSR polymorphisms in Chinese PCOS. *Reprod BioMed Online*. 2014;29(2):239–244.
365. Goodarzi MO, Louwers YV, Taylor KD, Jones MR, Cui J, Kwon S, et al. Replication of association of a novel insulin receptor gene polymorphism with polycystic ovary syndrome. *Fertility and Sterility*. 2011;95(5):1736–1741.
366. Lee EJ, Oh B, Lee JY, Kimm K, Lee SH, Baek KH. A novel single nucleotide polymorphism of INSR gene for polycystic ovary syndrome. *Fertility and Sterility*. 2008;89(5):1213–1220.
367. Siegel S, Futterweit W, Davies TF, Concepcion ES, Greenberg DA, Villanueva R, et al. A C/T single nucleotide polymorphism at the tyrosine kinase domain of the insulin receptor gene is associated with polycystic ovary syndrome. *Fertility and Sterility*. 2002;78(6):1240–1243.
368. Shi X, Xie X, Jia Y, Li S. Associations of insulin receptor and insulin receptor substrates genetic polymorphism with polycystic ovary syndrome: A systemic review and meta-analysis. *J Obstet Gynaecol Rev*. 2016;42(7):844–854.

References

369. Baba T, Endo T, Sata F, Honnma H, Kitajima Y, Hayashi T, et al. Polycystic ovary syndrome is associated with genetic polymorphism in the insulin signaling gene IRS-1 but not ENPP1 in a Japanese population. *Am J Physiol.* 200;81(10):850-854.
370. Christopoulos P, Mastorakos G, Gazouli M, Deligeoroglou E, Katsikis I, Diamanti-Kandarakis E, et al. Study of association of IRS-1 and IRS-2 genes polymorphisms with clinical and metabolic features in women with polycystic ovary syndrome. Is there an impact? *Gynecol Endocrinol.* 2010;26(9):698–703.
370. Yan Q, Hong J, Gu W, Zhang Y, Liu Q, Su Y, et al. Association of the common rs9939609 variant of FTO gene with polycystic ovary syndrome in Chinese women. *Endocrine.* 2009;36(3):377–382.
371. Barber TM, Bennett AJ, Groves CJ, Sovio U, Ruukonen A, Martikainen H, et al. Association of variants in the fat mass and obesity associated (FTO) gene with polycystic ovary syndrome. *Diabetologia.* 2008;51(7):1153–1158.
372. Wehr E, Schweighofer N, Möller R, Giuliani A, Pieber TR, Obermayer-Pietsch B. Association of FTO gene with hyperandrogenemia and metabolic parameters in women with polycystic ovary syndrome. *Metabolism.* 2010;59(4):575–580.
373. Kowalska I, Malecki MT, Strączkowski M, Skupien J, Karczewska-Kopczewska M, Nikolajuk A, et al. The FTO gene modifies weight, fat mass and insulin sensitivity in women with polycystic ovary syndrome, where its role may be larger than in other phenotypes. *Diabetes Metab.* 2009;35(4):328–331.
374. Tan S, Scherag A, Janssen OE, Hahn S, Lahner H, Dietz T, et al. Large effects on body mass index and insulin resistance of fat mass and obesity associated gene (FTO) variants in patients with polycystic ovary syndrome (PCOS). *BMC Med Genet.* 2010;11:1–9.
375. Li T, Wu K, You L, Xing X, Wang P, Cui L, et al. Common variant rs9939609 in gene FTO confers risk to polycystic ovary syndrome. *PLoS ONE.* 2013;8(7):66250.
376. Yun J-H, Choi J-W, Lee K-J, Shin J-S, Baek K-H. The promoter -1031(T/C) polymorphism in tumor necrosis factor- α associated with polycystic ovary syndrome. *Reprod Biol Endocrinol.* 2011;9:131–137.
377. Tumu VR, Govatati S, Guruvaiah P. An interleukin-6 gene promoter polymorphism is associated with polycystic ovary syndrome in South Indian women. *J Assist Reprod Genet.* 2013;30(12):1541–1546.
378. Guo R, Zheng Y, Yang J, Zheng N. Association of TNF- α , IL-6 and IL-1 β gene polymorphisms with polycystic ovary syndrome: a meta-analysis. *BMC Genetics.* 2015;16(1):1-13.
379. Shi Y, Zhao H, Cao Y, Yang D, Li Z, Zhang B. Genome-wide association study identifies eight new risk loci for polycystic ovary syndrome. *Nature.* 2012;44(9):1020–1027.
380. Chen ZJ, Zhao H, He L, Shi Y, Qin Y, Li Z. Genome-wide association study identifies susceptibility loci for polycystic ovary syndrome on chromosome 2p16.3, 2p21 and 9q33.3. *Nature.* 2011;43(1):55–60.

References

381. Hayes MG, Urbanek M, Ehrmann DA. Genome-wide association of polycystic ovary syndrome implicates alterations in gonadotropin secretion in European ancestry populations. *Nat Commun.* 2015;6:7502–7514.
382. Barker D. The developmental origins of adult disease. *J Am Coll Nutr.* 2004;23:588–595.
383. Barker DJP, Eriksson JG, Forsén T, Osmond C. Fetal origins of adult disease: strength of effects and biological basis. *Int J Epidemiol.* 2003;31(6):1235–1239.
384. Barker DJ. The fetal and infant origins of adult disease. *BMJ: British Medical Journal.* 1990;69(5):467–468.
385. Symonds ME, Sebert SP, Hyatt MA. Nutritional programming of the metabolic syndrome. *Nat Rev Endocrinol.* 2009;5(11):604–610.
386. Alfaradhi MZ, Ozanne SE. Developmental programming in response to maternal overnutrition. *Front Genet.* 2011;2:27.
387. Lakshmy R. Metabolic syndrome: Role of maternal undernutrition and fetal programming. *Rev Endoc Metab Disord.* 2013;14(3):229–240.
388. Wickstrom R. Effects of nicotine during pregnancy: Human and experimental evidence. *Curr Neuropharmacol.* 2007;5(3):213–222.
389. Entringer S. Impact of stress and stress physiology during pregnancy on child metabolic function and obesity risk. *Curr Opin Clin Nutr Metab Care.* 2013;16(3):320–327.
390. Roseboom TJ, Painter RC, van Abeelen AFM, Veenendaal MVE, de Rooij SR. Hungry in the womb: What are the consequences? Lessons from the Dutch famine. *Maturitas.* 2011;70(2):141–145.
391. Portrait F, Teeuwiszen E, Deeg D. Early life undernutrition and chronic diseases at older ages: The effects of the Dutch famine on cardiovascular diseases and diabetes. *Soc Sci Med.* 2011;73(5):711–718.
392. Handel AE, Ebers GC, Ramagopalan SV. Epigenetics: molecular mechanisms and implications for disease. *Trends Mol Med.* 2010;16(1):7–16.
393. Barnes RB, Rosenfield RL, Ehrmann DA. Ovarian hyperandrogenism as a result of congenital adrenal virilizing disorders: evidence for perinatal masculinization of neuroendocrine function in women. *J Clin Endocrinol Metab.* 1994;79(5):1328–1333.
394. Hague WM, Adams J, Rodda C, Brook CG, de Bruyn R, Grant DB, et al. The prevalence of polycystic ovaries in patients with congenital adrenal hyperplasia and their close relatives. *Clin Endocrinol.* 1990;33(4):501–510.
395. Falbo A, Rocca M, Russo T, D'Ettore A, Tolino A, Zullo F, et al. Changes in androgens and insulin sensitivity indexes throughout pregnancy in women with polycystic ovary syndrome (PCOS): relationships with adverse outcomes. *J Ovarian Res.* 2010;3:23–31.

References

396. Maliqueo M, Lara HE, Sánchez F, Echiburú B, Crisosto N, Sir-Petermann T. Placental steroidogenesis in pregnant women with polycystic ovary syndrome. *Eur J Obstet Gynecol Reprod Biol.* 2013;166(2):151–155.
397. Sir-Petermann T, Maliqueo M, Angel B, Lara HE, Perez-Bravo F, Recabarren SE. Maternal serum androgens in pregnant women with polycystic ovarian syndrome: possible implications in prenatal androgenization. *Hum Reprod.* 2002;17(10):2573–2579.
398. Mehrabian F, Kelishadi R. Comparison of the metabolic parameters and androgen level of umbilical cord blood in newborns of mothers with polycystic ovary syndrome and controls. *J Res Med Sci.* 2012;17(3):207–211.
399. Barry JA, Kay AR, Navaratnarajah R, Iqbal S, Bamfo JEAK, David AL, et al. Umbilical vein testosterone in female infants born to mothers with polycystic ovary syndrome is elevated to male levels. *J Obstet Gynaecol.* 2010;30(5):444–446.
400. Crisosto N, Echiburú B, Maliqueo M, Pérez V, de Guevara AL, Preisler J, et al. Improvement of hyperandrogenism and hyperinsulinemia during pregnancy in women with polycystic ovary syndrome: possible effect in the ovarian follicular mass of their daughters. *Fertility and Sterility.* 2011;97(1):218–224.
401. Sir-Petermann T, Codner E, Maliqueo M, Echiburú B, Hitschfeld C, Crisosto N, et al. Increased anti-Müllerian hormone serum concentrations in prepubertal daughters of women with polycystic ovary syndrome. *J Clin Endocrinol Metab.* 2006;91(8):3105–3109.
402. Bridges NA, Cooke A, Healy MJ, Hindmarsh PC, Brook CG. Standards for ovarian volume in childhood and puberty. *Fertility and Sterility.* 1993;60(3):456–460.
403. Thompson EA, Siiteri PK. The involvement of human placental microsomal cytochrome P-450 in aromatization. *J Biol Chem.* 1974;249(17):5373–5378.
404. Palomba S, Russo T, Falbo A, Di Cello A, Tolino A, Tucci L, et al. Macroscopic and microscopic findings of the placenta in women with polycystic ovary syndrome. *Hum Reprod.* 2013;28(10):2838–2847.
405. Sir-Petermann T, Echiburú B, Maliqueo MM, Crisosto N, Sánchez F, Hitschfeld C, et al. Serum adiponectin and lipid concentrations in pregnant women with polycystic ovary syndrome. *Hum Reprod.* 2007;22(7):1830–1836.
406. Nestler JE. Modulation of aromatase and P450 cholesterol side-chain cleavage enzyme activities of human placental cytotrophoblasts by insulin and insulin-like growth factor I. *Endocrinology.* 1987;121(5):1845–1852.
407. Nestler JE. Insulin and insulin-like growth factor-I stimulate the 3 α -hydroxysteroid dehydrogenase activity of human placental cytotrophoblasts. *Endocrinology.* 1989;125(4):2127–2133.
408. Uzelac PS, Li X, Lin J, Neese LD, Lin L, Nakajima ST, et al. Dysregulation of leptin and testosterone production and their receptor expression in the human placenta with gestational diabetes mellitus. *Placenta.* 2010;31(7):581–588.

References

409. Barbieri RL, Saltzman DH, Torday JS, Randall RW, Frigoletto FD, Ryan KJ. Elevated concentrations of the β -subunit of human chorionic gonadotropin and testosterone in the amniotic fluid of gestations of diabetic mothers. *Am J Obstet Gynecol*. 1986;154(5):1039–1043.
410. McNeilly AS, Duncan WC. Rodent models of polycystic ovary syndrome. *Mol Cell Endocrinol*. 2012;373(1-2):2–7.
411. Hogg K, Wood C, McNeilly AS, Duncan WC. The in utero programming effect of increased maternal androgens and a direct fetal intervention on liver and metabolic function in adult sheep. *PLoS ONE*. 2011;6(9):24877.
412. Hogg K, Young JM, Oliver EM, Souza CJ, McNeilly AS, Duncan WC. Enhanced thecal androgen production is prenatally programmed in an ovine model of polycystic ovary syndrome. *Endocrinology*. 2012;153(1):450–461.
413. Dumesic DA, Abbott DH, Eisner JR, Goy RW. Prenatal exposure of female rhesus monkeys to testosterone propionate increases serum luteinizing hormone levels in adulthood. *Fertility and Sterility*. 1997;67(1):155–163.
414. Abbott DH, Barnett DK, Bruns CM, Dumesic DA. Androgen excess fetal programming of female reproduction: a developmental aetiology for polycystic ovary syndrome? *Hum Reprod Update*. 2005;11(4):357–374.
415. Veiga-Lopez A, Ye W, Phillips DJ, Herkimer C, Knight PG, Padmanabhan V. Developmental programming: deficits in reproductive hormone dynamics and ovulatory outcomes in prenatal, testosterone-treated sheep. *Biol Reprod*. 2007;78(4):636–647.
416. Eisner JR, Barnett MA, Dumesic DA, Abbott DH. Ovarian hyperandrogenism in adult female rhesus monkeys exposed to prenatal androgen excess. *Fertility and Sterility*. 2002;77(1):167–172.
417. Indran IR, Lee BH, Yong E-L. Cellular and animal studies: insights into pathophysiology and therapy of PCOS. *Best Prac Res Clin Obstet Gynaecol*. 2016;37:12–24.
418. Abbott DH, Tarantal AF, Dumesic DA. Fetal, infant, adolescent and adult phenotypes of polycystic ovary syndrome in prenatally androgenized female rhesus monkeys. *Am J Primatol*. 2009;71(9):776–784.
419. Eisner JR, Dumesic DA, Kemnitz JW, Colman RJ, Abbott DH. Increased adiposity in female rhesus monkeys exposed to androgen excess during early gestation. *Obes Res*. 2003;11(2):279–286.
420. Zhou R, Bird IM, Dumesic DA, Abbott DH. Adrenal hyperandrogenism is induced by fetal androgen excess in a rhesus monkey model of polycystic ovary syndrome. *J Clin Endocrinol Metab*. 2005;90(12):6630–6637.
421. Abbott DH, Bruns CR, Barnett DK, Dunaif A, Goodfriend TL, Dumesic DA, et al. Experimentally induced gestational androgen excess disrupts glucoregulation in rhesus monkey dams and their female offspring. *Am J Physiol Endocrinol Metab*. 2010;299(5):741–751.

References

422. Abbott DH, Nicol LE, Levine JE, Xu N, Goodarzi MO, Dumesic DA. Nonhuman primate models of polycystic ovary syndrome. *Mol Cell Endocrinol.* 2013;373(1-2):21–28.
423. Padmanabhan V, Veiga-Lopez A. Sheep models of polycystic ovary syndrome phenotype. *Mol Cell Endocrinol.* 2013;373(1-2):8–20.
424. Manikkam M, Crespi EJ, Doop DD, Herkimer C, Lee JS, Yu S, et al. Fetal programming: Prenatal testosterone excess leads to fetal growth retardation and postnatal catch-up growth in sheep. *Endocrinology.* 2004;145(2):790–798.
425. Birch RA, Birch RA, Padmanabhan V, Foster DL, Padmanabhan V, Foster DL, et al. Prenatal programming of reproductive neuroendocrine function: fetal androgen exposure produces progressive disruption of reproductive cycles in sheep. *Endocrinology.* 2003;144(4):1426–1434.
426. Padmanabhan V, Veiga-Lopez A, Abbott DH, Recabarren SE, Herkimer C. Developmental programming: Impact of prenatal testosterone excess and postnatal weight gain on insulin sensitivity index and transfer of traits to offspring of overweight females. *Endocrinology.* 2010;151(2):595–605.
427. Steckler TL, Herkimer C, Dumesic DA, Padmanabhan V. Developmental programming: excess weight gain amplifies the effects of prenatal testosterone excess on reproductive cyclicity-implication for polycystic ovary syndrome. *Endocrinology.* 2008;150(3):1456–1465.
428. Manikkam M, Thompson RC, Herkimer C, Welch KB, Flak J, Karsch FJ, et al. Developmental programming: impact of prenatal testosterone excess on pre- and postnatal gonadotropin regulation in sheep. *Biol Reprod.* 2008;78(4):648–660.
429. Smith P, Steckler TL, Veiga-Lopez A, Padmanabhan V. Developmental programming: Differential effects of prenatal testosterone and dihydrotestosterone on follicular recruitment, depletion of follicular reserve, and ovarian morphology in sheep. *Biol Reprod.* 2009;80(4):726–736.
430. Steckler TL, Roberts EK, Doop DD, Lee TM, Padmanabhan V. Developmental programming in sheep: administration of testosterone during 60-90 days of pregnancy reduces breeding success and pregnancy outcome. *Theriogenology.* 2006;67(3):459–467.
431. Rae M, Grace C, Hogg K, Wilson LM, McHaffie SL, Ramaswamy S, et al. The pancreas is altered by in utero androgen exposure: implications for clinical conditions such as polycystic ovary syndrome (PCOS). *PLoS ONE.* 2013;8(2):56263.
432. Livak KJ, Schmittgen TD. Analysis of relative gene expression data using real-time quantitative PCR and the $2^{-\Delta\Delta CT}$ method. *Methods.* 2001;25(4):402–408.
433. Ruijter JM, Pfaffl MW, Zhao S, Spiess AN, Boggy G, Blom J, et al. Evaluation of qPCR curve analysis methods for reliable biomarker discovery: Bias, resolution, precision, and implications. *Methods.* 2013;59(1):32–46.

References

434. The Rotterdam ESHRE/ASRM-sponsored PCOS consensus workshop group. Revised 2003 consensus on diagnostic criteria and long-term health risks related to polycystic ovary syndrome (PCOS). *Hum Reprod.* 2004;19(1):41–47.
435. Bates GW, Legro RS. Longterm management of polycystic ovarian syndrome (PCOS). *Mol Cell Endocrinol.* 2012;373(1-2):91–97.
436. Moran LJ, Teede HJ, Norman RJ. Metabolic risk in PCOS: phenotype and adiposity impact. *Trends Endocrinol Metab.* 2015;26(3):136–143.
437. Chen L, Xu WM, Zhang D. Association of abdominal obesity, insulin resistance, and oxidative stress in adipose tissue in women with polycystic ovary syndrome. *Fertility and Sterility.* 2014;102(4):1167–1174.
438. Zheng S-H, Li X-L. Visceral adiposity index as a predictor of clinical severity and therapeutic outcome of PCOS. *Gynecol Endocrinol.* 2015;32(3):177–183.
439. Androulakis II, Kandaraki E, Karachalios A, Christakou C, Marinakis E, Paterakis T, et al. Visceral adiposity index (VAI) is related to the severity of anovulation and other clinical features in women with polycystic ovary syndrome. *Clin Endocrinol.* 2014;81(3):426–431.
440. Messinis IE, Messini CL, Anifondis G, Dafopoulos K. Polycystic ovaries and obesity. *Best Prac Res Clin Obstet Gynaecol.* 2015;29(4):479–488.
441. Magnuson A, Foster M, Booth A. Detrimental and protective fat: body fat distribution and its relation to metabolic disease. *Horm Mol Biol Clin Investig.* 2014;17(1):13-27.
442. Serfaty D, Rein M, Schwarzfuchs D, Shelef I, Gepner Y, Bril N, et al. Abdominal fat sub-depots and energy expenditure: Magnetic resonance imaging study. *Clin Nutr.* 2017;36(3):804-811.
443. Park HT, Lee ES, Cheon Y-P, Lee DR, Yang K-S, Kim YT, et al. The relationship between fat depot-specific preadipocyte differentiation and metabolic syndrome in obese women. *Clin Endocrinol.* 2011;76(1):59–66.
444. McLaughlin T, Lamendola C, Liu A, Abbasi F. Preferential fat deposition in subcutaneous versus visceral depots is associated with insulin sensitivity. *J Clin Endocrinol Metab.* 2011;96(11):1756–1760.
445. Tran TT, Yamamoto Y, Gesta S, Kahn CR. Beneficial effects of subcutaneous fat transplantation on metabolism. *Cell Metabolism.* 2008;7(5):410–420.
446. Porter SA, Massaro JM, Hoffmann U, Vasani RS, O'Donnell CJ, Fox CS. Abdominal subcutaneous adipose tissue: A protective fat depot? *Diabetes Care.* 2009;32(6):1068–1075.
447. Hamdy O, Porramatikul S, Al-Ozairi E. Metabolic obesity: the paradox between visceral and subcutaneous fat. *Curr Diabetes Rev.* 2008;2(4):367–373.

References

448. Maliqueo M, Maliqueo M, Pérez-Bravo F, Galgani JE, Galgani JE, Pérez F, et al. Relationship of serum adipocyte-derived proteins with insulin sensitivity and reproductive features in pre-pubertal and pubertal daughters of polycystic ovary syndrome women. *Eur J Obstet Gynecol Reprod Biol.* 2012;161(1):56–61.
449. Goossens GH, Goossens GH. The role of adipose tissue dysfunction in the pathogenesis of obesity-related insulin resistance. *Physiol Behav.* 2007;94(2):206–218.
450. Lafontan M. Adipose tissue and adipocyte dysregulation. *Diabetes Metab.* 2014;40(1):16–28.
451. Galic S, Oakhill JS, Steinberg GR. Adipose tissue as an endocrine organ. *Mol Cell Endocrinol.* 2010;316(2):129–139.
452. Slawik M, Vidal-Puig AJ. Adipose tissue expandability and the metabolic syndrome. *Genes Nutr.* 2008;2(1):41–45.
453. Virtue S, Vidal-Puig A. Adipose tissue expandability, lipotoxicity and the metabolic syndrome-an allostatic perspective. *Biochim Biophys Acta.* 2010;1801(3):338–349.
454. Cristancho AG, Lazar MA. Forming functional fat: a growing understanding of adipocyte differentiation. *Nat Rev Mol Cell Biol.* 2011;12(11):722–734.
455. Rosen ED, MacDougald OA. Adipocyte differentiation from the inside out. *Nat Rev Mol Cell Biol.* 2006;7(12):885–896.
456. Ge K, Lee JE. Transcriptional and epigenetic regulation of PPAR γ expression during adipogenesis. *Cell Biosci.* 2014;4(1):29.
457. Galarraga M, Campión J, Muñoz-Barrutia A, Boqué N, Moreno H, Martínez JA, et al. Adiposoft: automated software for the analysis of white adipose tissue cellularity in histological sections. *J Lipid Res.* 2012;53(12):2791–2796.
458. Virtue S, Vidal-Puig A. It's not how fat you are, It's what you do with it that counts. *PLoS Biology.* 2008;6(9):237.
459. Kim JY, van de Wall E, Laplante M, Azzara A, Trujillo ME, Hofmann SM, et al. Obesity-associated improvements in metabolic profile through expansion of adipose tissue. *J Clin Invest.* 2007;117(9):2621–2637.
460. Gesta S, Tseng Y-H, Kahn CR. Developmental origin of fat: tracking obesity to its source. *Cell.* 2007;131(2):242–256.
461. Gustafson B, Hedjazifar S, Gogg S, Hammarstedt A, Smith U. Insulin resistance and impaired adipogenesis. *Trends Endocrinol Metab.* 2015;26(4):193–200.
462. Keller E, Chazenbalk GD, Aguilera P, Madrigal V, Elashoff D, Grogan T, et al. Impaired preadipocyte differentiation into adipocytes in subcutaneous abdominal adipose of PCOS-like female rhesus monkeys. *Endocrinology.* 2014;155(7):2696–2703.

References

463. Veiga-Lopez A, Moeller J, Patel D, Moeller J, Patel D, Ye W, et al. Developmental programming: impact of prenatal testosterone excess on insulin sensitivity, adiposity, and free fatty acid profile in postpubertal female sheep. *Endocrinology*. 2013;154(5):1731–1742.
464. Chang E, Park C-Y, Park SW. Role of thiazolidinediones, insulin sensitizers, in non-alcoholic fatty liver disease. *J Diabetes Investig*. 2013;4(6):517–524.
465. Westermark PO, Arner E, Bernard S, Bergmann O, Hoffstedt J, Blomqvist L, et al. Dynamics of fat cell turnover in humans. *Nature*. 2008;453(7196):783–787.
466. Singh P, Somers VK, Romero-Corral A, Sert-Kuniyoshi FH, Pusalavidyasagar S, Davison DE, et al. Effects of weight gain and weight loss on regional fat distribution. *Am J Clin Nutr*. 2012;96(2):229–233.
467. Gurr MI, Jung RT, Robinson MP, James WP. Adipose tissue cellularity in man: the relationship between fat cell size and number, the mass and distribution of body fat and the history of weight gain and loss. *Int J Obes*. 1982;6(5):419–436.
468. MacLean PS, Higgins JA, Giles ED, Sherk VD, Jackman MR. The role for adipose tissue in weight regain after weight loss. *Obesity Reviews*. 2015;16:45–54.
469. Lonn M, Mehlig K, Bengtsson C, Lissner L. Adipocyte size predicts incidence of type 2 diabetes in women. *FASEB J*. 2009;24(1):326–331.
470. Hammarstedt A, Graham TE, Kahn BB. Adipose tissue dysregulation and reduced insulin sensitivity in non-obese individuals with enlarged abdominal adipose cells. *Diabetol Metab Syndr*. 2012;4(1):42.
471. Kim JI, Huh JY, Sohn JH, Choe SS, Lee YS, Lim CY, et al. Lipid-overloaded enlarged adipocytes provoke insulin resistance independent of inflammation. *Mol Cell Biol*. 2015;35(10):1686–1699.
472. Manneras-Holm L, Leonhardt H, Kullberg J, Jennische E, Oden A, Holm G, et al. Adipose tissue has aberrant morphology and function in PCOS: Enlarged adipocytes and low serum adiponectin, but not circulating sex steroids, are strongly associated with insulin resistance. *J Clin Endocrinol Metab*. 2011;96(2):304–311.
473. Permana PA. Subcutaneous abdominal preadipocyte differentiation in vitro inversely correlates with central obesity. *Am J Physiol Endocrinol Metab*. 2004;286(6 49-6):958962.
474. Heilbronn L, Smith SR, Ravussin E. Failure of fat cell proliferation, mitochondrial function and fat oxidation results in ectopic fat storage, insulin resistance and type II diabetes mellitus. *Int J Obes Relat Metab Disord*. 2004;28:12–21.
475. Jack MM, Yang X, Cam MC, Jansson PA, Cushman SW, Carvalho E, et al. Evidence of impaired adipogenesis in insulin resistance. *Biochem Biophys Res Commun*. 2004;317(4):1045–1051.
476. Kokosar M, Benrick A, Perfilyev A, Fornes R, Nilsson E, Maliqueo M, et al. Epigenetic and transcriptional alterations in human adipose tissue of polycystic ovary syndrome. *Sci Rep*. 2016;6:22883.

References

477. Tontonoz P, Spiegelman BM. Fat and beyond: The diverse biology of PPAR γ . *Biochemistry*. 2008;77(1):289–312.
478. Adams M, Montague CT, Prins JB, Holder JC, Smith SA, Sanders L, et al. Activators of peroxisome proliferator-activated receptor gamma have depot-specific effects on human preadipocyte differentiation. *J Clin Invest*. 1997;100(12):3149–3153.
479. Carey DG, Cowin GJ, Galloway GJ, Jones NP, Richards JC, Biswas N, et al. Effect of rosiglitazone on insulin sensitivity and body composition in type 2 diabetic patients. *Obes Res*. 2012;10(10):1008–1015.
480. Lefebvre AM, Laville M, Vega N, Riou JP, van Gaal L, Auwerx J, et al. Depot-specific differences in adipose tissue gene expression in lean and obese subjects. *Diabetes*. 1998;47(1):98–103.
481. Degawa-Yamauchi M, Moss KA, Bovenkerk JE, Shankar SS, Morrison CL, Lelliott CJ, et al. Regulation of adiponectin expression in human adipocytes: Effects of adiposity, glucocorticoids, and tumor necrosis factor α . *Obes Res*. 2012;13(4):662–669.
482. Haque WA, Shimomura I, Matsuzawa Y, Garg A. Serum adiponectin and leptin levels in patients with lipodystrophies. *J Clin Endocrinol Metab*. 2002;87(5):2395–2395.
483. Lihn AS, Bruun JM, He G, Pedersen SB, Jensen PF, Richelsen B. Lower expression of adiponectin mRNA in visceral adipose tissue in lean and obese subjects. *Mol Cell Endocrinol*. 2004;219(1-2):9–15.
484. Kadowaki T. Adiponectin and adiponectin receptors in insulin resistance, diabetes, and the metabolic syndrome. *J Clin Invest*. 2006;116(7):1784–1792.
485. Lihn AS, Pedersen SB, Richelsen B. Adiponectin: action, regulation and association to insulin sensitivity. *Obesity Reviews*. 2005;6(1):13–21.
486. Fu Y, Fu Y, Luo N, Luo N, Klein RL, Klein RL, et al. Adiponectin promotes adipocyte differentiation, insulin sensitivity, and lipid accumulation. *J Lipid Res*. 2005;46(7):1369–1379.
487. do Carmo Avides M, Domingues L, Vicente A, Teixeira J. Differentiation of human pre-adipocytes by recombinant adiponectin. *Prot Express Purif*. 2008;59(1):122–126.
488. Mirza SS, Shafique K, Shaikh AR, Khan NA, Anwar Qureshi M, Qureshi MA. Association between circulating adiponectin levels and polycystic ovarian syndrome. *J Ovarian Res*. 2014;7(1):18.
489. Sharifi F, Hajhosseini R, Mazloomi S. Decreased adiponectin levels in polycystic ovary syndrome, independent of body mass index. *Metab Syndr Relat Disord*. 2010;8(1):47-52.

References

490. Cankaya S, Demir B, Aksakal SE, Dilbaz B, Demirtas C, Goktolga U. Insulin resistance and its relationship with high molecule weight adiponectin in adolescents with polycystic ovary syndrome and a maternal history. *Fertility and Sterility*. 2014;102(3):826–830.
491. Sarray S, Madan S, Saleh LR, Mahmoud N, Almawi WY. Validity of adiponectin-to-leptin and adiponectin-to-resistin ratios as predictors of polycystic ovary syndrome. *Fertility and Sterility*. 2015;104(2):460–466.
492. Al-Awadi AM, Sarray S, Arekat MR, Saleh LR, Mahmood N, Almawi WY. The high-molecular weight multimer form of adiponectin is a useful marker of polycystic ovary syndrome in Bahraini Arab women. *Clinical Nutrition ESPEN*. 2016;13:33–38.
493. Groth SW. Adiponectin and polycystic ovary syndrome. *Biol Res Nurs*. 2010;12(1):62–72.
494. Nishizawa H, Shimomura I, Kishida K, Maeda N, Kuriyama H, Nagaretani H, et al. Androgens decrease plasma adiponectin, an insulin-sensitizing adipocyte-derived protein. *Diabetes*. 2002;51(9):2734–2741.
495. Berra M, Armillotta F, D'Emidio L, Costantino A, Martorana G, Pelusi G, et al. Testosterone decreases adiponectin levels in female to male transsexuals. *Asian J Androl*. 2006;8(6):725–729.
496. Frederiksen L, Højlund K, Hougaard DM, Mosbech TH, Larsen R, Flyvbjerg A, et al. Testosterone therapy decreases subcutaneous fat and adiponectin in aging men. *Eur J Endocrinol*. 2012;166(3):469–476.
497. Page ST, Herbst KL, Amory JK, Coviello AD, Anawalt BD, Matsumoto AM, et al. Testosterone administration suppresses adiponectin levels in men. *J Androl*. 2004;26(1):85–92.
498. Riestra P, Garcia-Anguita A, Ortega L, Garces C. Relationship of adiponectin with sex hormone levels in adolescents. *Horm Res Paediatr*. 2013;79(2):83–87.
499. Böttner A, Kratzsch J, Müller G, Kapellen TM, Blüher S, Keller E, et al. Gender Differences of adiponectin levels develop during the progression of puberty and are related to serum androgen levels. *J Clin Endocrinol Metab*. 2004;89(8):4053–4061.
500. Comim FV, Hardy K, Franks S. Adiponectin and its receptors in the ovary: Further evidence for a link between obesity and hyperandrogenism in polycystic ovary syndrome. *PLoS ONE*. 2013;8(11):80416.
501. Maleszka A, Smolinska N, Nitkiewicz A, Kiezun M, Chojnowska K, Dobrzyn K, et al. Adiponectin expression in the porcine ovary during the oestrous cycle and its effect on ovarian steroidogenesis. *Int J Endocrinol*. 2014;2014(4):1–9.
502. Motoshima H, Wu X, Sinha MK, Hardy VE, Rosato EL, Barbot DJ, et al. Differential regulation of adiponectin secretion from cultured human omental and subcutaneous adipocytes: effects of insulin and rosiglitazone. *J Clin Endocrinol Metab*. 2002;87(12):5662–5667.

References

503. Fasshauer M, Klein J, Neumann S, Eszlinger M, Paschke R. Hormonal regulation of adiponectin gene expression in 3T3-L1 adipocytes. *Biochem Biophys Res Commun.* 2002;290(3):1084–1089.
504. Möhlig M, Wegewitz U, Osterhoff M, Isken F, Ristow M, Pfeiffer AFH, et al. Insulin decreases human adiponectin plasma levels. *Horm Metab Res.* 2002;34(11/12):655–658.
505. Matsubara M, Matsubara M, Katayose S, Katayose S, Maruoka S, Maruoka S. Decreased plasma adiponectin concentrations in nondiabetic women with elevated homeostasis model assessment ratios. *Eur J Endocrinol.* 2003;148(3):343–350.
506. Liu BH, Wang YC, Wu SC, Mersman HJ, Cheng WT, Gimig ST. Insulin regulates the expression of adiponectin and adiponectin receptors in porcine adipocytes. *Domest Anim Endocrinol.* 2008;34(4):352-359.
507. Brown LM, Clegg DJ. Central effects of estradiol in the regulation of food intake, body weight, and adiposity. *Journal Steroid Biochem Mol Biol.* 2010;122(1-3):65–73.
508. Edmunds SE, Stubbs AP, Santos AA, Wilkinson ML. Estrogen and androgen regulation of sex hormone binding globulin secretion by a human liver cell line. *J Steroid Biochem Mol Biol.* 1990;37(5):733–739.
509. Yasui T, Matsui S, Tani A, Kunimi K, Yamamoto S, Irahara M. Androgen in postmenopausal women. *J Med Invest.* 2012;59(1-2):12–27.
510. Elbers JMH, Elbers J, Asscheman H, Seidell JC. Long-term testosterone administration increases visceral fat in female to male transsexuals. *J Clin Endocrinol Metab.* 1997;82(7):2044-2047.
511. Elbers JM, de Jong S, Teerlink T, Asscheman H, Seidell JC, Gooren LJ. Changes in fat cell size and in vitro lipolytic activity of abdominal and gluteal adipocytes after a one-year cross-sex hormone administration in transsexuals. *Metabolism.* 1999;48(11):1371–1377.
512. Lee M-J, Pramyothin P, Karastergiou K, Fried SK. Deconstructing the roles of glucocorticoids in adipose tissue biology and the development of central obesity. *Biochem Biophys Acta.* 2013;1842(3):473–481.
513. Singh R, Artaza JN, Taylor WE, Braga M, Yuan X, Gonzalez-Cadavid NF, et al. Testosterone inhibits adipogenic differentiation in 3T3-L1 cells: nuclear translocation of androgen receptor complex with beta-catenin and T-cell factor 4 may bypass canonical Wnt signaling to down-regulate adipogenic transcription factors. *Endocrinology.* 2005;147(1):141–154.
514. Fujioka K, Fujioka K, Kajita K, Kajita K, Wu Z, Hanamoto T, et al. Dehydroepiandrosterone reduces preadipocyte proliferation via androgen receptor. *Am J Physiol Endocrinol Metab.* 2012;302(6):694–704.

References

515. Singh R, Artaza JN, Taylor WE, Bhasin S, Gonzalez-Cadavid NF. Androgens stimulate myogenic differentiation and inhibit adipogenesis in C3H 10T1/2 pluripotent cells through an androgen receptor-mediated pathway. *Endocrinology*. 2003;144(11):5081–5088.
516. Gupta V, Bhasin S, Guo W, Singh R, Miki R, Chauhan P, et al. Effects of dihydrotestosterone on differentiation and proliferation of human mesenchymal stem cells and preadipocytes. *Mol Cell Endocrinol*. 2008;296(1-2):32–40.
517. McNelis JC, Manolopoulos KN, Gathercole LL, Bujalska IJ, Stewart PM, Tomlinson JW, et al. Dehydroepiandrosterone exerts antiglucocorticoid action on human preadipocyte proliferation, differentiation, and glucose uptake. *Am J Physiol Endocrinol Metab*. 2013;305(9):1134–1144.
518. Blouin K, Nadeau M, Perreault M, Veilleux A, Drolet R, Marceau P, et al. Effects of androgens on adipocyte differentiation and adipose tissue explant metabolism in men and women. *Clin Endocrinol*. 2010;72(2):176–188.
519. Jeong S, Yoon M. 17 β -Estradiol inhibition of PPAR γ -induced adipogenesis and adipocyte-specific gene expression. *Acta Pharmacol Sin*. 2011;32(2):230–238.
520. Zhang R, Su D, Zhu W, Huang Q, Liu M, Xue Y, et al. Estrogen suppresses adipogenesis by inhibiting S100A16 expression. *J Mol Endocrinol*. 2014;52(3):235–244.
521. Roncari DA, Van RL. Promotion of human adipocyte precursor replication by 17 β -estradiol in culture. *J Clin Invest*. 1978;62(3):503–508.
522. Dieudonne MN, Pecquery R, Leneuve MC, Giudicelli Y. Opposite effects of androgens and estrogens on adipogenesis in rat preadipocytes: Evidence for sex and site-related specificities and possible involvement of insulin-like growth factor 1 receptor and peroxisome proliferator-activated receptor. *Endocrinology*. 2000;141(2):649–656.
523. Tomlinson JJ, Boudreau A, Wu D, Atlas E, Haché RJG. Modulation of early human preadipocyte differentiation by glucocorticoids. *Endocrinology*. 2006;147(11):5284–5293.
524. Pantoja C, Huff JT, Yamamoto KR. Glucocorticoid signaling defines a novel commitment state during adipogenesis in vitro. *Mol Biol Cell*. 2008;19(10):4032–4041.
525. Ayala JT, Ayala-Sumuano J-T, Velez-delValle C, Beltrán-Langarica A, Marsch-Moreno M, Hernandez-Mosqueira C, et al. Glucocorticoid paradoxically recruits adipose progenitors and impairs lipid homeostasis and glucose transport in mature adipocytes. *Sci Rep*. 2013;3:2573.
526. Campbell JE, Peckett AJ, D'souza AM, Hawke TJ, Riddell MC. Adipogenic and lipolytic effects of chronic glucocorticoid exposure. *AJP: Cell Physiology*. 2010;300(1):C198–C209.
527. Marsden PJ, Murdoch AP, Taylor R. Tissue insulin sensitivity and body weight in polycystic ovary syndrome. *Clin Endocrinol*. 2001;55(2):191–199.

References

528. User N, Abel ED, Peroni O, Kim JK, Kim YB, Hadro E, et al. Adipose-selective targeting of the GLUT4 gene impairs insulin action in muscle and liver. *Nature*. 2001;409(6821):729–733.
529. Smith U. Impaired ('diabetic') insulin signaling and action occur in fat cells long before glucose intolerance- is insulin resistance initiated in the adipose tissue? *Int J Obes*. 2002;26(7):897–904.
530. Carvalho E, Carvalho E, Jansson P-A, Nagaev I, Wentzel A-M, Smith U. Insulin resistance with low cellular IRS-1 expression is also associated with low GLUT4 expression and impaired insulin-stimulated glucose transport. *The FASEB journal*. 2001;15(6):1401-103.
531. Zhang HH, Huang J, Düvel K, Boback B, Wu S, Squillace RM, et al. Insulin stimulates adipogenesis through the Akt-TSC2-mTORC1 pathway. *cPLoS ONE*. 2009;4(7):6189.
532. Groeneveld MP, Brierley GV, Rocha NM, Siddle K, Semple RK. Acute knockdown of the insulin receptor or its substrates Irs1 and 2 in 3T3-L1 adipocytes suppresses adiponectin production. *Sci Rep*. 2016;6:21105.
533. Cinti S, Eberbach S, Castellucci M, Accili D. Lack of insulin receptors affects the formation of white adipose tissue in mice. A morphometric and ultrastructural analysis. *Diabetologia*. 1998;41(2):171–177.
534. Miki H, Yamauchi T, Suzuki R, Komeda K, Kubota N, Tsuchida A, et al. Essential role of insulin receptor substrate 1 (IRS-1) and IRS-2 in adipocyte differentiation. *Mol Cell Biol*. 2001;21(7):2521–2532.
535. Hannon TS, Janosky J, Arslanian SA. Longitudinal study of physiologic insulin resistance and metabolic changes of puberty. *Pediatr Res*. 2006;60(6):759–763.
536. Goran MI, Gower BA. Longitudinal study on pubertal insulin resistance. *Diabetes*. 2001;50(11):2444-2450.
537. Sam S. Obesity and polycystic ovary syndrome. *Obes Manag*. 2007;3(2):69–73.
538. Lim SS, Davies MJ, Norman RJ, Moran LJ. Overweight, obesity and central obesity in women with polycystic ovary syndrome: a systematic review and meta-analysis. *Hum Reprod Update*. 2012;18(6):618–37.
539. Ezeh U, Pall M, Mathur R, Azziz R. Association of fat to lean mass ratio with metabolic dysfunction in women with polycystic ovary syndrome. *Hum Reprod*. 2014;29(7):1508-1517.
540. Huang ZH, Manickam B, Ryvkin V. PCOS is associated with increased CD11c expression and crown-like structures in adipose tissue and increased central abdominal fat depots independent of obesity. *J Clin Endocrinol Metab*. 2012;98(1):17-24.

References

541. Borruel S, Fernandez-Duran E, Alpanes M, Marti D, Alvarez-Blasco F, Luque-Ramirez M, et al. Global adiposity and thickness of intraperitoneal and mesenteric adipose tissue depots are increased in women with polycystic ovary syndrome (PCOS). *J Clin Endocrinol Metab.* 2013;98(3):1254–1263.
542. Cosar E, Üçok K, Sahin FK, Köken G, Akgün L, Arioz DT, et al. Body fat composition and distribution in women with polycystic ovary syndrome. *Gynecol Endocrinol.* 2008;24(8):428432.
543. Dokras A, Sarwer DB, Allison KC, Milman L, Kris-Etherton PM, Kunselman AR, et al. Weight loss and lowering androgens predict improvements in health-related quality of life in women with PCOS. *J Clin Endocrinol Metab.* 2016;101(8):2966–2974.
544. Legro RS, Dodson WC, Kris-Etherton PM, Kunselman AR, Stetter CM, Williams NI, et al. Randomized controlled trial of preconception interventions in infertile women with polycystic ovary syndrome. *J Clin Endocrinol Metab.* 2015;100(11):4048–4058.
545. Azziz R, Carmina E, Chen Z, Dunaif A, Laven JSE, Legro RS, et al. Polycystic ovary syndrome. *Nat Rev Dis Primers.* 2016;2:16057.
546. Larsson I, Hulthén L, Landén M, Pålsson E, Janson P, Stener-Victorin E. Dietary intake, resting energy expenditure, and eating behavior in women with and without polycystic ovary syndrome. *Clin Nutr.* 2015;35(1):213–218.
547. Wright CE, Zborowski JV, Talbott EO. Dietary intake, physical activity, and obesity in women with polycystic ovary syndrome. *Intl J Obes.* 2004;28(8):1026-1032.
548. Coffey S, Bano G, Mason HD. Health-related quality of life in women with polycystic ovary syndrome: a comparison with the general population using the Polycystic Ovary Syndrome Questionnaire (PCOSQ) and the Short Form-36 (SF-36). *Gynecol Endocrinol.* 2006;22(2):80–86.
549. Churchill SJ, Wang ET, Bhasin G, Alexander C, Bresee C, Pall M, et al. Basal metabolic rate in women with PCOS compared to eumenorrheic controls. *Clinical Endocrinology.* 2015;83(3):384–388.
550. Cosar E, Köken G, Sahin FK, Akgün L, Üçok K, Genç A, et al. Resting metabolic rate and exercise capacity in women with polycystic ovary syndrome. *Int J Gynecol Obstet.* 2008;101(1):31-34.
551. Segal KR, Dunaif A. Resting metabolic rate and postprandial thermogenesis in polycystic ovarian syndrome. *Int J Obes.* 1990;14(7):559–567.
552. Saito M. Brown adipose tissue as a regulator of energy expenditure and body fat in humans. *Diabetes Metab J.* 2013;37(1):22–29.
553. Dulloo AG, Seydoux J, Jacquet J. Adaptive thermogenesis and uncoupling proteins: a reappraisal of their roles in fat metabolism and energy balance. *Phys Behav.* 2004;83(4):587–602.

References

554. Lowell BB, Spiegelman BM. Towards a molecular understanding of adaptive thermogenesis. *Nature*. 2000;404(6778):652–660.
555. Watanabe T, Nomura M, Nakayasu K, Kawano T, Ito S, Nakaya Y. Relationships between thermic effect of food, insulin resistance and autonomic nervous activity. *J Med Invest*. 2006;53(1-2):153–158.
556. Binns A, Gray M, Di Brezzo R. Thermic effect of food, exercise, and total energy expenditure in active females. *J Sci Med Sport*. 2015;18(2):204-208.
557. Schutz Y, Bessard T, Jéquier E. Diet-induced thermogenesis measured over a whole day in obese and nonobese women. *Am J Clin Nutr*. 1984;40(3):542–52.
558. Smith RE, Horwitz BA. Brown fat and thermogenesis. *Physiol Rev*. 1969;40(2):320–425.
559. Kajimura S, Saito M. A new era in brown adipose tissue biology: Molecular control of brown fat development and energy homeostasis. *Annu Rev Physiol*. 2014;76(1):225–249.
560. Bargut TCL, Aguila MB, Mandarim-de-Lacerda CA. Brown adipose tissue: Updates in cellular and molecular biology. *Tissue and Cell*. 2016;48(5):452-460.
561. Morrison SF, Madden CJ, Tupone D. Central neural regulation of brown adipose tissue thermogenesis and energy expenditure. *Cell Metabolism*. 2014;19(5):741–756.
562. Nedergaard J, Cannon B. UCP1 mRNA does not produce heat. *Biochim Biophys Acta*. 2013;1831(5):943-949.
563. Lee P, Ho KY, Swarbrick MM. Brown adipose tissue in adult humans: A metabolic renaissance. *Endocrine Reviews*. 2013;34(3):413-438.
564. Seale P, Bjork B, Yang W, Kajimura S, Chin S, Kuang S, et al. PRDM16 controls a brown fat/skeletal muscle switch. *Nature*. 2008;454(7207):961–967.
565. Timmons JA, Wennmalm K, Larsson O, Walden TB, Lassmann T, Petrovic N, et al. Myogenic gene expression signature establishes that brown and white adipocytes originate from distinct cell lineages. *Proc Natl Acad Sci USA*. 2007;104(11):4401-4406.
566. Kubota K, Gygi SP, Spiegelman BM, Kajimura S, Lunsford E, Frangioni JV, et al. Initiation of myoblast to brown fat switch by a PRDM16-C/EBP- β transcriptional complex. *Nature*. 2009;460(7259):1154-1158.
567. Wu J, Boström P, Sparks LM, Ye L, Choi JH, Giang AH, et al. Beige adipocytes are a distinct type of thermogenic fat cell in mouse and human. *Cell*. 2012;150(2):366-376.
568. Nigro M, Santos AT, Barthem CS, Louzada RAN, Fortunato RS, Ketzer LA, et al. A change in liver metabolism but not in brown adipose tissue thermogenesis is an early event in ovariectomy-induced obesity in rats. *Endocrinology*. 2014;155(8):2881–2891.

References

569. Ohno H, Shinoda K, Spiegelman BM, Kajimura S. PPAR γ agonists induce a white-to-brown fat conversion through stabilization of PRDM16 protein. *Cell Metab.* 2012;15(3):395-404.
570. Schulz TJ, Huang TL, Tran TT, Zhang H, Townsend KL, Shadrach JL, et al. Identification of inducible brown adipocyte progenitors residing in skeletal muscle and white fat. *PNAS.* 2011;108(1):143–148.
571. Walden TB, Hansen IR, Timmons JA. Recruited vs. nonrecruited molecular signatures of brown, “brite,” and white adipose tissues. *AJP: Endocrinol Metab.* 2012;302(1):19-31.
572. Sharp LZ, Shinoda K, Ohno H, Scheel DW, Tomoda E, Ruiz L, et al. Human BAT possesses molecular signatures that resemble beige/brite cells. *PLoS ONE.* 2012;7(11):49452.
573. Rothwell NJ, Stock MJ. Luxuskonsumtion, diet-induced thermogenesis and brown fat: the case in favour. *Clin Sci.* 1983;64(1):19–23.
574. Tseng Y-H, Cypess AM, Kahn CR. Cellular bioenergetics as a target for obesity therapy. *Nat Rev Drug Discov.* 2010 ;9(6):465–482.
575. Rothwell NJ, Stock MJ. A role for brown adipose tissue in diet-induced thermogenesis. *Nature.* 1979;281(5726):31–35.
576. Ouellet V, Routhier A. Outdoor temperature, age, sex, body mass index, and diabetic status determine the prevalence, mass, and glucose-uptake activity of 18F-FDG-detected BAT in humans. *J Clin Endocrinol Metab.* 2011;96(1):192-199.
577. Symonds ME, Pope M, Sharkey D, Budge H. Adipose tissue and fetal programming. *Diabetologia.* 2012;55(6):1597–1606.
578. Bessard T, Schutz Y, Jéquier E. Energy expenditure and postprandial thermogenesis in obese women before and after weight loss. *Am J Clin Nutr.* 1983;38(5):680–693.
579. Henry BA, Loughnan R, Hickford J, Young IR, John JCS, Clarke I. Differences in mitochondrial DNA inheritance and function align with body conformation in genetically lean and fat sheep. *J Anim Sci.* 2015;93(5):2083–2093.
580. Brandon LJ, Granata GP. The thermic effect of food and obesity: Discrepant results and methodological variations. *Nutrition Reviews.* 2002;60(8):223–333.
581. Wang TW, Chao JC, Wei HJ, Ho HJ, Hsu CY, Tsai YH, et al. Dietary intake, glucose metabolism and sex hormones in women with polycystic ovary syndrome (PCOS) compared with women with non-PCOS-related infertility. *Br J Nutr.* 2013;109(12):2190-2198.
582. Ahmadi A, Akbarzadeh M, Mohammadi F, Akbari M, Jafari B, Tolide-Ie HR. Anthropometric characteristics and dietary pattern of women with polycystic ovary syndrome. *Indian J Endocrinol Metab.* 2013;17(4):672–676.

References

583. Alves BC, Spritzer PM, Mário FM, Graff SK. Dietary glycemic index is associated with less favorable anthropometric and metabolic profiles in polycystic ovary syndrome women with different phenotypes. *Fertility and Sterility*. 2013;100(4):1081-1088.
584. Toscani MK, Mario FM, Radavelli-Bagatini S, Spritzer PM. Insulin resistance is not strictly associated with energy intake or dietary macronutrient composition in women with polycystic ovary syndrome. *Nutrition Research*. 2011;31(2):97-103.
585. Altieri P, Cavazza C, Pasqui F, Morselli AM, Gambineri A, Pasquali R. Dietary habits and their relationship with hormones and metabolism in overweight and obese women with polycystic ovary syndrome. *Clin Endocrinol*. 2012;78(1):52–59.
586. Gower BA, Douglas CC, Norris LE, Azziz R, Darnell BE, Oster RA. Difference in dietary intake between women with polycystic ovary syndrome and healthy controls. *Fertility and Sterility*. 2006;86(2):411-417.
587. Alvarez-Blasco F, Luque-Ramirez M, Escobar-Morreale HF. Diet composition and physical activity in overweight and obese premenopausal women with or without polycystic ovary syndrome. *Gynecol Endocrinol*. 2011;27(12):978–81.
588. Shishehgar F, Tehrani FR, Mirmiran P, Hajian S, Baghestani AR, Moslehi N. Factors influencing physical activity in women with polycystic ovary syndrome in comparison to eumenorrheic non hirsute women. *Glob J Health Sci*. 2016;8(10):56382.
589. Diamanti-Kandarakis E. Insulin Resistance in PCOS. *Endocrine*. 2006;30(1):13-17.
590. Dunaif A. Insulin resistance and the polycystic ovary syndrome: Mechanism and implications for pathogenesis. *Endocrine Reviews*. 1997;18(6):774-800.
591. Galluzzo A, Amato MC, Giordano C. Insulin resistance and polycystic ovary syndrome. *Nutr Metab Cardiovasc Dis*. 2008;18(7):511–518.
592. DeUgarte CM, Bartolucci AA, Azziz R. Prevalence of insulin resistance in the polycystic ovary syndrome using the homeostasis model assessment. *Fertility and Sterility*. 2005;83(5):1454-1460.
593. Ciampelli M, Fulghesu AM, Cucinelli F, Pavone V, Caruso A, Mancuso S, et al. Heterogeneity in beta cell activity, hepatic insulin clearance and peripheral insulin sensitivity in women with polycystic ovary syndrome. *Hum Reprod*. 1997;12(9):1897–1901.
594. Holte J, Bergh T, Berne C, Berglund L, Lithell H. Enhanced early insulin response to glucose in relation to insulin resistance in women with polycystic ovary syndrome and normal glucose tolerance. *J Clin Endocrinol Metab*. 1994;78(5):1052–1058.
595. Goodarzi MO, Erickson S, Port SC, Jennrich RI, Korenman SG. Beta-cell function: a key pathological determinant in polycystic ovary syndrome. *J Clin Endocrinol Metab*. 2004;90(1):310–315.

References

596. Ramaswamy S, Grace C, Mattei AA, Siemienowicz K, Brownlee W, MacCallum J, et al. Developmental programming of polycystic ovary syndrome (PCOS): prenatal androgens establish pancreatic islet α/β cell ratio and subsequent insulin secretion. *Sci Rep*. 2016;6:27408.
597. Nicol LE, O'Brien TD, Dumesic DA, Grogan T, Tarantal AF, Abbott DH. Abnormal infant islet morphology precedes insulin resistance in PCOS-like monkeys. *PLoS ONE*. 2014;9(9):106527.
598. Shanik MH, Xu Y, Škrha J, Dankner R, Zick Y. Insulin resistance and hyperinsulinemia is hyperinsulinemia the cart or the horse? *Diabetes Care*. 2008;31:262-268.
599. Ravussin E, Acherson KJ, Vernet O, Danforth E, Jequier E. Evidence that insulin resistance is responsible for the decreased thermic effect of glucose in human obesity. *J Clin Invest*. 1985;76(3):1268-1273.
600. Del Prato S, Rett K, Weck M, Bonora E, Ferrannini E, Camastra S. Effect of obesity and insulin resistance on resting and glucose-induced thermogenesis in man. *Int J Obes*. 1999;23(12):1307-1313.
601. Robinson S, Niththyanathan R, Anyaoku V, Elkeles R, Beard R, Johnston DG. Reduced postprandial energy expenditure in women predisposed to type 2 diabetes. *Diabet Med*. 1994;11(6):545-550.
602. Golay A. Blunted glucose-induced thermogenesis: a factor contributing to relapse of obesity. *Int J Obes Relat Metab Disord*. 1993;17:23-27.
603. Gumbiner B, Thorburn AW, Henry RR. Reduced glucose-induced thermogenesis is present in noninsulin-dependent diabetes mellitus without obesity. *J Clin Endocrinol Metab*. 1991;72(4):801-807.
604. Benedict C, Brede S, Schioth HB, Lehnert H, Schultes B, Born J, et al. Intranasal insulin enhances postprandial thermogenesis and lowers postprandial serum insulin levels in healthy men. *Diabetes*. 2010;60(1):114-118.
605. Laron Z. Insulin and the brain. *Arch Physiol Biochem*. 2009;115(2):112-116.
606. Cetinkalp S, Simsir IY, Ertek S. Insulin resistance in brain and possible therapeutic approaches. *Curr Vascul Pharmacol*. 2014;12(4):553-564.
607. Hallschmid M, Schultes B. Central nervous insulin resistance: a promising target in the treatment of metabolic and cognitive disorders? *Diabetologia*. 2009;52(11):2264-2269.
608. Sanchez-Alavez M, Tabarean IV, Osborn O, Mitsukawa K, Schaefer J, Dubins J, et al. Insulin causes hyperthermia by direct inhibition of warm-sensitive neurons. *Diabetes*. 2009;59(1):43-50.
609. Shibata H, Pérusse F, Bukowiecki LJ. The role of insulin in nonshivering thermogenesis. *Can J Physiol Pharmacol*. 1987;65(2):152-158.

References

610. Orava J, Nuutila P, Lidell ME, Oikonen V, Nojonen T, Viljanen T, et al. Different metabolic responses of human brown adipose tissue to activation by cold and insulin. *Cell Metabolism*. 2011;14(2):272–279.
611. Hitchcox KM, Townsend KL, Nygaard EB, Nakano K, Markan KR, Middelbeek RJ, et al. Brown adipose tissue regulates glucose homeostasis and insulin sensitivity. *J Clin Invest*. 2013;123(1):215–223.
612. Cantó C, Auwerx J. PGC-1 α , SIRT1 and AMPK, an energy sensing network that controls energy expenditure. *Curr Opin Lipidol*. 2009;20(2):98–105.
613. Liang H, Ward WF. PGC-1 α : a key regulator of energy metabolism. *Adv Physiol Educ*. 2006;30(4):145–151.
614. Tiraby C, Tavernier G, Lefort C, Larrouy D, Bouillaud F, Ricquier D, et al. Acquisition of brown fat cell features by human white adipocytes. *J Biol Chem*. 2003;278(35):33370–33376.
615. Leone TC, Saffitz JE, Lehman JJ, Finck BN, Semenkovich CF, Schmidt RE, et al. PGC-1 α deficiency causes multi-system energy metabolic derangements: Muscle dysfunction, abnormal weight control and hepatic steatosis. *PLoS Biology*. 2005;3(4):101.
616. Boutant M, Cantó C. SIRT1: A novel guardian of brown fat against metabolic damage. *Obesity*. 2016;24(3):554.
617. Nemoto S, Fergusson MM, Finkel T. SIRT1 functionally interacts with the metabolic regulator and transcriptional coactivator PGC-1 α . *J Biol Chem*. 2005;280(16):16456–16460.
618. Rodgers JT, Lerin C, Haas W, Gygi SP. Nutrient control of glucose homeostasis through a complex of PGC-1 α and SIRT1. *Nature*. 2005;434(7029):113–118.
619. Cantó C, Auwerx J. Targeting Sirtuin 1 to improve metabolism: All you need is NAD(+)? *Pharmacol Rev*. 2012;64(1):166–187.
620. Boutant M, Joffraud M, Kulkarni SS, García-Casarrubios E, García-Roves PM, Ratajczak J, et al. SIRT1 enhances glucose tolerance by potentiating brown adipose tissue function. *Molecular Metabolism*. 2014;4(2):118–131.
621. Qiang L, Wang L, Kon N, Zhao W, Lee S, Zhang Y, et al. Brown remodeling of white adipose tissue by Sirt1-dependent deacetylation of Ppar γ . *Cell*. 2012;150(3):620–632.
622. Pfluger PT, Herranz D, Velasco-Miguel S, Serrano M, Tschöp MH. Sirt1 protects against high-fat diet-induced metabolic damage. *Proc Natl Acad Sci USA*. 2008;105(28):9793–9798.
623. Xu F, Zheng X, Lin B, Liang H, Cai M, Cao H, et al. Diet-induced obesity and insulin resistance are associated with brown fat degeneration in SIRT1-deficient mice. *Obesity*. 2016;24(3):634–642.

References

624. Harms M, Seale P. Brown and beige fat: development, function and therapeutic potential. *Nat Med.* 2013;19(10):1252–1263.
625. Lee M-W, Odegaard JI, Mukundan L, Qiu Y, Molofsky AB, Nussbaum JC, et al. Activated type 2 innate lymphoid cells regulate beige fat biogenesis. *Cell.* 2014;160(1-2):74–87.
626. Rothwell NJ, Stock MJ. Regulation of energy balance. *Annu Rev Nutr.* 1981;1:235–256.
627. Nedergaard J, Raasmaja A, Cannon B. Parallel increases in amount of (3H)GDP binding and thermogenin antigen in brown-adipose-tissue mitochondria of cafeteria-fed rats. *Biochem Biophys Res Commun.* 1984;122(3):1328-1336.
628. Apfelbaum M, Falcou R, Ricquier D, Bouillaud F, Mory G. Increase of uncoupling protein and its mRNA in brown adipose tissue of rats fed on “cafeteria diet.” *Biochem J.* 1985;231(1):241-244.
629. Trayhurn P, Fuller L. The development of obesity in genetically diabetic-obese (db/db) mice pair-fed with lean siblings. *Diabetologia.* 1980;19(2):148-153.
630. Thurlby PL, Trayhurn P. The role of thermoregulatory thermogenesis in the development of obesity in genetically-obese (ob/ob) mice pair-fed with lean siblings. *Br J Nutr.* 1979;42(03):377-385.
631. Ashwell M, Holt S, Jennings G, Stirling DM. Measurement by radioimmunoassay of the mitochondrial uncoupling protein from brown adipose tissue of obese (ob/ob) mice and Zucker (fa/fa) rats at different ages. *FEBS Letters.* 1985;179(2):233-237.
632. Knehans AW, Romsos DR. Reduced norepinephrine turnover in brown adipose tissue of ob/ob mice. *Am J Physiol.* 1982;242(4):253–261.
633. Boyer BB, Himms-Hagen J, Flier JS, Hamann A, Kozak LP, Lowell BB, et al. Development of obesity in transgenic mice after genetic ablation of brown adipose tissue. *Nature.* 1993;366(6457):740-742.
634. Feldmann HM, Golozoubova V, Cannon B, Nedergaard J. UCP1 ablation induces obesity and abolishes diet-induced thermogenesis in mice exempt from thermal stress by living at thermoneutrality. *Cell Metabolism.* 2009;9(2):203–209.
635. Trayhurn P. Origins and early development of the concept that brown adipose tissue thermogenesis is linked to energy balance and obesity. *Biochimie.* 2017;134:62-70.
636. Nagai N, Sakane N, Ueno LM. The– 3826 A→ G variant of the uncoupling protein-1 gene diminishes postprandial thermogenesis after a high fat meal in healthy boys. *J Clin Endocrinol Metab.* 2003;88(12):5661-5667.
637. Lee P, Smith S, Linderman J, Courville AB, Brychta RJ, Dieckmann W, et al. Temperature-acclimated brown adipose tissue modulates insulin sensitivity in humans. *Diabetes.* 2014;63(11):3686–98.

References

638. Chechi K, van Marken Lichtenbelt WD, Richard D. Brown and beige adipose tissue: phenotype and metabolic potential in mice and men. *J Appl Physiol.* 2017;10:1152.
639. Hibi M, Oishi S, Matsushita M, Yoneshiro T, Yamaguchi T, Usui C, et al. Brown adipose tissue is involved in diet-induced thermogenesis and whole-body fat utilization in healthy humans. *Int J Obes.* 2016;40(11):1655-1661.
640. Azzu V, Brand MD. The on-off switches of the mitochondrial uncoupling proteins. *Trends Biochem Sci.* 2009;35(5):298–307.
641. Esteves TC, Brand MD. The reactions catalysed by the mitochondrial uncoupling proteins UCP2 and UCP3. *Biochim Biophys Acta.* 2005;1709(1):35–44.
642. Bouillaud F, Alves-Guerra M-C, Ricquier D. UCPs, at the interface between bioenergetics and metabolism. *Biochim Biophys Acta.* 2016;1863(10):2443–2456.
643. Fleury C, Neverova M, Collins S, Raimbault S, Champigny O, Levi-Meyrueis C, et al. Uncoupling protein-2: a novel gene linked to obesity and hyperinsulinemia. *Nature.* 1997;15(3):269–272.
644. Costford SR, Chaudhry SN, Crawford SA, Salkhordeh M, Harper M-E. Long-term high-fat feeding induces greater fat storage in mice lacking UCP3. *AJP: Endocrinol Metab.* 2008;295(5):1018–1024.
645. Fuller PM, Warden CH, Barry SJ, Fuller CA. Effects of 2-G exposure on temperature regulation, circadian rhythms, and adiposity in UCP2/3 transgenic mice. *J Appl Physiol.* 2000;89(4):1491–1498.
646. Horvath TL, Diano S, Miyamoto S, Barry S, Gatti S, Alberati D, et al. Uncoupling proteins-2 and 3 influence obesity and inflammation in transgenic mice. *Int J Obes Relat Metab Disord.* 2003;27(4):433–442.
647. Brondani LA, Assmann TS, de Souza BM, Bouças AP, Canani LH, Crispim D. Meta-analysis reveals the association of common variants in the uncoupling protein (UCP) 1-3 genes with body mass index variability. *PLoS ONE.* 2014;9(5):96411.
648. Xu X, Liu X, Gu R, Qian L, Xu K, Yang T, et al. UCP2 -866G/A, Ala55Val and UCP3 -55C/T polymorphisms in association with obesity susceptibility - a meta-analysis study. *PLoS ONE.* 2013;8(4):58939.
649. Acosta A, Camilleri M, Shin A, Vazquez-Roque MI, Iturrino J, Lanza IR, et al. Association of UCP-3 rs1626521 with obesity and stomach functions in humans. *Obesity.* 2015;23(4):898–906.
650. Zhang CY, Baffy G, Perret P, Krauss S, Peroni O, Grujic D, et al. Uncoupling protein-2 negatively regulates insulin secretion and is a major link between obesity, beta cell dysfunction, and type 2 diabetes. *Cell.* 2001;105(6):745–755.
651. Vidal-Puig AJ, Grujic D, Zhang CY, Hagen T, Boss O, Ido Y, et al. Energy metabolism in uncoupling protein 3 gene knockout mice. *J Biol Chem.* 2000;275(21):16258–16266.

References

652. Kurylowicz A, Jonas M, Wicik Z, Chmura A, Jonas M, Puzianowska-Kuznicka M, et al. Obesity is associated with a decrease in expression but not with the hypermethylation of thermogenesis-related genes in adipose tissues. *J Translat Med.* 2015;13(1):31.
653. Affourtit C, Crichton PG, Parker N, Brand MD. Novel uncoupling proteins. *Novartis Foundation Symposium.* 2007;287:70-80.
654. Samec S, Seydoux J, Dulloo AG. Interorgan signaling between adipose tissue metabolism and skeletal muscle uncoupling protein homologs: is there a role for circulating free fatty acids? *Diabetes.* 1998;47(11):1693-1698.
655. Bezaire V, Spriet LL, Campbell S, Sabet N, Gerrits M, Bonen A, et al. Constitutive UCP3 overexpression at physiological levels increases mouse skeletal muscle capacity for fatty acid transport and oxidation. *FASEB J.* 2005;19(8):977-979.
656. Khalfallah Y, Fages S, Laville M, Langin D, Vidal H. Regulation of uncoupling protein-2 and uncoupling protein-3 mRNA expression during lipid infusion in human skeletal muscle and subcutaneous adipose tissue. *Diabetes.* 2000;49(1):25-31.
657. Shabalina IG, Hoeks J, Kramarova TV, Schrauwen P, Cannon B, Nedergaard J. Cold tolerance of UCP1-ablated mice: a skeletal muscle mitochondria switch toward lipid oxidation with marked UCP3 up-regulation not associated with increased basal, fatty acid- or ROS-induced uncoupling or enhanced GDP effects. *Biochem Biophys Acta.* 2010;1797(6-7):968-980.
658. Hilse KE, Kalinovich AV, Rupprecht A, Smorodchenko A, Zeitz U, Staniek K, et al. The expression of UCP3 directly correlates to UCP1 abundance in brown adipose tissue. *Biochim Biophys Acta.* 2016;1857(1):72-78.
659. Thompson MP, Kim D. Links between fatty acids and expression of UCP2 and UCP3 mRNAs. *FEBS Letters.* 2004;568(1-3):4-9.
660. Fedorenko A, Lishko PV, Kirichok Y. Mechanism of fatty-acid-dependent UCP1 uncoupling in brown fat mitochondria. *Cell.* 2012;151(2):400-413.
661. Zurlo F, Lillioja S, Esposito-Del Puente A, Nyomba BL, Raz I, Saad MF, et al. Low ratio of fat to carbohydrate oxidation as predictor of weight gain: Study of 24-h RQ. *Am J Physiol.* 1990;259(5 22-5):650-657.
662. Ellis AC, Hyatt TC, Hunter GR, Gower BA. Respiratory quotient predicts fat mass gain in premenopausal women. *Obesity.* 2010;18(12):2255-2259.
663. Bachman ES, Dhillon H, Zhang CY, Cinti S, Bianco AC, Kobilka BK, Lowell BB. Beta AR signaling required for diet-induced thermogenesis and obesity resistance. *Science.* 2002;297(5582):843-845.
664. Wijers SLJ, Saris WHM, van Marken Lichtenbelt WD. Individual thermogenic responses to mild cold and overfeeding are closely related. *J Clin Endocrinol Metab.* 2007;92(11):4299-4305.

References

665. Welle S, Lilavivat U, Campbell RG. Thermic effect of feeding in man: Increased plasma norepinephrine levels following glucose but not protein or fat consumption. *Metabolism*. 1981;30(10):953-958.
666. Glick Z, Raum WJ. Norepinephrine turnover in brown adipose tissue is stimulated by a single meal. *Am JP*. 1986;251(1):13-17.
667. Schwartz RS, Jaeger LF, Silberstein S, Veith RC. Sympathetic nervous system activity and the thermic effect of feeding in man. *IntJ Obes*. 1987;11(2):141-149.
668. Lansdown A, Rees DA. The sympathetic nervous system in polycystic ovary syndrome: a novel therapeutic target? *Clinical Endocrinology*. 2012;77(6):791-801.
669. Ek I, Arner P, Bergqvist A, Carlström K, Wahrenberg H. Impaired adipocyte lipolysis in nonobese women with the polycystic ovary syndrome: A possible link to insulin resistance? *J Clin Endocrinol Metab*. 1997;82(4):1147-1153.
670. Gennarelli G, Holte J, Stridsberg M, Niklasson F, Berne C, Bäckström T. The counterregulatory response to hypoglycaemia in women with the polycystic ovary syndrome. *Clinical Endocrinology*. 1997;46(2):167-174.
671. Rahmouni K, Morgan DA, Morgan GM, Liu X, Sigmund CD, Mark AL, et al. Hypothalamic PI3K and MAPK differentially mediate regional sympathetic activation to insulin. *J Clin Invest*. 2004;114(5):652-658.
672. Straznicky NE, Lambert GW, Masuo K, Dawood T, Eikelis N, Nestel PJ, et al. Blunted sympathetic neural response to oral glucose in obese subjects with the insulin-resistant metabolic syndrome. *Am J Clin Nutri*. 2009;89(1):27-36.
673. Rowland LA, Bal NC, Periasamy M. The role of skeletal muscle based thermogenic mechanisms in vertebrate endothermy. *Biological Reviews*. 2015;90(4):1279-1297.
674. van den Berg SA, van Marken Lichtenbelt W, van Dijk KW, Schrauwen P. Skeletal muscle mitochondrial uncoupling, adaptive thermogenesis and energy expenditure. *Curr Opin Clin Nutri Metab Care*. 2011;14(3):243-249.
675. Khalfallah Y, Fages S, Laville M, Langin D, Vidal H. Regulation of uncoupling protein-2 and uncoupling protein-3 mRNA expression during lipid infusion in human skeletal muscle and subcutaneous adipose tissue. *Diabetes*. 2000;49(1):25-31.
676. Almond K, Manieri M, Sivitz WI. Ectopic brown adipose tissue in muscle provides a mechanism for differences in risk of metabolic syndrome in mice. *Proc Natl Acad of Sci USA*. 2007;104(7):2366-2371.
677. Lee TK, Clarke IJ, St John J, Young IR, Leury BL, Rao A, et al. High cortisol responses identify propensity for obesity that is linked to thermogenesis in skeletal muscle. *FASEB J*. 2014;28(1):35-44.
678. Henry BA, Dunshea FR, Gould M, Clarke IJ. Profiling postprandial thermogenesis in muscle and fat of sheep and the central effect of leptin administration. *Endocrinology*. 2008;149(4):2019-2026.

References

679. Wu J, Cohen P, Spiegelman BM. Adaptive thermogenesis in adipocytes: is beige the new brown? *Genes Dev.* 2013;27(3):234–250.
680. Seale P, Kajimura S, Yang W, Chin S, Rohas LM, Uldry M, et al. Transcriptional control of brown fat determination by PRDM16. *Cell Metabolism.* 2007;6(1):38–54.
681. Kajimura S, Seale P, Tomaru T. Regulation of the brown and white fat gene programs through a PRDM16/CtBP transcriptional complex. *Genes Dev.* 2008;22(10):1397-1409.
682. Cohen P, Levy JD, Zhang Y, Frontini A, Kolodin DP, Svensson KJ, et al. Ablation of PRDM16 and beige adipose causes metabolic dysfunction and a subcutaneous to visceral fat switch. *Cell.* 2014;156(1):304-316.
683. Tai T, Jennermann C, Brown KK, Oliver BB, MacGinnitie MA, Wilkison WO, et al. Activation of the nuclear receptor peroxisome proliferator-activated gamma promotes brown adipocyte differentiation. *J Biol Chem.* 1996;271(47):29909–29914.
684. Karamanlidis G, Karamitri A, Docherty K. C/EBP β reprograms white 3T3-L1 preadipocytes to a brown adipocyte pattern of gene expression. *J Biol Chem.* 2007;282(34):24660-24669.
685. Carmona MC, Hondares E, la Concepción de MLR, Rodríguez-Sureda V, Peinado-Onsurbe J, Poli V, et al. Defective thermoregulation, impaired lipid metabolism, but preserved adrenergic induction of gene expression in brown fat of mice lacking C/EBPbeta. *Biochem J.* 2005;389:47–56.
686. Wang Q, Zhang M, Xu M, Gu W, Xi Y, Qi L, et al. Brown adipose tissue activation is inversely related to central obesity and metabolic parameters in adult human. *PLoS ONE.* 2015;10(4):0123795.
687. Choi DK, Oh TS, Choi JW, Mukherjee R. Gender difference in proteome of brown adipose tissues between male and female rats exposed to a high fat diet. *CellPhysiol Biochem.* 2011;28(5):933-948.
688. Rodriguez-Cuenca S, Monjo M, Frontera M, Gianotti M, Proenza AM, Roca P. Sex steroid receptor expression profile in brown adipose tissue. Effects of hormonal status. *Cell Physiol Biochem.* 2007;20(6):877-886.
689. Rodriguez AM, Monjo M, Roca P, Palou A. Opposite actions of testosterone and progesterone on UCP1 mRNA expression in cultured brown adipocytes. *Cell Mol Life Sci.* 2002;59(10):1714-1723.
690. Rodriguez-Cuenca S, Monjo M, Gianotti M, Proenza AM, Roca P. Expression of mitochondrial biogenesis-signaling factors in brown adipocytes is influenced specifically by 17beta-estradiol, testosterone, and progesterone. *AJP: Endocrinol Metabol.* 2006;292(1):340-346.
691. Laudenslager M, Wilkinson C, Carlisle H, Hammel H, laude. Energy balance in ovariectomized rats with and without estrogen replacement. *Am J Physiol.* 1980;238(5):400-405.

References

692. Carlisle H, Laudenslager M, Calvano SE. Increased heat loss in ovariectomized hypothyroid rats treated with estradiol. *Am J Physiol.* 1982;243(1):70–6.
693. Quarta C, Mazza R, Pasquali R, Pagotto U. Role of sex hormones in modulation of brown adipose tissue activity. *J Mol Endocrinol.* 2012;49(1):1–7.
694. Pedersen SB, Bruun JM, Kristensen K, Richelsen B. Regulation of UCP1, UCP2, and UCP3 mRNA expression in brown adipose tissue, white adipose tissue, and skeletal muscle in rats by estrogen. *Biochem Biophys Res Commun.* 2001;288(1):191-197.
695. Heine PA, Taylor JA, Iwamoto GA, Lubahn DB, Cooke PS. Increased adipose tissue in male and female estrogen receptor-alpha knockout mice. *Proc Natl Acad Sci US A.* 2000;97(23):12729–12734.
696. Trayhurn P. Thermogenesis and the energetics of pregnancy and lactation. *Can J Physiol Pharmacol.* 1989;67(4):370–375.
697. Trayhurn P, Wusteman MC. Sympathetic activity in brown adipose tissue in lactating mice. *Am J Physiol.* 1987;253:515–520.
698. Nedergaard J, Bengtsson T, Cannon B. Three years with adult human brown adipose tissue. *Ann N Y Acad Sci.* 2010;1212(1):20–36.
699. Rogers NH. Brown adipose tissue during puberty and with aging. *Ann Med.* 2015;47(2):142–149.
700. Monjo M, Rodríguez AM, Palou A, Roca P. Direct effects of testosterone, 17 β -estradiol, and progesterone on adrenergic regulation in cultured brown adipocytes: potential mechanism for gender-dependent thermogenesis. *Endocrinology.* 2003;144(11):4923-4930.
701. Yuan X, Hu T, Zhao H, Huang Y, Ye R, Lin J, et al. Brown adipose tissue transplantation ameliorates polycystic ovary syndrome. *Proc Natl Acad Sci USA.* 2016;113(10):2708–2713.
702. Berlanga A, Guiu-Jurado E, Porrás JA, Auguet T. Molecular pathways in non-alcoholic fatty liver disease. *Clin Exp Gastroenterol.* 2014;7:221–239.
703. Byrne CD, Targher G. NAFLD: a multisystem disease. *J Hepatol.* 2015;62:47–64.
704. Machado M, Marques-Vidal P, Cortez-Pinto H. Hepatic histology in obese patients undergoing bariatric surgery. *J Hepatol.* 2006;45(4):600-606.
705. Blachier M, Leleu H, Peck-Radosavljevic M, Valla D-C, Roudot-Thoraval F. The burden of liver disease in Europe: A review of available epidemiological data. *J Hepatol.* 2013;58(3):593-608.
706. Schwimmer JB, Deutsch R, Kahen T, Lavine JE, Stanley C, Behling C. Prevalence of fatty liver in children and adolescents. *Pediatrics.* 2006;118(4):1388–1393.

References

707. Anderson EL, Howe LD, Jones HE, Higgins JPT, Lawlor DA, Fraser A. The prevalence of non-alcoholic fatty liver disease in children and adolescents: A systematic review and meta-analysis. *PLoS ONE*. 2015;10(10):0140908.
708. Targher G, Rossini M, Lonardo A. Evidence that non-alcoholic fatty liver disease and polycystic ovary syndrome are associated by necessity rather than chance: a novel hepato-ovarian axis? *Endocrine*. 2015;51(2):211–221.
709. Mofrad P, Contos MJ, Haque M, Sargeant C, Fisher RA, Luketic VA, et al. Clinical and histologic spectrum of nonalcoholic fatty liver disease associated with normal ALT values. *Hepatology*. 2003;37(6):1286–1292.
710. Musso G, Gambino R, Cassader M. Meta-analysis: natural history of non-alcoholic fatty liver disease (NAFLD) and diagnostic accuracy of non-invasive tests for liver disease severity. *Ann Med*. 2011;43(8):617.
711. Adams LA, Waters OR, Knudman MW. NAFLD as a risk factor for the development of diabetes and the metabolic syndrome: an eleven-year follow-up study. *Am J Gastroenterol*. 2009;104(4):861–867.
712. Lonardo A, Ballestri S, Marchesini G, Angulo P, Loria P. Nonalcoholic fatty liver disease: a precursor of the metabolic syndrome. *Dig Liver Dis*. 2014;47(3):181–190.
713. Katsagoni CN, Georgoulis M, Papatheodoridis GV, Panagiotakos DB, Kontogianni MD. Effects of lifestyle interventions on clinical characteristics of patients with non-alcoholic fatty liver disease: A meta-analysis. *Metabolism*. 2016;68:119–132.
714. Oh MK, Winn J, Poordad F. Review article: diagnosis and treatment of non-alcoholic fatty liver disease. *Aliment Pharmacol Ther*. 2008;28(5):503–522.
715. Sun X, Zhang Y, Xie M. Review. The role of peroxisome proliferator-activated receptor in the treatment of non-alcoholic fatty liver disease. *Acta Pharm*. 2017;67(1):1–13.
716. Romeo S, Kozlitina J, Xing C, Pertsemlidis A, Cox D, Pennacchio LA, et al. Genetic variation in PNPLA3 confers susceptibility to nonalcoholic fatty liver disease. *Nature*. 2008;40(12):1461–1465.
717. Utzschneider KM, Kahn SE. Review: The role of insulin resistance in nonalcoholic fatty liver disease. *J Clin Endocrinol Metab*. 2006;91(12):4753–4761.
718. Mota M, Banini BA, Cazanave SC, Sanyal AJ. Molecular mechanisms of lipotoxicity and glucotoxicity in nonalcoholic fatty liver disease. *Metabolism*. 2016;65(8):1049–1061.
719. Feldstein AE, Werneburg NW, Canbay A, Guicciardi ME, Bronk SF, Rydzewski R, et al. Free fatty acids promote hepatic lipotoxicity by stimulating TNF- α expression via a lysosomal pathway. *Hepatology*. 2004;40(1):185–194.
720. Donnelly KL, Smith CI, Schwarzenberg SJ, Jessurun J, Boldt MD, Parks EJ. Sources of fatty acids stored in liver and secreted via lipoproteins in patients with nonalcoholic fatty liver disease. *J Clin Invest*. 2005;115(5):1343–1351.

References

721. Ramezani-Binabaj M, Motalebi M, Karimi-Sari H, Rezaee-Zavareh MS, Alavian SM. Are women with polycystic ovarian syndrome at a high risk of non-alcoholic fatty liver disease; a meta-analysis. *Hepat Mon.* 2014;14(11):23235.
722. Baranova A, Tran TP, Bireddinc A, Younossi ZM. Systematic review: association of polycystic ovary syndrome with metabolic syndrome and non-alcoholic fatty liver disease. *Aliment Pharmacol Ther.* 2011;33(7):801–814.
723. Brzozowska MM, Ostapowicz G. An association between non-alcoholic fatty liver disease and polycystic ovarian syndrome. *J Gastroenterol Hepatol.* 2009;24(2):243-247.
724. Macut D, Tziomalos K, Božić-Antić I, Bjekić-Macut J, Katsikis I, Papadakis E, et al. Non-alcoholic fatty liver disease is associated with insulin resistance and lipid accumulation product in women with polycystic ovary syndrome. *Hum Reprod.* 2016;31(6):1347–1353.
725. Cerda C, Pérez-Ayuso RM, Riquelme A, Soza A, Villaseca P, Sir-Petermann T, et al. Nonalcoholic fatty liver disease in women with polycystic ovary syndrome. *J Hepatol.* 2007;47(3):412–417.
726. Romanowski MD, Parolin MB, Freitas ACT, Piazza MJ, Basso J, Urbanetz AA. Prevalence of non-alcoholic fatty liver disease in women with polycystic ovary syndrome and its correlation with metabolic syndrome. *Arq Gastroenterol.* 2015;52(2):117–123.
727. Grobe YG, Rodriguez GP, Ramos MH, Uribe M, Sanchez NM. Prevalence of non-alcoholic fatty liver disease in premenopausal, postmenopausal and polycystic ovary syndrome women. The role of estrogens. *Gynecoll Endocrinol.* 2010;9(4):402–409.
728. Ayonrinde OT, Adams LA, Doherty DA, Mori TA, Beilin LJ, Oddy WH, et al. Adverse metabolic phenotype of adolescent girls with non-alcoholic fatty liver disease plus polycystic ovary syndrome compared with other girls and boys. *J Gastroenterol Hepatol.* 2016;31(5):980–987.
729. Jones H, Sprung VS, Pugh C. Polycystic ovary syndrome with hyperandrogenism is characterized by an increased risk of hepatic steatosis compared to nonhyperandrogenic PCOS phenotypes and healthy controls, independent of obesity and insulin resistance. *J Clin Endocrinol Metab.* 2012;97(10):3709-3716.
730. Vassilatou E, Lafoyianni S, Vryonidou A, Ioannidis D, Kosma L, Katsoulis K, et al. Increased androgen bioavailability is associated with non-alcoholic fatty liver disease in women with polycystic ovary syndrome. *Hum Reprod.* 2010;25(1):212–220.
731. Kauffman RP, Baker TE, Baker V, Kauffman MM, Castracane VD. Endocrine factors associated with non-alcoholic fatty liver disease in women with polycystic ovary syndrome: Do androgens play a role? *Gynecol Endocrinol.* 2010;26(1):39–46.
732. Petersen KF, Dufour S, Savage DB, Bilz S, Solomon G, Yonemitsu S, et al. The role of skeletal muscle insulin resistance in the pathogenesis of the metabolic syndrome. *Proc Natl Acad Sci USA.* 2007;104(31):12587–12594.

References

733. Jornayvaz FR, Samuel VT. The role of muscle insulin resistance in the pathogenesis of atherogenic dyslipidemia and nonalcoholic fatty liver disease associated with the metabolic syndrome. *Annu Rev Nutr.* 2010;30(1):273-290.
734. Dunaif A, Segal KR, Shelley DR, Green G, Dobrjansky A, Licholai T. Evidence for distinctive and intrinsic defects in insulin action in polycystic ovary syndrome. *Diabetes.* 1992;41(10):1257–1266.
735. Mehlem A, Hagberg CE, Muhl L, Eriksson U, Falkevall A. Imaging of neutral lipids by oil red O for analyzing the metabolic status in health and disease. *Nat Protoc.* 2013;8(6):1149–1154.
736. Kazantzis M, Stahl A. Fatty acid transport proteins, implications in physiology and disease. *Biochim Biophys Acta.* 2012;1821(5):852-857.
737. Doege H, Stahl A. Protein-mediated fatty acid uptake: Novel insights from in vivo models. *Physiology.* 2006;21(4):259–268.
738. Falcon A, Doege H, Fluit A, Tsang B, Watson N, Kay MA, et al. FATP2 is a hepatic fatty acid transporter and peroxisomal very long-chain acyl-CoA synthetase. *AJP: Endocrinol Metabol.* 2010;299(3):384–393.
739. Doege H, Grimm D, Falcon A, Tsang B, Storm TA, Xu H, et al. Silencing of hepatic fatty acid transporter protein 5 in vivo reverses diet-induced non-alcoholic fatty liver disease and improves hyperglycemia. *J Biol Chem.* 2008;283(32):22186–22192.
740. Mitsuyoshi H, Yasui K, Harano Y, Endo M, Tsuji K, Minami M, et al. Analysis of hepatic genes involved in the metabolism of fatty acids and iron in nonalcoholic fatty liver disease. *Hepato Res.* 2008;39(4):366–373.
741. Auinger A, Valenti L, Pfeuffer M, Helwig U, Herrmann J, Fracanzani AL, et al. A promoter polymorphism in the liver-specific fatty acid transport protein 5 is associated with features of the metabolic syndrome and steatosis. *Horm Metab Res.* 2010;42(12):854–859.
742. Méndez-Giménez L, Rodríguez A, Balaguer I, Frühbeck G. Role of aquaglyceroporins and caveolins in energy and metabolic homeostasis. *Mol Cell Endocrinol.* 2014;397(1-2):78-92.
743. Parton RG, Simons K. The multiple faces of caveolae. *Nat Rev Mol Cell Biol.* 2007;8(3):185-194.
744. Scherer PE, Okamoto T, Chun M. Identification, sequence, and expression of caveolin-2 defines a caveolin gene family. *Proc Natl Acad Sci USA.* 1996;93(1):131–135.
745. Mastrodonato M, Calamita G, Rossi R, Mentino D, Bonfrate L, Portincasa P, et al. Altered distribution of caveolin-1 in early liver steatosis. *Eur J Clin Invest.* 2011;41(6):642–651.
746. Fernandez-Rojo MA, Ramm GA. Caveolin-1 function in liver physiology and disease. *Trends Mol Med.* 2016;22(10):889-904.

References

747. Sowa G. Novel insights into the role of caveolin-2 in cell- and tissue-specific signaling and function. *Biochem Res Int.* 2011;2011:809259.
748. Moreno M, Molina H, Amigo L, Zanlungo S, Arrese M, Rigotti A, et al. Hepatic overexpression of caveolins increases bile salt secretion in mice. *Hepatology.* 2003;38(6):1477–1488.
749. Furuhashi M, Saitoh S, Shimamoto K, Miura T. Fatty acid-binding protein 4 (FABP4): pathophysiological insights and potent clinical biomarker of metabolic and cardiovascular diseases. *Clin Med Insights Cardiol.* 2015;8:23–33.
750. Westerbacka J, Kolak M, Kiviluoto T, Arkkila P. Genes involved in fatty acid partitioning and binding, lipolysis, monocyte/macrophage recruitment, and inflammation are overexpressed in the human fatty liver of insulin-resistant subjects *Diabetes.* 2007;56(11):2759-2765.
751. Greco D, Kotronen A, Westerbacka J, Puig O, Arkkila P, Kiviluoto T, et al. Gene expression in human NAFLD. *Am J Physiol Gastrointest Liver Physiol.* 2008;294(5):1281–1287.
752. Bradbury MW. Lipid metabolism and liver inflammation. Hepatic fatty acid uptake: possible role in steatosis. *Am J Physiol Gastrointest Liver Physiol.* 2006;290(2):194–198.
753. Horton JD, Goldstein JL, Brown MS. SREBPs: activators of the complete program of cholesterol and fatty acid synthesis in the liver. *J Clin Invest.* 2002;109(9):1125–1131.
754. Azzout-Marniche D, Bécard D, Guichard C, Foretz M, Ferré P, Foufelle F. Insulin effects on sterol regulatory-element-binding protein-1c (SREBP-1c) transcriptional activity in rat hepatocytes. *Biochem J.* 2000;350(2):389–393.
755. Shimomura I, Bashmakov Y, Ikemoto S, Horton JD, Brown MS, Goldstein JL. Insulin selectively increases SREBP-1c mRNA in the livers of rats with streptozotocin-induced diabetes. *Proc Natl Acad Sci USA.* 1999;96(24):13656–13661.
756. Kohjima M, Enjoji M, Higuchi N, Kato M, Kotoh K, Yoshimoto T, et al. Re-evaluation of fatty acid metabolism-related gene expression in nonalcoholic fatty liver disease. *Int J Mol Med.* 2007;20(3):351–358.
757. Dorn C, Riener M-O, Kirovski G, Saugspier M, Steib K, Weiss TS, et al. Expression of fatty acid synthase in nonalcoholic fatty liver disease. *IntJ Clin Exp Pathol.* 2010;3(5):505–514.
758. Mao J, DeMayo FJ, Li H, Abu-Elheiga L, Gu Z, Shaikenov TE, et al. Liver-specific deletion of acetyl-CoA carboxylase 1 reduces hepatic triglyceride accumulation without affecting glucose homeostasis. *Proc Natl Acad Sci USA.* 2006;103(22):8552–8557.

References

759. Savage DB, Choi CS, Samuel VT, Liu Z-X, Zhang D, Wang A, et al. Reversal of diet-induced hepatic steatosis and hepatic insulin resistance by antisense oligonucleotide inhibitors of acetyl-CoA carboxylases 1 and 2. *J Clin Invest*. 2006;116(3):817–824.
760. Montagner A, Polizzi A, Fouché E, Ducheix S, Lippi Y, Lasserre F, et al. Liver PPAR α is crucial for whole-body fatty acid homeostasis and is protective against NAFLD. *Gut*. 2016;65(7):1202–1214.
761. Harano Y, Yasui K, Toyama T, Nakajima T, Mitsuyoshi H, Mimani M, et al. Fenofibrate, a peroxisome proliferator-activated receptor alpha agonist, reduces hepatic steatosis and lipid peroxidation in fatty liver Shionogi mice with hereditary fatty liver. *Liver Int*. 2006;26(5):613–620.
762. Xu A, Wang Y, Keshaw H, Xu LY, Lam KSL, Cooper GJS. The fat-derived hormone adiponectin alleviates alcoholic and nonalcoholic fatty liver diseases in mice. *J Clin Invest*. 2003;112(1):91–100.
763. Polyzos SA, Toulis KA, Goulis DG, Zavos C, Kountouras J. Serum total adiponectin in nonalcoholic fatty liver disease: a systematic review and meta-analysis. *Metabolism*. 2010;60(3):313–326.
764. Sanal MG, Sarin SK. Serum adipokine profile in Indian men with nonalcoholic steatohepatitis: Serum adiponectin is paradoxically decreased in lean vs. obese patients. *Diabet Metab Syndr Clin Res Rev*. 2009;3(4):198-203.
765. Polyzos SA, Kountouras J, Zavos C. Adiponectin as a potential therapeutic agent for nonalcoholic steatohepatitis. *Hepatol Res*. 2010;40(4):446–447.
766. Inoue M, Ohtake T, Saito H, Motomura W, Takahashi N, Kohgo Y, et al. Increased expression of PPAR γ in high fat diet-induced liver steatosis in mice. *Biochem Biophys Res Commun*. 2005;336(1):21-222.
767. Pettinelli P, Videla LA. Up-regulation of PPAR-gamma mRNA expression in the liver of obese patients: an additional reinforcing lipogenic mechanism to SREBP-1c induction. *J Clin Endocrinol Metab*. 2011;96(5):1424–1430.
768. Francque S, Verrijken A, Caron S, Prawitt J, Paumelle R, Derudas B, et al. PPAR α gene expression correlates with severity and histological treatment response in patients with non-alcoholic steatohepatitis. *J Hepatol*. 2015;63(1):164–173.
769. Moran-Salvador E, Lopez-Parra M, Garcia-Alonso V, Titos E, Martinez-Clemente M, Gonzalez-Periz A, et al. Role for PPAR in obesity-induced hepatic steatosis as determined by hepatocyte- and macrophage-specific conditional knockouts. *FASEB J*. 2011;25(8):2538-2550.
770. Majumdar N, Subbaiah PV, Greenstein AW, Yang P, Cordoba-Chacon J, Kineman RD. Hepatocyte-specific, PPAR γ -regulated mechanisms to promote steatosis in adult mice. *J Endocrinol*. 2017;232(1):107-121.
771. Pawlak M, Gross B, Staels B, Lefebvre P. PPARs in obesity-induced T2DM, dyslipidaemia and NAFLD. *Nat Rev Endocrinol*. 2017;13(1):36-49.

References

772. Nan Y-M, Han F, Kong L-B, Zhao S-X, Wang R-Q, Wu W-J, et al. Adenovirus-mediated peroxisome proliferator activated receptor gamma overexpression prevents nutritional fibrotic steatohepatitis in mice. *Scand J Gastroenterol*. 2010;46(3):358–369.
773. Gupte AA, Liu JZ, Ren Y, Minze LJ, Wiles JR, Collins AR, et al. Rosiglitazone attenuates age- and diet-associated nonalcoholic steatohepatitis in male low-density lipoprotein receptor knockout mice. *Hepatology*. 2010;52(6):2001–2011.
774. Ratziu V, Giral P, Jacqueminet S, Charlotte F, Hartemann-Heurtier A, Serfaty L, et al. Rosiglitazone for nonalcoholic steatohepatitis: one-year results of the randomized placebo-controlled Fatty Liver Improvement with Rosiglitazone Therapy (FLIRT) Trial. *Gastroenterology*. 2008;135(1):100–110.
775. Polyzos SA, Mantzoros CS. Adiponectin as a target for the treatment of nonalcoholic steatohepatitis with thiazolidinediones: A systematic review. *Metabolism*. 2016;65(9):1297–1306.
776. Liu C, Lin JD. PGC-1 coactivators in the control of energy metabolism. *Acta Biochim Biophys Sin*. 2011;43(4):248–257.
777. Aharoni-Simon M, Hann-Obercyger M, Pen S, Madar Z, Tirosh O. Fatty liver is associated with impaired activity of PPAR gamma-coactivator 1 alpha (PGC1 alpha) and mitochondrial biogenesis in mice. *Lab Invest* 2011;91(7):1018–1028.
778. Sookoian S, Rosselli MS, Gemma C, Burgueño AL, Gianotti TF, Castaño GO, et al. Epigenetic regulation of insulin resistance in nonalcoholic fatty liver disease: impact of liver methylation of the peroxisome proliferator-activated receptor γ coactivator 1 α promoter. *Hepatology*. 2010;52(6):1992–2000.
779. Yoon JC, Puigserver P, Chen GX, Donovan J, Wu ZD, Rhee J, et al. Control of hepatic gluconeogenesis through the transcriptional coactivator PGC-1. *Nature*. 2001;413(6852):131–138.
780. Ren Y, Yu Y, Li R, Zhao H, Qiao J, Zhao Y, et al. Epigenetic regulation of an adverse metabolic phenotype in polycystic ovary syndrome: the impact of the leukocyte methylation of PPARGC1A promoter. *Fertility and Sterility*. 2017;107(2):467-474.
781. Puigserver P, Rhee J, Donovan J, Walkey CJ, Yoon JC. Insulin-regulated hepatic gluconeogenesis through FOXO1–PGC-1 α interaction. *Nature*. 2003;423(6939):550-555.
782. Koo SH, Satoh H, Herzig S, Lee CH, Hedrick S. PGC-1 promotes insulin resistance in liver through PPAR- α -dependent induction of TRB-3. *Nat Med*. 2004;10(5):530-534.
783. Burnol A-F, Postic C, Guilmeau S, Richards P, Ourabah S, Montagne J. MondoA/ChREBP: The usual suspects of transcriptional glucose sensing; Implication in pathophysiology. *Metabolism*. 2017;70:133-151.
784. Iizuka K, Horikawa Y. ChREBP: A glucose-activated transcription factor involved in the development of metabolic syndrome. *Endocr J*. 2008;55(4):617–624.

References

785. Barclay JL, Nelson CN, Ishikawa M, Murray LA, Kerr LM, McPhee TR, et al. GH-dependent STAT5 signaling plays an important role in hepatic lipid metabolism. *Endocrinology*. 2011;152(1):181–192.
786. Kineman RD, Yakar S, Cronstein BN, Muzumdar R, Cordoba-Chacon J, Gong Z, et al. Growth hormone control of hepatic lipid metabolism. *Diabetes*. 2016;65(12):3598–3609.
787. Ichikawa T, Hamasaki K, Ishikawa H, Ejima E, Eguchi K, Nakao K. Non-alcoholic steatohepatitis and hepatic steatosis in patients with adult onset growth hormone deficiency. *Gut*. 2003;52(6):914.
788. Fan Y, Menon RK, Cohen P, Hwang D, Clemens T, DiGirolamo DJ, et al. Liver-specific deletion of the growth hormone receptor reveals essential role of growth hormone signaling in hepatic lipid metabolism. *J Biol Chem*. 2009;284(30):19937–19944.
789. Cui Y, Hosui A, Sun R, Shen K, Gavrilova O, Chen W, et al. Loss of signal transducer and activator of transcription 5 leads to hepatosteatosis and impaired liver regeneration. *Hepatology*. 2007;46(2):504–513.
790. Baik M, Nam YS, Piao MY, Kang HJ, Park SJ, Lee J-H. Liver-specific deletion of the signal transducer and activator of transcription 5 gene aggravates fatty liver in response to a high-fat diet in mice. *J Nutri Biochem*. 2015;29:56–63.
791. Mueller KM, Themanns M, Friedbichler K, Kornfeld J-W, Esterbauer H, Tuckermann JP, et al. Hepatic growth hormone and glucocorticoid receptor signaling in body growth, steatosis and metabolic liver cancer development. *Mol Cell Endocrinol*. 2012;361(1):1-11.
792. Jaffe CA, Ocampo-Lim B, Guo W, Krueger K, Sugahara I, DeMott-Friberg R, et al. Regulatory mechanisms of growth hormone secretion are sexually dimorphic. *J Clin Invest*. 1998;102(1):153–164.
793. Oshida K, Waxman DJ, Corton JC. Chemical and hormonal effects on STAT5b-dependent sexual dimorphism of the liver transcriptome. *PLoS ONE*. 2016;11(3):0150284.
794. Clodfelter KH, Holloway MG, Hodor P, Park S-H, Ray WJ, Waxman DJ. Sex-dependent liver gene expression is extensive and largely dependent upon signal transducer and activator of transcription 5b (STAT5b): STAT5b-dependent activation of male genes and repression of female genes revealed by microarray analysis. *Mol Endocrinol*. 2006;20(6):1333–13351.
795. Ramirez MC, Luque GM, Ornstein AM, Becu-Villalobos D. Differential neonatal testosterone imprinting of GH-dependent liver proteins and genes in female mice. *J Endocrinol*. 2010;207(3):301–308.
796. Finck BN, Kelly DP. PGC-1 coactivators: inducible regulators of energy metabolism in health and disease. *J Clin Invest*. 2006;116(3):615–622.

References

797. Shimoura I, Matsuda M, Hammer RE, Bashmakov Y, Brown MS, Goldstein JL. Decreased IRS-2 and increased SREBP-1c lead to mixed insulin resistance and sensitivity in livers of lipodystrophic and ob/ob mice. *Molecular Cell*. 2000;6(1):77–86.
798. Vigouroux C, Caron-Debarle M, Le Dour C, Magré J, Capeau J. Molecular mechanisms of human lipodystrophies: from adipocyte lipid droplet to oxidative stress and lipotoxicity. *Int J Biochem Cell Biol*. 2011;43(6):862–876.
799. Ajluni N, Meral R, Neidert AH, Brady GF, Buras E, McKenna B, et al. Spectrum of disease associated with partial lipodystrophy: lessons from a trial cohort. *Clin Endocrinol*. 2017;86(5):698–707.
800. Zadeh ES, Lungu AO, Cochran EK, Brown RJ, Ghany MG, Heller T, et al. The liver diseases of lipodystrophy: The long-term effect of leptin treatment. *J Hepatol*. 2013;59(1):131-137.
801. Fiorenza CG, Chou SH, Mantzoros CS. Lipodystrophy: pathophysiology and advances in treatment. *Nat Rev Endocrinol*. 2011;7(3):137-150.
802. Huang Y, Gao JM, Zhang CM, Zhao HC, Zhao Y, Li R, Yu Y, Qiao J. Assessment of growth and metabolic characteristics in offspring of dehydroepiandrosterone-induced polycystic ovary syndrome adults. *Reproduction*. 2016;152(6):705-714.
803. Itoh N. Hormone-like (endocrine) Fgfs: their evolutionary history and roles in development, metabolism, and disease. *Cell Tissue Res*. 2010;342(1):1–11.
804. Beenken A, Mohammadi M. The FGF family: biology, pathophysiology and therapy. *Nat Rev Drug Discov*. 2009;8(3):235–253.
805. Kelleher FC, O'Sullivan H, Smyth E, McDermott R, Viterbo A. Fibroblast growth factor receptors, developmental corruption and malignant disease. *Carcinogenesis*. 2013;34(10):2198–2205.
806. Adams AC, Cheng CC, Coskun T, Kharitonov A. FGF21 requires β klotho to act in vivo. *PLoS ONE*. 2012;7(11):49977.
807. Fisher FM, Maratos-Flier E. Understanding the physiology of FGF21. *Annu Rev Physiol*. 2015;78(1):223-241.
808. Markan KR, Naber MC, Ameka MK, Anderegg MD. Circulating FGF21 is liver derived and enhances glucose uptake during refeeding and overfeeding. *Diabetes*. 2014;63(12):4057-4063.
809. Yang C, Jin C, Li X, Wang F, McKeenan WL, Luo Y. Differential specificity of endocrine FGF19 and FGF21 to FGFR1 and FGFR4 in complex with KLB. *PLoS ONE*. 2012;7(3):33870.
810. Fisher FM, Estall JL, Adams AC, Antonellis PJ, Bina HA, Flier JS, et al. Integrated regulation of hepatic metabolism by fibroblast growth factor 21 (FGF21) in vivo. *Endocrinology*. 2011;152(8):2996–3004.

References

811. Kharitonov A, Shiyanova TL, Koester A, Ford AM, Micanovic R, Galbreath EJ, et al. FGF-21 as a novel metabolic regulator. *J Clin Invest*. 2005;115(6):1627–1635.
812. Dutchak PA, Katafuchi T, Bookout AL, Choi JH, Yu RT, Mangelsdorf DJ, et al. Fibroblast growth factor-21 regulates PPAR γ activity and the antidiabetic actions of thiazolidinediones. *Cell*. 2012;148(3):556–567.
813. Kharitonov A, Wroblewski VJ, Koester A, Chen Y-F, Clutinger CK, Tigno XT, et al. The metabolic state of diabetic monkeys is regulated by fibroblast growth factor-21. *Endocrinology*. 2006;148(2):774–781.
814. Xu J, Stanislaus S, Chinookoswong N, Lau YY, Hager T, Patel J, et al. Acute glucose-lowering and insulin-sensitizing action of FGF21 in insulin-resistant mouse models-association with liver and adipose tissue effects. *Am J Physiol Endocrinol Metab*. 2009;297(5):1105–1114.
815. Lin Z, Tian H, Lam KSL, Lin S, Hoo RCL, Konishi M, et al. Adiponectin mediates the metabolic effects of FGF21 on glucose homeostasis and insulin sensitivity in mice. *Cell Metab*. 2013;17(5):779–789.
816. Holland WL, Adams AC, Brozinick JT, Bui HH, Miyauchi Y, Kusminski CM, et al. An FGF21-adiponectin-ceramide axis controls energy expenditure and insulin action in mice. *Cell Metab*. 2013;17(5):790–797.
817. Coskun I, Bina HA, Schneider MA, Dunbar JD, Hu CC, Chen Y, et al. Fibroblast growth factor 21 corrects obesity in mice. *Endocrinology*. 2008;149(12):6018–6027.
818. Fisher FM, Kleiner S, Douris N, Fox EC, Mepani RJ, Verdeguer F, et al. FGF21 regulates PGC-1 α and browning of white adipose tissues in adaptive thermogenesis. *Genes Dev*. 2012;26(3):271–281.
819. Lee P, Brychta RJ, Linderman J, Smith S. Mild cold exposure modulates fibroblast growth factor 21 (FGF21) diurnal rhythm in humans: relationship between FGF21 levels, lipolysis, and cold-induced thermogenesis. *J Clin Endocrinol Metab*. 2012;98(1):98–102.
820. Dushay J, Chui PC, Gopalakrishnan GS, Varela-Rey M, Crawley M, Fisher FM, et al. Increased fibroblast growth factor 21 in obesity and nonalcoholic fatty liver disease. *Gastroenterology*. 2010;139(2):456–463.
821. Fisher FM, Chui PC, Antonellis PJ, Bina HA, Kharitonov A, Flier JS, et al. Obesity is a fibroblast growth factor 21 (FGF21)-resistant state. *Diabetes*. 2010;59(11):2781–2789.
822. Chui PC, Antonellis PJ, Bina HA, Kharitonov A. Obesity is a fibroblast growth factor 21 (FGF21)-resistant state. *Diabetes*. 2010;59(11):2781–2789.
823. Gallego-Escuredo JM, Gómez-Ambrosi J, Catalan V, Domingo P, Giral M, Frühbeck G, et al. Opposite alterations in FGF21 and FGF19 levels and disturbed expression of the receptor machinery for endocrine FGFs in obese patients. *Int J Obes*. 2014;39(1):121–129.

References

824. Fazeli PK, Misra M, Goldstein M, Miller KK, Klibanski A. Fibroblast growth factor-21 may mediate growth hormone resistance in anorexia nervosa. *J Clin Endocrinol Metab.* 2009;95(1):369–374.
825. Zhang X, Yeung DC, Karpisek M, Stejskal D, Zhou ZG, Liu F, et al. Serum FGF21 levels are increased in obesity and are independently associated with the metabolic syndrome in humans. *Diabetes.* 2008;57(5):1246–1253.
826. Suomalainen A. Fibroblast growth factor 21: a novel biomarker for human muscle-manifesting mitochondrial disorders. *Expert Opin Med Diagn.* 2013;7(4):313–317.
827. Kim KH, Jeong YT, Oh H, Kim SH, Cho JM, Kim Y-N, et al. Autophagy deficiency leads to protection from obesity and insulin resistance by inducing Fgf21 as a mitokine. *Nat Med.* 2012;19(1):83–92.
828. Lee CH, Hui EYL, Woo YC, Yeung CY, Chow WS, Yuen MMA, et al. Circulating fibroblast growth factor 21 levels predict progressive kidney disease in subjects with type 2 diabetes and normoalbuminuria. *J Clin Endocrinol Metab.* 2015;100(4):1368–1375.
829. Lin Z, Zhou Z, Liu Y, Gong Q, Yan X, Xiao J, et al. Circulating FGF21 levels are progressively increased from the early to end stages of chronic kidney diseases and are associated with renal function in Chinese. *PLoS ONE.* 2011;6(4):18398.
830. De Sousa-Coelho AL, Marrero PF, Haro D. Activating transcription factor 4-dependent induction of FGF21 during amino acid deprivation. *Biochem J.* 2012;443(1):165–171.
831. Lundasen T, Hunt MC, Nilsson L-M, Sanyal S, Angelin B, Alexson SE, et al. PPARalpha is a key regulator of hepatic FGF21. *Biochem Biophys Res Commun.* 2007;360(2):437–440.
832. Gälman C, Lundåsen T, Kharitonov A, Bina HA, Eriksson M, Hafström I, et al. The circulating metabolic regulator FGF21 is induced by prolonged fasting and PPARalpha activation in man. *Cell Metab.* 2008;8(2):169–174.
833. Badman MK, Pissios P, Kennedy AR, Koukos G, Flier JS, Maratos-Flier E. Hepatic fibroblast growth factor 21 is regulated by PPARalpha and is a key mediator of hepatic lipid metabolism in ketotic states. *Cell Metab.* 2007;5(6):426–37.
834. Badman MK, Koester A, Flier JS, Kharitonov A, Maratos-Flier E. Fibroblast growth factor 21-deficient mice demonstrate impaired adaptation to ketosis. *Endocrinology.* 2009;150(11):4931–4940.
835. Vienberg SG, Brøns C, Nilsson E, Astrup A, Vaag A, Andersen B. Impact of short-term high-fat feeding and insulin-stimulated FGF21 levels in subjects with low birth weight and controls. *Eur J Endocrinol.* 2012;167(1):49–57.
836. Sánchez J, Palou A, Picó C. Response to carbohydrate and fat refeeding in the expression of genes involved in nutrient partitioning and metabolism: striking effects on fibroblast growth factor-21 induction. *Endocrinology.* 2009;150(12):5341–5350.

References

837. Uebanso T, Taketani Y, Yamamoto H, Amo K, Ominami H, Arai H, et al. Paradoxical regulation of human FGF21 by both fasting and feeding signals: is FGF21 a nutritional adaptation factor? *PLoS ONE*. 2011;6(8):22976.
838. Kim KH, Lee M-S. FGF21 as a stress hormone: The roles of FGF21 in stress adaptation and the treatment of metabolic diseases. *Diabetes Metab J*. 2014;38(4):245-251.
839. Gómez-Sámamo MÁ, Grajales-Gómez M, Zuarth-Vázquez JM, Navarro-Flores MF, Martínez-Saavedra M, Juárez-León ÓA, et al. Fibroblast growth factor 21 and its novel association with oxidative stress. *Redox Biology*. 2016;11:335–341.
840. Boström P, Wu J, Jedrychowski MP, Korde A, Ye L. A PGC1- α -dependent myokine that drives brown-fat-like development of white fat and thermogenesis. *Nature*. 2012;481(7382):463-468.
841. Lee P, Linderman JD, Smith S, Brychta RJ, Wang J, Idelson C, et al. Irisin and FGF21 are cold-induced endocrine activators of brown fat function in humans. *Cell Metab*. 2014;19(2):302–309.
842. Jedrychowski MP, Wrann CD, Paulo JA, Gerber KK, Szpyt J, Robinson MM, et al. Detection and quantitation of circulating human irisin by tandem mass spectrometry. *Cell Metab* 2015;22(4):734–740.
843. Huh JY, Panagiotou G, Mougios V, Brinkoetter M, Vamvini MT, Schneider BE, et al. FNDC5 and irisin in humans: I. Predictors of circulating concentrations in serum and plasma and II. mRNA expression and circulating concentrations in response to weight loss and exercise. *Metabolism*. 2012;61(12):1725–1738.
844. Anastasilakis AD, Polyzos SA, Saridakis ZG, Kynigopoulos G, Skouvaklidou EC, Molyvas D, et al. Circulating irisin in healthy, young individuals: day-night rhythm, effects of food intake and exercise, and associations with gender, physical activity, diet, and body composition. *J Clin Endocrinol Metab*. 2014;99(9):3247–3255.
845. Daskalopoulou SS, Cooke AB, Gomez Y-H, Mutter AF, Filippaios A, Mesfum ET, et al. Plasma irisin levels progressively increase in response to increasing exercise workloads in young, healthy, active subjects. *Eur J Endocrinol*. 2014;171(3):343–352.
846. Kraemer RR, Shockett P, Webb ND, Shah U, Castracane VD. A transient elevated irisin blood concentration in response to prolonged, moderate aerobic exercise in young men and women. *Horm Metab Res*. 2013;46(2):150–154.
847. Polyzos SA, Kountouras J, Anastasilakis AD, Geladari EV, Mantzoros CS. Irisin in patients with nonalcoholic fatty liver disease. *Metabolism*. 2014;63(2):207-217.
848. Liu J-J, Wong MDS, Toy WC, Tan CSH, Liu S, Ng XW, et al. Lower circulating irisin is associated with type 2 diabetes mellitus. *J Diabetes Complications*. 2013;27(4):365–369.
849. Zhang H-J, Zhang X-F, Ma Z-M, Pan L-L, Chen Z, Han H-W, et al. Irisin is inversely associated with intrahepatic triglyceride contents in obese adults. *J Hepatol*. 2013;59(3):557–562.

References

850. Moreno-Navarrete JM, Ortega F, Serrano M, Guerra E, Pardo G, Tinahones F, et al. Irisin is expressed and produced by human muscle and adipose tissue in association with obesity and insulin resistance. *J Clin Endocrinol Metab.* 2013;98(4):769–778.
851. Kurdiova T, Balaz M, Vician M, Maderova D, Vlcek M, Valkovic L, et al. Effects of obesity, diabetes and exercise on Fndc5 gene expression and irisin release in human skeletal muscle and adipose tissue: in vivo and in vitro studies. *J Physiol.* 2013;592(5):1091–1107.
852. Choi Y-K, Kim M-K, Bae K-H, Seo H-A, Jeong J-Y, Lee W-K, et al. Serum irisin levels in new-onset type 2 diabetes. *Diabetes Res Clin Pract.* 2013;100(1):96-101.
853. Timmons JA, Baar K, Davidsen PK, Atherton PJ. Is irisin a human exercise gene? *Nature.* 2012;488(7413):9-10.
854. Norheim F, Langleite TM, Hjorth M, Holen T. The effects of acute and chronic exercise on PGC-1 α , irisin and browning of subcutaneous adipose tissue in humans. *FEBS J.* 2014;281(3):739-749.
855. Albrecht E, Norheim F, Thiede B, Holen T, Ohashi T, Schering L, et al. Irisin - a myth rather than an exercise-inducible myokine. *Sci Rep.* 2015;5:8889.
856. Raschke S, Elsen M, Gassenhuber H, Sommerfeld M, Schwahn U, Brockmann B, et al. Evidence against a beneficial effect of irisin in humans. *PLoS ONE.* 2013;8(9):73680.
857. Crujeiras AB, Pardo M, Casanueva FF. Irisin: “fat” or artefact. *ClinEndocrinol.* 2015;82(4):467–474.
858. Stengel A, Hofmann T, Goebel-Stengel M, Elbelt U, Kobelt P, Klapp BF. Circulating levels of irisin in patients with anorexia nervosa and different stages of obesity-correlation with body mass index. *Peptides.* 2012;39:125–130.
859. Park KH, Zaichenko L, Brinkoetter M, Thakkar B, Sahin-Efe A, Joung KE, et al. Circulating irisin in relation to insulin resistance and the metabolic syndrome. *J Clin Endocrinol Metab.* 2013;98(12):4899–4907.
860. Chen N, Li Q, Liu J, Jia S. Irisin, an exercise- induced myokine as a metabolic regulator: an updated narrative review. *Diabetes Metab Res Rev.* 2016;32(1):51-59.
861. Crujeiras AB, Pardo M, Arturo R-R, Navas-Carretero S, Zulet MA, Martínez JA, et al. Longitudinal variation of circulating irisin after an energy restriction-induced weight loss and following weight regain in obese men and women. *Am J Hum Biol.* 2013;26(2):198–207.
862. Pardo M, Crujeiras AB, Amil M, Aguera Z, Jiménez-Murcia S, Baños R, et al. Association of irisin with fat mass, resting energy expenditure, and daily activity in conditions of extreme body mass index. *Int J Endocrinol.* 2014;2014:857270.
863. Roca-Rivada A, Castelao C, Senin LL, Landrove MO, Baltar J, Crujeiras AB, et al. FNDC5/irisin is not only a myokine but also an adipokine. *PLoS ONE.* 2013;8(4):60563.

References

864. So WY, Cheng Q, Xu A, Lam KSL, Leung PS. Loss of fibroblast growth factor 21 action induces insulin resistance, pancreatic islet hyperplasia and dysfunction in mice. *Cell Death Dis.* 2015;6(3):1707.
865. Tanaka N, Takahashi S, Zhang Y, Krausz KW, Smith PB, Patterson AD, et al. Role of fibroblast growth factor 21 in the early stage of NASH induced by methionine- and choline-deficient diet. *Biochim Biophys Acta.* 2015;1852(7):1242–1252.
866. Zhu S, Wu Y, Ye X, Ma L, Qi J, Yu D, et al. FGF21 ameliorates nonalcoholic fatty liver disease by inducing autophagy. *Mol Cell Biochem.* 2016;420(1-2):107–119.
867. Liu Y, Zhao C, Xiao J, Liu L, Zhang M, Wang C, et al. Fibroblast growth factor 21 deficiency exacerbates chronic alcohol-induced hepatic steatosis and injury. *Sci Rep.* 2016;6(1):31026.
868. Yilmaz Y, Eren F, Yonal O, Kurt R, Aktas B, Celikel CA, et al. Increased serum FGF21 levels in patients with nonalcoholic fatty liver disease. *Eur J Clin Invest.* 2010;40(10):887–892.
869. Li H, Fang Q, Gao F, Fan J, Zhou J, Wang X, et al. Fibroblast growth factor 21 levels are increased in nonalcoholic fatty liver disease patients and are correlated with hepatic triglyceride. *J Hepatol.* 2010;53(5):934–940.
870. Yan H, Xia M, Chang X, Xu Q, Bian H, Zeng M, et al. Circulating fibroblast growth factor 21 levels are closely associated with hepatic fat content: a cross-sectional study. *PLoS ONE.* 2011;6(9):24895.
871. Giannini C, Feldstein AE, Santoro N. Circulating levels of FGF-21 in obese youth: associations with liver fat content and markers of liver damage. *J Clin Endocrinol Metab.* 2013;98(7):2993-3000.
872. Alisi A, Ceccarelli S, Panera N, Prono F, Petrini S, De Stefanis C, et al. Association between serum atypical fibroblast growth factors 21 and 19 and pediatric nonalcoholic fatty liver disease. *PLoS ONE.* 2013;8(6):67160.
873. Reinehr T, Karges B, Meissner T, Wiegand S, Fritsch M, Holl RW, et al. Fibroblast growth factor 21 and fetuin-A in obese adolescents with and without type 2 diabetes. *J Clin Endocrinol Metab.* 2015;100(8):3004–3010.
874. Reinehr T, Woelfle J, Wunsch R, Roth CL. Fibroblast growth factor 21 (FGF-21) and its relation to obesity, metabolic syndrome, and nonalcoholic fatty liver in children: a longitudinal analysis. *J Clin Endocrinol Metab.* 2012;97(6):2143–2150.
875. Xu J, Lloyd DJ, Hale C, Stanislaus S, Chen M, Sivits G, et al. Fibroblast growth factor 21 reverses hepatic steatosis, increases energy expenditure, and improves insulin sensitivity in diet-induced obese mice. *Diabetes.* 2008;58(1):250–259.
876. Zhu S, Ma L, Wu Y, Ye X, Zhang T, Zhang Q, et al. FGF21 treatment ameliorates alcoholic fatty liver through activation of AMPK-SIRT1 pathway. *Acta Biochim Biophys Sin.* 2014;46(12):1041–1048.
877. Friedman J. The long road to leptin. *J Clin Invest.* 2016;126(12):4727-4734.

References

878. Paz-Filho G, Mastronardi CA, Licinio J. Leptin treatment: Facts and expectations. *Metabolism*. 2015;64(1):146-156.
879. Tan BK, Hallschmid M, Adya R, Kern W, Lehnert H, Randeve HS. Fibroblast growth factor 21 (FGF21) in human cerebrospinal fluid: relationship with plasma FGF21 and body adiposity. *Diabetes*. 2011;60(11):2758–2762.
880. Zhang X, Yeung D, Karpisek M, Stejskal D. Serum FGF21 levels are increased in obesity and are independently associated with the metabolic syndrome in humans. *Diabetes*. 2008;57(5):1246-1253.
881. Dostalova I, Kavalkova P, Haluzikova D, Lacinova Z, Mraz M, Papezova H, et al. Plasma concentrations of fibroblast growth factors 19 and 21 in patients with anorexia nervosa. *J Clin Endocrinol Metab*. 2008;93(9):3627–3632.
882. del Rocio Ibarra-Reynoso L, Pisarchyk L, Perez-Luque EL, Garay-Sevilla ME, Malacara JM. Dietary restriction in obese children and its relation with eating behavior, fibroblast growth factor 21 and leptin: a prospective clinical intervention study. *Nutr Metab*. 2015;12(1):31.
883. Asrih M, Veyrat-Durebex C, Poher A-L, Lyautey J, Rohner-Jeanrenaud F, Jornayvaz FR. Leptin as a potential regulator of FGF21. *Cell Physiol Biochem*. 2016;38(3):1218–1225.
884. Miehle K, Ebert T, Kralisch S, Hoffmann A, Kratzsch J, Schlögl H, et al. Serum concentrations of fibroblast growth factor 21 are elevated in patients with congenital or acquired lipodystrophy. *Cytokine*. 2016;83:239–244.
885. Spolcova A, Holubova M, Mikulaskova B, Nagelova V, Stofkova A, Lacinova Z, et al. Changes in FGF21 serum concentrations and liver mRNA expression in an experimental model of complete lipodystrophy and insulin-resistant diabetes. *Diabetes*. 2014;63(4):483–490.
886. Véniant MM, Hale C, Helmering J, Chen MM, Stanislaus S, Busby J, et al. FGF21 promotes metabolic homeostasis via white adipose and leptin in mice. *PLoS ONE*. 2012;7(7):40164.
887. Kurosu H, Choi M, Ogawa Y, Dickson AS, Goetz R, Eliseenkova AV, et al. Tissue-specific expression of betaKlotho and fibroblast growth factor (FGF) receptor isoforms determines metabolic activity of FGF19 and FGF21. *J Biol Chem*. 2007;282(37):26687–26695.
888. Wang H, Qiang L, Farmer SR. Identification of a domain within peroxisome proliferator-activated receptor γ regulating expression of a group of genes containing fibroblast growth factor 21 that are selectively repressed by SIRT1 in adipocytes. *Mol Cell Biol*. 2008;28(1):188-200.
889. Spiegelman BM. PPAR-gamma: adipogenic regulator and thiazolidinedione receptor. *Diabetes*. 1998;47(4):507-514.

References

890. Hotta Y, Nakamura H, Konishi M, Murata Y, Takagi H, Matsumura S, et al. Fibroblast growth factor 21 regulates lipolysis in white adipose tissue but is not required for ketogenesis and triglyceride clearance in liver. *Endocrinology*. 2009;150(10):4625–4633.
891. Inagaki T, Dutchak P, Zhao G, Ding X, Gautron L, Parameswara V, et al. Endocrine regulation of the fasting response by PPARalpha-mediated induction of fibroblast growth factor 21. *Cell Metab*. 2007;5(6):415–425.
892. Ding X, Boney-Montoya J, Owen BM, Bookout AL, Coate KC, Mangelsdorf DJ, et al. β Klotho is required for fibroblast growth factor 21 effects on growth and metabolism. *Cell Metab*. 2012;16(3):387–393.
893. Samms RJ, Cheng CC, Kharitonov A, Gimeno RE, Adams AC. Overexpression of β -Klotho in adipose tissue sensitizes male mice to endogenous FGF21 and provides protection from diet-induced obesity. *Endocrinology*. 2016;157(4):1467–1480.
894. Diaz-Delfin J, Hondares E, Iglesias R, Giralt M, Caelles C, Villarroya F. TNF- α represses β -Klotho expression and impairs FGF21 action in adipose cells: involvement of JNK1 in the FGF21 pathway. *Endocrinology*. 2012;153(9):4238–4245.
895. Liu Q, Feng T, Gao Y, Xu A, Hui X. The FGF21–adiponectin axis in controlling energy and vascular homeostasis. *J Mol Cell Biol*. 2016;8(2):110-119.
896. Kubota N, Terauchi Y, Kubota T, Kumagai H, Itoh S, Satoh H, et al. Pioglitazone ameliorates insulin resistance and diabetes by both adiponectin-dependent and -independent pathways. *J Biol Chem*. 2006;281(13):8748–8755.
897. Nawrocki AR, Rajala MW, Tomas E, Pajvani UB, Saha AK, Trumbauer ME, et al. Mice lacking adiponectin show decreased hepatic insulin sensitivity and reduced responsiveness to peroxisome proliferator-activated receptor gamma agonists. *J Biol Chem*. 2005;281(5):2654–2660.
898. Talukdar S, Zhou Y, Li D, Rossulek M, Dong J, Somayaji V, et al. A Long-acting FGF21 molecule, PF-05231023, decreases body weight and improves lipid profile in non-human primates and type 2 diabetic subjects. *Cell Metab*. 2016;23(3):427–440.
899. Gaich G, Chien JY, Fu H, Glass LC, Deeg MA, Holland WL, et al. The effects of LY2405319, an FGF21 analog, in obese human subjects with type 2 diabetes. *Cell Metab*. 2013;18(3):333–340.
900. Gil-Campos M, Cañete RR, Gil A. Adiponectin, the missing link in insulin resistance and obesity. *Clin Nutr*. 2004;23(5):963–974.
901. Morrice N, Mcilroy GD, Tammireddy SR, Reekie J, Shearer KD, Doherty MK, et al. Elevated Fibroblast growth factor 21 (FGF21) in obese, insulin resistant states is normalised by the synthetic retinoid Fenretinide in mice. *Sci Rep*. 2017;7:43782.

References

902. Degawa-Yamauchi M, Moss KA, Bovenkerk JE, Shankar SS, Morrison CL, Lelliott CJ, et al. Regulation of adiponectin expression in human adipocytes: Effects of adiposity, glucocorticoids, and tumor necrosis factor alpha. *Obes Res.* 2005;13(4):662–669.
903. Liu M, Liu F. Transcriptional and post-translational regulation of adiponectin. *Biochem J.* 2010;425(1):41-52.
904. Nygaard EB, Møller CL, Kievit P, Grove KL, Andersen B. Increased fibroblast growth factor 21 expression in high-fat diet-sensitive non-human primates (*Macaca mulatta*). *Int J Obes.* 2013;38(2):183–191.
905. Chavez AO, Molina-Carrion M, Abdul-Ghani MA, Folli F, DeFronzo RA, Tripathy D. Circulating fibroblast growth factor-21 is elevated in impaired glucose tolerance and type 2 diabetes and correlates with muscle and hepatic insulin resistance. *Diabetes Care.* 2009;32(8):1542–1546.
906. Cheng X, Zhu B, Jiang F, Fan H. Serum FGF-21 levels in type 2 diabetic patients. *Endocrine Res.* 2011;36(4):142–148.
907. Hojman P, Pedersen M, Nielsen AR, Krogh-Madsen R, Yfanti C, Akerstrom T, et al. Fibroblast growth factor-21 is induced in human skeletal muscles by hyperinsulinemia. *Diabetes.* 2009;58(12):2797–2801.
908. Jeon JY, Choi S-E, Ha ES, Kim TH, Jung JG, Han SJ, et al. Association between insulin resistance and impairment of FGF21 signal transduction in skeletal muscles. *Endocrine.* 2016;53(1):97–106.
909. Mashili FL, Austin RL, Deshmukh AS, Fritz T, Caidahl K, Bergdahl K, et al. Direct effects of FGF21 on glucose uptake in human skeletal muscle: implications for type 2 diabetes and obesity. *Diabetes Metab Res Rev.* 2011;27(3):286–297.
910. Izumiya Y, Oishi K, Uchida D, Bina HA, Ouchi N, Ishida N, et al. FGF21 is an Akt-regulated myokine. *FEBS Letters.* 2008;582(27):3805–3810.
911. Kintscher U, Law RE. PPARgamma-mediated insulin sensitization: the importance of fat versus muscle. *Am J Physiol Endocrinol Metab.* 2005;288(2):287–291.
912. Norris AW, Chen L, Fisher SJ, Szanto I, Ristow M, Jozsi AC, et al. Muscle-specific PPARgamma-deficient mice develop increased adiposity and insulin resistance but respond to thiazolidinediones. *J Clin Invest.* 2003;112(4):608–618.
913. Hevener AL, He W, Barak Y, Le J, Bandyopadhyay G. Muscle-specific Pparg deletion causes insulin resistance. *Nat Med.* 2003;9(12):1491-1497.
914. Ko B-J, Kim SM, Park KH, Park HS, Mantzoros CS. Levels of circulating selenoprotein P, fibroblast growth factor (FGF) 21 and FGF23 in relation to the metabolic syndrome in young children. *Int J Obes.* 2014;38(12):1497–1502.
915. Bisgaard A, Sorensen K, Johannsen T, Helge J, Andersson AM, Juul A. Significant gender difference in serum levels of fibroblast growth factor 21 in Danish children and adolescents. *Int J Pediatr Endocrinol.* 2014;2014(1):7.

References

916. Hanks LJ, Casazza K, Ashraf AP, Wallace S, Gutiérrez OM. Fibroblast growth factor-21, body composition, and insulin resistance in pre-pubertal and early pubertal males and females. *Clin Endocrinol.* 2014;82(4):550–556.
917. Li G, Yin J, Fu J, Li L, Grant SFA, Li C, et al. FGF21 deficiency is associated with childhood obesity, insulin resistance and hypoadiponectinaemia: The BCAMS Study. *Diabetes Metab.* 2017;43(3):253-260.
918. Hanssen MJ, Broeders E, Samms RJ, Vosselman MJ, van der Lans AJ, Cheng CC, et al. Serum FGF21 levels are associated with brown adipose tissue activity in humans. *Scientific Reports.* 2015;5:10275.
919. Owen BM, Bookout AL, Ding X, Lin VY, Atkin SD. FGF21 contributes to neuroendocrine control of female reproduction. *Nat Med.* 2013;19(9):1153-1156.
920. Díaz M, Gallego-Escuredo JM, de Zegher F, Villarroya F, Ibáñez L. Effects of ethinylestradiol-cyproterone acetate vs. pioglitazone-flutamide-metformin on plasma FGF21 levels in adolescent girls with androgen excess. *Diabetes Metab.* 2015;42(3):196–199.
921. Sahin SB, Ayaz T, Cure MC, Sezgin H, Ural UM, Balik G, et al. Fibroblast growth factor 21 and its relation to metabolic parameters in women with polycystic ovary syndrome. *Scand J Clin Lab Invest.* 2014;74(6):465–469.
922. Gorar S, Culha C, Uc ZA, Dellal FD, Serter R, Aral S, et al. Serum fibroblast growth factor 21 levels in polycystic ovary syndrome. *Gynecol Endocrinol.* 2010;26(11):819–826.
923. Olszanecka-Glinianowicz M, Madej P, Wdowczyk M, Owczarek A, Chudek J. Circulating FGF21 levels are related to nutritional status and metabolic but not hormonal disturbances in polycystic ovary syndrome. *Eur J Endocrinol.* 2014;172(2):173–179.
924. Schlessinger K, Li W, Tan Y, Liu F, Souza SC, Tozzo E, et al. Gene expression in WAT from healthy humans and monkeys correlates with FGF21-induced browning of WAT in mice. *Obesity.* 2015;23(9):1818–1829.
925. Hondares E, Iglesias R, Giralt A, Gonzalez FJ, Giralt M, Mampel T, et al. Thermogenic activation induces FGF21 expression and release in brown adipose tissue. *J Biol Chem.* 2011;286(15):12983–12990.
926. Véniant MM, Sivits G, Helmering J, Komorowski R, Lee J, Fan W, et al. Pharmacologic effects of FGF21 are independent of the “browning” of white adipose tissue. *Cell Metab.* 2015;21(5):731–738.
927. Chau MDL, Gao J, Yang Q, Wu Z, Gromada J. Fibroblast growth factor 21 regulates energy metabolism by activating the AMPK-SIRT1-PGC-1alpha pathway. *Proc Natl Acad Sci USA* 2010;107(28):12553–12558.
928. Coskun T, Bina HA, Schneider MA, Dunbar JD. Fibroblast growth factor 21 corrects obesity in mice. *Endocrinology.* 2008;149(12):6018-6027.

References

929. BonDurant LD, Ameka M, Naber MC, Markan KR, Idiga SO, Acevedo MR, et al. FGF21 regulates metabolism through adipose-dependent and -independent mechanisms. *Cell Metab.* 2017;25(4):935-944.
930. Owen BM, Ding X, Morgan DA, Coate KC, Bookout AL, Rahmouni K, et al. FGF21 acts centrally to induce sympathetic nerve activity, energy expenditure, and weight loss. *Cell Metab.* 2014;20(4):670-677.
931. Potthoff MJ, Inagaki T, Satapati S, Ding X, He T, Goetz R, et al. FGF21 induces PGC-1 α and regulates carbohydrate and fatty acid metabolism during the adaptive starvation response. *Proc Natl Acad Sci USA.* 2009;106(26):10853–10858.
932. Xiong X-Q, Chen D, Sun H-J, Ding L, Wang J-J, Chen Q, et al. FNDC5 overexpression and irisin ameliorate glucose/lipid metabolic derangements and enhance lipolysis in obesity. *Biochim Biophys Acta.* 2015;1852(9):1867–1875.
933. Rahman S, Al-Daghri NM, McTernan PG, Amer OE, Chrousos GP, Piya MK, et al. Habitual physical activity is associated with circulating irisin in healthy controls but not in subjects with diabetes mellitus type 2. *Eur J Clin Invest.* 2015;45(8):775-781.
934. Choi HY, Kim S, Park JW, Lee NS, Hwang SY, Huh JY, et al. Implication of circulating irisin levels with brown adipose tissue and sarcopenia in humans. *J Clin Endocrinol Metab.* 2014;99(8):2778–2785.
935. Ijiri N, Kanazawa H, Asai K, Watanabe T, Hirata K. Irisin, a newly discovered myokine, is a novel biomarker associated with physical activity in patients with chronic obstructive pulmonary disease. *Respirology.* 2015;20(4):612–617.
936. Huh JY, Siopi A, Mougios V, Park KH, Mantzoros CS. Irisin in response to exercise in humans with and without metabolic syndrome. *J Clin Endocrinol Metab.* 2014;100(3):453–457.
937. Park KH, Zaichenko L, Brinkoetter M. Circulating irisin in relation to insulin resistance and the metabolic syndrome. *J Clin Endocrinol Metab.* 2013;98(12):4899-4907.
938. Perakakis N, Triantafyllou GA, Fernández-Real JM, Huh JY, Park KH, Seufert J, et al. Physiology and role of irisin in glucose homeostasis. *Nat Rev Endocrinol.* 2017;13(06):324-337.
939. Moreno M, Moreno-Navarrete JM, Serrano M, Ortega F, Delgado E, Sanchez-Ragnarsson C, et al. Circulating irisin levels are positively associated with metabolic risk factors in sedentary subjects. *PLoS ONE.* 2015;10(4):0124100.
940. Sesti G, Andreozzi F, Fiorentino TV, Mannino GC, Sciacqua A, Marini MA, et al. High circulating irisin levels are associated with insulin resistance and vascular atherosclerosis in a cohort of nondiabetic adult subjects. *Acta Diabetol.* 2014;51(5):705–713.
941. Sanchis-Gomar F, Alis R, Pareja-Galeano H, Sola E, Victor VM, Rocha M, et al. Circulating irisin levels are not correlated with BMI, age, and other biological parameters in obese and diabetic patients. *Endocrine.* 2014;46(3):674–677.

References

942. Völzke H, Nauck M, Friedrich N, Oelmann S, Bahls M. Circulating irisin concentrations are associated with a favourable lipid profile in the general population. *PLoS ONE*. 2016;11(4):0154319.
943. Varela-Rodríguez BM, Cordido F, Juiz-Valiña P, Pena-Bello L, Vidal-Bretal B, Sangiao-Alvarellos S. FNDC5 expression and circulating irisin levels are modified by diet and hormonal conditions in hypothalamus, adipose tissue and muscle. *Sci Rep*. 2016;6(1):29898.
944. Al-Daghri NM, Alkharfy KM, Rahman S, Amer OE, Vinodson B, Sabico S, et al. Irisin as a predictor of glucose metabolism in children: sexually dimorphic effects. *Eur J Clin Invest*. 2013;44(2):119–124.
945. Zügel M, Schumann U, Bosnyák E, Müller D, Steinacker JM, Weigt C, et al. The role of sex, adiposity, and gonadectomy in the regulation of irisin secretion. *Endocrine*. 2016;54(1):101-110.
946. Li M, Yang M, Zhou X, Fang X, Hu W, Zhu W, et al. Elevated circulating levels of irisin and the effect of metformin treatment in women with polycystic ovary syndrome. *J Clin Endocrinol Metab*. 2015;100(4):1485–1493.
947. Bostancı MS, Akdemir N, Cinemre B, Cevrioglu AS, Özden S, Ünal O. Serum irisin levels in patients with polycystic ovary syndrome. *Eur Rev Med PharmacolSci*. 2015;19(23):4462–4468.
948. Chang CL, Huang SY, Soong YK. Circulating irisin and glucose-dependent insulinotropic peptide are associated with the development of polycystic ovary syndrome. *J Clin Endocrinol Metab*. 2014;99(12):2539-2548.
949. Adamska A, Karczewska-Kupczewska M, Lebkowska A, Milewski R, Górska M, Otziomek E, et al. Serum irisin and its regulation by hyperinsulinemia in women with polycystic ovary syndrome. *Endocr J*. 2016;63(12):1107–1112.
950. Abali R, Yuksel IT, Yuksel MA, Bulut B, Imamoglu M, Emirdar V, et al. Implications of circulating irisin and Fabp4 levels in patients with polycystic ovary syndrome. *J Obstet Gynaecol*. 2016;36(7):897–901.
951. Ali SH, Al-nuaimi AMA, Al-musawi BJ. Serum irisin and leptin levels in obese and non-obese women with polycystic ovary syndrome with reference to glucose homeostasis. *Int J Pharmacy Pharmaceut Sci*. 2016;8(10):276-283.
952. Gao S, Cheng Y, Zhao L, Chen Y, Liu Y. The relationships of irisin with bone mineral density and body composition in PCOS patients. *Diabetes Metab Res Rev*. 2016;32(4):421–428.
953. Li H, Xu X, Wang X, Liao X, Li L, Yang G, et al. Free androgen index and Irisin in polycystic ovary syndrome. *J Endocrinol Invest*. 2015;39(5):549–556.
954. Li D-J, Huang F, Lu W-J, Jiang G-J, Deng YP, Shen F-M. Metformin promotes irisin release from murine skeletal muscle independently of AMP-activated protein kinase activation. *Acta Physiol*. 2014;213(3):711–721.

References

955. Waxman DJ, Holloway MG. Sex differences in the expression of hepatic drug metabolizing enzymes. *Mol Pharmacol*. 2009;76(2):215–228.
956. Horst Ter KW, Gilijamse PW, de Weijer BA, Kilicarslan M, Ackermans MT, Nederveen AJ, et al. Sexual dimorphism in hepatic, adipose tissue, and peripheral tissue insulin sensitivity in obese humans. *Front Endocrinol*. 2015;6:182.
957. Hedrington MS, Davis SN. Sexual dimorphism in glucose and lipid metabolism during fasting, hypoglycemia, and exercise. *Front Endocrinol*. 2015;6:61.
958. Seidell JC, Cigolini M, Charzewska J, Ellsinger BM, Björntorp P, Hautvast JG, et al. Fat distribution and gender differences in serum lipids in men and women from four European communities. *Atherosclerosis*. 1991;87(2-3):203–210.
959. Bellentani S, Scaglioni F, Marino M, Bedogni G. Epidemiology of non-alcoholic fatty liver disease. *Digestive Dis*. 2010;28(1):155-161.
960. Geer EB, Shen W. Gender differences in insulin resistance, body composition, and energy balance. *Gender Med*. 2009;6:60–75.
961. Nordström A, Hadrévi J, Olsson T, Franks PW, Nordström P. Higher prevalence of type 2 diabetes in men than in women is associated with differences in visceral fat mass. *J Clin Endocrinol Metab*. 2016;101(10):3740–3746.
962. Bhatnagar P, Wickramasinghe K, Williams J, Rayner M. The epidemiology of cardiovascular disease in the UK 2014. *BMJ: British Medical Journal*. 2015;101(15):1182–1189.
963. Tafeit E, Moller R, Rackl S, Giuliani A, Urdl W, Freytag U, et al. Subcutaneous adipose tissue pattern in lean and obese women with polycystic ovary syndrome. *Exp Biol Med*. 2003;228(6):710–716.
964. Villa J, Pratley RE. Adipose tissue dysfunction in polycystic ovary syndrome. *Curr Diab Rep*. 2011;11(3):179–184.
965. Sir-Petermann T, Codner E, Pérez V, Echiburú B, Maliqueo M, Ladrón de Guevara A, et al. Metabolic and reproductive features before and during puberty in daughters of women with polycystic ovary syndrome. *J Clin Endocrinol Metab*. 2009;94(6):1923–1930.
966. Torchen LC, Idkowiak J, Fogel NR, O'Neil DM, Shackleton CHL, Arlt W, et al. Evidence for increased 5 α -reductase activity during early childhood in daughters of women with polycystic ovary syndrome. *J Clin Endocrinol Metab*. 2016;101(5):2069–2075.
967. Wu C, Jiang Z, Wei K. 5 α -reductase activity in women with polycystic ovary syndrome: A systematic review and meta-analysis. *Reprod Biol Endocrinol*. 2017;15(1):21.
968. Kelsey MM, Zeitler PS. Insulin resistance of puberty. *Curr Diab Rep*. 2016;16(7):64.

References

969. Franks S, Robinson S, Willis DS. Nutrition, insulin and polycystic ovary syndrome. *Rev Reprod.* 1996;1(1):47–53.
970. Shaw L, Elton S. Polycystic ovary syndrome: a transgenerational evolutionary adaptation. *BJOG.* 2008;115(2):144–148.
971. Zhang J, Li Y. Fibroblast growth factor 21 analogs for treating metabolic disorders. *Front Endocrinol.* 2015;6:168.
972. Du Q, Yang S, Wang YJ, Wu B, Zhao YY, Bin Fan. Effects of thiazolidinediones on polycystic ovary syndrome: a meta-analysis of randomized placebo-controlled trials. *Adv Ther.* 2012;29(9):763–774.